Trinity College Dublin
Coláiste na Tríonóide, Baile Átha Cliath
The University of Dublin

Beyond Haemostasis: Crosstalk between Human Platelets and Multiple Myeloma Cells

By

Anushka Kulkarni

A dissertation submitted for the degree of Doctor of Philosophy

at the

University of Dublin, Trinity College

This research was conducted in the School of Pharmacy and Pharmaceutical Sciences, Trinity College, Dublin 2, Ireland

Under the direction and supervision of

Dr. Maria José Santos-Martinez and Dr. Despina Bazou

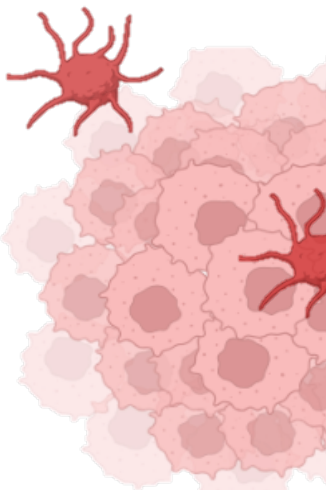

2026

DECLARATION

I declare that this thesis has not been submitted as an exercise for a degree at this or any other university and it is entirely my own work. Except where stated otherwise, the work described in this report has been carried out by the author alone.

I agree to deposit this thesis in the University's open access institutional repository or allow the Library to do so on my behalf, subject to Irish Copyright Legislation and Trinity College Library conditions of use and acknowledgement.

I consent to the examiner retaining a copy of the thesis beyond the examining period, should they so wish (EU GDPR May 2018).

_____

Anushka Kulkarni

SUMMARY

Multiple myeloma (MM) is a haematological malignancy characterised by unhindered proliferation of plasma cells. It is well established that cancer cells can aggregate platelets, a phenomenon known as tumour cell induced platelet aggregation (TCIPA). TCIPA correlates with tumour progression in solid tumours, but little is known about its role in haematological malignancies, in particular MM.

The overall aim of this thesis is to investigate the multifaceted mechanisms of myeloma–human blood platelet crosstalk, integrating platelet aggregation assays, proteomics, invasion and migration assays, and PI-based cell death assays to determine how platelets influence MM cell behaviour, proteomic adaptation, and the therapeutic response to bortezomib. For this purpose, washed platelets were prepared from whole blood obtained from healthy volunteers and exposed to MM cell lines (MM.1S, JJN-3, KMS-27 and U266) under specific experimental conditions.

Results from light transmission aggregometry (LTA) demonstrated that MM cells induce platelet aggregation in a cell line–dependent manner. MM.1S and KMS-27 cells consistently induced platelet aggregation, whereas JJN-3 and U266 did not, highlighting intrinsic heterogeneity in platelet responsiveness to each cell line. Pharmacological modulation indicated that TCIPA involves distinct combinations of ADP-, TXA_2-, and MMP-dependent pathways, varying by cell type. Differences in platelet aggregation under quasi-static (LTA) versus static (ultrasound standing wave trap) conditions further revealed that effective platelet activation may depend upon direct, sustained MM–platelet contact, with tumour cell number affecting the platelet response.

Proteomic profiling across MM.1S, KMS-27, JJN-3, and U266 cell lines showed that platelets' interaction with those cell lines profoundly remodels the myeloma secretome, reshaping pathways linked to metabolism, cytoskeletal organisation, and proteostasis. Enrichment of metabolic enzymes (e.g., G6PD, ENO1), adhesion molecules (VINC, TLN1, GELS), and stress-response proteins (HSP90, HSPB1) revealed platelet-induced metabolic reprogramming and activation of adhesion-

mediated survival signalling. Few of the proteins were found to be strongly associated with drug resistance and myeloma progression after a literature search. A conserved signature of 14 proteins across all the MM cell lines, included CAP1, ARRB1, CALM, and COTL1, impliying an adaptive response promoting proliferation, immune modulation, and therapy resistance.

Based on results of proteomics, invasion and migration assays were performed. These assays showed that MM cell-platelet co-culture alters MM motility and invasion in a context-dependent manner. While the co-incubation of platelets induced an increased MMP-2 and MMP-9 activity, they restricted invasion in matrix-based assays. The most clinically relevant finding was that co-incubation significantly increased the migratory capacity of MM.1S and U266 cells, with comparable donor-dependent responses observed in KMS-27 and JJN-3. The use of platelets or platelet releasate as chemoattractants reduced cell migration, except in MM.1S cells. These findings indicate that physical platelet–cell interactions maybe the principal drivers of MM cell motility, underscoring important mechanistic differences from adherent solid tumour models. Further studies are required to investigate the role of MM cell-platelet releasate co-incubation in migration of MM cells.

Finally, analysis of proteasome inhibitor sensitivity indicated that platelet association may reduce bortezomib-induced cytotoxicity, though technical constraints prevented definitive quantification. Further experiments using cells secretome suggested that protection against bortezomib involves contact-dependent, not entirely through soluble factors, if there are any.

Collectively, this work demonstrates that MM cells can aggregate platelets in vitro and that platelets, in turn, modulate the myeloma microenvironment. Further studies are necessary to validate the exact molecular pathways involved during this process.

ACKNOWLEDGEMENTS

First and foremost, I would like to express my deepest gratitude to my supervisor, Prof. Maria Jose Santos Martinez, for her constant support throughout my three-year PhD journey. Your guidance, kindness, and leadership played a pivotal role in shaping the researcher I am today. Despite the many challenges we faced during these years, you always greeted me with a warm smile and words of encouragement, which meant more to me than you know. You are truly an inspiring role model, and I am incredibly grateful to have had you as my supervisor.

I would also like to sincerely thank my co-supervisor, Dr. Despina Bazou. Your positive attitude, strong work ethic, and unwavering belief in me continuously motivated me to push myself and improve. I am truly thankful for your support and encouragement throughout this journey.

I am grateful to my thesis committee members, Dr. Carlos Medina and Dr. Oliviero Gobbo, for taking the time to review my work each year and for providing valuable feedback. I would also like to thank Dr. Nadhim Kamil Hante for teaching me western blotting techniques and for always being willing to help whenever I had questions in the lab.

My sincere thanks go to Dr. Paul Dowling for assisting with the processing of my samples for proteomics at Maynooth University, Dublin, and for carrying out the LC-MS analysis. Your advice, guidance, and friendly presence made my visits to the university an absolute pleasure. I would also like to extend my heartfelt thanks to all the participants who generously donated blood for this study, without whom this research would not have been possible.

A huge thank you to the technical staff in the school. In particular, I would like to thank Mr. Brian Talbot for his patience and assistance whenever lab equipment decided not to cooperate, and Dr. Gavin McManus for introducing me to the real-time imaging system, Incucyte, which proved invaluable when other techniques were not working as planned.

I am incredibly grateful to the many people I met during my PhD journey, with whom I formed friendships that I will cherish forever. I would like to thank the other labs in the Pharmacy Department for allowing me to use their equipment, borrow chemicals, and for sharing coffee and lunch breaks. Those lunchtime chats were always a welcome escape from work. In particular, I would like to thank Thomson, Almu, Sukanya, Ayushi, and Abeer for the great teamwork while sharing a lab. I am also thankful to Sara (Dr. Sara Toselli) for showing me around the labs and introducing me to people during my early days. Special thanks go to two exceptional master's students, Swarali and Aarthi, for helping me with my thesis as part of their master's projects.

I would like to thank my friends outside the university who have been a constant source of support over the past four years and have witnessed my laughter, tears, and endless complaints about life. A very special thank you to Ajit, you have been like family to me in a new country. Thank you for listening to me talk about the same research problem a thousand times, even when you couldn't understand a word of it. Thank you for cooking dinner and picking me up from college when I worked late into the night. I am immensely grateful to you.

Lastly, I would like to thank my family, my Aai (mother) and Baba (father), as I call them, for their unconditional love, unwavering support and for giving me the courage to move to another country to pursue my studies. Everything I am today, I owe to you.

PUBLICATIONS AND PRESENTATIONS

Publications

Kulkarni A, Bazou D, Santos-Martinez MJ., Bleeding and Thrombosis in Multiple Myeloma: Platelets as Key Players during Cell Interactions and Potential Use as Drug Delivery Systems, *International Journal of Molecular Sciences,* 24, (21), 2023, p15855

Presentations

Kulkarni A, Bazou D, Santos-Martinez MJ., Proteomic profile of multiple myeloma cell-platelet interaction, *44th All Ireland School of Pharmacy Conference, Cork 4-5/9/25*
Poster, 2025

Kulkarni A, Bazou D, Santos-Martinez MJ., Platelets and MMPs in multiple myeloma: role in TCIPA and invasion, *43rd All Ireland School of Pharmacy Conference, Dublin, 27-28/08/2024*
Poster 2024

Kulkarni A, Bazou D, Santos-Martinez MJ., The role of Platelets in Multiple Myeloma, *EACR-AACR Basic and Translational Research Conference: How to Bring Basic Science Discoveries to the Clinic, Dublin, 27-29/2/2024*
Poster 2024

Kulkarni A, Bazou D, Santos-Martinez MJ., The Role of Platelets in Multiple Myeloma *The Trinity St James's Cancer Institute Christmas Research Blitz, Dublin 8/12/23*
Oral Presentation, 2023

Kulkarni A, Bazou D, Santos-Martinez MJ.,The role of platelets in multiple myeloma, *Irish Association of Pharmacologists Annual Meeting, Cork, 3/11/2023*
Oral Presentation, 2023

TABLE OF CONTENTS

SUMMARY ..... **III**
ACKNOWLEDGEMENTS ..... **V**
PUBLICATIONS AND PRESENTATIONS ..... **VII**
TABLE OF CONTENTS ..... **VIII**
LIST OF FIGURES ..... **XI**
LIST OF TABLES ..... **XIII**
LIST OF ABBREVIATIONS ..... **XIV**
CHAPTER 1 INTRODUCTION **1:0**
1.1 MULTIPLE MYELOMA 1:1
1.1.1 Pathogenesis and evolution of MM 1:1
1.1.2 Clinical stages and diagnostic criteria 1:3
1.1.3 Clinical management of MM 1:6
1.1.4 MM and its microenvironment 1:9
1.2 HAEMOSTASIS AND CANCER 1:13
1.2.1 Primary haemostasis 1:13
1.2.2 Secondary Haemostasis 1:16
1.3 HAEMOSTASIS AND CANCER INTERPLAY 1:18
1.3.1 Platelets in Haematological Malignancies 1:21
1.3.2 Platelets in MM Clinical Context 1:22
1.4 MATRIX METALLOPROTEINASES AND CANCER 1:24
1.4.1 Matrix Metalloproteinases 1:24
1.4.2 Matrix metalloproteinases in solid cancers 1:25
1.4.3 Matrix metalloproteinases in MM 1:26
1.5 AIMS 1:27
CHAPTER 2 MULTIPLE MYELOMA CELL-INDUCED PLATELET AGGREGATION AND ITS PHARMACOLOGICAL MODULATION **2:28**
2.1 INTRODUCTION 2:29
2.1.1 Light transmission aggregometry 2:29
2.1.2 Ultrasound standing wave trap 2:30
2.1.3 Modulation of tumour cell-induced platelet aggregation 2:31
2.1.4 Gelatin zymography 2:33
2.2 METHODS 2:33
2.2.1 Reagents 2:33
2.2.2 Ethical Approval, Blood Collection And, Preparation Of Washed Platelets 2:33
2.2.3 Cell Lines Used And Cell Culture Conditions 2:34
2.2.4 Light Transmission Aggregometry 2:34
2.2.5 Optical Microscopy 2:35
2.2.6 Ultrasound Wave Trap 2:35
2.2.7 Immunoblotting (Western Blot) 2:35
2.2.8 Gelatin Zymography 2:36
2.3 RESULTS 2:37
2.3.1 Tumour cell-induced platelet aggregation: light transmission aggregometry 2:37
2.3.2 Drug Modulation of TCIPA 2:44
2.3.3 Tumour cell-induced platelet aggregation: ultrasound standing wave trap 2:48
2.3.4 Immunoblotting (Western Blot) 2:51

2.3.5 Gelatin Zymography 2:51
2.4 DISCUSSION 2:52
2.5 CONCLUSIONS 2:58

CHAPTER 3 LOOKING AT THE PROTEOME OF PLATELET–MYELOMA CROSSTALK: IDENTIFYING DRIVERS OF METABOLIC SHIFT AND THERAPEUTIC RESISTANCE 3:59

3.1 INTRODUCTION 3:60
3.1.1 Mass spectrometry 3:60
3.1.2 Label Free Quantification 3:61
3.2 METHODS 3:62
3.2.1 Reagents 3:62
3.2.2 Washed platelet preparation 3:62
3.2.3 Cell lines used and collection of conditioned media 3:63
3.2.4 Platelet response to MM conditioned media 3:63
3.2.5 Proteomics 3:64
3.3 RESULTS 3:67
3.3.1 Platelet response to MM conditioned media 3:67
3.3.2 Proteomics 3:68
3.4 DISCUSSION 3:117
3.5 CONCLUSIONS 3:126

CHAPTER 4 PLATELETS–MULTIPLE MYELOMA CELL INTERACTIONS DRIVING INVASION AND MIGRATION OF MYELOMA CELLS 4:129

4.1 INTRODUCTION 4:130
4.2 METHODS 4:131
4.2.1 Cell lines employed in this chapter 4:131
4.2.2 Washed platelets and platelet releaseate preparation 4:131
4.2.3 Invasion Studies 4:132
4.2.4 Gelatin Zymography 4:132
4.2.5 Migration Studies 4:133
4.2.6 Quantification of cell migration using IncuCyte system 4:133
4.2.7 Statistical Analysis 4:133
4.3 RESULTS 4:134
4.3.1 Invasion Studies 4:134
4.3.2 Gelatin zymography 4:136
4.3.3 Migration Studies 4:137
4.4 DISCUSSION 4:141
4.5 CONCLUSIONS 4:145

CHAPTER 5 EVALUATING PLATELET INVOLVEMENT IN MULTIPLE MYELOMA: CONTRIBUTORS TO RESISTANCE MECHANISMS OR INNOCENT BYSTANDERS 5:146

5.1 INTRODUCTION 5:147
5.2 METHODS 5:149
5.2.1 WP preparation 5:149
5.2.2 Cell lines used 5:150
5.2.3 BTZ EC_{50} 5:150
5.2.4 Effect of BTZ on MM cells co-incubated in the presence and absence of platelets 5:150
5.2.5 Effect of BTZ on MM cells co-incubated in the presence of MM cell secretome and MM cell-platelet secretome 5:150
5.3 RESULTS 5:151
5.3.1 Calculation of EC_{50} value of BTZ 5:151
5.3.2 Effect of BTZ on MM cells co-incubated in the presence and absence of platelets 5:152
5.3.3 Effect of BTZ on MM cells co-incubated in the presence of MM.1S cell secretome and MM.1S cell-platelet secretome 5:153
5.4 DISCUSSION 5:153
5.5 CONCLUSIONS 5:155

DISCUSSION 5:157
CONCLUSIONS AND FUTURE DIRECTIONS.....5:160
REFERENCES.....CLXII

LIST OF FIGURES

FIGURE 1 GENOMIC AND CLINICAL MODELS OF CLONAL EVOLUTION IN MULTIPLE MYELOMA (MM).[30][31]
FIGURE 2 SYSTEMIC MANIFESTATIONS OF MULTIPLE MYELOMA (MM)
FIGURE 3 PRIMARY HAEMOSTASIS
FIGURE 4 SECONDARY HAEMOSTASIS
FIGURE 5 INTERACTION BETWEEN PLATELETS AND TUMOUR CELLS.
FIGURE 6 PRINCIPLE OF LIGHT TRANSMISSION AGGREGOMETRY.
FIGURE 7 SCHEMATIC DIAGRAM OF THE ULTRASOUND STANDING WAVE TRAP [174]
FIGURE 8 POTENTIAL PHARMACOLOGICAL MODULATION OF TCIPA
FIGURE 9 MM.1S CELLS INDUCED PLATELET AGGREGATION USING LTA
FIGURE 10 KMS-27 CELLS INDUCED PLATELET AGGREGATION USING LTA
FIGURE 11 EFFECT OF U266 CELLS ON PLATELET AGGREGATION
FIGURE 12 EFFECT OF JJN-3 CELLS ON PLATELETS
FIGURE 13 MODULATION OF MM.1S CELLS INDUCED PLATELET AGGREGATION
FIGURE 14 OPTICAL MICROSCOPY PERFORMED AFTER FIXING WP EXPOSED TO DIFFERENT CONCENTRATION OF MM.1S CELLS AND ANTIPLATELET AGENTS
FIGURE 15 MODULATION OF KMS-27 TCIPA
FIGURE 16 OPTICAL MICROSCOPY PERFORMED AFTER FIXING THE WP EXPOSED TO 200,000 KMS-27 CELLS/ML AND DIFFERENT ANTIPLATELET AGENTS
FIGURE 17 INVESTIGATION OF TCIPA BY MM.1S AND KMS-27 CELLS USING AN ULTRASOUND STANDING WAVE TRAP
FIGURE 18 IMMUNOBLOTTING OF P53. THE EXPRESSION OF P53 WAS DETERMINED BY WESTERN BLOTTING. A MOLECULAR WEIGHT PROTEIN LADDER (FIRST WELL) WAS USED AS A REFERENCE FOR THE MOLECULAR WEIGHT. B-ACTIN WAS USED AS LOADING CONTROL.
FIGURE 19 GELATINASE ACTIVITY AS MEASURED BY ZYMOGRAPHY
FIGURE 20 PROCEDURE FOR CARRYING OUT PLATELET FUNCTIONAL STUDIES.
FIGURE 21 PROCEDURE CARRIED OUT FOR COLLECTING THE SAMPLE AND SAMPLE PROCESSING FOR PROTEOMIC ANALYSIS.
FIGURE 22 AGGREGATION OF PLATELETS RESUSPENDED IN THE CONDITIONED MEDIA FROM MM.1S, KMS-27, U266 AND JJN-3 CELLS IN THE PRESENCE OF A) COLLAGEN (2μG/ML) B) ARACHIDONIC ACID (500 μG/ML) C) U46619 (1 μM).
FIGURE 23 STRING PROTEIN INTERACTION MAP DEPICTING ALL THE PROTEINS EXPRESSED ONLY IN THE MM.1S-PLATELET SECRETOME.
FIGURE 24 THE ENRICHMENT ANALYSIS OF PROTEINS PRESENT EXCLUSIVELY IN THE PRESENCE OF PLATELETS AND MM.1S CELLS BASED ON (I) KEGG PATHWAY, (II) BIOLOGY PROCESS (GENE ONTOLOGY), PROVIDED BY THE STRING DATABASE.
FIGURE 25 STRING PROTEIN INTERACTION MAP DEPICTING ALL THE PROTEINS INCREASED IN ABUNDANCE IN THE MM.1S CELL-PLATELET SECRETOME.
FIGURE 26 THE ENRICHMENT ANALYSIS OF PROTEINS INCREASED IN ABUNDANCE BY THE CO-INCUBATION OF MM.1S CELLS WITH PLATELETS, BASED ON (I) KEGG PATHWAY AND, (II) BIOLOGICAL PROCESS (GENE ONTOLOGY), PROVIDED BY THE STRING DATABASE.
FIGURE 27 DIFFERENTIAL PROTEIN ABUNDANCE IN THE MM.1S CELL-PLATELET SECRETOME
FIGURE 28 STRING PROTEIN INTERACTION MAP DEPICTING ALL THE PROTEINS ENRICHED ONLY BY JJN-3 CELL-PLATELET SECRETOME.
FIGURE 29 THE ENRICHMENT ANALYSIS OF PROTEINS EXPRESSED ONLY BY THE CO-INCUBATION OF PLATELETS AND JJN-3 CELLS, BASED ON (I) KEGG PATHWAY AND (II) BIOLOGICAL PROCESS (GENE ONTOLOGY), PROVIDED BY THE STRING DATABASE
FIGURE 30 STRING PROTEIN INTERACTION MAP DEPICTING PROTEINS INCREASED IN ABUNDANCE IN JJN-3 CELL-PLATELET SECRETOME (FOLD CHANGE ≥ 1.5 AND P VALUE ≤ 0.05)
FIGURE 31 THE ENRICHMENT ANALYSIS OF PROTEINS INCREASED IN ABUNDANCE IN THE PRESENCE OF JJN-3 CELLS AND PLATELETS, BASED ON (I) KEGG PATHWAY AND (II) BIOLOGICAL PROCESS (GENE ONTOLOGY), PROVIDED BY THE STRING DATABASE.
FIGURE 32 DIFFERENTIAL PROTEIN ABUNDANCE IN THE JJN-3 CELL-PLATELET SECRETOME
FIGURE 33 STRING PROTEIN INTERACTION MAP DEPICTING ALL THE PROTEINS ENRICHED ONLY BY THE KMS-27- PLATELET INTERACTION

FIGURE 34 THE ENRICHMENT ANALYSIS OF PROTEINS EXPRESSED BY THE CO-INCUBATION OF PLATELETS AND KMS-27 CELLS, BASED ON THE BIOLOGICAL PROCESS (GO) PATHWAY, PROVIDED BY THE STRING DATABASE
FIGURE 35 STRING PROTEIN INTERACTION MAP DEPICTING PROTEINS INCREASED IN ABUNDANCE IN KM2-27 CELL-PLATELET SECRETOME (FOLD CHANGE ≥ 1.5 AND P VALUE ≤ TO 0.05)
FIGURE 36 THE ENRICHMENT ANALYSIS OF PROTEINS INCREASED IN ABUNDANCE IN KMS-27 CELL-PLATELET SECRETOMES, BASED ON (I) KEGG PATHWAY AND (II) BIOLOGICAL PROCESS (GO), PROVIDED BY THE STRING DATABASE
FIGURE 37 DIFFERENTIAL PROTEIN ABUNDANCE IN THE KMS-27 CELL-PLATELET SECRETOME
FIGURE 38 STRING PROTEIN INTERACTION MAP DEPICTING PROTEINS ENRICHED IN THE U266 CELLS- PLATELET SECRETOME
FIGURE 39 THE ENRICHMENT ANALYSIS OF PROTEINS EXPRESSED BY THE CO-INCUBATION OF PLATELETS AND U266 CELLS, BASED ON (I) KEGG PATHWAY AND (II) BIOLOGICAL PROCESS (GO) PATHWAY, PROVIDED BY THE STRING DATABASE
FIGURE 40 STRING PROTEIN INTERACTION MAP DEPICTING PROTEINS INCREASED IN ABUNDANCE IN THE U266 CELLS-PLATELET SECRETOME (FOLD CHANGE ≥ 1.5 AND P VALUE ≤ 0.05)
FIGURE 41 THE ENRICHMENT ANALYSIS OF PROTEINS INCREASED IN ABUNDANCE IN THE U266 CELL-PLATELET SECRETOME, BASED ON (I) KEGG PATHWAY AND (II) BIOLOGICAL PROCESS (GO), PROVIDED BY THE STRING DATABASE
FIGURE 42 DIFFERENTIAL PROTEIN ABUNDANCE IN THE U266 CELL-PLATELET SECRETOMES
FIGURE 43 COMPARATIVE PROTEOMIC ANALYSIS OF CELL-PLATELET SECRETOMES[250]
FIGURE 44 SCHEMATIC OVERVIEW OF THE EXPERIMENTAL DESIGN UTILISED FOR (A) INVASION AND (B) MIGRATION STUDIES.
FIGURE 45 MATRIGEL INVASION ASSAYS OF MM.1S
FIGURE 46 MATRIGEL INVASION ASSAYS OF JJN-3
FIGURE 47 MMP ACTIVITY DURING MM.1S AND JJN-3 INVASION WAS ASSESSED BY GELATIN ZYMOGRAPHY
FIGURE 48 MIGRATION OF MM.1S AND U266 CELLS IN THE PRESENCE OR ABSENCE OF PLATELETS.
FIGURE 49 MIGRATION OF KMS-27 AND JJN-3 CELLS IN THE PRESENCE OR ABSENCE OF PLATELETS.
FIGURE 50 MIGRATION ASSAY OF MULTIPLE MYELOMA CELLS WITH AND WITHOUT PLATELETS
FIGURE 51 MECHANISM OF ACTION OF BORTEZOMIB (BTZ).
FIGURE 52 PROCEDURE FOLLOWED TO STUDY THE EFFECT OF BORTEZOMIB (BTZ) ON CELL DEATH OF MM CELLS CO-INCUBATED WITH AND WITHOUT MM CELL-PLATELET SECRETOME.
FIGURE 53 HALF-MAXIMAL EFFECTIVE CONCENTRATION (EC50) CURVE OF BTZ IN MM.1S CELL LINE
FIGURE 54 EFFECT OF BORTEZOMIB ON CELL DEATH OF MM CELLS CO-INCUBATED IN THE PRESENCE AND ABSENCE OF PLATELETS.
FIGURE 55 EFFECT OF BTZ ON MM.1S CELLS RESUSPENDED IN MM.1S CELL SECRETOME AND MM.1S CELL-PLATELET SECRETOME

LIST OF TABLES

TABLE 1 REVISED INTERNATIONAL STAGING SYSTEM (R-ISS)
TABLE 2 MATRIX METALLOPROTEINASES (MMPS) CLASSIFICATION, THEIR KEY SUBSTRATES AND FUNCTIONAL ROLE
TABLE 3 SAMPLES COLLECTED FOR PROTEOMICS ANALYSIS AND TERMS USED THROUGHOUT THE THESIS
TABLE 4 PROTEINS PRESENT ONLY IN MM.1S CELL-PLATELET SECRETOME, ALONG WITH THEIR BIOLOGICAL ROLE
TABLE 5 TOP 10 PROTEINS INCREASED IN ABUNDANCE IN MM.1S CELL-PLATELET SECRETOME COMPARED TO MM.1S CELL SECRETOME
TABLE 6 TOP 10 PROTEINS INCREASED IN ABUNDANCE IN MM.1S CELL-PLATELET SECRETOME COMPARED TO PLATELET RELEASATE
TABLE 7 LIST OF ALL THE PROTEINS ENRICHED ONLY IN JJN-3 CELL-PLATELET SECRETOME ALONG WITH THEIR BIOLOGICAL ROLE
TABLE 8 TOP 10 PROTEINS INCREASED IN ABUNDANCE IN JJN-3 CELL-PLATELET SECRETOME VS JJN-3 CELLS ALONE
TABLE 9 TOP 10 PROTEINS INCREASED IN ABUNDANCE IN JJN-3 CELL-PLATELET SECRETOME COMPARED TO RELEASATE CONTROL
TABLE 10 BIOLOGICAL FUNCTION OF ALL THE PROTEINS EXPRESSED ONLY IN THE KMS-27 CELL- PLATELET SECRETOME
TABLE 11 TOP 10 PROTEINS INCREASED IN ABUNDANCE IN THE KMS-27 CELL-PLATELET SECRETOME WHEN COMPARED TO THE KMS-27 CELL SECRETOME
TABLE 12 TOP 10 PROTEINS INCREASED IN ABUNDANCE IN THE KMS-27 CELL-PLATELET SECRETOME WHEN COMPARED TO THE PLATELET RELEASATE
TABLE 13 PROTEINS ENRICHED ONLY IN THE U266 CELL-PLATELET SECRETOME ALONG WITH THEIR BIOLOGICAL ROLE
TABLE 14 TOP 10 PROTEINS INCREASED IN ABUNDANCE IN THE U266 CELL-PLATELET SECRETOME WHEN COMPARED TO THE U266 CELL SECRETOME
TABLE 15 TOP 10 PROTEINS INCREASED IN ABUNDANCE IN THE U266 CELL-PLATELET SECRETOME WHEN COMPARED TO THE PLATELET RELEASATE
TABLE 16 MM CELL-PLATELET SECRETOME PROTEINS CONSISTENTLY REGULATED ACROSS FOUR CELL LINES

LIST OF ABBREVIATIONS

1433F	14-3-3 protein eta
1433Z	14-3-3 protein zeta/delta
1B44	HLA class I histocompatibility antigen, B-44 alpha chain
2AAA	Serine/threonine-protein phosphatase 2A 65 kDa regulatory subunit A alpha isoform
6PGD	6-phosphogluconate dehydrogenase
6PGL	6-phosphogluconolactonase
A16A1	Aldehyde dehydrogenase family 16 member A1
A1AT	Alpha-1-antitrypsin
ABHEB	Alpha/beta hydrolase domain-containing protein 14B
ABRAL	Actin-binding Rho-activating protein-like
ACLY	ATP-citrate synthase
ACPH	Acylamino-acid-releasing enzyme
ACTN1	Alpha-actinin-1
ACTN4	Alpha-actinin-4
ACTZ	Alpha-centractin
ADA10	Disintegrin and metalloproteinase domain-containing protein 10
ADHX	Alcohol dehydrogenase class-3
ADP	Adenosine diphosphate
AIMP1	Aminoacyl tRNA synthase complex-interacting multifunctional protein 1
AKT	Protein kinase B
AL	Amyloid light-chain
ALDOA	Fructose-bisphosphate aldolase A
ALDOC	Fructose-bisphosphate aldolase C
ALL	Acute lymphoid leukaemia
AML	Acute myeloid leukaemia
AN32A	Acidic leucine-rich nuclear phosphoprotein 32 family member A
Ang-2/Tie-2	Angiopoietin-2 and its receptor Tie-2
ANOVA	One-way analysis of variance
ANXA2	Annexin A2
ANXA3	Annexin A3
ANXA5	Annexin A5
AP1B1	AP-1 complex subunit beta-1
APT	Adenine phosphoribosyltransferase
Apy	Apyrase
ARC1B	Actin-related protein 2/3 complex subunit 1B
ARF3	ADP-ribosylation factor 3
ARHL2	Poly(ADP-ribose) glycohydrolase ARH3
ARK72	Aflatoxin B1 aldehyde reductase member 2
ARP3	Actin-related protein 3
ARRB1	Beta-arrestin-1
AS1	Antisense RNA 1.
ASA	Aspirin
ASCT	Autologous stem cell transplantation
ASML	N-acetylserotonin O-methyltransferase-like protein
BCMA	B-cell maturation antigen
BIEA	Biliverdin reductase A
BLVRB	Flavin reductase (NADPH)
BMPC	Bone marrow plasma cells
BMSC	Bone marrow stromal cells
BPNT1	3(2),5-bisphosphate nucleotidase 1

BTK	Bruton tyrosine kinase
BTZ	Bortezomib
C1RL	Complement C1r subcomponent-like protein
CA123	Complex associated with ABC proteins protein 1
CAB39	Calcium-binding protein 39
CAH1	Carbonic anhydrase 1
CAH13	Carbonic anhydrase 13
CALM	Calmodulin
CAM-DR	Cell adhesion mediated drug resistance
cAMP	Cyclic adenosine monophosphate
CAND1	Cullin-associated NEDD8-dissociated protein 1
CAP1	Adenylyl cyclase-associated protein 1
CAPZB	F-actin-capping protein subunit beta
CASP3	Caspase-3
CATA	Catalase
CAZA1	F-actin-capping protein subunit alpha-1
CAZA2	F-actin-capping protein subunit alpha-2
CBR1	Carbonyl reductase [NADPH] 1
CCL2	C-C motif chemokine ligand 2
CCND1	Cyclin D1 gene
CCS	Copper chaperone for superoxide dismutase
CD14	Monocyte differentiation antigen CD14
CD226	CD226 antigen
CD3	cluster of differentiation 3
CD9	CD9 antigen
CDC42	Cell division control protein 42 homolog
CELMoD	Cereblon E3 ligase modulator
cGMP	Cyclic guanosine monophosphate
CID	Collision-induced dissociation
CLC1B	Clathrin light chain B
CLH1	Clathrin heavy chain 1
CLIC1	Chloride intracellular channel protein 1
CLIC4	Chloride intracellular channel protein 4
CNDP2	Cytosolic non-specific dipeptidase
CNPY2	Protein canopy homolog 2
CO2	Carbon dioxide
COF1	Cofilin-1
COPD	Coatomer subunit delta
COPG1	Coatomer subunit gamma-1
COR1A	Coronin-1A
COR1B	Coronin-1B
COTL1	Coactosin-like protein
CP	Cancer procoagulant
CRAB	Hyper-calcemia, renal failure, anaemia, bone pain
CRLF3	Cytokine receptor-like factor 3
CRS	Cytokine release syndrome
CSK	Tyrosine-protein kinase CSK
CSN4	COP9 signalosome complex subunit 4
CSN5	COP9 signalosome complex subunit 5
CXCL12	C-X-C motif chemokine ligand 12
CXCL8	C-X-C motif chemokine ligand 8
DAG	Diacylglycerol
DCTN1	Dynactin subunit 1
DCTN2	Dynactin subunit 2
DCUP	Deoxycytidylate deaminase

DDA	Data dependent acquisition
DDAH2	Dimethylarginine dimethylaminohydrolase 2
DDB1	DNA damage-binding protein 1
DEST	Destrin (Actin-depolymerizing factor)
DHAK	Bifunctional ATP-dependent dihydroxyacetone kinase/FAD-AMP lyase (cyclizing)
DHPR	Dihydropteridine reductase
DNAM-1	DNAX accessory molecule-1.
DNM1L	Dynamin-1-like protein
DOPD	D-dopachrome decarboxylase
DP13B	DCC-interacting protein 13-beta
DPP3	Dipeptidyl peptidase 3
DPYL2	Dihydropyrimidinase-related protein 2
DREB	Drebrin
DUS3	Dual specificity protein phosphatase 3
DVT	Deep vein thrombosis
ECM	Extracellular matrix
EDTA	Ethylenediaminetetraacetic acid
EF1G	Elongation factor 1-gamma
EF2	Elongation factor 2
EFNB1	Ephrin-B1
EHA	European Hematology Association
EHD1	EH domain-containing protein 1
EHD3	EH domain-containing protein 3
ELOB	Elongin-B
ELOC	Transcription elongation factor B polypeptide 1
EMAL2	Echinoderm microtubule-associated protein-like 2
ENOA	Alpha-enolase
ENOG	Gamma-enolase
ENOPH	Enolase-phosphatase E1
ERK	Extracellular signal-regulated kinase
ERP29	Endoplasmic reticulum resident protein 29
ESAM	Endothelial cell-selective adhesion molecule
ESI	Electrospray ionization
ESMO	European Society for Medical Oncology
ESYT1	Extended synaptotagmin-1
ETD	Electron transfer dissociation
EVs	Extracellular vesicles
F13A	Coagulation factor XIII A chain
FA10	Coagulation factor X
FA49B	Protein FAM49B
FA63A	Protein FAM63A
FA9	Coagulation factor IX
FAAA	Fumarylacetoacetase
FABP5	Fatty acid-binding protein, epidermal
FAS	Fatty acid synthase
FCN3	Ficolin-3
FGF-2	Fibroblast growth factor 2
FGFR3	Fibroblast growth factor receptor 3
FHL1	Four and a half LIM domains protein 1
FKB1A	Peptidyl-prolyl cis-trans isomerase FKBP1A
FKBP3	Peptidyl-prolyl cis-trans isomerase FKBP3
FN3K	Fructosamine-3-kinase
FPPS	Farnesyl pyrophosphate synthase
FUMH	Fumarate hydratase, mitochondrial

G6B	Platelet receptor Gi24
G6PD	Glucose-6-phosphate 1-dehydrogenase
GALM	Aldose 1-epimerase
GBB1	Guanine nucleotide-binding protein G(I)/G(S)/G(T) subunit beta-1
GDIA	Rho GDP-dissociation inhibitor 1
GDIB	Rho GDP-dissociation inhibitor 2 (RhoGDI beta)
GDIR2	Rho GDP-dissociation inhibitor 2
GDS1	Rho GDP-dissociation inhibitor 1
GELS	Gelsolin
GGCT	Gamma-glutamylcyclotransferase
GLGB	1,4-alpha-glucan-branching enzyme
GLO2	Hydroxyacylglutathione hydrolase
GLOD4	Glyoxalase domain-containing protein 4
GLRX3	Glutaredoxin-3
GLU2B	Glucosidase 2 subunit beta
GLYC	Serine hydroxymethyltransferase, cytosolic
GLYG	Glycogenin-1
GMFG	Glia maturation factor gamma
GNAI2	Guanine nucleotide-binding protein G(i) subunit alpha-2
GNS	N-acetylglucosamine-6-sulfatase
GoF	Gain of function
GP1BB	Platelet glycoprotein Ib beta chain
GPCR	G-protein–coupled receptors
GPIX	Platelet glycoprotein IX
GPX1	Glutathione peroxidase 1
GPX3	Glutathione peroxidase 3
GPX4	Glutathione peroxidase 4
GRAP2	GRB2-related adapter protein 2
GRB2	Growth factor receptor-bound protein 2
GSH0	Glutamate--cysteine ligase regulatory subunit
GSHB	Glutathione synthetase
GSHR	Glutathione reductase, mitochondrial
GSTM1	Glutathione S-transferase Mu 1
GSTO1	Glutathione S-transferase omega-1
GTPB2	GTP-binding protein 2
HCD	Higher-energy collisional dissociation
HDGF	Hepatoma-derived growth factor
HDHD2	Haloacid dehalogenase-like hydrolase domain-containing protein 2
HGF	Hepatocyte growth factor
HLA-G	Human Leukocyte Antigen G
HS105	Heat shock protein 105 kDa
HS90A	Heat shock protein HSP 90-alpha
HS90B	Heat shock protein HSP 90-beta
HSP71	Heat shock 70 kDa protein 1A
HSP77	Heat shock 70 kDa protein 7 (HSPA7)
HSP7C	Heat shock cognate 71 kDa protein
HSPB1	Heat shock protein beta-1
HV206	Ig heavy chain V-II region WAH
ICANS	Immune effector cell-associated neurotoxicity syndrome
IDHC	Isocitrate dehydrogenase [NADP] cytoplasmic
IDHC	Isocitrate dehydrogenase [NADP], cytoplasmic
IF4A1	Eukaryotic initiation factor 4A-I
IF4A2	Eukaryotic initiation factor 4A-II
IF6	Eukaryotic translation initiation factor 6
IFN-γ	Interferon-gamma

IGF	Insulin-like growth factor
IgG	Immunoglobin G
IgH	Immuoglobulin heavy chain
IGHD	Ig delta chain C region
ILEU	Isoleucine--tRNA ligase
ILK	Integrin-linked kinase
IMB1	Importin subunit beta-1
IMiD	Immunomodulatory drug
IMPA1	Inositol monophosphatase 1
IMWG	International myeloma working group
IP3	Inositol 1,4,5-trisphosphate
IQGA2	Ras GTPase-activating-like protein IQGAP2
ISOC1	Isochorismatase domain-containing protein 1
ITA2B	Integrin alpha-IIb
ITA6	Integrin alpha-6
ITAM	Immunoreceptor tyrosine–based activation motif
ITB3	Integrin beta-3
KAD1	Adenylate kinase isoenzyme 1
KAD2	Adenylate kinase 2, mitochondrial
KAP0	cAMP-dependent protein kinase type I-alpha regulatory subunit
KAP3	cAMP-dependent protein kinase type II-beta regulatory subunit
KAPCB	cAMP-dependent protein kinase catalytic subunit beta
KCC1A	Calcium/calmodulin-dependent protein kinase type 1
KCY	UMP-CMP kinase
KIF2A	Kinesin-like protein
KRAS	Kirsten rat sarcoma viral oncogene homolog
KV105	Ig kappa chain V-I region AG
LAG-3	Lymphocyte-activation gene 3
LAMP2	Lysosome-associated membrane protein 2
LDHA	L-lactate dehydrogenase A chain
LFQ	Label-free quantification
LGALS1	Galectin-1
LIMS1	LIM and senescent cell antigen-like domains protein 1
LIS1	Platelet-activating factor acetylhydrolase IB subunit alpha
LKHA4	Leukotriene A-4 hydrolase
lncRNA	Long non-coding RNAs
LoF	Loss of function
LOX12	Arachidonate 12-lipoxygenase
LRC59	Leucine-rich repeat-containing protein 59
LRRF2	Leucine-rich repeat flightless-interacting protein 2
LTA	Light transmission aggregometry
LV104	Ig lambda chain V-I region NIG-64
LV405	Ig lambda chain V-IV region
LXN	Latexin
LY66F	Lymphocyte antigen 6 complex locus protein G6f
MAGA4	Melanoma-associated antigen 4
MALDI	Matrix-assisted laser desorption/ionization
MAOX	NADP-dependent malic enzyme, mitochondrial
MAPK	Mitogen-activated protein kinase
MCP	Membrane cofactor protein
MDHM	Malate dehydrogenase, mitochondrial
MDSCs	Myeloid-derived suppressor cells
MGUS	Monoclonal gammopathy of unknown significance
MIF	Macrophage migration inhibitory factor
MIP-1α	Chemokine macrophage inflammatory protein-1α

MK01	Mitogen-activated protein kinase 1
ML12A	Myosin light chain 12A
MLEC	Malectin
MM	Multiple myeloma
MMECs	multiple myeloma endothelial cells
MMP-2	Matrix metalloproteinases 2
MMP-9	Matrix metalloproteinases 9
MMSET	Multiple myeloma SET domain
MOB1A	MOB kinase activator 1A
MPI	Mannose-6-phosphate isomerase
MRD	Minimal residual disease
MSCs	Mesenchymal stromal cells
MUCB	Ig mu heavy chain disease protein
MVP	Major vault protein
MYH9	Myosin-9
MYLK	Myosin light chain kinase
NAGK	N-acetyl-D-glucosamine kinase
NAMPT	Nicotinamide phosphoribosyltransferase
NF-κB	Nuclear factor kappa-light-chain-enhancer of activated B cells
NHLC2	NHL repeat-containing protein 2
NIT1	Nitrilase homolog 1
NIT2	Omega-amidase NIT2
NK	Natural killer
NKG2D	Natural Killer Group 2, member D
NO	Nitric oxide
NOS	Nitric oxide synthase
NP1L1	Nucleosome assembly protein 1-like 1
NP1L1	Niemann-Pick C1-like protein 1
NRAS	Neuroblastoma RAS viral oncogene homolog
NSCLC	Non small-cell lung cancer
NSD2	Nuclear receptor–binding SET domain protein 2
NSF1C	NSFL1 cofactor p47
NTF2	Nuclear transport factor 2
NUDT3	Diphosphoinositol polyphosphate phosphohydrolase 1
OLA1	Obg-like ATPase 1
OPG	Osteoprotegerin
$P2Y_1/P2Y_{12}$	Purinergic receptors
PA2G4	Proliferation-associated protein 2G4
PACN2	Protein kinase C and casein kinase substrate in neurons protein 2
PAGE2	P antigen family member 2
PAR	Protease-Activated Receptor
PARVB	Parvin beta
PBMCs	Peripheral blood mononuclear cells
PD-1	Programmed cell death protein 1
PD-L1	Programmed death-ligand 1
PDE5A	cGMP-specific 3',5'-cyclic phosphodiesterase 5A
PDGF	Platelet derived growth factor
PDIA1	Protein disulfide-isomerase A1
PDIA3	Protein disulfide-isomerase A3
PDLI1	PDZ and LIM domain protein 1
PDLI7	PDZ and LIM domain protein 7
PEA15	Astrocytic phosphoprotein PEA-15
PECA1	Platelet endothelial cell adhesion molecule
PEG	Polyethylene glycol

PF4	Platelet factor 4
PFD1	Prefoldin subunit 1
PFD2	Prefoldin subunit 2
PFD3	Prefoldin subunit 3
PFKAL	ATP-dependent 6-phosphofructokinase, liver type
PGAM1	Phosphoglycerate mutase 1
PGI_2	Prostacyclin
PGM1	Phosphoglucomutase-1
PGM2	Phosphoglucomutase-2
PI	Proteasome inhibitor
PI3K	Phosphoinositide 3-kinase
PI42A	Phosphatidylinositol 4-phosphate 5-kinase type I alpha
PIN1	Peptidyl-prolyl cis-trans isomerase NIMA-interacting 1
PKHL1	Fibrocystin-L
PLC	Phospholipase C
PLCG2	1-phosphatidylinositol 4,5-bisphosphate phosphodiesterase gamma-2
PLEK	Pleckstrin
PLSL	Plastin-2
PLST	Plastin-3
PNCB	Nicotinate phosphoribosyltransferase
PP2AA	Serine/threonine-protein phosphatase 2A catalytic subunit alpha isoform
PP2BA	Serine/threonine-protein phosphatase 2B catalytic subunit alpha isoform
PPCE	Prolyl endopeptidase
PPIL1	Peptidyl-prolyl cis-trans isomerase-like 1
PPM1A	Protein phosphatase 1A
PPM1F	Protein phosphatase 1F
PPP	Platelet poor plasma
PRDC1	Phosphoribosyltransferase domain-containing protein 1
PRDX1	Peroxiredoxin-1
PRDX4	Peroxiredoxin-4
PRDX5	Peroxiredoxin-5, mitochondrial
PRDX6	Peroxiredoxin-6
PRIO	Major prion protein
PROZ	Vitamin K-dependent protein Z
PRP	Platelet rich plasma
PRPS2	Ribose-phosphate pyrophosphokinase 2
PSA1	Proteasome subunit alpha type-1
PSA2	Proteasome subunit alpha type-2
PSA3	Proteasome subunit alpha type-3
PSA4	Proteasome subunit alpha type-4
PSB2	Proteasome subunit beta type-2
PSB4	Proteasome subunit beta type-4
PSB6	Proteasome subunit beta type-6
PSB7	Proteasome subunit beta type-7
PSB8	Proteasome subunit beta type-8
PSB9	Proteasome subunit beta type-9
PSD10	26S proteasome non-ATPase regulatory subunit 10
PSD11	26S proteasome non-ATPase regulatory subunit 11
PSD13	26S proteasome non-ATPase regulatory subunit 13
PSMD1	26S proteasome non-ATPase regulatory subunit 1
PSMD6	26S proteasome non-ATPase regulatory subunit 6
PSME1	Proteasome activator complex subunit 1
PSME2	Proteasome activator complex subunit 2

PTN6	Tyrosine-protein phosphatase non-receptor type 6 (SHP-1)
PTPA	Serine/threonine-protein phosphatase 2A activator
PTPRJ	Receptor-type tyrosine-protein phosphatase eta
PUR4	Phosphoribosylformylglycinamidine synthase
PUR6	Multifunctional protein ADE2
PUR9	Bifunctional purine biosynthesis protein PURH
PYGB	Glycogen phosphorylase, brain form
PYGL	Glycogen phosphorylase, liver form
PYR1	CAD protein
PZP	Pregnancy zone protein
QORX	Quinone oxidoreductase PIG3
R-ISS	Revised international staging system
RAB14	Ras-related protein Rab-14
RAB2A	Ras-related protein Rab-2A
RAB5A	Ras-related protein Rab-5A
RAC1	Ras-related C3 botulinum toxin substrate 1
RAC2	Ras-related C3 botulinum toxin substrate 2
RADI	Radixin
RANG	Ran-specific GTPase-activating protein
RANKL	Receptor activator of nuclear factor kappa-B ligand
RANKR	Receptor activator of nuclear factor kappa-B receptor
RAP1B	Ras-related protein Rap-1b
RB11B	Ras-related protein Rab-11B
RD23B	UV excision repair protein RAD23 homolog B
RENBP	N-acylglucosamine 2-epimerase
RGS10	Regulator of G-protein signaling 10
RHG01	Rho GTPase-activating protein 1
RHOA	Transforming protein RhoA
RINI	Ribonuclease inhibitor
RLA2	60S acidic ribosomal protein P2
RPE	Ribulose-phosphate 3-epimerase
RPMI	Roswell Park Memorial Institute
RUNX2	Runt-related transcription factor 2
SAA4	Serum amyloid A-4 protein
SAP (APCS)	Serum amyloid P-component
SCRN1	Secernin-1
SD	Standard deviation
SDC4	Syndecan-4
SDS-PAGE	Sodium dodecyl sulfate-polyacrylamide gel electrophoresis
SEM	Standard error of mean
SEM4A	Semaphorin-4A
SEM4D	Semaphorin-4D
SEPT02	Septin-2
SEPT06	Septin-6
SERC	Phosphoserine aminotransferase
SH3L1	SH3 domain-containing protein 1
SH3L2	SH3 domain-binding glutamic acid-rich-like protein 2
SLAMF7	Signaling Lymphocytic Activation Molecule Family Member 7
SMM	Smoldering multiple myeloma
SNAA	Alpha-soluble NSF attachment protein
SNAP	S-Nitroso-N-acetylpenicillamine
SND1	Staphylococcal nuclease domain-containing protein 1
SNHG16	small nucleolar RNA host gene 16
SORT1	Sortilin 1
SPB6	Serpin B6

SPB9	Serpin B9
SPTB2	Spectrin beta chain, non-erythrocytic 1
ST1A3	Sulfotransferase 1A3/1A4
STIP1	Stress-induced-phosphoprotein 1
STOM	Erythrocyte band 7 integral membrane protein
STXB2	Syntaxin-binding protein 2
SYAC	Alanine--tRNA ligase, cytoplasmic
SYDC	Aspartyl-tRNA synthetase, cytoplasmic
SYEP	Bifunctional glutamate/proline--tRNA ligase
SYG	Glycine--tRNA ligase
SYHC	Histidine--tRNA ligase, cytoplasmic
SYNC	Asparagine--tRNA ligase, cytoplasmic
SYSC	Serine--tRNA ligase, cytoplasmic
SYTC	Threonine--tRNA ligase, cytoplasmic
SYWC	Tryptophan--tRNA ligase, cytoplasmic
SYYC	Tyrosine--tRNA ligase, cytoplasmic
TALDO	Transaldolase
TAMs	Tumour associated macrophages
TBA1B	Tubulin alpha-1B chain
TBA4A	Tubulin alpha-4A chain
TBA8	Tubulin alpha-8 chain
TBB1	Tubulin beta-1 chain
TBB4B	Tubulin beta-4B chain
TBB5	Tubulin beta-5 chain
TBB8	Tubulin beta-8 chain
TBC13	TBC1 domain family member 13
TBCA	Tubulin-specific chaperone A
TBCB	Tubulin-folding cofactor B
TCIPA	Tumour cell-induced platelet aggregation
Tcons	Conventional T-cells
TCPA	T-complex protein 1 subunit alpha
TCPB	T-complex protein 1 subunit beta
TCPD	T-complex protein 1 subunit delta
TCPH	T-complex protein 1 subunit eta
TCPQ	T-complex protein 1 subunit theta
TCPZ	T-complex protein 1 subunit zeta
TEBP	Prostaglandin E synthase 3
TF	Tissue factor
TGF-β	Transforming growth factor-beta
THIC	Acetyl-CoA acetyltransferase, cytosolic
TIM-3	T-cell immunoglobulin and mucin-domain containing protein 3
TKT	Transketolase
TLN1	Talin-1
TNG2	TGN-site integral membrane protein 2
TPD54	Tumor protein D54
TPIS	Triosephosphate isomerase
TPM4	Tropomyosin alpha-4 chain
TPP2	Tripeptidyl-peptidase 2
Tregs	Regulatory T cells
TSN	Translin
TSN14	Tetraspanin-14
TSN9	Tetraspanin-9
TTP	Thrombocytopenic purpura
TXA2	Thromboxane A_2
TXNL1	Thioredoxin-like protein 1

UB2D2	Ubiquitin-conjugating enzyme E2 D2
UB2L3	Ubiquitin-conjugating enzyme E2 L3
UB2V1	Ubiquitin-conjugating enzyme E2 variant 1
UB2V2	Ubiquitin-conjugating enzyme E2 variant 2
UBA1	Ubiquitin-like modifier-activating enzyme 1
UBA7	Ubiquitin-like modifier-activating enzyme 7
UBE2K	Ubiquitin-conjugating enzyme E2 K
UBE2V2	Ubiquitin-conjugating enzyme E2 variant 2
UBP14	Ubiquitin carboxyl-terminal hydrolase 14
UBP5	Ubiquitin carboxyl-terminal hydrolase 5
UBS3B	Ubiquitin-associated and SH3 domain-containing protein B
UCHL3	Ubiquitin carboxyl-terminal hydrolase isozyme L3
UFC1	Ubiquitin-fold modifier-conjugating enzyme 1
UGPA	UTP--glucose-1-phosphate uridylyltransferase
URP2	Urotensin-II-related peptide
VATA	V-type proton ATPase catalytic subunit A
VEGF	Vascular endothelial growth factor
VEGFR2	Vascular endothelial growth factor receptor 2
VIME	Vimentin
VINC	Vinculin
VPS35	Vacuolar protein sorting-associated protein 35
VPS4B	Vacuolar protein sorting-associated protein 4B
VTE	Venous thromboembolism
vWF	Von Willebrand factor
WDR1	WD repeat-containing protein 1
WP	Washed platelets
XPO1	Exportin-1
XPO7	Exportin-7
XPP1	Xaa-Pro aminopeptidase 1

Chapter 1
Introduction

1.1 MULTIPLE MYELOMA

Cancer is a condition caused by over-proliferation of abnormal cells in the body. Every year, 44,000 people are diagnosed with cancer in Ireland, with around 2,000 people affected by haematological cancers [1,2].

Multiple myeloma (MM) is a bone marrow malignancy that accounts for 1% of all cancer types and for 10% of all haematological cancers. Around 380 people are diagnosed with MM each year in Ireland. It is more common in people aged 60 or older, particularly in men [3].

1.1.1 Pathogenesis and evolution of MM

MM is characterised by uncontrolled proliferation of plasma cells in the bone marrow. The expansion of these cells affects multiple organ systems, most notably, the spine, ribs, kidney, blood and brain, leading to several biochemical and clinical manifestations including hyper**C**alcemia, **R**enal failure, **A**naemia and **B**one pain due to the presence of lytic lesions (collectively referred to as the CRAB criteria) [4].

The pathogenesis of MM involves a multistep transformation process driven by genetic, epigenetic, and microenvironmental interactions. A hallmark of MM is the acquisition of cytogenetic abnormalities, including chromosomal translocations, copy number variations, and mutations in genes regulating cell cycle, survival, and genomic stability [5]. MM can be divided into hyperdiploid (characterised by multiple extra chromosomes) and non-hyperdiploid genetic subtypes. Among the latter, translocations involving the immunoglobulin heavy chain (IgH) are early clonal events and hallmark initiating lesions, occurring in nearly 40% of cases and representing a more aggressive phenotype associated with shorter survival [6]. Notably, *t(11;14)(q13;q32)* results in overexpression of cyclin D1 gene (CCND1), which promotes G1/S cell cycle progression and is often associated with lymphoplasmacytic morphology and a relatively indolent disease with favourable prognosis [7,8]. Conversely, *t(4;14)(p16;q32)* leads to upregulation of both fibroblast growth factor receptor 3 (FGFR3) and nuclear receptor–binding SET domain protein 2 (NSD2) / multiple myeloma SET domain (MMSET), the latter being a histone methyltransferase that drives oncogenic programming and is linked to a poor prognosis due to its role in chromatin remodelling and increased

proliferation, a process termed 'myelomagenesis' [9,10]. Similarly, *t(14;16)(q32;q23)* drives expression of the musculoaponeurotic fibrosarcoma (c-MAF) transcription factor, enhancing adhesion and potentially, migration and angiogenesis [11,12]

The TP53 gene, located on chromosome 17p, is a fundamental tumour suppressor governing cell cycle arrest, apoptosis, and genome integrity [13]. Mutations in this gene can result in Loss of Function (LoF) of its tumour suppressor activity or in the acquisition of Gain of Function (GoF) properties in p53, thereby acting as a tumour promoter. Its role has been studied in several types of solid tumours, including lung, pancreas, breast and ovarian cancer, among others, and is used as a biomarker for cancer risk diagnosis and prognosis [14–16]. In fact, any loss/mutation in the TP53 gene has been shown to worsen prognosis and overall survival in MM patients [17,18]. In addition, the presence of different isoforms of p53: α, β, γ, from the transactivation domain (TA), long, and short isoforms, has recently been proven to play a role in the prognosis of MM patients as well [24]. In fact, patients with low levels of the short isoforms and high levels of the β/γ TA isoforms have a worse prognosis, suggesting that this expression pattern is associated with more aggressive disease behaviour [19].

MM progression is further driven by activating mutations in key oncogenic signalling pathways, most prominently upregulating the mitogen-activated protein kinase (RAS/RAF/MAPK) and Phosphoinositide 3-Kinase (PI3K) / Protein Kinase B (AKT) pathway cascades. Mutations in Kirsten rat sarcoma viral oncogene homolog (KRAS) and Neuroblastoma RAS viral oncogene homolog (NRAS) collectively occur in approximately 40% of MM patients, while activating B-Raf proto-oncogene serine/threonine kinase (BRAF) mutations (especially V600E) are present in a smaller subset (~4–6%), resulting in sustained extracellular signal-regulated kinase (ERK) activation and uncontrolled proliferation [20,21]. Concurrently, dysregulation of the PI3K/AKT pathway contributes to increased metabolic activity, enhanced survival, and resistance to apoptosis. These mutations are often subclonal and may become diverse and evolving at relapse, further complicating MM treatment due to its heterogeneity [22].

1.1.2 Clinical stages and diagnostic criteria

MM usually begins as an asymptomatic premalignant condition known as **monoclonal gammopathy of unknown significance (MGUS),** in which an abnormal protein produced by a population of plasma cells in the bone marrow, called a monoclonal (M) protein, is found in the blood. While serum and urine M-protein levels are elevated in these patients, clinical symptoms (CRAB) are absent. According to the International Myeloma Working Group (IMWG), diagnosis of MGUS requires serum M-protein less than 3 g/dL and very low or absent in urine and clonal bone marrow plasma cells (BMPC) less than 10%. The long-term risk of progression to MM is small but persistent, averaging around 1% per year. Patients require regular clinical and analytical monitoring, but treatment is not indicated, as it provides no survival benefit [23] .

Smouldering multiple myeloma (SMM) is an intermediate, asymptomatic stage with a higher clonal burden than MGUS but no end-organ damage (no CRAB) or myeloma-defining biomarkers that meet the criteria for treatment. According to IMWG [5,6], SMM is characterized by 10–60% clonal BM plasma cells, higher serum (≥3 g/dL) and urine M-protein levels (≥500 mg/day), and carries a much higher risk of progression to active MM, of approximately 10% per year for the first 5 years, after which the risk declines [24]. However, this risk is heterogeneous across patients' cytogenetics, with some SMM patients at low risk and others at higher risk. Risk models are used to stratify clinical management [25].

The presence of myeloma-defining events (MDEs) such as any CRAB feature, or one of the IMWG biomarkers such as clonal plasma cell expansion greater than 60%, serum Free Light Chain ratio (FLC) ≥100 and/or the identification of at least one bone focal lesion 5mm in size or greater identified by Magnetic Resonance Imaging (MRI), are defining features of **active MM**. These patients are at a very high risk of progression to end-organ damage and therefore warrant treatment. **Figure 1** (a) summarises the different genetic alterations occurring during MM progression and (b) the IMWG staging criteria.

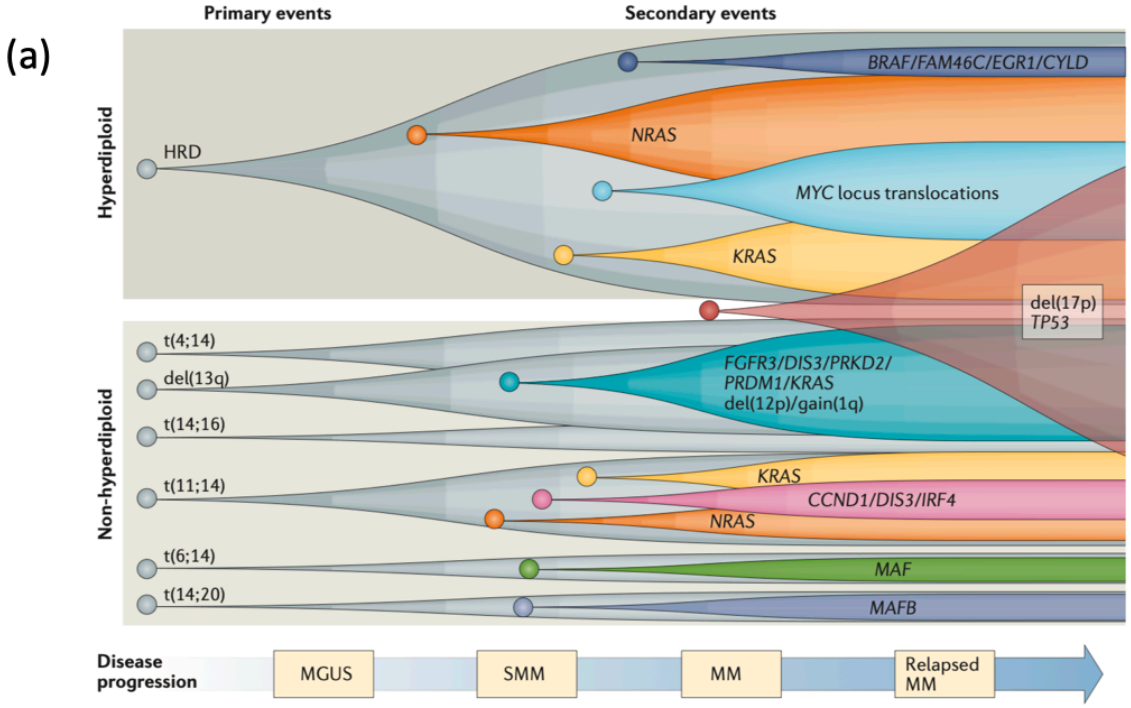

(b)

Disease stage	MGUS	SMM	Active MM
Serum M-protein	<3 g/dL	≥3 g/dL	≥1 myeloma defining events + (1) or (2): End-organ damage (CRAB): any one of • Hypercalcemia, renal insufficiency, anemia, bone lesions Biomarkers of malignancy: • ≥60% clonal BM plasma cells, • Serum involved/uninvolved free light chain ratio ≥100 • >1 focal lesion on MRI ≥5mm in size (1) Clonal bone marrow plasma cells ≥10% or (2) Biopsy proven plasmacytoma
Urine M-protein	N/A	≥500 mg/day	
% BM plasma cells	<10%	10-60%	
Myeloma defining events	Absence of myeloma defining events or amyloidosis		
Progression risk	1% per year	10% per year (1st 5y) 3% per year (next 5y)	

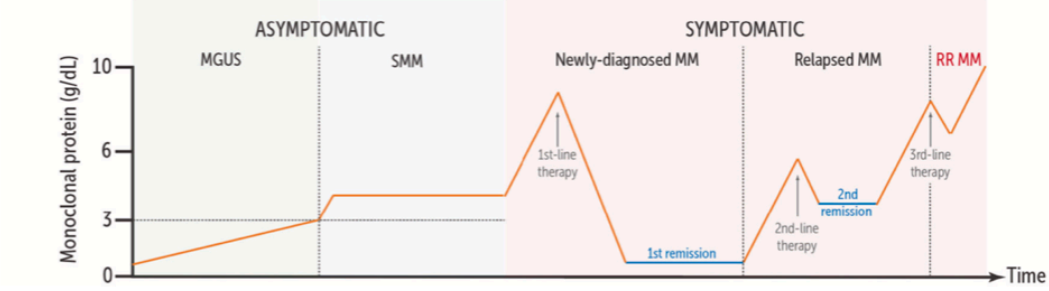

Figure 1 Genomic and Clinical Models of Clonal Evolution in Multiple Myeloma (MM). (a) Proposed model of clonal evolution in MM based on genomic events that drive clonal evolution from monoclonal gammopathy of undetermined significance (MGUS) to active MM. HRD- Hyperdiploid tumours (reproduced from Manier et al [26]) (b) Clinical model of disease progression in MM according to the IMWG criteria (Reproduced from Ho et al [27])

The clinical manifestations of MM are summarised in **Figure 2** . These manifestations include neutropenia, thrombocytopenia, anaemia and the characteristic rouleaux formation seen on peripheral blood smear. This is due to overabundance of paraproteins or M-proteins that negate the negative repelling

charges on red blood cells that lead to their aggregation in coin-like stacks [28] . Immunoparesis or the suppression of uninvolved polyclonal immunoglobulins (antibodies) in blood is fairly common resulting in immune dysfunction and recurrent infections [29]. Thrombotic complications, including deep vein thrombosis (DVT) and venous thromboembolism (VTE), arise through a pro-coagulant tumour microenvironment and elevated paraprotein-driven hyper viscosity [30]. Amyloid light-chain (AL) amyloidosis, resulting from the tissue deposition of misfolded immunoglobulin light chains, contributes to cardiomyopathy and peripheral neuropathy. Peripheral neuropathy may also be due to direct plasma cell infiltration of the nerve root and compression of the spinal cord [31].

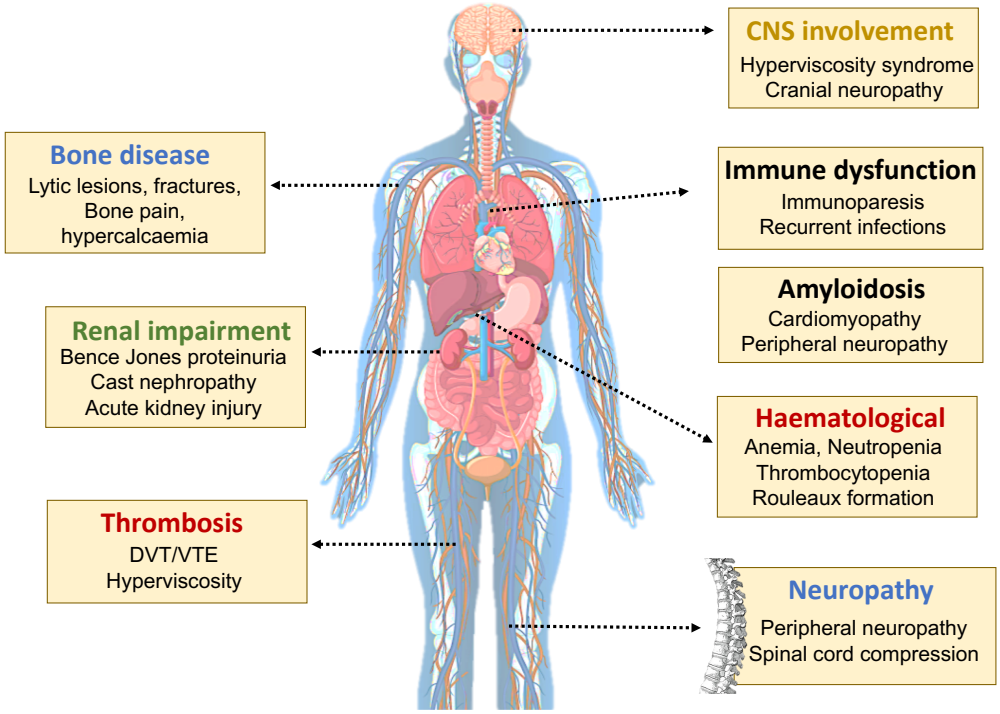

Figure 2 Systemic manifestations of multiple myeloma (MM) . Schematic overview of the major organ systems affected by MM and their associated clinical and biochemical features. DVT- deep vein thrombosis; VTE- venous thromboembolism. Figure *created using Microsoft Powerpoint.*

The Revised International Staging System (R-ISS) for MM incorporates molecular abnormalities and biochemical markers to classify MM into three prognostic stages. Table 1 summarises the key criteria, including the gradual acquisition of cytogenetic abnormalities (translocations and insertion/deletion of

chromosomes), the number of plasma cells in the bone marrow (BMPC) and lactate dehydrogenase (LDH), FLC ratio and β2 microglobulins and albumin levels in serum [32].

Table 1 Revised International Staging System (R-ISS)

R-ISS Stage	Criteria	
I	Sβ2M[1] Serum albumin Chromosomal abnormalities by iFISH[2] LDH[3]	< 3.5 mg/L ≥3.5 g/dL Standard-risk Normal (<upper normal limit)
II	Not R-ISS stage I or III	
III	Sβ2M **and either** Chromosomal abnormalities by FISH **or** LDH	≥ 5.5 mg/L *High-risk High (>upper normal limit)

[1]Sβ2M - Serum β2 microglobulin; [2] FISH- Fluorescence In-Situ Hybridization; [3]LDH lactate dehydrogenase. Reproduced from the International Myeloma Foundation [32]
*High risk is defined as: presence of del(17p) and/or translocation t(4;14) and/or translocation t(14;16)

1.1.3 Clinical management of MM

The clinical management of MM has evolved substantially over the past two decades, driven by improved understanding of disease biology, advances in risk stratification, and the development of novel therapeutic agents. Current evidence-based guidelines published by the International Myeloma Foundation, the European Haematology Association (EHA), and the European Society for Medical Oncology (ESMO) provide a structured framework for treatment decisions across the disease continuum, from newly diagnosed to relapsed and refractory MM [33,34]. These recommendations integrate results from numerous clinical trials

and real-world studies, ensuring that therapeutic strategies align with both efficacy and tolerability considerations.

For newly diagnosed patients, triplet therapy including an immunomodulatory drug (IMID) such as lenalidomide, a proteasome inhibitor (PI) such as bortezomib (BTZ), and the corticosteroid dexamethasone is preferred. Patients who are eligible subsequently proceed to autologous stem cell transplantation (ASCT), which remains a cornerstone of MM therapy due to its ability to induce deep remissions and prolong progression-free survival. For transplant-ineligible patients, dose-adjusted triplet regimens or daratumumab-based quadruplet therapies are increasingly used due to favourable tolerability profiles in older or frail individuals [35].

Disease relapse is inevitable for the majority of MM patients, and therapeutic selection in the second-line setting depends on prior treatment exposure, duration of response, cytogenetic risk profile, and patient comorbidities. Guidelines recommend alternating classes of IMiDs and PIs to overcome acquired resistance. Commonly used regimens include carfilzomib-based combinations, pomalidomide-based regimens, and daratumumab combined with either PIs or IMiDs. PI-based strategies (e.g., carfilzomib–dexamethasone) demonstrate efficacy even in BTZ-exposed patients, partly due to differential proteasome-binding kinetics [36–38].

The introduction of monoclonal antibodies has reshaped MM therapy, particularly in relapsed and refractory MM. Key agents include daratumumab (targets CD38), elotuzumab (targets SLAMF7 and enhances natural killer (NK)-cell mediated cytotoxicity) and isatuximab (anti-CD38 antibody). These antibodies are typically combined with PIs or IMiDs to enhance response depth and duration of response [39].

Over the past few years, bispecific antibodies (antibodies with two binding sites on them for different antigens or epitopes of the same antigen [40]) have shown great responses in relapsed/refractory MM patients with 1-3 prior therapies. Talquetamab is a bispecific antibody that targets the novel receptor GPRC5D (NCT04634552), which is highly expressed on plasma cells, and engages T cells via

CD3. It is marketed by Janssen under the name Talvey® and has been conditionally approved by the US-FDA and the European Commission [41]. Janssen's teclistamab (TECVAYLI®) and Pfizer's Elrexfio™ (elranatamab-bcmm) are bispecific antibodies that target the B-cell maturation antigen (BCMA) and cluster of differentiation 3 (CD3) (NCT04557098, NCT04649359) and are used in relapsed/refractory MM patients [42,43]. These bispecific agents offer substantial clinical benefit, including high rates of minimal residual disease (MRD) negativity and manageable toxicity profiles, though risks such as cytokine release syndrome (CRS) and immune effector cell-associated neurotoxicity syndrome (ICANS) require specialised monitoring [44].

Building upon the clinical success already established by bispecific antibodies, trispecific antibodies also represent a rapidly emerging frontier in the treatment of relapsed/refractory MM. Unlike bispecific antibodies, trispecific antibodies simultaneously bind to three distinct targets, in the case of JNJ-79635322 (JNJ-5322), BCMA and GPRC5D on MM cells, as well as CD3 on T-cells, with the goal of overcoming tumor heterogeneity and preventing the development of resistance. Theoretical advantages of this dual-antigen targeting include increased sensitivity, along with increased specificity and a potential reduction in toxicities due to reduced off-target binding. Phase 1 data on JNJ-79635322 in patients with relapsed or refractory MM were recently presented at the 2025 American Society of Clinical Oncology (ASCO) and European Hematology Association (EHA) meetings, where it was confirmed that among the 36 patients who received the recommended phase 2 dose, the overall response rate was 86.1%. In the 27 patients who were naive to BCMA- and GPRC5D-directed therapies, the overall response rate was 100% [45,46].

To overcome lenalidomide or pomalidomide resistance, novel agents such as cereblon E3 ligase modulators (CELMoD) are under investigation. One such agent, Mezigdomide, demonstrated an approximately 86% overall response rate and 17.5-month progression-free survival in lenalidomide-refractory patients [47].

1.1.4 MM and its microenvironment

1.1.4.1 Plasma cell development

Plasma cells develop in the bone marrow from hematopoietic stem cells through several distinct stages. During this process, they finally become IgM-expressing immature B cells. At this point, they are considered immature B lymphocytes. These cells leave the bone marrow and travel to secondary lymphoid organs such as the spleen and lymph nodes, where they complete their maturation. Upon activation, B lymphocytes can migrate into a transient structure within the secondary lymphoid organs known as the germinal centre. Inside the germinal centre, they multiply rapidly and undergo processes such as class switching and somatic hypermutation. These changes allow some cells to become long-lasting memory B lymphocytes, while others develop into plasma cells that secrete antibodies. Many plasma cells then return to the bone marrow, where they can survive for extended periods and continue to produce antibodies [48].

1.1.4.2 Interaction of myeloma cells with the bone marrow microenvironment

The development and progression of MM depend not only on intrinsic oncogenic mutations but also on dynamic interactions between malignant plasma cells and the bone marrow microenvironment. The bone marrow niche comprises cellular components consisting of mesenchymal stromal cells (MSCs) and their descendant stromal cells, osteoblasts, osteoclasts, endothelial cells, immune effector and suppressor cells, along with non-cellular components such as the extracellular matrix (ECM), extracellular vesicles (EVs) and soluble factors. Together, these elements establish a highly dynamic ecosystem that malignant plasma cells exploit to support homing, clonal expansion, drug resistance, and immune evasion. Interactions between MM and BM cells can thus occur through either direct cell-cell interaction or via soluble factors. This process ultimately promotes homing, survival, and growth of plasma cells [49].

1.1.4.2.1 Interactions with cellular components

MSCs are multipotent cells that differentiate into osteoblasts, adipocytes, fibroblasts, and chondrocytes and play a central role in maintaining bone homeostasis and supporting haematopoiesis. Research has demonstrated that MM cells profoundly alter MSC function. For instance, MM cells stimulate bone

marrow–derived MSCs to release exosomes that remodel the microenvironment, thereby fostering tumour growth and facilitating the spread of malignant plasma cells [50]. A hallmark of MM-associated bone disease is the suppression of osteoblastogenesis coupled with enhanced osteoclast activation. MM cells stimulate osteoblasts to produce receptor activator of nuclear factor kappa-B ligand (RANKL) and downregulate osteoprotegerin (OPG), leading to overstimulation of RANK and therefore osteoclast activity. MM cells also secrete the chemokine macrophage inflammatory protein-1α (MIP-1α), creating a perpetuating cycle of bone resorption and release of matrix-embedded growth factors that fuel tumour growth [51]. Furthermore, MSCs can induce BTZ resistance via cell–cell contact by directly increasing Bcl-2 expression and enhancing NF-κB activity [52,53]. Murine models have shown MSC differentiation being skewed away from its osteogenic lineage toward adipogenesis, generating adipocytes enriched in growth factors such as vascular endothelial growth factor (VEGF), insulin-like growth factor (IGF), CXCL12, and pro-inflammatory signals, promoting MM proliferation, osteoclastogenesis, chemoresistance, and immune modulation [54].

Angiogenesis is a defining feature of MM progression. Endothelial cells, isolated from MM patients, termed multiple myeloma endothelial cells (MMECs), acquire an activated phenotype, characterised by elevated secretion of pro-angiogenic mediators VEGF, fibroblast growth factor 2 (FGF-2), matrix metalloproteinases 2 and 9 (MMP-2/9), hepatocyte growth factor (HGF), angiopoietin-2 and its receptor Tie-2 (Ang-2/Tie-2), C-X-C motif chemokine ligand 8 (CXCL8/IL-8), C-X-C motif chemokine ligand 12 (CXCL12/SDF-1), and C-C motif chemokine ligand 2 (CCL2/MCP-1) [55,56]. MMECs also recruit $CD133^{+}$ endothelial progenitor cells, facilitating the formation of new blood vessels [57]. This helps to sustain tumour growth and facilitate the dissemination of MM cells.

Myeloid-derived suppressor cells (MDSCs), particularly monocytic MDSCs ($CD14^{+}$HLA-DR^low) are significantly elevated in both newly diagnosed and relapsed MM patients [58]. These cells exert potent immunosuppressive effects by inhibiting cytotoxic T-cell activation. Furthermore, a recent study in a murine model has shown that MM-derived IL-18 induced MDSC activity, suppressed T cell

response, enhancing MM progression, whereas mice lacking IL-18 showed significant protection against the progression of MM [59].

Tumour-associated macrophages (TAMs), likewise, contribute to MM progression by secreting IL-6 and IL-10 while suppressing IL-12 and TNF-α, thereby promoting cell proliferation, angiogenesis, and immunosuppression [60].

The MM microenvironment is profoundly immunosuppressed. T-cell dysfunction manifests as reduced numbers of $CD4^+$ and $CD8^+$ T cells along with increased exhaustion markers such as PD-1, LAG-3, and TIM-3 [61,62]. Regulatory T cells (Tregs), in particular $CD38^+$ Tregs, are increased early in MM, contributing to immune suppression by inhibiting cytotoxic T-cell and NK-cell activity. Ex-vivo cocultures of MM cells, peripheral blood mononuclear cells (PBMCs) and conventional T-cells (Tcons) have showed that MM cells stimulate the induction of induced Tregs or iTregs (CD38+), while targeting CD38+ with isatuximab restored Tcon cells and reduced iTREGs -induced immunosuppression, underscoring the therapeutic relevance of immune checkpoint modulation [63].

NK cells from MM patients' bone marrow aspirates show impaired cytolytic activity due to downregulation of activating receptors (e.g., NKG2D, DNAM-1) and overexpression of inhibitory receptors such as PD-1 [62]. MDSCs exacerbate this by secreting immunosuppressive factors like arginase-1 and nitric oxide, further impairing T-cell function [64]. Dendritic cells (DCs) from MM patients exhibit reduced antigen-presenting capacity due to downregulation of co-stimulatory molecules such as CD40, CD80, and CD86, thereby preventing adaptive immune response [65].

1.1.4.2.2Interactions with non-cellular components

The ECM provides essential structural and biochemical support within the bone marrow, thereby maintaining hematopoietic homeostasis. It is composed of fibrous proteins such as collagen, fibronectin, laminin, and proteoglycans and can regulate cell adhesion, migration, proliferation, and differentiation through either direct receptor-mediated signalling via integrins or by modulating the availability of cytokines and growth factors. In MM, however, this finely tuned ECM is pathologically remodelled by both malignant plasma cells and altered stromal

populations. MM cells also express MMP-2 and MMP-9 [66], which degrade key ECM components, facilitating tumour invasion and angiogenesis [67]. Moreover, MM progression is associated with altered ECM protein composition, including increased deposition of galectin-1 (LGALS1) and annexin A2 (ANXA2), which promote cell adhesion, immunosuppression, and angiogenesis [63]. These changes create a growth-permissive microenvironment and also inhibit normal immune cell infiltration and function. Furthermore, ECM components- hyaluronan and fibronectin have shown to be involved in drug resistance through different pathways, as shown in vitro using different MM cells [68]. Thus, targeting ECM components or their downstream signalling pathways holds promise for overcoming microenvironment-driven drug resistance and immune evasion in MM.

IL-6, secreted by both BMSCs and MM tumour cells [69] and IGF-1, secreted by BMSCs and osteoblasts, trigger activation of MEK/MAPK, and PI3K/Akt signalling pathway [70,71] and upregulate anti-apoptotic proteins. Clinically, elevated serum IL-6 levels are associated with a poor prognosis and reflect the proliferation fraction of MM cells within patients [72].

EVs have emerged as a third, increasingly recognised mode of intercellular communication within the MM bone marrow microenvironment. EVs, including exosomes, mediate short- and long-range signalling by delivering functional intracellular molecules and inducing epigenetic changes in recipient cells [73] transporting cargo comprising proteins, lipids, and nucleic acids, including miRNAs and lncRNAs [74]. MM cell-derived EVs remodel the bone marrow niche on multiple fronts- they enhance angiogenesis, promote osteoclast activation, and suppress osteogenesis through the transfer of lncRUNX2-AS1 to MSCs, where it represses RUNX2 expression and impairs osteoblast differentiation [75] Phenotypic profiling revealed increased expression of immune checkpoint molecules HLA-G, PD-1, and PD-L1 on MM patient-derived EVs compared to healthy controls, which suppressed T cell activation as demonstrated by reduced IFN-γ production and CD4+ T cell proliferation [76]. Additionally, exosome-mediated transfer of lncRNA SNHG16, from side population to main population of MM cells confered dexamethasone resistance [77]. In lenalidomide-resistant MM cells, EV secretion and cell adhesion abilities are significantly elevated compared

to parental drug-sensitive lines. Whole-transcriptome analysis revealed that SORT1 and LAMP2 were the key regulators of EV secretion, and silencing these genes resulted in decreased EV secretion and loss of cell adhesion in resistant cells, resulting in restored sensitivity to lenalidomide [78].

Megakaryocytes and platelets, once considered passive bystanders, are increasingly recognised as active modulators of MM progression. In the context of MM, platelets can be 'functionally reprogrammed' to support malignant plasma cell survival, immune evasion, and therapy resistance. The role of platelets in MM remains underexplored relative to stromal and immune components, warranting deeper investigation. This underlines the importance of examining the interactions between platelets and MM. The following section will explore the dynamic role of platelets in MM pathophysiology, with particular attention to their cross-talk with MM cells and thus, in the long run, their contribution to MM progression.

1.2 HAEMOSTASIS AND CANCER

1.2.1 Primary haemostasis

Thrombocytes or platelets, with a diameter of just about 3 μm, are the smallest elements in the blood. These are discoid-shaped elements in their resting state. Under electron microscopy, this discoid shape reveals a highly organised cytoskeleton composed of microtubules and actin filaments that maintain their structure. Platelets also contain α-granules, δ-granules and lysosomes (containing hydrolytic enzymes). Upon activation, platelets undergo morphological changes, including shape change to a more spherical form, extension of filopodia and lamellipodia, and degranulation, which facilitates interaction with other platelets and the endothelium [79].

Platelet activation under physiological conditions during blood vessel damage is induced by contact between exposed collagen and GPVI and GPIa/IIa platelet receptors, and by von Willebrand factor (vWF), which bridges this interaction via the GPIb/IX/V receptor complex. The activation of platelets leads to internal signalling, causing cytoskeletal organisation, shape change, and the release of their contents from δ-granules and α-granules, translocation of the P-selectin receptor (CD62P), and activation of the integrin αIIbβ3 (GPIIb/IIIa) receptor. The upregulation of P-selectin on the platelet surface allows for interactions with

leukocytes, while activation of GPIIb/IIIa enables platelet aggregation via fibrinogen, forming the initial haemostatic plug. The α-granules, 200-500 nm in diameter, mainly contain vWF, Platelet Factor 4 (PF4) and β-thromboglobulin, whereas the δ-granules, approximately 250 nm in size, contain adenosine diphosphate (ADP), serotonin, and calcium, that are released upon platelet activation. The release of granule content, together with the synthesis of thromboxane A_2 (TXA_2) and the generation of thrombin, contributes to the recruitment and activation of more platelets. Finally, soluble fibrinogen binds to the activated GPIIb/IIIa receptor, establishing bridges between platelets and forming the platelet clot [80,81]. Major platelet receptors, mediators involved in platelet activation/aggregation, and signalling pathways involved in primary haemostasis are depicted in **Figure 3**.

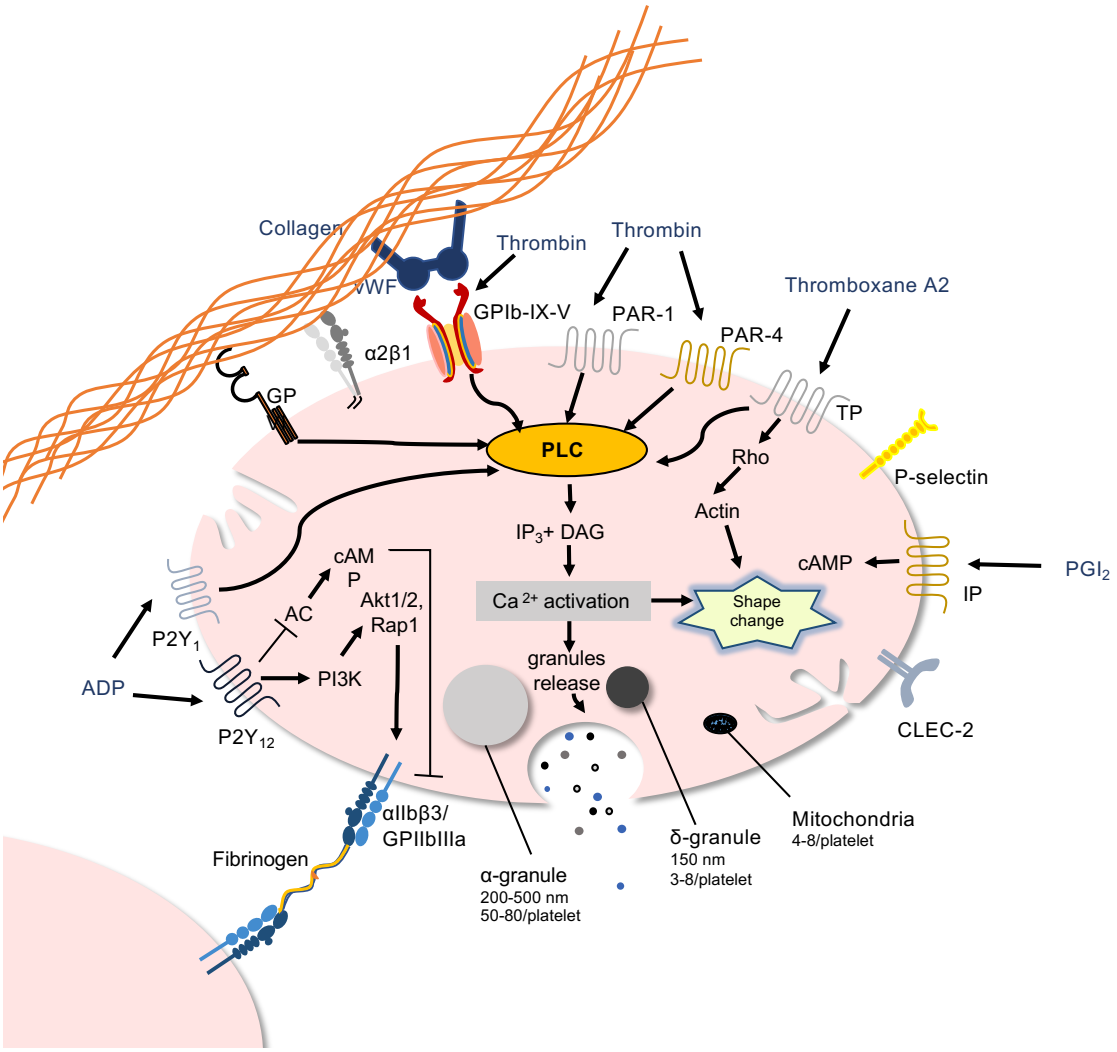

Figure 3 Primary Haemostasis. As a part of primary haemostasis, the diagram illustrates the principal receptors that regulate platelet activation, adhesion, and aggregation. G-protein–coupled receptors (GPCRs)—including thrombin (PAR1/PAR4), thromboxane A2 (TP), adenosine diphosphate (ADP) (P2Y1/P2Y12), activate intracellular signalling pathways that converge on phospholipase C (PLC). PLC generates the second messengers inositol 1,4,5-trisphosphate (IP3) and diacylglycerol (DAG), which together elevate intracellular Ca^{2+} levels and contribute to the inhibition of adenylate cyclase. These signals drive the release of contents from α-granules and δ-granules, supporting platelet activation and recruitment. Immunoreceptor tyrosine–based activation motif (ITAM)–coupled receptors, such as GPVI (the collagen receptor), initiate signalling leading to further PLC activation and intracellular Ca^{2+} mobilisation. The integrin αIIbβ3 (GPIIb/IIIa) receptor transitions from a low-affinity to a high-affinity conformation in response to inside-out signalling, enabling fibrinogen binding and promoting platelet aggregation. Additional adhesive and activating receptors include GPIb-IX-V, which mediates von Willebrand factor (VWF)–dependent adhesion under high shear, and CLEC-2, which binds podoplanin and triggers platelet activation and aggregation. *Figure created using Microsoft Powerpoint*

1.2.2 Secondary Haemostasis

Secondary haemostasis constitutes the coagulation-dependent phase of clot formation and stabilises the initially formed platelet plug by generating an insoluble fibrin network. It involves two pathways, extrinsic and intrinsic. In vivo, the extrinsic pathway primarily initiates haemostasis, whereas the intrinsic pathway primarily amplifies and sustains coagulation (not required for the initiation of haemostasis in vivo). Both pathways converge on a common pathway that activates factor X. Most coagulation factors are zymogens (inactive precursors of serine proteases) that are sequentially activated by proteolytic cleavage. Some factors require cofactors [such as factor V, factor VIII, and tissue factor (TF)] to form active enzyme complexes that efficiently propagate the coagulation cascade and generate thrombin, ultimately converting fibrinogen into insoluble fibrin.

The **extrinsic coagulation pathway** is initiated when vascular injury exposes subendothelial tissue factor (TF, factor III), which binds to circulating factor VIIa to form a high-affinity complex. Factor VII is a vitamin K–dependent zymogen, and the TF–VIIa complex catalyses the conversion of factor X to factor Xa, which functions primarily as a biochemical trigger. Activated factor Xa, together with cofactor factor Va (partially released from platelet α-granules and activated mainly by thrombin) and calcium, forms the prothrombinase complex, which converts prothrombin (factor II) into thrombin (factor IIa). The modest quantity of thrombin generated during initiation is essential because it activates platelets and several critical cofactors, namely factors V, VIII and factor XI to XIa, thereby amplifying the **intrinsic coagulation pathway** and creating a highly efficient catalytic surface on activated platelet membranes. On activated platelets, factor XI is bound to glycoprotein Ib/IX, and thrombin converts it to factor XIa, which then activates factor IX. Factor IXa, together with cofactor VIIIa and calcium, forms the intrinsic tenase complex, which efficiently activates factor X. The extrinsic tenase complex (TF–VIIa–Ca^{2+}) and intrinsic tenase complex (IXa–VIIIa–Ca^{2+}) both converge to produce factor Xa, linking the pathways. Furthermore, as part of the intrinsic coagulation pathway, XII is activated to XIIa on exposure to endothelial collagen. The surge in thrombin production catalysed by the prothrombinase complex (factor Xa, factor Va and Ca^{2+}) directly cleaves soluble fibrinogen (factor I) into fibrin monomers, which subsequently polymerise into protofibrils and

assemble into a three-dimensional fibrin network. Thrombin also activates factor XIII, which cross-links fibrin strands and antifibrinolytic proteins such as α2-antiplasmin, thereby rendering the clot mechanically stable and resistant to proteolytic degradation. Collectively, these processes transform a transient platelet aggregate into a fibrin-stabilised thrombus (**Figure 4**)[80,81].

In addition to their well-established roles in haemostasis and thrombosis, platelets play a vital and multifaceted role in vascular protection. Platelets support the semi-permeable barrier function of the resting endothelium through at least four distinct mechanisms[82]: physically blocking potential gaps in the vascular lining, promoting the proliferation and survival of endothelial cells [83], maintaining endothelial ultrastructure, and releasing soluble factors, including angiopoietin-1 [84], sphingosine-1-phosphate [85], and lysophosphatidic acid [86], that actively reduce endothelial permeability and enhance endothelial barrier function. Platelets and platelet microparticles have been shown to play a role in development of blood vessels and lymphatic vessels after vascular injury [87,88]. Platelets also protect the vasculature against inflammation. A study carried out in mice model showed that thrombocytopenic mice were highly susceptible to haemorrhage induced by inflammatory stimulus either in skin or internal organs [89]. Apart from that, platelets are also involved in cancer, as discussed in the next section [90].

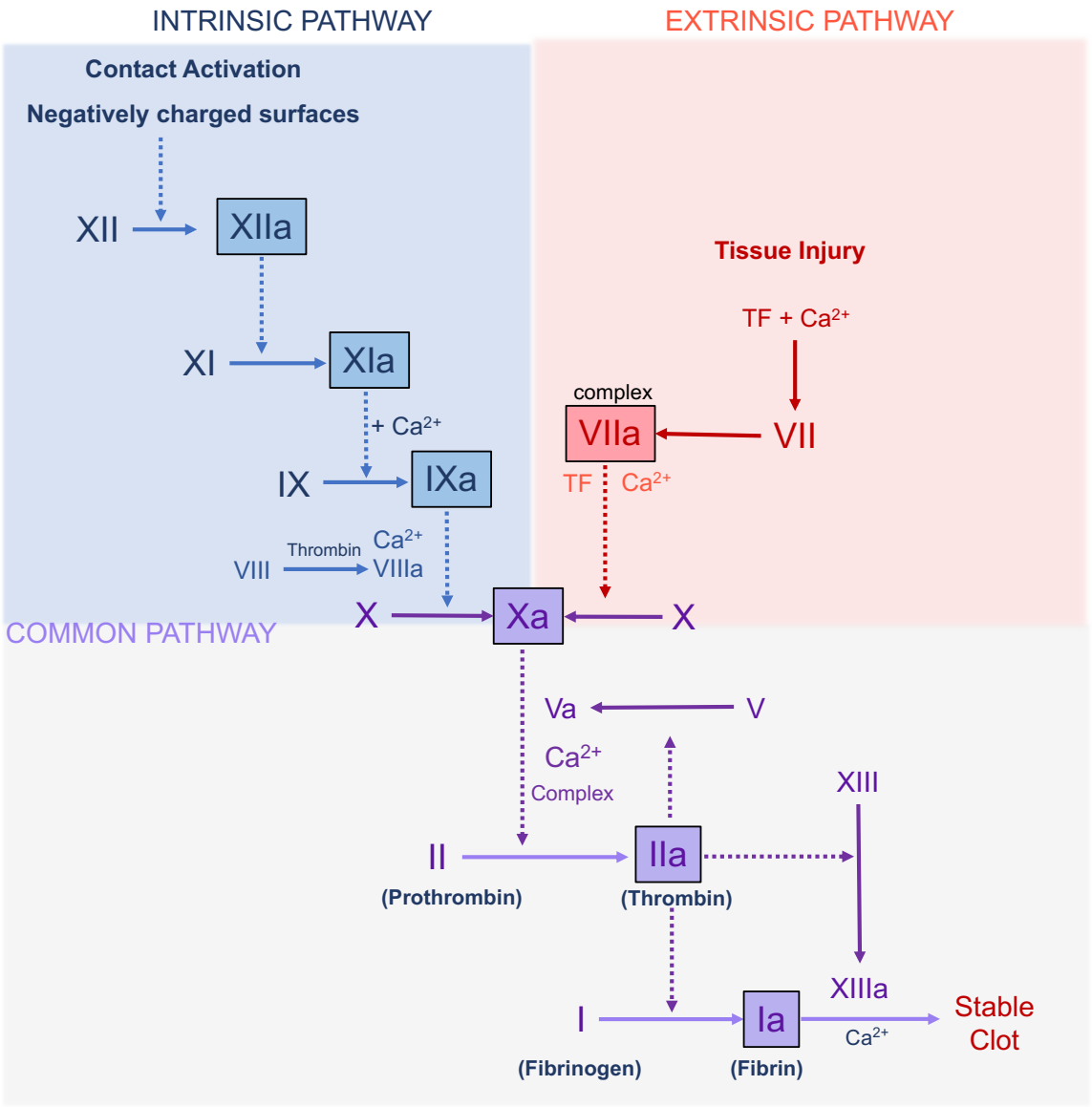

Figure 4 Secondary haemostasis. As a part of secondary haemostasis, tissue factor (TF) and exposed collagen activates clotting factors, leading to thrombin generation and conversion of fibrinogen to fibrin. Fibrin strands stabilize the primary platelet plug, forming a firm, cross-linked clot. Solid arrows indicate the conversion of a zymogen into its active form, while dashed arrows represent proteolytic activity. *Figure created using Microsoft Powerpoint.*

1.3 HAEMOSTASIS AND CANCER INTERPLAY

When cancer cells enter the vascular circulation, they encounter multiple stresses, including shear forces generated by blood flow, immune surveillance, and mechanical damage resulting from deformation within narrow capillaries and collisions with blood and endothelial cells [91]. Wood in 1953 demonstrated experimentally that tumour cells injected intravenously into a rabbit ear model adhered to capillary endothelial cells and associated with fibrin and platelets [92].

We now know that tumour cells can aggregate platelets through a phenomenon commonly called tumour cell-induced platelet aggregation (TCIPA). TCIPA confers a variety of advantages to cancer cells. When covered by platelets, tumour cells can evade immune recognition. Indeed, it has been shown that platelets protect cancer cells from TNF-α-mediated cytotoxicity [93]. Secondly, platelets surround the tumour cells, protecting them from shear stress imposed by flowing blood [94]. Moreover, platelets can help tumour cells proliferate, extravasate into nearby tissues, and avoid detachment-induced apoptosis [76], thereby promoting tumour progression and metastasis.

The interaction of cancer cells with platelets leads to the secretion of platelet factors, including ADP [95], TXA_2, transforming growth factor (TGF-β) [96], Lysophosphatidic Acid (LPA) [97], and MMP-2 [98], leading to the activation of more platelets and eventually to the promotion of TCIPA.

Studies conducted across different cancer cell lines have shown that tumour cells can release substances and express proteins/receptors on their cell membranes that can directly or indirectly affect platelet aggregation. Lung cancer cells have been shown to release thrombin, thereby activating platelets. Thrombin binds to PAR-1 and PAR-4 receptors present on platelets, promoting platelet aggregation [99]. TF has been found to be expressed in several types of cancers, like breast [100], lung [101], prostate [102] and colorectal cancer [103]. TF expression promotes cancer cell migration and angiogenesis [104,105]. Cancer procoagulant (CP) is a cysteine proteinase that directly activates factor X. CP has been found in malignant tissues, and its levels correlate with disease stage in colorectal and lung cancers [106]. CP may also play a role in angiogenesis, as demonstrated by increased VEGF and angiogenin production in MCF-7 and MDA-MB-231 breast cancer cell lines, respectively, when exposed to CP in vitro [107]. Some cancer cell lines, such as MCF7 breast carcinoma express GPIIb/IIIa and GP1b-IX-V-like receptors that may bind to vWF and facilitate metastasis [108,109]. However, in another study, Terraube et al. suggested that vWF plays a protective role by preventing metastasis, as they found that administration of B16-BL6 melanoma and Lewis lung carcinoma cells in vWF-deficient mice led to a substantial increase in metastasis compared to wild-type mice [110]. Breast cancer cell lines can release cathepsin K known to promote tumour progression and to induce platelet

activation and aggregation [111]. Cathepsin G, expressed by acute myeloid leukaemia (AML) and acute lymphoid leukaemia (ALL) cells [112], can also trigger platelet aggregation by binding to the PAR-4 receptor on platelets. It has been reported that Immunoglobin G (IgG) is released by human epithelial cancer cells [113] and can interact with platelets via the Fc receptor (FcyRIIa), thereby activating platelets [114]. Different melanoma cell lines have been shown to release ADP at varying concentrations. The cell line releasing the highest concentration of ADP induced irreversible platelet aggregation, whereas the cell line releasing the lowest concentration of ADP did not [115] .

However, some cancer cells can also secrete molecules that inhibit platelet activation and aggregation. One such agent is nitric oxide (NO). NO has been called the 'double-edged sword' [116] because it may exert both tumoricidal and tumour-promoting effects depending on its concentration, cellular source, and microenvironmental context. Activity of nitric oxide synthase (NOS), the enzyme responsible for catalysing the conversion of L-arginine to NO, has been found in various types of cancer tissues, including breast [117,118], colon [119], lung [120], bladder [121], and prostate [122]. In addition to NO, ectonucleotidases such as CD39 (ecto-ADPase/ENTPDase1) can modulate platelet responses by metabolising extracellular ADP, a key agonist of platelet activation, to adenosine monophosphate (AMP), thereby reducing ADP-mediated platelet activation and aggregation. CD39 expression has been identified on tumour-associated stromal and immune cells and, in some malignancies, on tumour cells themselves, including haematological cancers such as chronic lymphocytic leukaemia [123,124]. Furthermore, platelet–tumour cell interactions have been shown to induce CD39 expression in tumour cells, suggesting a feedback mechanism whereby tumour cells may locally attenuate platelet activation [125]. The subsequent conversion of AMP to adenosine by CD73 further contributes to an anti-aggregatory environment, as adenosine suppresses platelet activation via P1 receptor signalling [126]. Collectively, these findings indicate that although tumour cells predominantly promote platelet activation, selected tumour-derived mediators, such as NO and ectonucleotidases, can, under specific conditions, counteract platelet activation and modulate TCIPA.

Potential interactions between tumour cells and platelets are depicted in **Figure 5.**

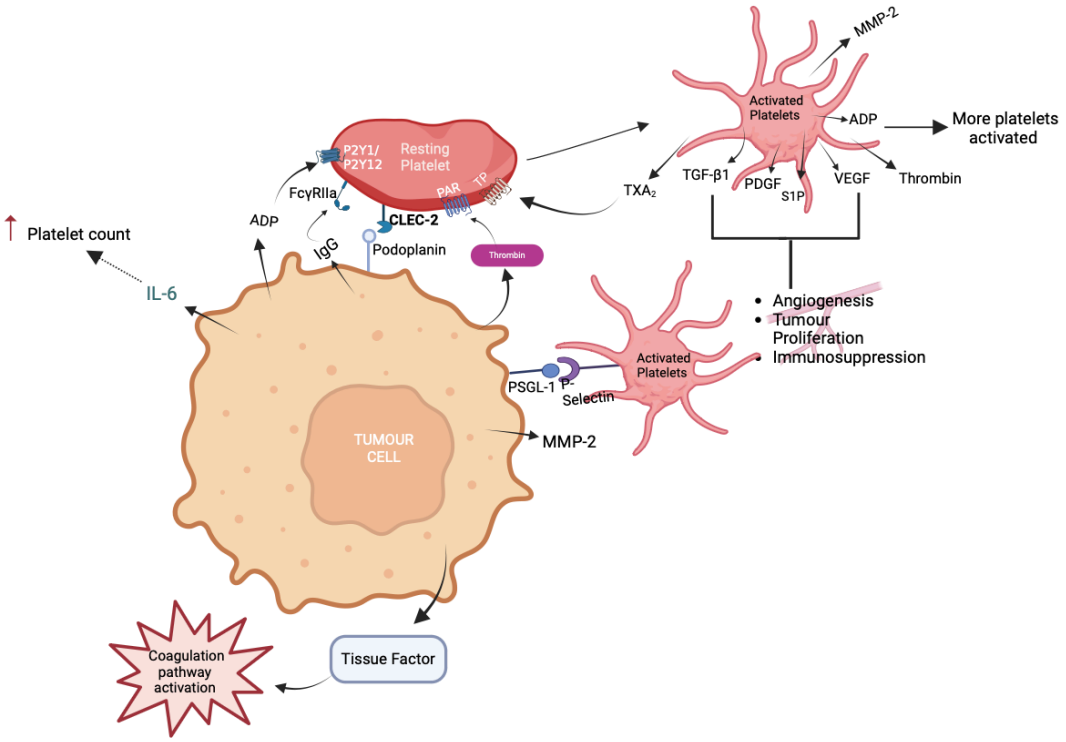

Figure 5 Interaction between platelets and tumour cells. Tumour cells are known to release molecules like MMP-2, ADP, IgG, thrombin and IL-6. MMP-2 plays a crucial role in metastasis and TCIPA, as it co-localises with the GPIIb/IIIa receptor and activates platelets. ADP and thrombin released by the tumour cells bind to the P2Y1/P2Y12 and the PAR receptors, respectively, on the platelet membrane, activating them. IL-6, released by some tumour cells, has shown to increase platelet count by increasing thrombopoietin production. Tumour cells also release Tissue Factor, which is correlated with poor prognosis, platelet activation, angiogenesis, and high metastatic potential. During activation and subsequent aggregation, platelets release several factors, including TGF-β1, PDGF, S1P and VEGF, that promote angiogenesis and tumour proliferation. In addition to these, platelets also release ADP, MMP-2, TXA2 and produce thrombin on their surface, activating more platelets. MMP-2: Matrix Metalloproteinase-2; ADP: Adenosine Diphosphate; IgG: Immunoglobulin G; IL-6: Interleukin-6; TCIPA: Tumour Cell-Induced Platelet Aggregation; PAR: Protease-Activated Receptor; TGF-β1: Transforming Growth Factor β1; PDGF: Platelet Derived Growth Factor; S1P: Sphingosine-1-phosphate; VEGF: Vascular Endothelial Growth Factor; TXA2: Thromboxane A2. *Image created using BioRender*

1.3.1 Platelets in Haematological Malignancies

Though platelet-tumour interactions are extensively studied in solid tumours, there are a limited number of studies in haematological cancers, and more

specifically on MM. One of the oldest studies on patient samples with leukaemia, conducted by Cowan et al. in 1975, indicated that platelets exhibited altered structure, with excessive δ-granules and α-granules, but reduced ATP and ADP release in the presence of circulating tumour cells [108]. In early comparative studies, leukaemia and lymphoma cell lines failed to induce platelet aggregation in vitro, unlike osteogenic sarcoma cells, suggesting a distinct tumour cell-platelet interaction in blood-borne neoplasms [127].

In the case of MM, a study carried out by Takagi et al. demonstrated that several MM cell lines (KMS-11, U266, OPM-2 and H929), when co-cultured with platelets or platelet releasate (a collection of secreted factors by platelets upon activation by an agonist, in this case, thrombin receptor activating peptide), led to enhanced cell proliferation. When OPM-2 cells pre-exposed to platelets were injected into mice, increased tumour engraftment was observed. Takagi et al. attributed this effect to IL-1β upregulation, as the use of IL-1β OPM-2 knockout cells abrogated tumour engraftment [128]. MM cells have also been shown to release TNF-α [129], which is a potent platelet activator [130] that can promote tumour progression [131] but also induce cell death [132]. Impaired platelet activation as evaluated by P-Selectin expression in response to several agonists, including collagen, ADP, epinephrine, and PAR-1 activating peptide, has been observed in platelets from active MM patients [133]. However, in another study, significant differences in P-selectin expression were not found between healthy donors and MM patients at diagnosis [134]. Myeloma cells have been observed to produce IL-6 [135] that, apart from inhibiting their apoptosis [136] and increasing RANKL [137], can also increase platelet count by increasing thrombopoietin production [138].

1.3.2 Platelets in MM Clinical Context

Several studies have reported elevated platelet activation markers in MGUS and in patients with newly diagnosed MM. This is reflected in increased fibrinogen binding, P-selectin exposure, and enhanced integrin αIIbβ3 activation. These abnormalities persist even during BTZ, dexamethasone and lenalidomide treatment, indicating a pro-thrombotic tendency in those patients [139,140]. Emerging evidence indicates that MM patients exhibit reticulated platelets (RPs), or immature platelets. RP contain functional mRNA and can interact with stromal cells via ADP and P-selectin. They can therefore modify the bone marrow niche and

promote angiogenesis, thereby facilitating tumour cell extravasation. Since RPs are more reactive than active platelets, they lead to a higher thrombotic risk in MM patients, potentially contributing to disease burden and worsening prognosis [141]. In fact, VTE is commonly observed in MM. VTE can also be particularly prevalent during treatment with thalidomide and dexamethasone [142]. Rare cases of thrombocytopenic purpura (TTP) have also been reported, but these were mainly associated with chemotherapy [143].

Despite clear evidence of this pro-thrombotic state, MM and MGUS are simultaneously characterised by platelet hypo-responsivity and impaired haemostasis. For example, one study found that platelets from MGUS and MM patients showed reduced responsiveness to ADP, as indicated by lower P-selectin and PAC-1 expressio[124]pared to healthy controls [144]. Similarly, another study reported that platelets from patients with active MM showed decreased P-selectin exposure in response to multiple agonists, including collagen, ADP, epinephrine, and the PAR-1-activating peptide, relative to healthy individuals [133]. Other functional assays also show that a majority of MM patients exhibit impaired platelet secretion: approximately 60% have reduced αIIbβ3 activation, and around 67% show reduced ATP/dense granule release per platelet, particularly under stimulation, indicating a secretion deficit despite overall hyperreactivity [145].

Although less common, bleeding complications do also occur. Across multiple studies [146–149], the primary identified cause of bleeding was dysfibrinogenemia, resulting from interactions between various paraproteins and fibrinogen. Although these bleeding complications are generally not significant, they can lead to haemorrhagic shock if not properly managed. M proteins secreted by MM cells can coat the platelets or increase plasma viscosity and, thus, impair platelet aggregation [150].

A large retrospective cohort study showed that 25% of MM patients present with thrombocytopenia at diagnosis. Those exhibiting thrombocytopenia had poor overall survival [1.5 years in patients with moderate–severe thrombocytopenia (<100,000/μL); 3.7 years in patients with normal platelet counts (150,000–349,000/μL); and 2.9 years in those with thrombocytosis (≥350,000/μL)]. MM

patients with reduced platelet counts also demonstrated prolonged thrombin lag times [151].

Therefore, MM patients present a dual, seemingly paradoxical phenotype with a hypercoagulable and a hyporesponsive/bleeding-prone state. This duality underscores the complexity of platelet dysfunction in MM and highlights the need for individualised risk assessment for both thrombosis and bleeding.

1.4 MATRIX METALLOPROTEINASES AND CANCER

1.4.1 Matrix Metalloproteinases

MMPs play a pivotal role in TCIPA and tumour progression. MMPs are a family of zinc- and calcium-dependent endopeptidases that participate in the dynamic remodelling of the ECM and are essential for normal physiological processes like wound healing, angiogenesis, and tissue development. Since 1949, when the first MMPs were discovered as depolymerising enzymes, 23 types of MMPs have been identified. Based on substrate specificity, MMPs can be divided into 6 broad categories (**Table 2**) [152–154].

Table 2 Matrix metalloproteinases (MMPs) classification, their key substrates and functional role

MMP Type	Key Members	Substrates	Functional Role
Collagenases	MMP-1, -8, -13, -18	Interstitial collagen types I, II, III, IV and XI	Initiate collagen degradation
Gelatinases	MMP-2, -9	Gelatin, Collagen type IV, V, VIII, X, XI, XIV	Involved in ECM degradation, remodelling, osteogenesis, wound healing
Stromelysins	MMP-3, -10, -11	Proteoglycans, laminin, fibronectin, casein, non-helical region of collagen	Activate other MMPs, promote EMT, remodel ECM

Matrilysins	MMP-7, -26	Broad substrates, including ECM and non-ECM proteins	Cell surface protein cleavage; EMT induction; immune modulation
Membrane-type MMPs (MT-MMPs)	MMP-14,-15, -16, -17, -24,-25	ECM proteins, activate pro-MMPs	Direct pericellular proteolysis; MMP activation;
Others	MMP-12, -19, -20, -21, -22, -23, -27, -28	Variable	Tissue-specific roles
EMT: Epithelial mesenchymal transition; ECM: Extracellular matrix			

1.4.2 Matrix metalloproteinases in solid cancers

MMP overexpression and dysregulation have been implicated in nearly all stages of tumorigenesis, from invasion and metastasis to angiogenesis and immune evasion.

Gelatinases A (MMP-2) and B (MMP-9) are the most widely studied MMPs in cancer research. Invasion is an important step in cancer metastasis, including degradation of the basement membrane and stromal ECM. MMPs such as MMP-2, MMP-9, and MMP-14 play key roles in this process. MMP-2 and -9 expression levels have been shown to be significantly increased in breast cancer patients, and this overexpression was associated with higher disease grade, poor overall survival, and higher incidence of distant metastasis [155,156]. An observational study published in 2023 found a positive correlation between MMP-9 expression levels and the severity of colorectal cancer, as assessed by disease stage and histopathological grade [157].

MMPs in addition play a pivotal role in angiogenesis, a significant step in tumour progression [132]. Specifically, MMP-1 stimulates vascular endothelial growth factor receptor 2 (VEGFR2) and EC proliferation, and activates the NF-κB transcription factor in endothelial cells, thus, promoting angiogenesis [158]. Other

factors such as TNF-α and IL-8 also stimulate the synthesis of MMP-2 and MMP-9 in endothelial cells, therefore promoting angiogenesis [159] .

Furthermore, MMPs have the ability to facilitate immune cell trafficking by degrading ECM and affecting cytokine processing. For example, MMP-2 and MMP-9 have been implicated in the activation of TGF-β, a key cytokine for immune suppression and desmoplasia [160]. TNF-α can convert pro-MMP-2 into active MMP-2 in conjunction with MMP-14 or MT1-MMP [161]. In a rodent model of prostate cancer bone metastasis, MMP-7 was shown to be produced by osteoclasts at the tumour–bone interface and to cleave RANKL into a soluble form. The resulting soluble RANKL retained biological activity and promoted osteoclast activation and bone resorption, thereby contributing to prostate cancer-induced osteolysis [162]. Co-targeting MMPs may therefore be a promising avenue for the treatment of cancer. Although no MMP inhibitor has yet been approved for cancer therapy, selective agents such as andecaliximab (anti-MMP-9) did reach Phase III trials in gastric and gastroesophageal cancers, while preclinical and early-phase studies are exploring other monoclonal antibodies and engineered inhibitors targeting MMP-9 and MMP-14 [163,164].

1.4.3 Matrix metalloproteinases in MM

In MM, there is increasing evidence that suggests that MMPs, notably MMP-2 and MMP-9, play a crucial role in modifying the bone marrow microenvironment to favour tumour survival and dissemination [67]. In 1997, Barillé et al. reported that human myeloma cells express high levels of MMP-9 and that MMP-9-stromal cell coculture can induce MMP-1 and convert pro-MMP-2 into its active form, suggesting cross-talk that enhances tumour invasion and bone resorption [165]. Clinical studies in newly diagnosed MM patients have confirmed elevated bone marrow plasma levels of MMP-9 and tissue inhibitors of metalloproteinases (TIMP-1/2) compared with controls, with a higher MMP-9/TIMP-1 ratio and a correlation with advanced disease stage [166]. MM burden in a murine 5T2MM model was found to be associated with elevated expression of MMP-2 and MMP-9. Mice treatment with the non-selective MMP inhibitor, SC-964, suppressed MMP-9 activity (as measured by gelatin zymography), angiogenesis (~77 % reduction in micro vessel density), and provided a partially protective effect against osteolytic

lesions [167]. Thus, targeting MMPs in MM represents an attractive therapeutic strategy.

Various MMP inhibitors have been tested in MM cell lines and in murine models. These include a) batimastat (broad-spectrum MMP inhibitor) [168]; b) bisphosphonate-based tissue-selective MMP-2-specific inhibitors (BMMPIs) such as ML104 and ML115 [169]; and c) MT2-MMP siRNA to target MMP-15 (shown to reduce migration and proliferation of U266 myeloma cells) [170].

1.5 AIMS

The overall aim is to explore the potential role of platelet–MM interactions in MM biology and dissemination.

Chapter 2: This chapter investigates whether MM cells can induce platelet aggregation under controlled in vitro conditions—both quasi-static and static—and whether these interactions can be modulated pharmacologically. The goal is to shed light on a largely underexplored aspect of MM pathophysiology and to identify potential new therapeutic targets.

Chapter 3: To delineate whether MM cell-induced platelet aggregation is driven by direct physical contact or by secreted molecular signals. Comparative proteomic profiling was employed to identify the specific proteins responsible for the cell-line-specific effects seen in MM TCIPA.

Chapter 4: Building upon the results obtained from previous chapter, this chapter aims to understand how direct platelet-MM cell contact, along with platelets and platelet releasate as chemoattractants, may modulate the invasive and migratory potential of myeloma cells.

Chapter 5: Building upon the results from Chapter 3, the aim of this chapter is to investigate the role of platelets in therapeutic escape. Specifically, it aims to investigate whether co-incubation of MM cells with platelet- and cell-platelet secretome contributes to resistance against the proteasome inhibitor, BTZ.

Chapter 2

Multiple myeloma cell-induced platelet aggregation and its pharmacological modulation

2.1 INTRODUCTION

TCIPA describes the ability of cancer cells to aggregate platelets. This confers a variety of advantages to cancer cells, including acting as a protective shield against the sheer force of flowing blood in the vasculature and safeguarding against immune surveillance. In addition, this interaction leads to the release of numerous molecules and growth factors from platelets (as platelets aggregate), helping cancer cells proliferate and metastasise to different parts of the body. Cancer patients often present with increased platelet activation [171]. This significantly increases their risk of thrombosis, the second leading cause of death in cancer patients [172]. MM patients often experience platelet hyperactivation, even at the MGUS stage, increasing the chances of thrombosis development [139]. In parallel, MM prognosis is strongly influenced by genetic alterations. In particular, loss or mutation of TP53, a key tumour suppressor gene [13] is associated with significantly worsened clinical outcomes [17,18].

The aim of this chapter is to investigate whether MM cell lines with different p53 statuses are capable of inducing platelet aggregation under controlled in vitro conditions (quasi-static and static) and whether it is possible to pharmacologically modulate these interactions. To measure TCIPA, light transmission aggregometry (LTA) and an ultrasound wave trap were used.

2.1.1 Light transmission aggregometry

LTA is considered the gold standard to measure platelet function and platelet abnormalities in vitro. It was described by Born in 1962 [154] and is based on the principle of measuring the optical density of a platelet sample in a cuvette, continuously stirred over time, in response to platelet agonists. Upon addition of a platelet agonist, platelets are activated and begin to aggregate, resulting in a reduction in the sample's optical density, as measured by the instrument and displayed in real time as a curve on the computer screen (**Figure 6**). The time between the injection of an agonist and the initiation of platelet aggregation is called the lag phase. This method allows for real-time measurement of platelet activity by assessing both the rate of aggregation and the peak response. LTA provides accurate information on platelet function, including the rate of aggregation and the reversibility of aggregation. Therefore, it is useful for diagnosing bleeding/clotting disorders, monitoring anti-platelet therapy, testing

agonist concentrations and looking at synergism between agonists, among other applications [173].

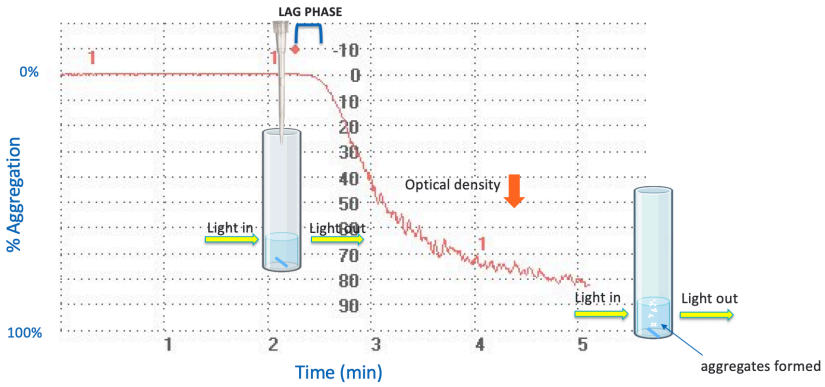

Figure 6 Principle of Light Transmission Aggregometry. The method involves detecting the optical density of a platelet sample in a cuvette under continuous stirring over time in response to platelet agonists. Platelets on their own limit the passage of light. However, when an agonist is added to the sample, platelets are activated and begin to aggregate, as shown by a decrease in optical density and an increase in light transmission. This is displayed as a real-time curve in the software. The time interval between the injection of the platelet agonist and the initiation of platelet aggregation is called the lag phase.

2.1.2 Ultrasound standing wave trap

The ultrasound wave trap (**Figure 7**) relies on the generation of an acoustic wave field in a chamber. When this wave reflects inside the chamber, it creates regions of pressure nodes (areas of minimal acoustic pressure) and antinodes (areas of maximum pressure). Particles or cells within the medium experience a net acoustic radiation force that drives them toward either the pressure nodes or antinodes, depending on their acoustic contrast factor, a function of density and compressibility relative to the medium. Cells for which the contrast factor is positive, move towards the pressure nodal plane. The arrangement of the pressure nodes is controlled by adjusting ultrasound frequency, amplitude, and the geometry of the chamber. Thus, acoustic waves can be utilised to non-invasively trap, cluster, and manipulate cells in a contact-free manner, without the need for surface adhesion or chemical binding [174].

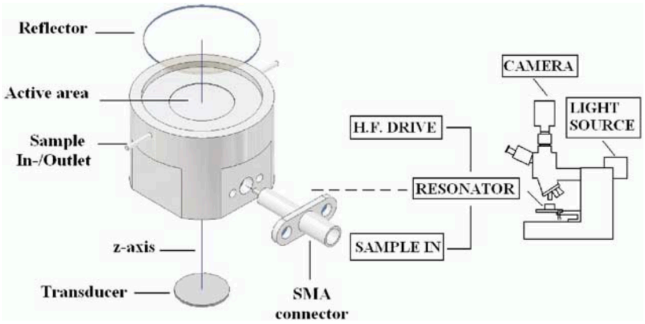

Figure 7 Schematic diagram of the ultrasound standing wave trap (Reproduced from Bazou et al., 2011 [174]) The device consists of a transducer in a housing of radial symmetry, an aqueous phase and a reflector that provides optical access to the device from above. A reflection epi-fluorescence microscope fitted with a high resolution digital camera along with an image acquisition software is used for monitoring and for capturing images.

2.1.3 Modulation of tumour cell-induced platelet aggregation

During TCIPA, platelet activation can be triggered by cell-platelet contact as well as local prothrombotic factors released by cancer cells and by platelets. For example, it has been demonstrated that both tumour cells and platelets can release ADP and thrombin, ensuing further platelet activation and aggregation. ADP acts on the purinergic receptors ($P2Y_1$ and $P2Y_{12}$) by direct signalling, causing platelet aggregation [175,176]. Thrombin can directly act on platelet receptors, PAR1 and PAR4, thereby causing platelet activation. Thrombin inhibitor, hirudin, has shown to completely inhibit TCIPA in non-small-cell lung cancer cell lines (NSCLC) [177]. Apyrase catalyses the hydrolysis of the released ADP, thus inhibiting platelet aggregation [178] and has been shown to inhibit TCIPA [174,179–181]. MMPs have also been directly involved in TCIPA, in particular MMP-1, MMP-2 and MMP-9 [182]. MMP-2 and MMP-9 have been implicated in breast cancer metastasis, tumour growth and tumour staging and thus, could be used as prognostic markers [183,184]. In addition, phenanthroline, a nonspecific MMP inhibitor that chelates the enzyme's Zn^{2+} cofactor, has been shown to modulate TCIPA in vitro [174,185]. Increased tumorigenesis and metastasis have also been associated with elevated levels of TXA_2, and breast, lung, prostate, colorectal, brain and ovarian cancer cells have been found to have an increased expression of TXA_2 synthase (TXA_2S) [186–190]. In this regard, although aspirin has failed to inhibit TCIPA in vitro at high concentrations in several investigations using different cell lines [174,191], it has inhibited metastasis via inhibition of COX-1 and preventing the increased production of TXA_2 in mice injected with platelet pre-exposed colorectal cancer cells [192]. Ethylenediamine tetra-acetic acid (EDTA) prevents platelet activation

by binding to the divalent calcium ion and acting as an effective anti-coagulant and anti-platelet agent [193] effectively inhibiting TCIPA [174]. Prostacyclin works by increasing cyclic adenosine monophosphate (cAMP) levels in platelets. It is continually released by endothelial cells and has a very short half-life (around 40s) [194]. NO is another potent antiplatelet agent, capable of increasing cyclic guanosine monophosphate (cGMP) within platelets and thereby reducing the calcium concentration required for platelet activation [185]. Both cyclic nucleotides, prostacyclin and NO donors, S-Nitroso-N-acetylpenicillamine (SNAP), have demonstrated to successfully modulate TCIPA in vitro [174,195–197].

Platelet activation pathways with their respective inhibitors with a potential effect of TCIPA is depicted in **Figure 8.**

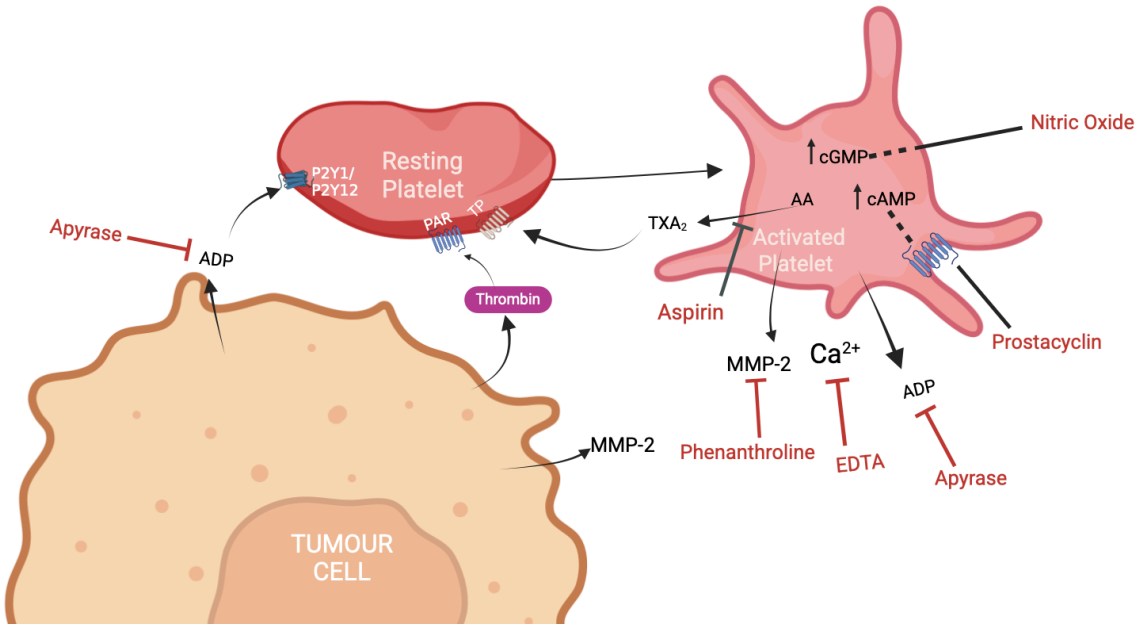

Figure 8 Potential pharmacological modulation of TCIPA. Tumour cells can release ADP, thrombin and (MMPs), in particular MMP-2, that can activate platelets and aggregate them. Once activated, platelets secrete TXA2, MMP-2, and ADP that can activate more platelets further. The platelet aggregation ability of these substances released by both the cancer cells and platelets can be inhibited by the use of Apyrase (ADP scavenger), aspirin (TXA2 inhibitor), phenanthroline (MMP inhibitor), EDTA (calcium chelator), prostacyclin (cAMP modulator) and nitric oxide (cGMP modulator). MMP- matrix metalloproteinases; ADP – Adenosine diphosphate; TXA2- Thromboxane A2; cAMP- cyclic adenosine monophosphate; cGMP- cyclic guanosine monophosphate; PAR - Protease-activated receptors; TP- thromboxane receptor; AA- arachidonic acid. *Image created using BioRender*

2.1.4 Gelatin zymography

Gelatin zymography is a highly sensitive electrophoretic technique used to assess the activity of gelatin-degrading enzymes, particularly MMP-2 (Gelatinase A) and MMP-9 (Gelatinase B), which play key roles in extracellular matrix remodelling. The method employs an SDS-PAGE gel copolymerised with gelatin as a substrate. Following electrophoresis, the gel is renatured and incubated under conditions that allow active enzymes to digest the embedded gelatine. Areas of proteolysis appear as clear bands against a stained background. The intensity of the bands in the gel correlates with the relative amount of each gelatinase in the sample, enabling qualitative and semi-quantitative evaluation of enzyme activity based on molecular weight. It has diverse applications, including studies of cancer invasion and metastasis, inflammatory diseases, and cardiovascular pathology, in which altered MMP activity is implicated [198].

2.2 METHODS

2.2.1 Reagents

All the reagents used for the methods were supplied from Sigma Aldrich, Ireland unless specified.

2.2.2 Ethical Approval, Blood Collection And, Preparation Of Washed Platelets

This study was approved by the School of Pharmacy and Pharmaceutical Sciences Research Ethics Committee from Trinity College Dublin, Ireland (2021-10-02). Blood was obtained from healthy volunteers following consent according to the Declaration of Helsinki. Whole blood (36 mL) was collected from the forearm of donors who had not been on any drugs that could affect platelet function during the previous 2 weeks, using a 21 G butterfly needle (Fisher Scientific Ltd, Ireland) attached to a 60 mL syringe. To prevent blood coagulation, blood was mixed with 10% v/v of 3.15% sodium citrate in a falcon tube and centrifuged at 250 x g for 20 min. The top-most layer, consisting of the PRP, was carefully collected and centrifuged once again at 900 x g for 10 min in the presence of prostacyclin to prevent platelet aggregation. The supernatant containing PPP was carefully removed and discarded. The pellet containing the platelets was resuspended in 5 mL of Tyrode's salts (Sigma-Aldrich, Ireland) and the concentration of WP counted

using a Z1 Beckman Coulter counter (Labplan Ltd, Ireland). The platelets were then diluted with Tyrode's salts to obtain a final concentration of 250,000 platelets/μL.

2.2.3 Cell Lines Used And Cell Culture Conditions

MM.1S (p53 wild type), U266 (p53 mutant), JJN-3 (p53 null), and KMS-27 (p53 wild type). MM cells were donated by Dr. Giada Bianchi (Dana Farber Cancer Institute, Boston, MA, U.S.A) and, Dr. Triona Ni Chonghaile (Royal College of Surgeons in Ireland, Dublin, Ireland). Gibco's Roswell Park Memorial Institute (RPMI) 1640 Medium, supplemented with 10% Fetal Bovine Serum (FBS) and 1% Antibiotic-Antimycotic (100X) (Thermo Fisher Ltd., Ireland) was used for culturing the cells that were maintained at 37°C/5% CO_2 in a cell culture incubator (GS Biotech, Medical Supply Company Ltd., UK). Cell growth and morphology were monitored daily by optical microscopy using an Olympus CKX41 (Mason Technology, Ireland) and sub-cultured when confluent.

2.2.4 Light Transmission Aggregometry

The PAP-8E Platelet Aggregometer (Bio/Data Corp., Brennan and Co., Ireland) was used for investigating the ability of MM cells to induce platelet aggregation. For this purpose, WP were prepared and allowed to rest for 60 min in order to ensure the total degradation of prostacyclin. The preservation of washed platelet's function (ability to aggregate in the presence of 2μg/mL of collagen) was always confirmed before running TCIPA experiments. Tumour cells were prepared by collecting the cells from the flasks and washing them twice and resuspending in Tyrode's salts. Cells were counted with a haemocytometer using trypan blue (0.4%) (Fisher Scientific Ltd., Ireland) as the staining dye.

MM cells were added to the WP at a concentration range of 20,000 – 2,000,000 cells/mL and their effect on platelet response was observed for 60 min. WP stirred on their own for 60 min without any agonist and cells were used as a negative control. To investigate the potential modulation of MM TCIPA, WP were incubated with different antiplatelet agents for 10 min- aspirin (150 μM); apyrase (150 μg/mL); ethylenediamine tetra-acetic acid (EDTA; 5mM); prostacyclin (100 ng/mL), phenanthroline (500 μM) or S-nitroso-N-acetylpenicillamine (SNAP; 100 μM). Then, 200,000 MM cells/mL were added to the incubated wells and their interaction with platelets was monitored for 80 min.

2.2.5 Optical Microscopy

The WP samples exposed to MM cancer cells, in the presence and absence of antiplatelet agents, were recovered after the LTA experiments and placed on a microscope slide using a cytocentrifuge. Briefly, the samples were fixed with 2% of paraformaldehyde solution, and 200 μL of the sample was cytospinned at 1,500 RPM for 10 min using a Cytospin™ 4 cytocentrifuge (ThermoFisher, UK). The slides were then visualised at 10x and 40x magnification using the Olympus BX51M reflection epi-fluorescence microscope. (Mason Technology, Ireland) and captured using the digital camera attached to it (Soft Imaging System, SIS, GmbH, Germany).

2.2.6 Ultrasound Wave Trap

The ultrasound standing wave trap used for the purpose of the experiments here, was manufactured in-house by Dr Bazou [199] and was used to monitor, in real time, the interactions between a cluster of MM cells and WP [8]. MM cells in suspension, were first introduced into the trap at a flow rate of 1 μL/min using a Gilson Minipuls 3 peristaltic pump (Anachem Ltd., UK). Under the influence of an acoustic field (2.385 MHz and 10 V) cells were allowed to levitate and form a 'cluster' for 30 min. WP were then introduced into the trap at a flow rate of 0.2 μL/min for 2 min until they formed a uniform layer around the MM cell cluster and the cluster-platelets interaction was observed for 40 min using the Olympus BX51M reflection epi-fluorescence microscope (Mason Technology, Ireland) fitted with a high resolution digital XM10 camera (Soft Imaging System, SIS, GmbH, Germany) along with the Cell D image acquisition software was used for monitoring and for capturing images during the procedure.

2.2.7 Immunoblotting (Western Blot)

Immunoblotting was carried out to confirm the presence/absence of p53 protein in the MM cell lines. The principle involves the separation of proteins based on their molecular weight and detection using specific antibodies. For this purpose, MM cells were lysed in lysis buffer (10 mM Tris, pH 7.4 100 mM NaCl, 1 mM EDTA, 1 mM NaF, 20 mM Na4P2O7, 2 mM Na3VO4, 1% TritonTM X-100, 10% glycerol, 0.1% SDS, 0.5% deoxycholate). The protein in the cell lysates was quantified using Bradford protein assay (Bio-Rad protein

assay kit II, Bio-Rad Laboratories, U.S.A). Bradford assay is a Coomassie dye-based colorimetric protein assay based on the binding of the dye to the denatured proteins in the sample and change in the absorption spectra of the sample, which can be measured at 595 nm. Following protein quantification, cell lysates containing equal amounts of protein were electrophoresed in 10% sodium dodecyl sulfate-polyacrylamide gel and then transferred to a PVDF (polyvinylidene difluoride) membrane. The membrane was incubated with p53 antibody mouse monoclonal (MA5-11296, Invitrogen, U.S.A) overnight followed by secondary antibody mouse anti-IgG (A4416, Sigma) for 1 hour at room temperature. Supersignal West Pico PLUS Chemiluminiscent substrate was used to analyse the bands using Gel Doc XR+ System (Bio-Rad Laboratories, Inc., U.S.A).

2.2.8 Gelatin Zymography

2.2.8.1 Protein quantification

Following TCIPA in the LTA, samples were centrifuged at 13,000 rpm for 5 min, and the resultant supernatant was collected. A Bradford assay (Bio-Rad, Ireland) was performed to measure the amount of protein in the samples by measuring their absorbance at 595 nm using a Fluorstar Optima microplate reader (BMG Labtech, Germany).

2.2.8.2 Electrophoresis and staining

Gels for zymography were prepared as per our research group protocol. Briefly, samples were run in 8% polyacrylamide gels co-polymerised with 2 mg/mL of bloom A gelatin for 1 hour 20 min. The gels were then washed thrice in 2.5% triton and twice in zymography buffer (50mM Tris-HCl pH 7.6, 150mM NaCl, 5mM $CaCl_2$ and 0.05% NaN_3) following electrophoresis. Gels were then incubated in zymography buffer for 6 days at 37^{o}C, to renature the enzymes, kept in staining solution (40% methanol, 10% acetic acid and 0.1% (w/v) Coomassie Blue R-250) for 3 hours to stain the gelatin, and de-stained (4% methanol and 8% acetic acid solution) for a day.

2.2.8.3 Measurement of matrix metalloproteinases activity

The intensity of the clear bands against the dark blue background was quantified using a Gel Doc XR+ System (Bio-Rad Laboratories, Inc., U.S.A). Conditioned media from HT-1080 cells stimulated with phorbol 12-myristate 13-acetate (PMA),

known to stimulate the production of gelatinases, was used as positive control for identifying the presence of MMP-2 and -9 in the gels [200].

2.2.8.4 Statistical Analysis

Data from at least 4 independent experiments were analysed with an unpaired student t-test or One-way analysis of variance (ANOVA) and Dunett's or Tukey multiple comparisons post-test when relevant, using GraphPad Prism 9 software (GraphPad Software, La Jolla, CA, U.S.A). Data are reported as mean+/-standard error of the mean (SEM). Statistical significance was considered at $p<0.05$.

2.3 RESULTS

2.3.1 Tumour cell-induced platelet aggregation: light transmission aggregometry

2.3.1.1 MM.1S cell line

MM.1S is a B cell line that expresses the p53 protein obtained from a 42-year-old patient affected with an immunoglobulin A lambda myeloma [201]. Exposure of the platelet suspension to different concentrations of cells resulted in platelet aggregation, as shown in **Figure 9 (A)**. The duration of the lag phase was inversely proportional to the cell concentration added to the sample. The lowest number of cells tested that consistently induced platelet aggregation was 20,000 cells/mL. The highest concentration of MM.1S (2,000,000 cells/mL) induced platelet aggregation in 17.4 ± 1.9 min. The presence of aggregates was corroborated by optical microscopy [**Figure 9 (C)**].

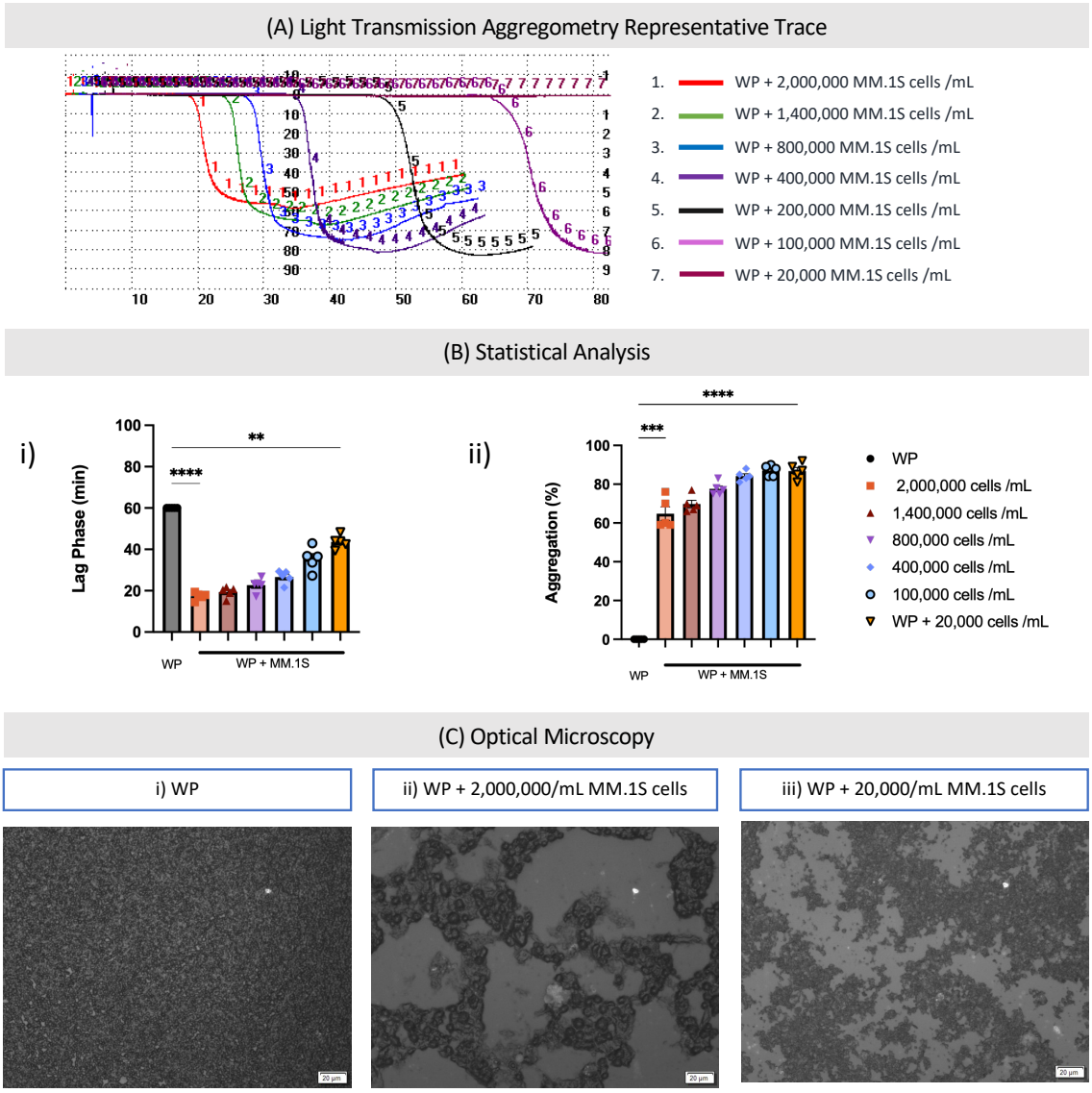

Figure 9 MM.1S cells induced platelet aggregation using LTA. (A) Representative trace from light transmission aggregometer (PAP-8E, BioData Corporation, U.S.A.) demonstrating platelet aggregation induced by MM.1S cells; (B) Statistical analysis of i) Lag phase (min) ii) Percentage of aggregation (%) after exposing platelets to varying concentrations of MM.1S cells. Data is presented as mean ± SEM; n=5; one-way ANOVA and Dunnett's post-test carried out using GraphPad Prism 9; **p<0.01; ***p<0.001 and ****p<0.0001 vs control (WP-stirring platelets); (C) Optical microscopy performed after fixing (i) WP (ii) WP exposed to 2,000,000 MM.1S cells/mL and (iii) to 20,000 MM.1S cells/ mL. Aggregates were visible against a clear background when washed platelets were exposed to MM.1S cells, whereas the control (WP- stirring platelets) showed a darker background with no visible aggregates. WP- washed platelets

2.3.1.2 KMS-27 Cell Line

KMS-27 is a cell line expressing the p53 protein. It was obtained from a 52-year-old male with plasmocytic leukaemia expressing immunoglobulin kappa antibody. When WP were exposed to KMS-27 cells at varying concentrations, the minimum number of cells required to aggregate platelets within 60 min of observation was

200,000 cells/mL. Similar to MM.1S cells, there was a decrease in the lag phase duration with the increasing number of cells, and all the concentrations tested were able to induce platelet aggregation. The presence of aggregates was corroborated with optical microscopy [**Figure 10**].

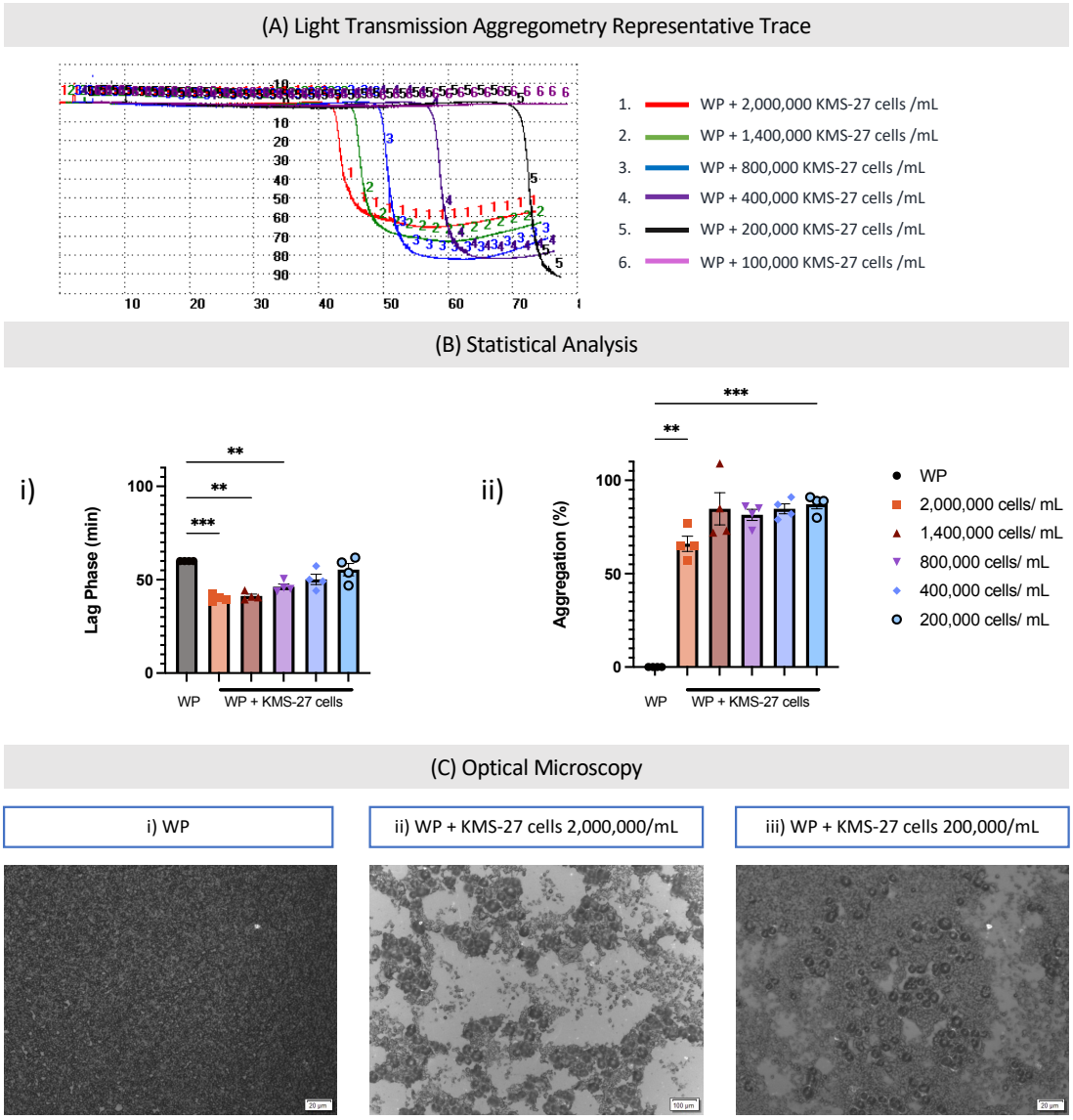

Figure 10 KMS-27 cells induced platelet aggregation using LTA. (A) Representative trace of KMS-27 cells inducing platelet aggregation using light transmission aggregometer (PAP-8E, BioData Corporation, U.S.A) (B) Statistical analysis performed on i) Lag phase (min) and ii) Percentage of aggregation after exposing WP to varying concentrations of KMS-27 cells. Data is presented as mean ± SEM; n=4; one-way ANOVA and Dunnett's post-test carried out using GraphPad Prism 9; **p<0.005 and ***p<0.001 vs control (WP- stirring platelets); (C) Optical microscopy performed after fixing (i) WP (ii) WP exposed to 2,000,000 cells/mL and (iii) 200,000 KMS-27 cells/mL. Aggregates were visible against a clear background when washed platelets were exposed to KMS-27 cells, whereas the control (WP-stirring platelets) showed a darker background with no visible aggregates. WP- Washed platelets

2.3.1.3 U266 Cell Line

U266 is a cell line with a mutant p53 protein. It was established from a 53-year-old male patient with immunoglobulin E, lambda light chain myeloma. When platelets were exposed to the p53 mutant U266 cell line at different concentrations (from 100,000 to 2,000,000 cells/mL) and monitored for 60 min, platelet aggregation occurred in only one blood donor out of six at the highest U266 cell concentrations (800,000 - 2,000,000- cells/mL) **Figure 11 (A)**. Microscopy images from the sample of the only donor, where U266 cells induced platelet aggregation, are provided in **Figure 11 (B)**, along with an image of a sample from one of the donors where U266 cells did not induce platelet aggregation.

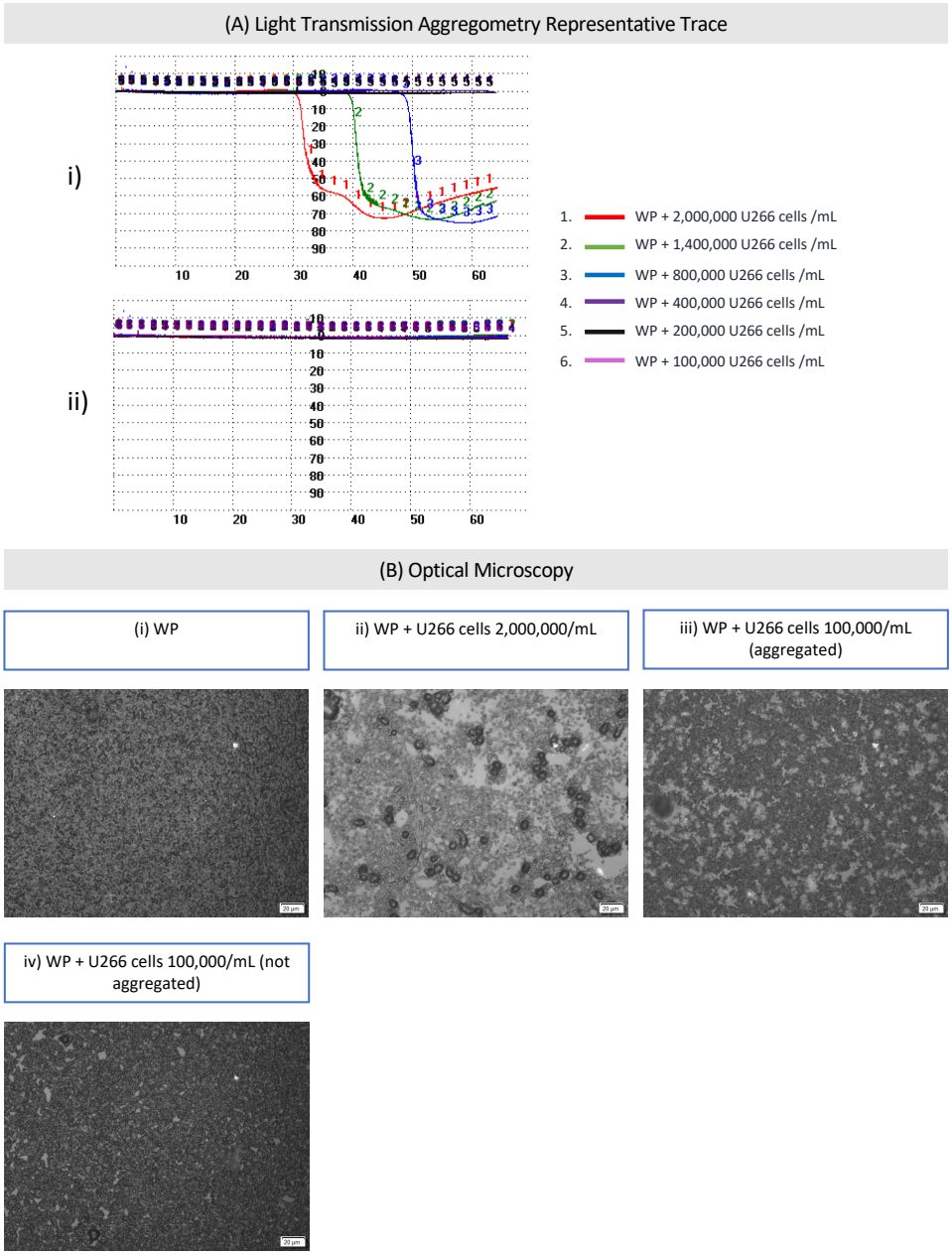

Figure 11 Effect of U266 cells on platelet aggregation. (A) Representative traces of the effect of U266 cells on platelet response using light transmission aggregometer (PAP-8E, BioData Corporation, U.S.A), observed for a time period of 60 min demonstrating i) TCIPA ii) lack of platelet aggregation at the same cell concentrations; (B) Optical microscopy performed after fixing i) WP (stirring platelets) ii) WP exposed to 2,000,000 and iii) 100,000 U266 cells/mL when U266 cells induced platelets aggregation (iv) when platelets did not aggregate after exposure to 100,000 cells/mL . Cell-platelet aggregates can be seen against a clear background with spaces between other cell-platelet aggregates whereas the control (WP-stirring platelets) showed a darker background without any aggregates. WP- washed platelets

2.3.1.4 JJN-3 Cell Line

JJN-3 is a cell line with a hemizygous deletion of TP53 and therefore does not express p53. It was established from a 57-year-old woman with plasma cell leukaemia expressing immunoglobulin A1 kappa. In this case, blood from 11 donors was used to run the experiments. Platelet aggregation was induced after exposure to the highest JJN-3 cell concentrations (2,000,000 cells/mL; 1,400,000 cells/mL; 800,000 cells/mL) and only in 6 out of the 11 platelet donors [**Figure 12 (A)** and **(B)**]. Microscopy images from one of the samples (n=6) where the platelets aggregated in the presence of JJN-3 cells are provided in **Figure 12 (C)**.

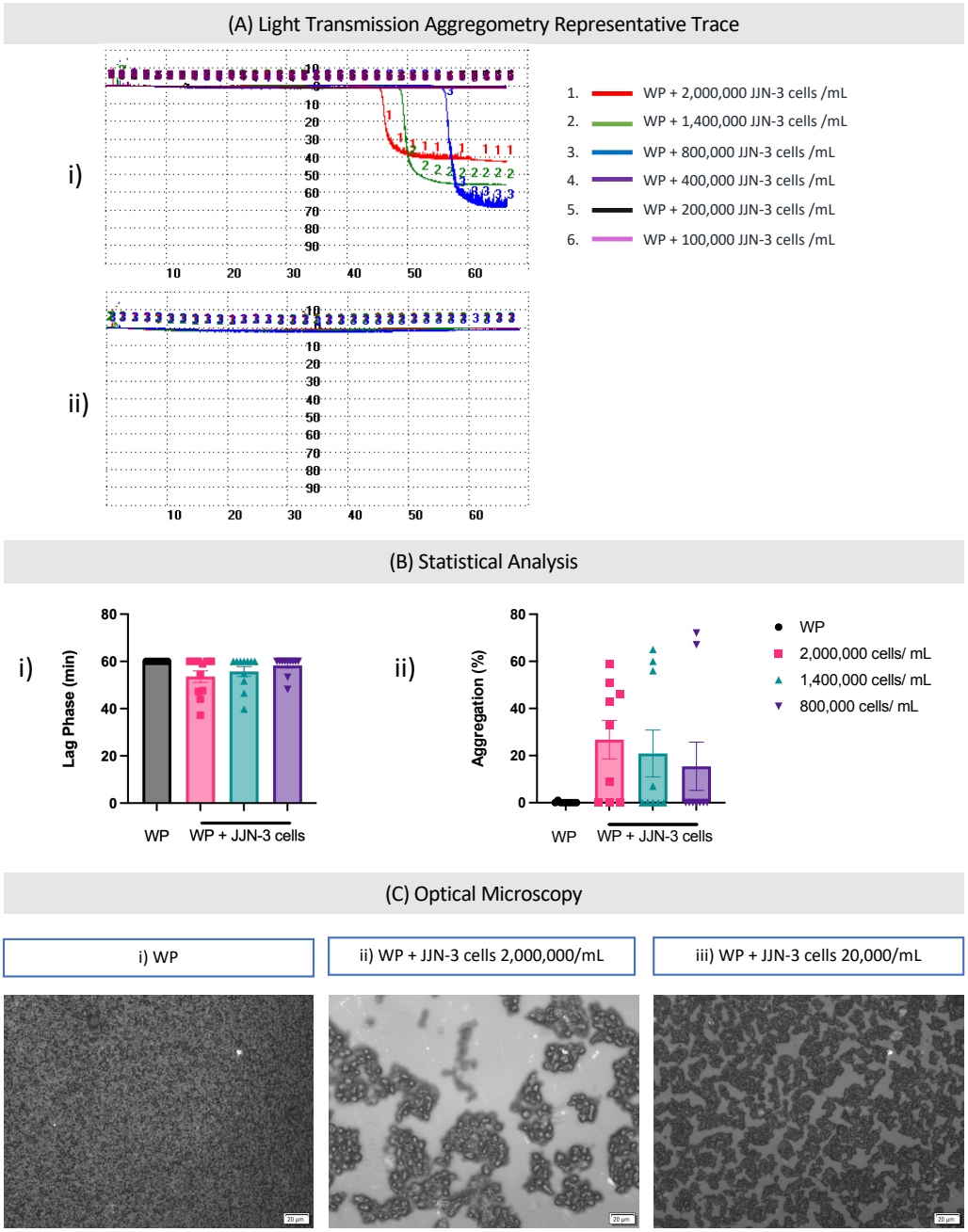

Figure 12 Effect of JJN-3 cells on platelets. (A) Representative traces of JJN-3 cells on platelet's response using light transmission aggregometer (PAP-8E, BioData Corporation, U.S.A), observed for a time period of 60 min demonstrating i) TCIPA ii) lack of platelet aggregation at the same cell concentrations; (B) Statistical analysis performed on i) lag phase (min) and ii) percentage of aggregation after exposing WP to varying concentrations of JJN-3 cells. Data is presented as mean ± SEM; n= 11; one-way ANOVA and Dunnett's post-test carried out using GraphPad Prism 9. (C) Optical microscopy performed after fixing (i) WP (stirring platelets), (ii) WP exposed to 2,000,000, and (iii) 20,000 cells JJN-3 cells/ mL. Presence of big aggregates can be seen when washed platelets were exposed to 2,000,000 JJN-3 cells /mL compared to when exposed to control (WP-stirring platelets) and 20,000 cells /mL from one of the donors where JJN-3 cells induced platelet aggregation. Cell-platelet aggregates can be seen against a clear background with spaces between other cell-platelet aggregates whereas the control (WP-stirring platelets) showed a darker background without any aggregates. WP- washed platelets

2.3.2 Drug Modulation of TCIPA

MM.1S and KMS-27 cells consistently induced platelet aggregation. Therefore, their potential modulation was investigated using different antiplatelet drugs.

2.3.2.1 Drug Modulation of MM.1S Induced platelet aggregation

Calcium chelator EDTA, cAMP modulator, prostacyclin and NO donor SNAP, were able to successfully inhibit TCIPA induced by MM.1S **Figure 13 (B)**. Although phenanthroline, a non-selective MMP inhibitor, did not inhibit TCIPA, it significantly delayed platelet aggregation compared with control (68.6 ± 5.422 min vs 50.58 ± 4.085 min). These results were corroborated by optical microscopy after sample fixation, as shown in **Figure 14**.

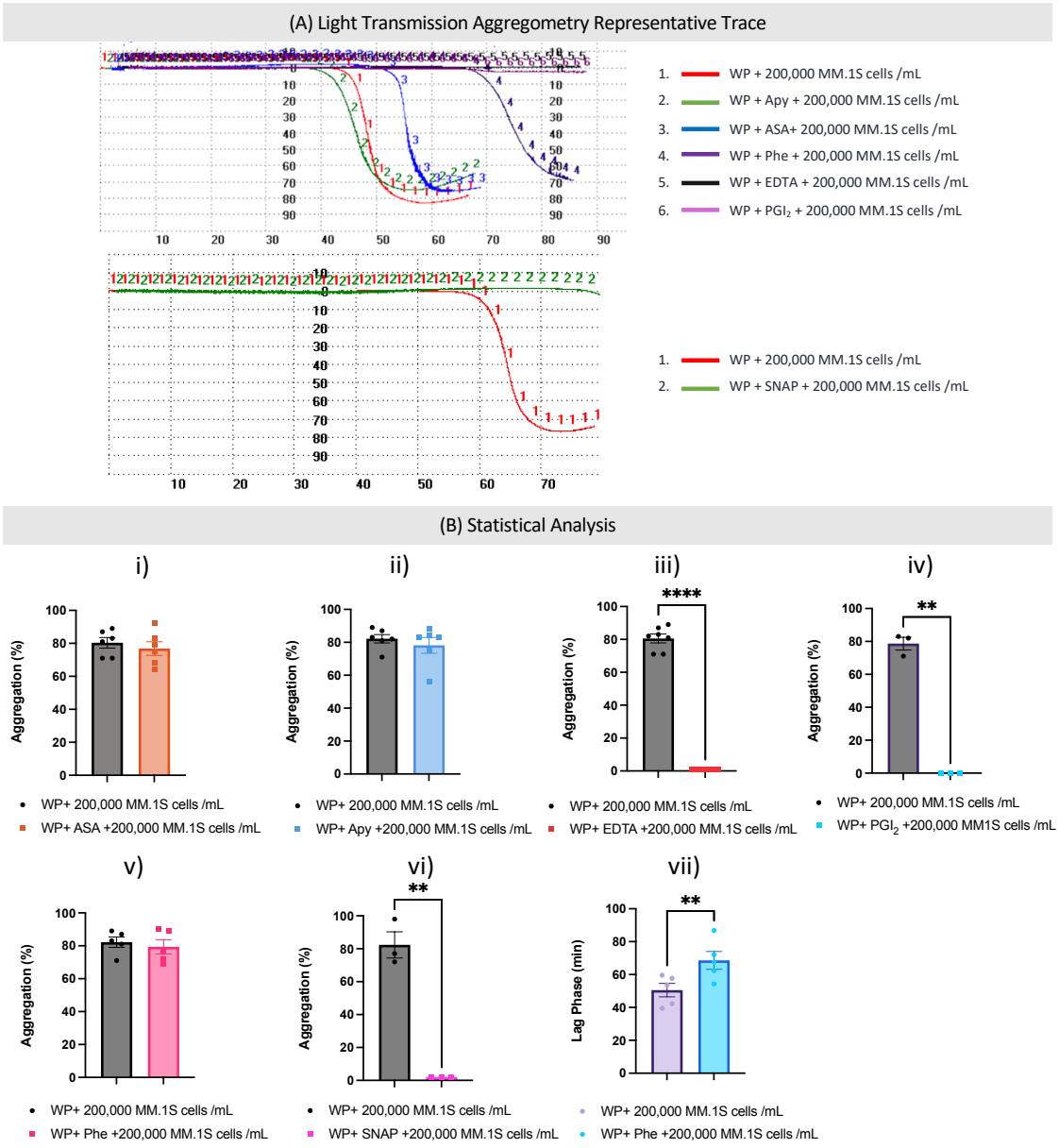

Figure 13 Modulation of MM.1S cells induced platelet aggregation. (A) Representative traces from the LTA using different anti-platelet agents. (B) Statistical analysis; Data is presented as mean ± SEM; two-tailed unpaired t-test; n≥3 ; **p<0.01; ****p<0.0001 vs control (WP+ 200,000 MM.1S cells/mL) carried out using GraphPad Prism 9. WP- Washed platelets; LTA- light transmission aggregometry; ASA- Aspirin (150 µM); Apy- Apyrase (150 µg/mL); Phe- Phenanthroline (500 µM); EDTA- Ethylenediamine tetraacetic acid (5 mM); PGI2- Prostacyclin (100 ng/mL).

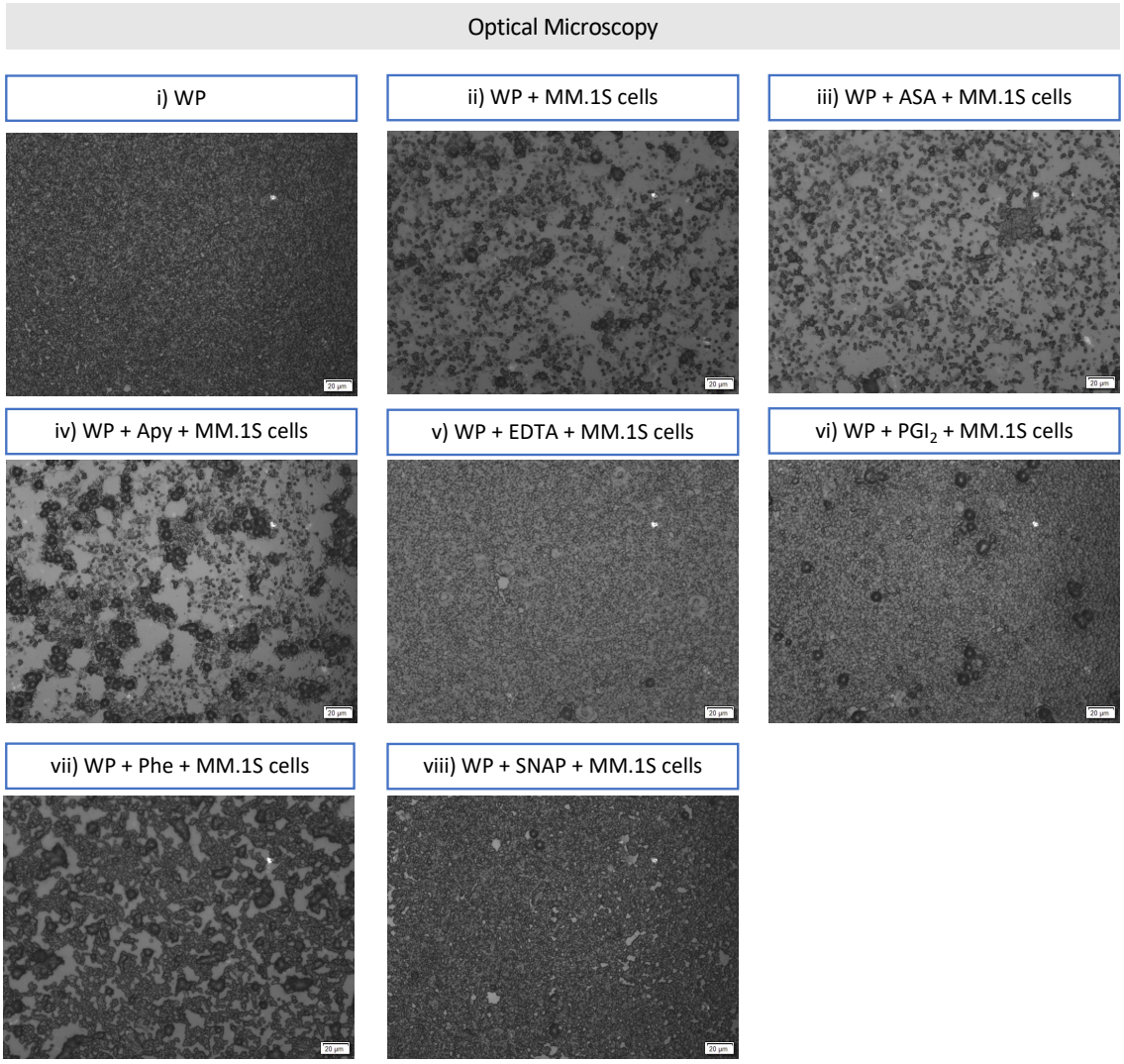

Figure 14 Optical microscopy performed after fixing WP exposed to different concentration of MM.1S cells and antiplatelet agents (i-viii). Aggregation can be seen by formation of cell-platelet aggregates against a clear background (white spaces in between) when platelets were incubated with (ii) MM.1S cells without any platelet modulator; (iii), MM.1S cells and ASA (iv) MM.1S cells and Apy and, (vii) MM.1S cells and Phe, WP- Washed platelets; LTA- light transmission aggregometry; ASA- Aspirin (150 µM); Apy- Apyrase (150 µg/mL); Phe- Phenanthroline (500 µM); EDTA- Ethylenediamine tetraacetic acid (5 mM); PGI2- Prostacyclin (100 ng/mL).

2.3.2.2 Drug Modulation Of KMS-27 Induced Platelet Aggregation

As shown in **Figure 15 (A),** all drugs tested inhibited TCIPA, suggesting the potential involvement of multiple platelet pathways (**Figure 8**) in this phenomenon. When platelets were incubated with EDTA, prostacyclin (PGI_2), phenanthroline (Phe) and SNAP, TCIPA was completely inhibited. However, although in the presence of apyrase (Apy) and aspirin (ASA), TCIPA was not completely inhibited, the percentage of aggregation was significantly reduced [apyrase (77.00%± 8.206 SD) and aspirin (73.8% ± 8.92 SD) vs control (85.8% ±

4.6 SD)]. Optical microscopy images after sample fixation are provided in **Figure 16.**

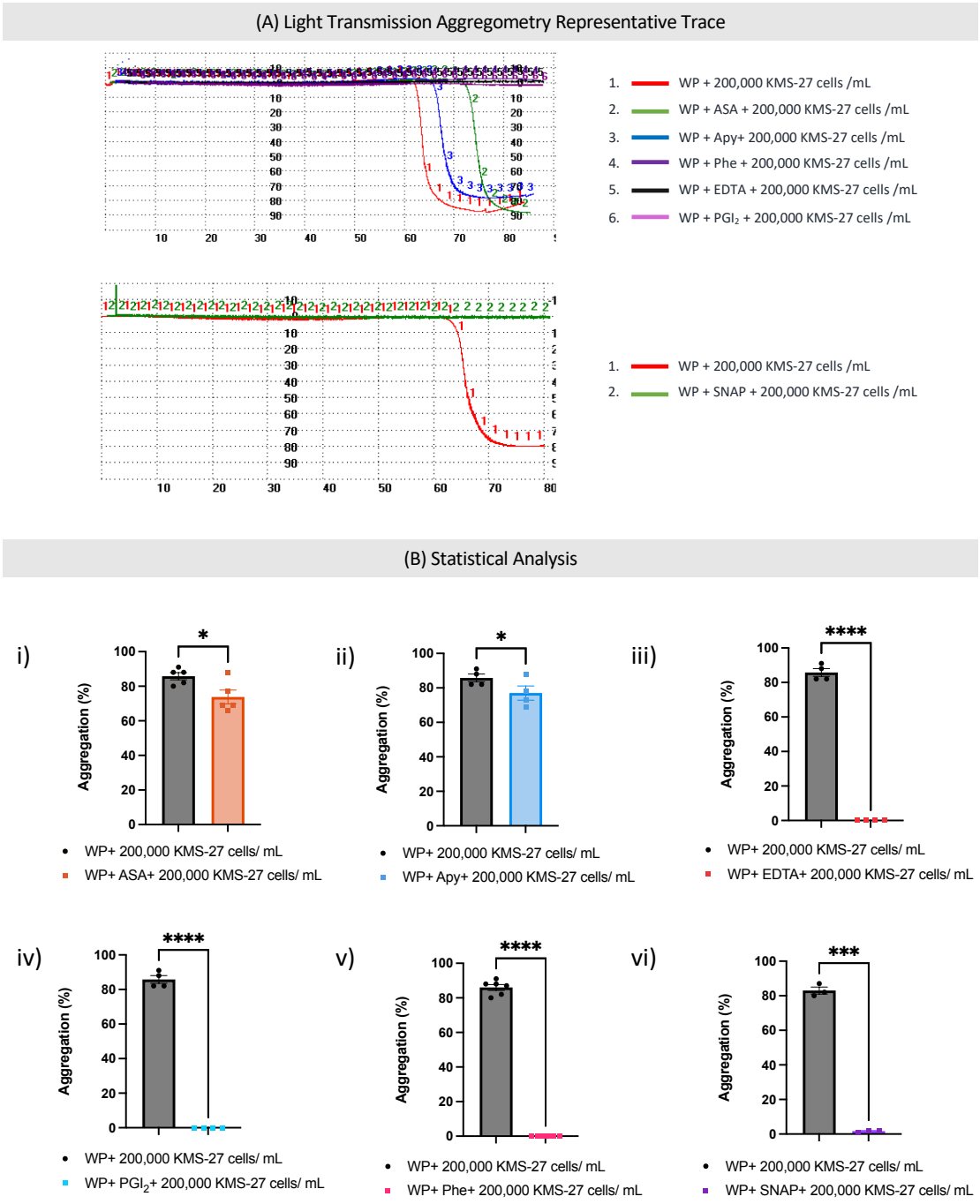

Figure 15 Modulation of KMS-27 TCIPA. (A) Representative traces of KMS-27 cells induced platelet aggregation modulated using different anti-platelet agents using light transmission aggregometer (PAP-8E, BioData Corporation, U.S.A). (B) Statistical analysis; Data is presented as mean ± SEM; n≥4; two- tailed unpaired t-test *p<0.05; ***p<0.001 ****p<0.0001 vs control (WP+ 100,000 KMS-27 cells) carried out using GraphPad Prism 9; WP- Washed platelets; ASA- Aspirin (150 µM); Apy- Apyrase (150 µg/mL); Phe- Phenanthroline (500 µM); EDTA- Ethylenediamine tetra acetic acid (5 mM); PGI2- Prostacyclin (100 ng/mL)

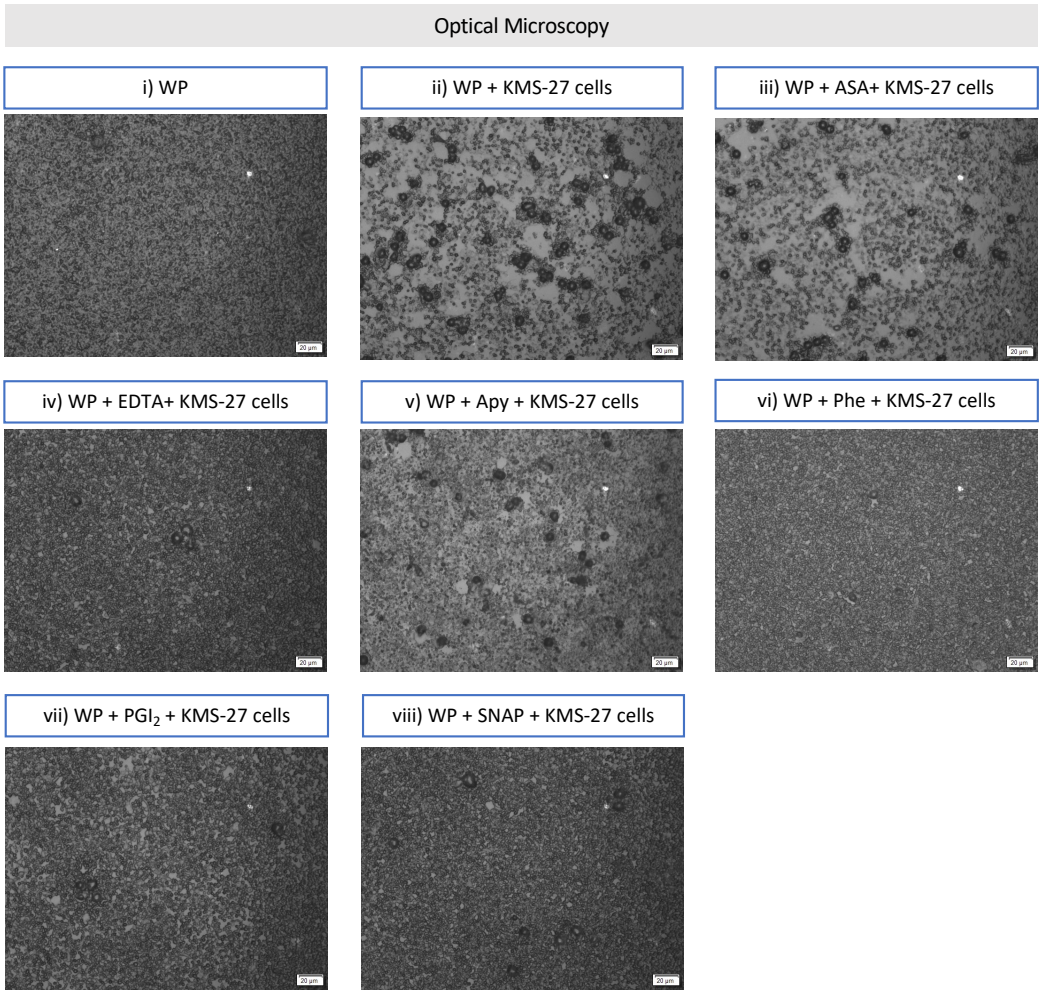

Figure 16 Optical microscopy performed after fixing the WP exposed to 200,000 KMS-27 cells/mL and different antiplatelet agents (ii-viii). Aggregation can be seen by the formation of cell-platelet aggregates against a clear background (clear spaces in between) when platelets were incubated with (ii) KMS-27 cells without any platelet modulator, (iii) KMS-27 cells and ASA and (v) KMS-27 cells and Apy. WP- Washed platelets; ASA- Aspirin (150 µM); Apy- Apyrase (150 µg/mL); Phe- Phenanthroline (500 µM); EDTA- Ethylenediamine tetra acetic acid (5 mM); PGI2- Prostacyclin (100 ng/mL)

2.3.3 Tumour cell-induced platelet aggregation: ultrasound standing wave trap

2.3.3.1 MM.1S and KMS-27 cell lines

To investigate TCIPA in real time under flowing blood conditions, an ultrasound standing-wave trap was used [174]. KMS-27 cells did not induce platelet aggregation (n=3) while MM.1S cells induced platelet aggregation within 22 ± 4.243 min (n=4) (**Figure 17**). Platelets surrounding the cluster cell, once aggregated, formed a gel-like coating that eventually broke off, taking along some

of the MM cells [**Figure 17 (i-iv)**], suggesting that they facilitate cancer cell dissemination in a similar manner.

2.3.3.2 Modulation of TCIPA by MM.1S cells using ultrasound standing wave trap

When platelets were incubated with phenanthroline and then injected into the trap, phenanthroline delayed platelet aggregation, as measured by the lag phase [**Figure 17 (vi)**]; however, this effect was not statistically significant ($p = 0.272$).

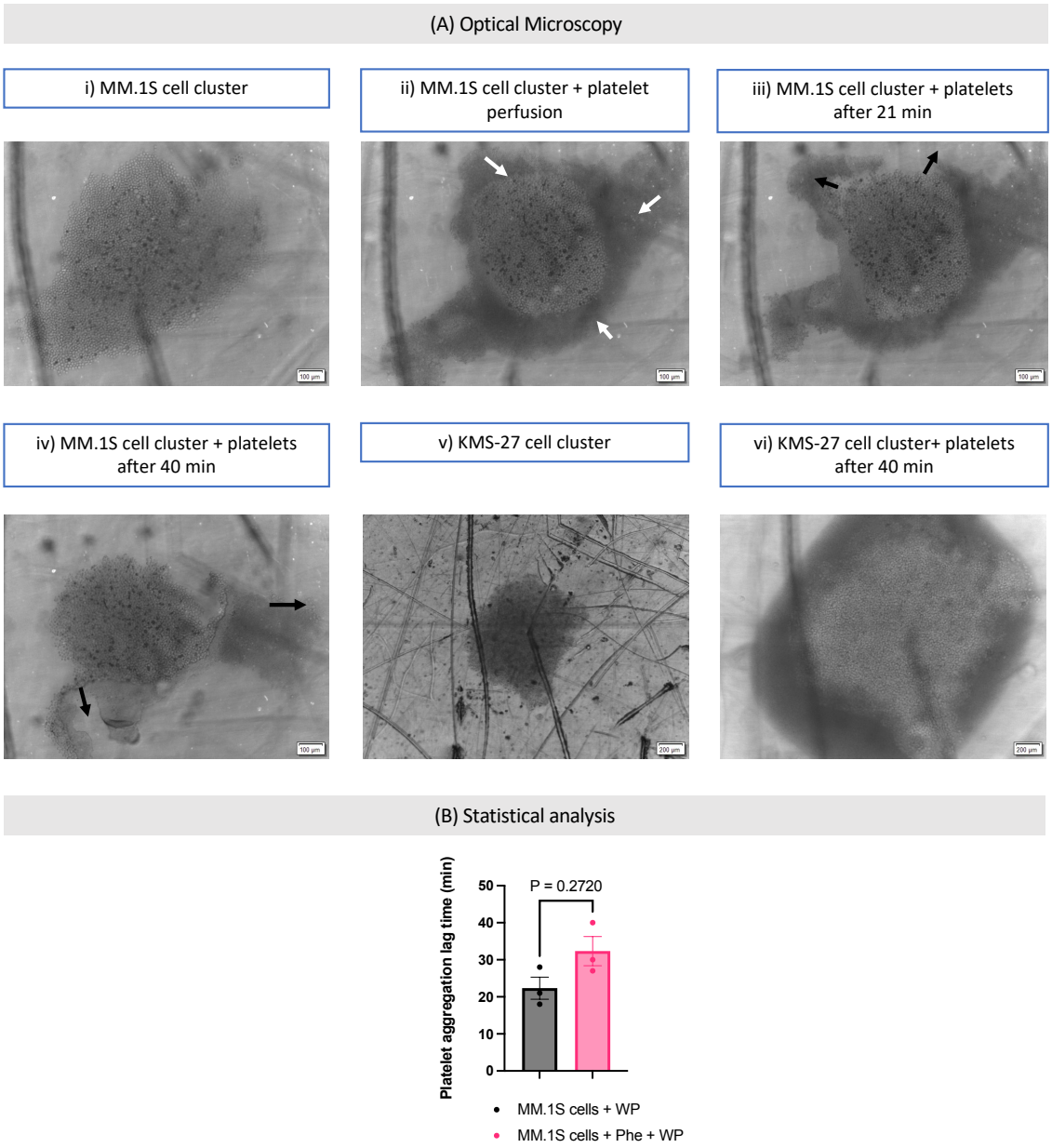

Figure 17 Investigation of TCIPA by MM.1S and KMS-27 cells using an ultrasound standing wave trap. (A) Optical microscopy i) Cluster of MM.1S; ii) Cluster of MM.1S surrounded by platelets (darker grey area); iii) Cluster of MM.1S cells 21 min post platelet perfusion showing platelet aggregation as seen by the formation of a gel-like coating (lighter grey area surrounding the cell cluster indicated by black arrows), that eventually breaks off iv) Cluster 40 min after perfusion of platelets, disrupted and completely surrounded by aggregated platelets (lighter grey area indicated by black arrows); v) Cluster of KMS-27 cells and vi) Cluster of KMS-27 surrounded by platelets (darker grey area) after 40 min of perfusion showing lack of platelet aggregation; (B) Statistical analysis; time taken by MM.1S cells to aggregate platelets in the presence and absence of phenanthroline (Phe) at 500 µM using the ultrasound standing wave trap. Data is presented as mean ± SEM; n= 3; two-tailed unpaired t-test, carried out using GraphPad Prism 9 (p= 0.272).

2.3.4 Immunoblotting (Western Blot)

A Western blot was performed to confirm the presence of p53 in the MM cell lines used in this study. The results showed that all MM cell lines used expressed p53 (**Figure 18**).

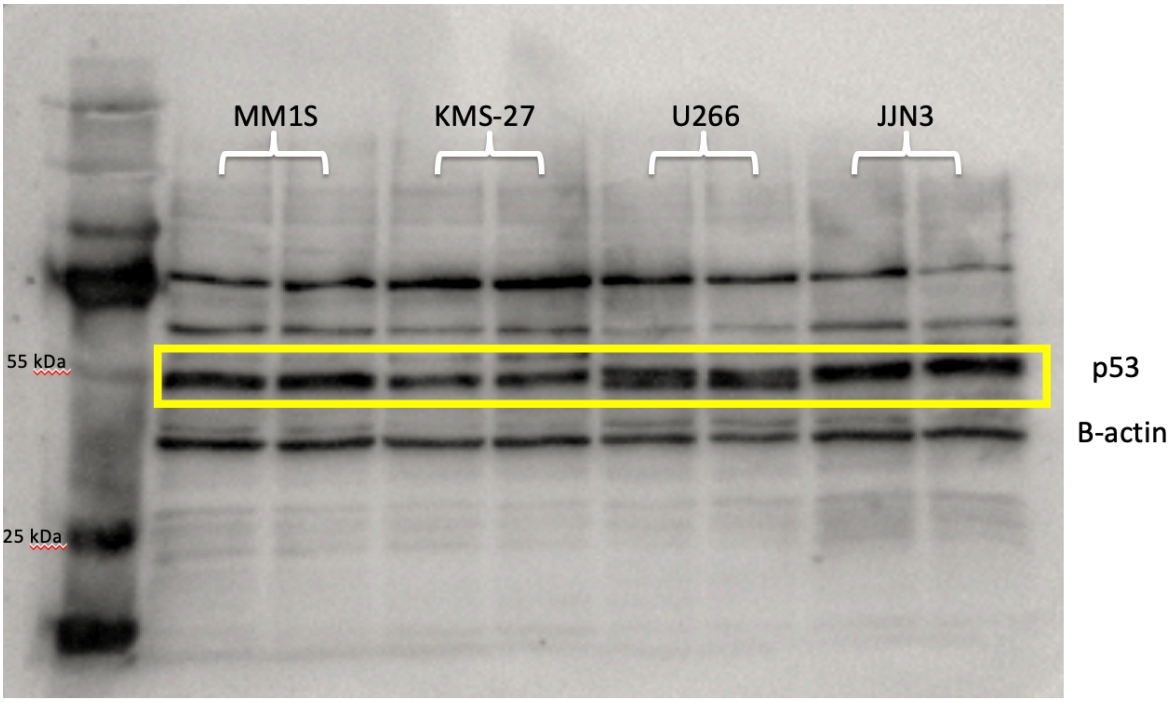

Figure 18 Immunoblotting of p53. The expression of p53 was determined by western blotting. A molecular weight protein ladder (first well) was used as a reference for the molecular weight. β-actin was used as loading control.

2.3.5 Gelatin Zymography

MMPs have shown to play a crucial role in cancer metastasis [202]. MMP-2 acts as a platelet agonist while MMP-9 acts as a platelet inhibitor [203]. Gelatin zymography analysis was carried out to measure the activity of gelatinases (MMP-2 and MMP-9) on platelet samples incubated with phenanthroline following platelet aggregation induced by collagen and KMS-27 cells in the LTA. Conditioned media from PMA-stimulated HT-1080 cells was used as a control for detecting gelatinase activity in the gels [**Figure 19 A (i)**].

While a significant decrease in the activity of MMP-2 was observed when phenanthroline was used to inhibit collagen-induced platelet aggregation [**Figure 19 B (i)**] , this difference was not observed when platelet aggregation was induced by KMS-27 cells [**Figure 19 B (iii)**] . Contrarily, while MMP-9 activity decreased

when phenanthroline was used to inhibit collagen- and KMS-27 cells-induced platelets aggregation, this decrease was not significant [**Figure 19 B (ii, iv)**].

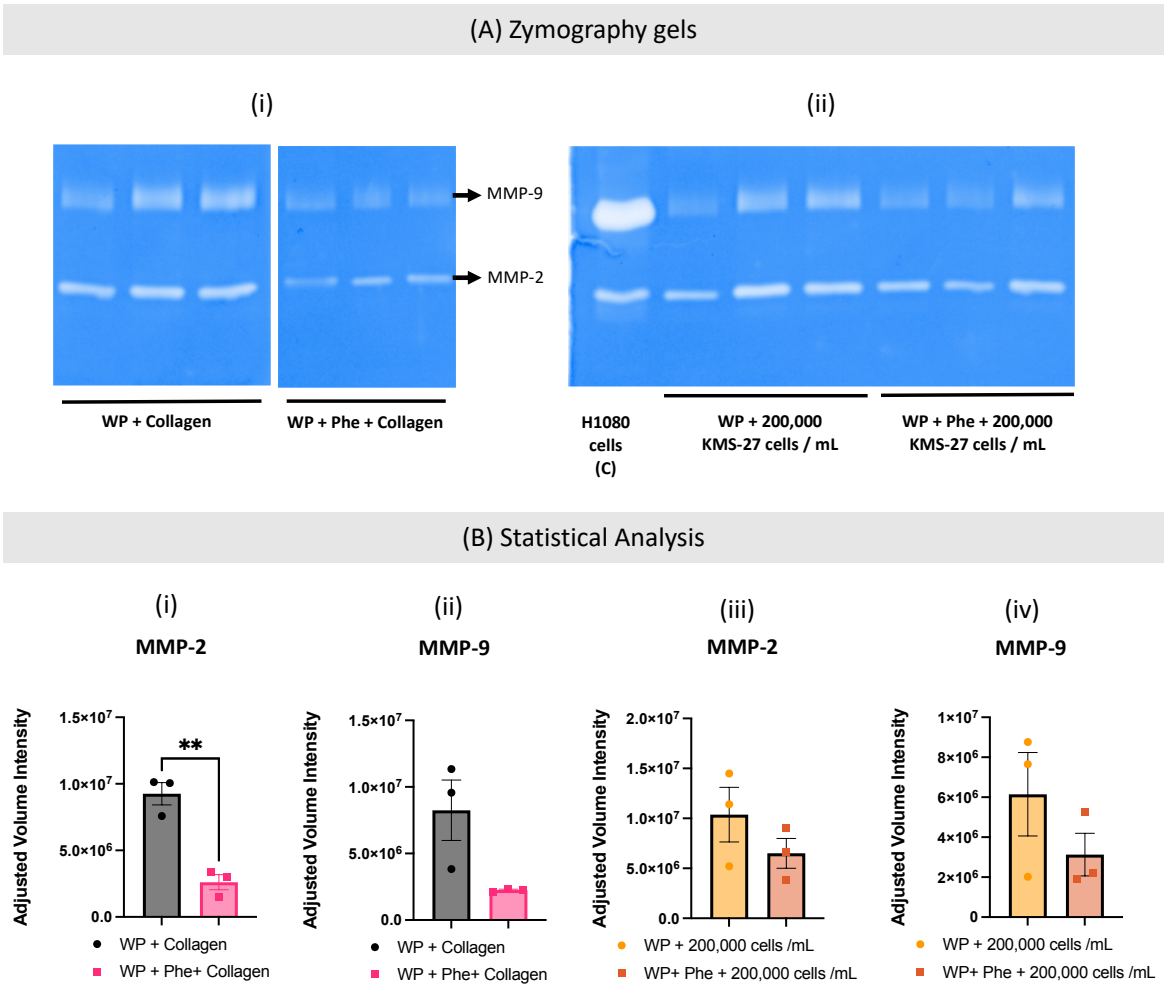

Figure 19 Gelatinase activity as measured by zymography. (A) Representative zymography gels containing supernatants after the exposure of WP in the absence and presence of Phe to (i) collagen and to (ii) KMS-27 cells at different concentrations. (B) Statistical Analysis; Data is represented as mean ± SEM; n= 3; two- tailed unpaired t-test carried using GraphPad Prism 9 performed on gelatinases activity of supernatants collected from (i-ii) collagen induced platelet aggregation, in the presence and absence of phenanthroline and, (iii-iv) KMS-27 induced platelet aggregation in the presence of phenanthroline Gelatinases activity was determined by adjusted volume intensity;**p<0.01. Phe-Phenanthroline

2.4 DISCUSSION

TCIPA is a well-recognised mechanism linking malignancy, thrombosis, and metastatic dissemination [204].

MM.1S and KMS-27 cell lines consistently induced platelet aggregation at all concentrations tested (200,000- 2,000,000 cells/mL), whereas the JJN-3 and U266 cell lines were inconsistent and induced platelet aggregation only at the highest cell concentrations (800,000- 2,000,000 cells/mL). However, while the highest concentration of MM.1S (2,000,000 cells/mL) induced platelet aggregation in 17.4 ± 1.9 min, the KMS-27 cells took longer (40.1 ± 1.9 min), suggesting that the MM.1S cells are more aggressive in their ability to aggregate platelets.

While TCIPA has been described in MM cell lines, including MM.1S, U266, KMS-11, OPM-2, and NCI-H929, in published studies [104], there are no previous reports specifically investigating platelet aggregation induced by KMS-27 and JJN-3 cells, indicating that these findings are novel.

Previous studies by Takagi et al. revealed that not only MM.1S, but U266 cells also induced platelet aggregation using LTA. The researchers, however, do not report the number of cells used or the duration of the experiments in their work. Furthermore, donor-specific factors also influence platelet reactivity. For example, sex-related differences have been observed: females exhibit greater platelet activation in response to TRAP and thrombin than males, and platelet responsiveness decreases with advancing age [205]. Genetic variability also plays a role, as demonstrated by the consistent platelet response profiles observed within individuals over time [206]. A larger sample size would be beneficial in further elucidating U266 and JJN-3-induced platelet aggregation. Nevertheless, MM cells can induce platelet aggregation, as shown clinically. Specifically, platelets from MM patients have been found to have increased surface P-selectin levels, α-granule depletion, and protruding filopodia on the plasma membrane, indicating platelet activation across disease stages from MGUS to active MM [128].

Tumour cells, apart from releasing several pro-aggregatory substances such as TF, thrombin, MMP-2, IL-6, ADP, cathepsin B, CP, can also release EVs, which have been shown to have thrombogenic potential [207], and demonstrated to be loaded with pro-aggregatory and pro-thrombotic cargo such as TF [208]. Papageorgiou et al. measured TF expression in both myeloma cells and myeloma cell-derived microparticles and thrombin generation in their presence using a calibrated

automated thrombogram assay (CAT) in normal human PPP and uncovered that myeloma cell-derived microparticles expressed an even higher procoagulant activity than myeloma cells. [209].

Modulating MM.1S and KMS-27 induced TCIPA

Since MM.1S and KMS-27 cells consistently induced platelet aggregation, the next step was to investigate whether this interaction could be modulated by different platelet inhibitors. MM.1S and KMS-27-induced TCIPA was consistently inhibited by EDTA, prostacyclin, and SNAP.

Previous TCIPA studies using solid tumour lines reported effective inhibition at low prostacyclin concentrations (10 ng/mL) over shorter assay times (15 min) [210,211]. However, due to the extended duration (60 min) of the experiments reported in this thesis and prostacyclin's short half-life, a higher concentration (100 ng/mL) was necessary to sustain inhibition. The differential effectiveness underscores the importance of experimental duration and agonist half-life in platelet inhibition assays, as well as the ability of haematological tumour cells to induce platelet aggregation compared with solid tumours.

Along with prostacyclin, NO is an important mediator generated from the endothelium [212]. NO, by mediating via cGMP, maintains vasodilation and inhibits both platelet adhesion to the endothelium and platelet aggregation [213]. Furthermore, NO can both promote and inhibit tumour progression and metastasis based on its exposure duration and concentration, cellular sensitivity to NO and localisation of nitric oxide synthase (NOS)[214]. Khan et al. showed that small amounts of NO from tumour cells and endothelium cells can promote angiogenesis and EMT, whereas large amounts of NO derived from inducible nitric oxide synthase (iNOS) expressing M1 and Th1 polarised macrophages and lymphocytes may exert an anti-tumour effect [215]. In our experiments, the NO donor used, SNAP, completely inhibited platelet aggregation. This result is consistent with previous studies showing SNAP's inhibitory effect on TCIPA [185]. EDTA completely inhibited platelet aggregation induced by both MM.1S and KMS-27 cells, underscoring the requirement for calcium in tumour cell-mediated platelet activation. Calcium is essential for multiple platelet activation pathways, including integrin αIIbβ3 activation and fibrinogen binding, and its chelation has

been consistently shown to abolish TCIPA [174]. EDTA not only chelates calcium but has also been shown to alter platelet morphology and function, including irreversible dissociation of the GPIIbIIIa receptor [216]. While calcium chelation completely inhibited MM TCIPA, EDTA has limited clinical significance as it is nephrotoxic in vivo [217].

MMPs play an important role in platelet aggregation. Intracellular MMP-2 activates platelets by cleaving talin, thereby facilitating inside-out GPIIbIIIa activation, whereas extracellular pro-MMP-2 can bind to activated GPIIbIIIa receptors on platelets, undergo conversion to MMP-2, and further activate them [218]. MMP-9 can counteract the effects of MMP-2 by decreasing platelet aggregation [219]. Phenanthroline is a non-selective inhibitor of MMPs, meaning it can inhibit both MMP-2 and MMP-9. MM.1S incubated with phenanthroline did not inhibit TCIPA but rather resulted in a significant delay of platelet aggregation (18.02 + 3.053 min) compared to the control (WP + 200,000 MM.1S cells/mL). The concentration of phenanthroline used (500 μM) has been shown to inhibit platelet aggregation induced by Caco-2 colorectal cancer cells [220], 59M ovarian adenocarcinoma and HT1080 fibrosarcoma cells [174]. This concentration (500 μM) may, however, be insufficient to inhibit platelet aggregation induced by MM.1S cells. Increasing the dose could prove effective, as demonstrated in HT-1080–induced platelet aggregation, where 1000 μM significantly inhibited TCIPA [185]. In the case of KMS-27-induced TCIPA, 500 μM of phenanthroline completely inhibited platelet aggregation in the presence of the same concentration of cells (200,000 cells/mL) used in MM.1S-induced TCIPA. This suggests that MM.1S cells may release more MMP-2 than KMS-27 cells. Alternatively, their more aggressive nature enables them to induce stronger platelet aggregation, potentially resulting in greater platelet-derived MMP-2 release. Assessment of MMP-2 and MMP-9 levels by gelatin zymography after TCIPA induced by KMS-27 cells revealed a discrepancy between aggregation and protease activity. Although LTA confirmed complete inhibition of KMS-27-mediated aggregation in the presence of phenanthroline, a corresponding reduction in gelatinase activity (MMP-2 or MMP-9) was not found to be significant. This suggests that other MMPs, such as MMP-1 [221] and MMP-14 [222] may also play a synergistic role in inhibiting platelet aggregation. While MMP-1 has not been found to be directly secreted by myeloma cells, MMP-14 [223] can activate pro-MMP-1 to generate active MMP-2.

ADP is another platelet agonist that is[96]eased by both tumour cells [115] and platelets' δ-granules upon activation. It is also released by damaged erythrocytes and endothelial cells [224]. Apyrase is an ADP scavenger that has shown to inhibit TCIPA [174,179–181]. While apyrase did not have any effect on MM. 1S-induced TCIPA, it marginally inhibited KMS-27-induced platelet aggregation, suggesting a role for ADP in KMS-27 TCIPA.

Aspirin (acetylsalicylic acid), a cyclooxygenase-1 (COX-1) inhibitor that suppresses thromboxane A_2 (TXA_2) synthesis, has historically been described as a weak inhibitor of TCIPA in vitro, even at high concentrations [174,191,225–227]. However, in the present study, aspirin successfully inhibited KMS-27-induced platelet aggregation, suggesting that KMS-27-mediated TCIPA may be more dependent on TXA_2-driven pathways than platelet aggregation induced by MM.1S. Recent findings show that suppression of COX-1 in platelets by aspirin helps to reduce tumour metastasis by reducing TXA_2 production and thus, preventing suppression of T-cell immunity by TXA_2 [228]. Clinically, aspirin has been shown to reduce thrombotic risk in MM patients receiving immunomodulatory agents [229], although its protective efficacy appears limited in individuals with a prior history of VTE [230]. Furthermore, aspirin may be used as a preventive medicine for MM, as shown by a 39% reduced risk of MM in participants with an average of ≥5 adult strength (325-mg) tablets per week than non-users, according to a prospective analysis of two large U.S. cohorts (the Health Professionals Follow-Up Study and Nurses' Health Study). Additionally, participants with ≥11 years of continuous regular aspirin use also showed a reduced MM risk [231]. In patients diagnosed with MM in the same cohorts, aspirin use post-diagnosis in those patients was also inversely associated with mortality related to MM [232] .

TCIPA using ultrasound standing wave trap

When MM cells were allowed to interact with platelets in a two-dimensional (2-D) cluster arrangement using the ultrasound wave trap, MM.1S cells induced platelet aggregation, as evidenced by the formation of gel-like platelet structures observed microscopically, followed by eventual disruption of the cell cluster. This pattern of aggregation is consistent with tumour cell–induced platelet aggregation previously reported by Bazou et al. [162] using the same experimental platform with 59 M

ovarian cell line [174]. Phenanthroline, in agreement with observations obtained using light LTA, delayed the onset of platelet aggregation in the wave trap but did not completely inhibit platelet aggregation, further supporting the involvement of metalloproteinase-dependent mechanisms that are not solely responsible for MM.1S-induced TCIPA. In contrast, although KMS-27 cells induced platelet aggregation in LTA, they failed to do so in the ultrasound wave trap. One reason could be that the cell-to-cell contact in the cell cluster may led to the release of platelet inhibitory substances such as NO or NTPDase1/CD39 (converts ATP to ADP and finally to adenosine preventing platelet aggregation [233]) preventing the interaction between tumour cells and platelets or that the potential release of pro-aggregatory factors by the MM cells does not take place under this specific conditions. Furthermore, it is important to consider that the number of tumour cells introduced into the trap allowed to form clusters (in the range of 30,000 cells) was substantially lower than the number of cells used in LTA experiments (100,000-1,000,000 cells), which may have contributed to the absence of detectable platelet aggregation.

The behaviour of MM cell lines with differing p53 status in inducing platelet aggregation suggests that p53 does not play a distinct or decisive role in MM-induced platelet aggregation. Although western blot analysis indicated p53 protein expression in all tested cell lines, this finding was unexpected for the JJN-3 cell line, which harbours a hemizygous TP53 deletion and has previously been reported not to express p53 [234,235]. The detection of p53 in JJN-3 cells in this study may be explained by several factors: (1) JJN-3 cells may indeed express low levels of p53, (2) the antibody used in the western blot may be non-specific, as suggested by the presence of multiple bands on the membrane (**Figure 18**), or (3) the detected band may not correspond to p53, as no positive reference control was included. Results from LTA demonstrated that MM.1S and KMS-27 cells, both of which express p53 protein, were capable of inducing platelet aggregation, while JJN-3 (p53 null) and U266 (p53 mutant) did not do so consistently. Moreover, results obtained using the ultrasound wave trap further underscored this complexity, as the two p53 wild-type cell lines exhibited distinct behaviours: MM.1S cells induced platelet aggregation, whereas KMS-27 cells did not. Therefore, it seems reasonable to conclude that p53 does **not** play a crucial role in MM-induced platelet aggregation. Therefore, the initial hypothesis, that p53 (tumour suppressor

protein) expression, would be inversely correlated with platelet aggregation potential, is not valid.

2.5 CONCLUSIONS

In conclusion, this study demonstrates that MM cells can induce TCIPA in a cell line–dependent manner. MM.1S and KMS-27 consistently induced platelet aggregation across all concentrations tested, whereas JJN-3 and U266 did so only at higher cell numbers, highlighting heterogeneity in MM–platelet interactions. Faster aggregation observed with MM.1S cells indicates a more potent pro-aggregatory phenotype. These findings are consistent with clinical evidence of platelet hyperactivation in MM patients and extend existing literature by providing novel data on KMS-27- and JJN-3-induced TCIPA. Difference in sensitivity to apyrase, aspirin, and phenanthroline suggests that MM.1S- and KMS-27-induced TCIPA rely on distinct combinations of ADP, TXA_2, and MMP-dependent pathways. The lack of significant changes in MMP-2 and MMP-9 activity despite TCIPA inhibition indicates that additional MMPs likely contribute to KMS-27-mediated platelet activation. Comparison of LTA with the ultrasound standing wave trap further revealed that tumour cell number and spatial organisation influence TCIPA. While MM.1S induced platelet aggregation in both systems, KMS-27 failed to do so in the ultrasound standing-wave trap, suggesting that effective platelet activation by certain MM cells may either require a higher number of tumour cells or involve specific cell–platelet contact dynamics. Although studies on the use of different platelet inhibitors are limited, future studies should aim to either modulate MM-induced TCIPA using selective MMP inhibitors or using a combination of inhibitors. Investigating the role of tumour-derived EVs will further clarify mechanisms of platelet activation in MM. Additionally, extending these findings to patient-derived MM cells or platelets may be essential to determine the clinical relevance of targeting platelet–tumour interactions as a therapeutic strategy to reduce thrombosis and potentially limit disease progression in MM.

Chapter 3

Looking at the proteome of platelet–myeloma crosstalk: Identifying drivers of metabolic shift and therapeutic resistance

3.1 INTRODUCTION

Proteomics, the large-scale study of proteins, offers a powerful and increasingly indispensable approach for understanding the functional landscape of cancer cells. While genomics identifies genetic predisposition, transcriptomics quantifies RNA expression, and proteomics captures the cell's functional state. By measuring proteins, the primary cell effectors, and their post-translational modifications, proteomics provides a direct view into the molecular mechanisms that, together with regulatory non-coding RNAs, drive disease phenotypes. In cancer, proteomic technologies have been instrumental in identifying biomarkers, uncovering mechanisms of drug resistance, and revealing novel therapeutic targets [236]. In the context of MM, proteomic profiling has revealed key insights into disease pathophysiology. They have revealed protein signatures linked to disease progression, patient risk groups, and responses to major treatment classes such as proteasome inhibitors and immunomodulatory drugs [237–241]. Moreover, analysis of the MM microenvironment secretome, including exosomes and soluble factors, has helped to understand how myeloma cells and the microenvironment can modulate their surroundings to promote immunosuppression and osteolysis [242–244]. Despite these advances, relatively little attention has been paid to how MM cells interact with circulating blood components, especially platelets. The molecular basis of these interactions in haematological cancers remains poorly defined, representing an important gap in our understanding of MM pathophysiology.

3.1.1 Mass spectrometry

One of the most indispensable tools for quantitative profiling of proteins and their modifications is mass spectrometry (MS) based proteomics. MS separates ions based on their mass/charge (m/z) ratio. MS-based proteomics can be divided into two sub-categories: a) targeted proteomics, b) untargeted or discovery proteomics. While targeted proteomics aims at a predefined set of proteins or peptides with high accuracy, untargeted or discovery proteomics aims to quantify as many proteins or peptides as possible within the biological sample. Discovery proteomics is designed to measure all proteins expressed in any tissue, cell line, or organism, compare proteomes across different conditions, or aid in biomarker discovery [245].

The process of untargeted proteomics starts with the isolation, denaturation, reduction, and alkylation of the proteins present in the sample. The unfolded proteins are then digested with an appropriate enzyme, typically trypsin. The digested samples are introduced into liquid chromatography-mass spectrometry (LC-MS). LC separates proteins based on their hydrophilicity. The hydrophobic/lipophilic peptides get attached to the non-polar stationary phase, with the hydrophilic peptides eluting first from the column. This step enhances accuracy by reducing sample complexity and improving sensitivity. The peptides in the eluent are then converted into charged gaseous ions by applying a high voltage using either electrospray ionisation (ESI) or matrix-assisted laser desorption/ionisation (MALDI). These are introduced into the MS either in data-dependent acquisition (DDA) mode, in which the MS selects the most intense peptide ions for fragmentation, or in data-independent acquisition (DIA) mode, in which the instrument fragments all ions within predefined m/z windows. The fragmentation techniques used are collision-induced dissociation (CID), higher-energy collision-induced dissociation (HCD), and electron transfer dissociation (ETD). Fragmentation breaks the peptides into predictable pieces, which are then used to determine the amino acid sequence. The resulting product ions are characterised by their mass-to-charge (m/z) ratios and relative abundances, producing a spectrum that is then matched to theoretical spectra in databases to identify the peptides [246].

3.1.2 Label Free Quantification

Once quantitative data from MS are gathered, they can be analysed using label-based and/or label-free methods. Label-free approaches can determine relative protein abundance across multiple biological samples without requiring isotopic or chemical labels. Label-free quantification (LFQ) broadly encompasses two major strategies: intensity-based and spectral counting. Both strategies have been widely applied in proteomic studies and are considered effective alternatives to labelling approaches due to their simplicity and cost-effectiveness. Intensity-based LFQ relies on measuring the signal intensities of peptide precursor ions, such as peak heights or areas under extracted ion chromatograms, to estimate relative protein abundance. In contrast, spectral counting methods derive relative protein abundance from the number of MS/MS spectra confidently matched to peptides of

a given protein, assuming that more abundant proteins yield more peptide identifications and therefore more spectra [247,248].

In the previous chapter, results indicated that MM.1S and KMS-27 cell lines induced platelet aggregation with varying sensitivity to different pharmacological agents, while JJN-3 and U266 failed to induce consistent aggregation, underscoring heterogeneity in tumour cell–platelet interactions. These results suggest that not all MM cell subtypes interact with platelets following the same activation pathways. Building on these observations, two approaches were used to elucidate the molecular pathways underlying platelet activation and to investigate whether direct physical contact between cells and platelets is required for this process. First, assess whether MM cell-conditioned media, independent of direct cell-platelet contact, can aggregate platelets or modulate platelet responses to platelet agonists. For this purpose, platelets were resuspended in conditioned media from MM cells and their function studied using LTA. Second, proteomic profiling of conditioned media from the same MM cell lines, with and without platelets, was also performed to identify potential pro-aggregatory or modulatory factors in this interaction. Together, these complementary approaches aimed to determine whether MM-secreted components alone could influence platelet behaviour and to elucidate the cell line-specific effects observed in TCIPA.

3.2 METHODS

3.2.1 Reagents

All the reagents were procured from Sigma-Aldrich, Ireland, unless otherwise stated.

3.2.2 Washed platelet preparation

Blood was obtained from healthy volunteers after obtaining informed consent, in accordance with the Declaration of Helsinki. Briefly, PRP was prepared from whole blood and centrifuged to prepare WP in the presence of prostacyclin to prevent platelet aggregation. The pellet containing the platelets was resuspended in serum-free RPMI 1640 and 1% Antibiotic-Antimycotic (100X) [Fisher Scientific Ltd., Ireland] or in MM cell-conditioned media to a final concentration of 250,000 platelets/μL. Platelet releasate (mixture of biologically active compounds released

by platelets upon activation) was prepared by inducing platelet aggregation with 4 µg/mL collagen using the LTA.

3.2.3 Cell lines used and collection of conditioned media

MM.1S, U266, JJN-3, KMS-27 MM cells cultured in RPMI 1640 Medium, supplemented with 10% FBS and 1% Antibiotic-Antimycotic (100X) were used for these experimental procedures. Once 70-80% confluent, cells were incubated in serum-free media for 48 hours, and the resultant supernatant (conditioned media) was collected, centrifuged and filtered through a 0.22 µm filter (PES syringe filters, Branchia, Labbox Labware, S.L.) for further use.

3.2.4 Platelet response to MM conditioned media

WP were resuspended in the MM conditioned media to a final concentration of 250,000 platelets/µL. They were stirred for 60 min to test whether the conditioned media could induce platelet aggregation. Platelets response to agonists targeting the different platelet activation pathways [Collagen (Chrono-log Corp., U.S.A); Arachidonic acid (Bio-Data Corp. U.S.A); U46619 (Tocris Biosciences, U.K)] was also tested and monitored using the PAP-8E Platelet Aggregometer (Bio/Data Corp., U.S.A) (Figure 20). WP resuspended in serum-free media and stimulated with the same platelet agonists served as a control. Data from 3 independent experiments were subjected to an unpaired Student's t-test using GraphPad Prism 9 software (GraphPad Software, La Jolla, CA, U.S.A). Data is reported as mean and SEM. Statistical significance was considered at $p < 0.05$.

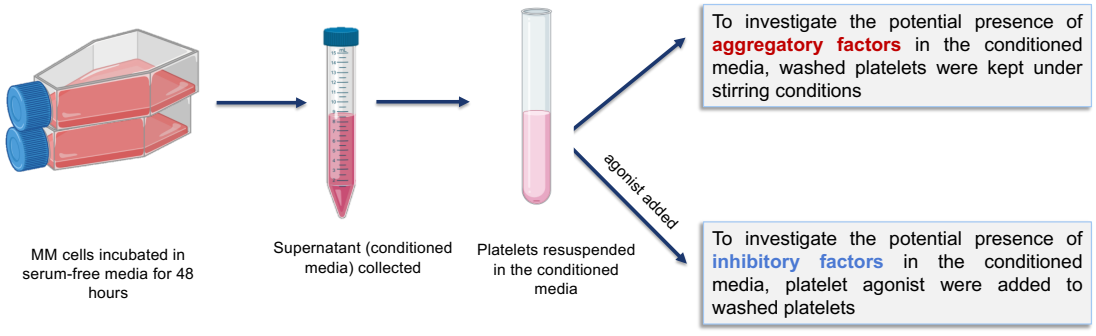

Figure 20 Procedure for carrying out platelet functional studies. LTA- Light transmission aggregometry. *Created using Biorender and Microsoft Powerpoint.*

3.2.5 Proteomics

3.2.5.1 Collection and concentration of secretome

MM cells were incubated in the presence of serum-free media, WP resuspended in serum-free media and platelet releasate. After incubating the flasks for 24 hours, the supernatant was collected, centrifuged, filtered through 0.22 μm and stored at -80^{o} C until further analysis. All the samples were concentrated to 1/10th of the volume using a 3KDa cut-off centrifugal device (Pall Corporation, USA). Briefly, 500 μL of each sample was added to the filter units and centrifuged at 4,000 rpm for 20 min at room temperature, reducing the volume to 50 μL. Then, an additional 500 μL of sample was added to the filter unit and centrifuged again at the same speed for the same duration until the volume was reduced to 100 μL.

3.2.5.2 Protein assay

The Pierce 660nm Protein Assay (Thermo Scientific, Ireland) was performed on all samples prior to sample preparation to measure protein concentration against a standard curve. The assay is based on the binding of its proprietary dye-metal complex to primarily basic amino acid residues, such as histidine, lysine, and arginine, present in proteins. Upon binding, the dye-metal complex changes to green colour, resulting in an absorbance shift to 660 nm.

3.2.5.3 Filter-aided sample preparation (FASP) of secretome

FASP protocol was used to prepare samples for proteomic analysis. 10 μg of protein containing sample was loaded up to a maximum volume of 400 μL with 8 M urea buffer in 0.1 M Tris/HCl on Vivaspin 5,000 MWCO PES membrane (Sartorius, U.K), centrifuged at 14,000 x g for 20 min. The disulfide bonds in the proteins were reduced with 1 M dithiothreitol (DTT), and the free cysteine residues were alkylated with 0.05 M Iodoacetamide (IAA), washed, charged with 100 mM ammonium bicarbonate (ABC) and digested with trypsin and ProteaseMAX Surfactant, which was added as an enhancer. Protein samples were then analysed using a Q-Exactive mass spectrometer (Thermo Scientific, Ireland) coupled to a Dionex RSLCnano (Thermo Scientific, Ireland). Peptides were separated using a 2–40% gradient of acetonitrile (A: 0.1% FA, B: 80% acetonitrile, 0.1% FA) over 65 min at a flow rate of 250 nL/min. The Q-Exactive was operated in the data-dependent mode, collecting a full MS scan from 300–1650 m/z at 70 K resolution and an AGC target of 1e6. The 10 most abundant ions per scan were selected for

MS/MS at 17.5 K resolution and AGC target of 1e5 and intensity threshold of 1 K. Maximum fill times were 10 ms and 100 ms for MS and MS/MS scans, respectively, with a dynamic exclusion of 60 s. Samples were analysed using 25 NCE (normalised collisional energy) with 20% stepped energy.

3.2.5.4 Analysis of proteomics data

For quantitative analysis, samples were analysed using MaxQuant (v1.5.2.8) and the Andromeda search engine to identify features against the UniProtKB/SwissProt database (Homo sapiens). The following search parameters were used: (i) first search peptide tolerance of 20 ppm, (ii) main search peptide tolerance of 4.5 ppm, (iii) cysteine carbamidomethylation set as a fixed modification, (iv) methionine oxidation set as a variable modification, (v) a maximum of two missed cleavage sites and (vi) a minimum peptide length of seven amino acids. The false discovery rate (FDR) was set to 1% for both peptides and proteins using a target-decoy approach. Perseus v.1.5.6.0 was used for data analysis. Label-free quantitation (LFQ) was performed. At least 2 LFQ values (max. 3 LFQ values) for each protein across samples were Log_2 transformed and used to compute mean LFQ values. LC-MS and analysis of the proteomics data until this point were carried out by Dr Paul Dowling, Maynooth University, Ireland.

Files were exported in MS Excel, and further downstream processing was carried out. Fold change was calculated using Log_2 fold change values as per the given formula:

$$Fold\ change\ (Sample\ A\ and\ B) = 2\hat{}(Log2\ \ Sample\ A\ mean - Log2\ Sample\ B\ mean)$$

A two-tailed unpaired Student t-test was carried out in Microsoft Excel using the function 'T.TEST' to calculate the p-value.

FASTA protein headers were searched and categorised by biological process (Gene Ontology) and Kyoto Encyclopaedia of Genes and Genomes (KEGG) pathway enrichment using the STRING Database (https://string-db.org). The STRING network visualises protein interactions as a graph where nodes represent proteins and edges represent interactions, with confidence scores indicating the likelihood of the association. The interaction score was set to high confidence (>0.7) [249]. This denotes >70% probability that an interaction is real. STRING can provide a

list of enriched KEGG pathways and Gene Ontology biological terms (e.g., "MAPK signalling pathway" and “immune response”, respectively) to determine whether specific pathways are statistically overrepresented using tests such as the hypergeometric test or Fisher’s exact test, with corrections for multiple comparisons. Volcano plots were created using R studio (version 2023.06.2+561).

Figure 21 depicts and briefly explains the proteomic sample collection, processing, and analysis.

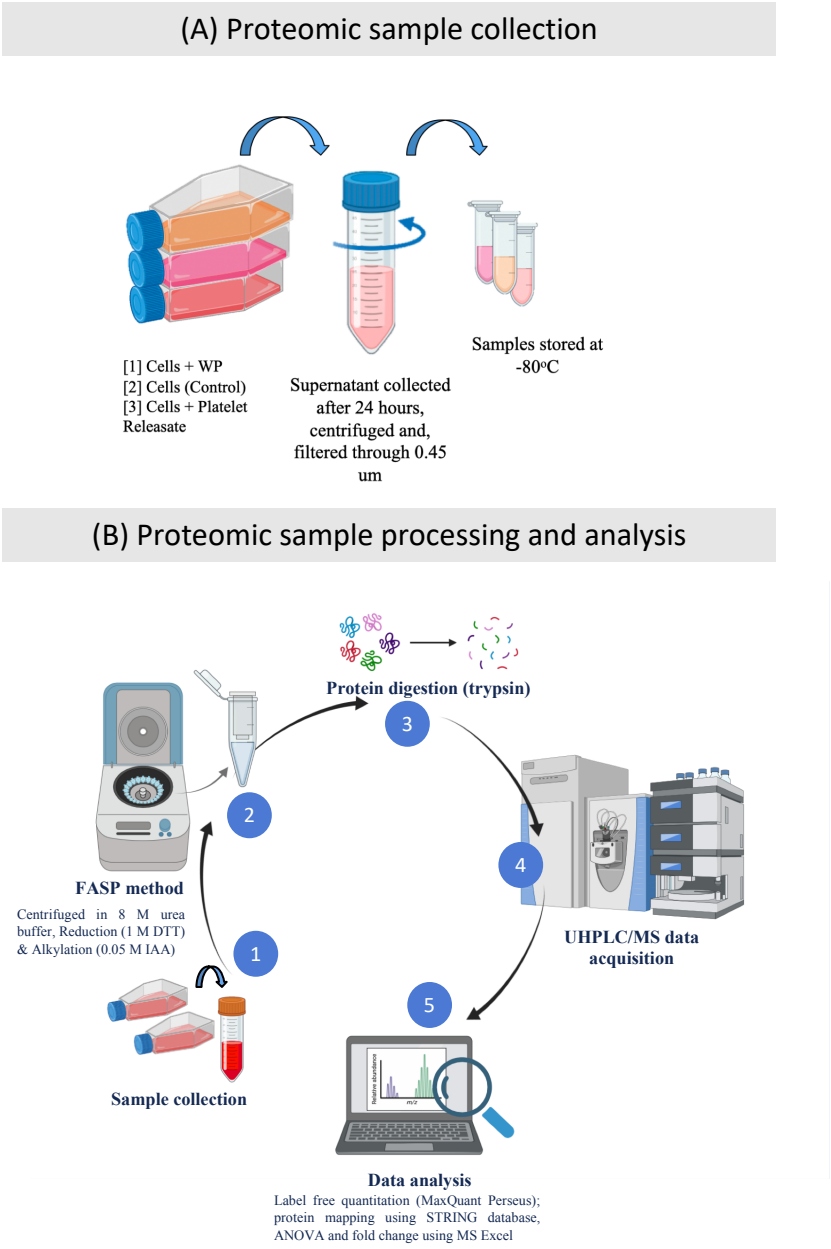

Figure 21 Procedure carried out for collecting the sample and sample processing for proteomic analysis.

3.3 RESULTS

3.3.1 Platelet response to MM conditioned media

Platelets were resuspended in conditioned media from MM.1S, KMS-27, U266 and JJN-3 cell lines, and LTA was used to investigate if the conditioned media could modulate platelet aggregation.

It was found that conditioned media from MM.1S, KMS-27, U266, and JJN-3 cell lines did not induce platelet aggregation (resuspended platelets were maintained under stirring conditions in the LTA for up to 60 min). Conditioned media did not exert an inhibitory effect when platelet aggregation was induced by collagen-, arachidonic acid- and U46619. Rather, when MM.1S conditioned media was used to resuspend platelets and platelet aggregation induced by collagen (2 μg/mL), increased platelet aggregation was observed when compared to platelets resuspended in free serum media (control). However, when conditioned media from the other 3 cell lines were used to resuspend platelets and stimulated with the same agonists, no significant differences were observed when compared to the control (**Figure 22**).

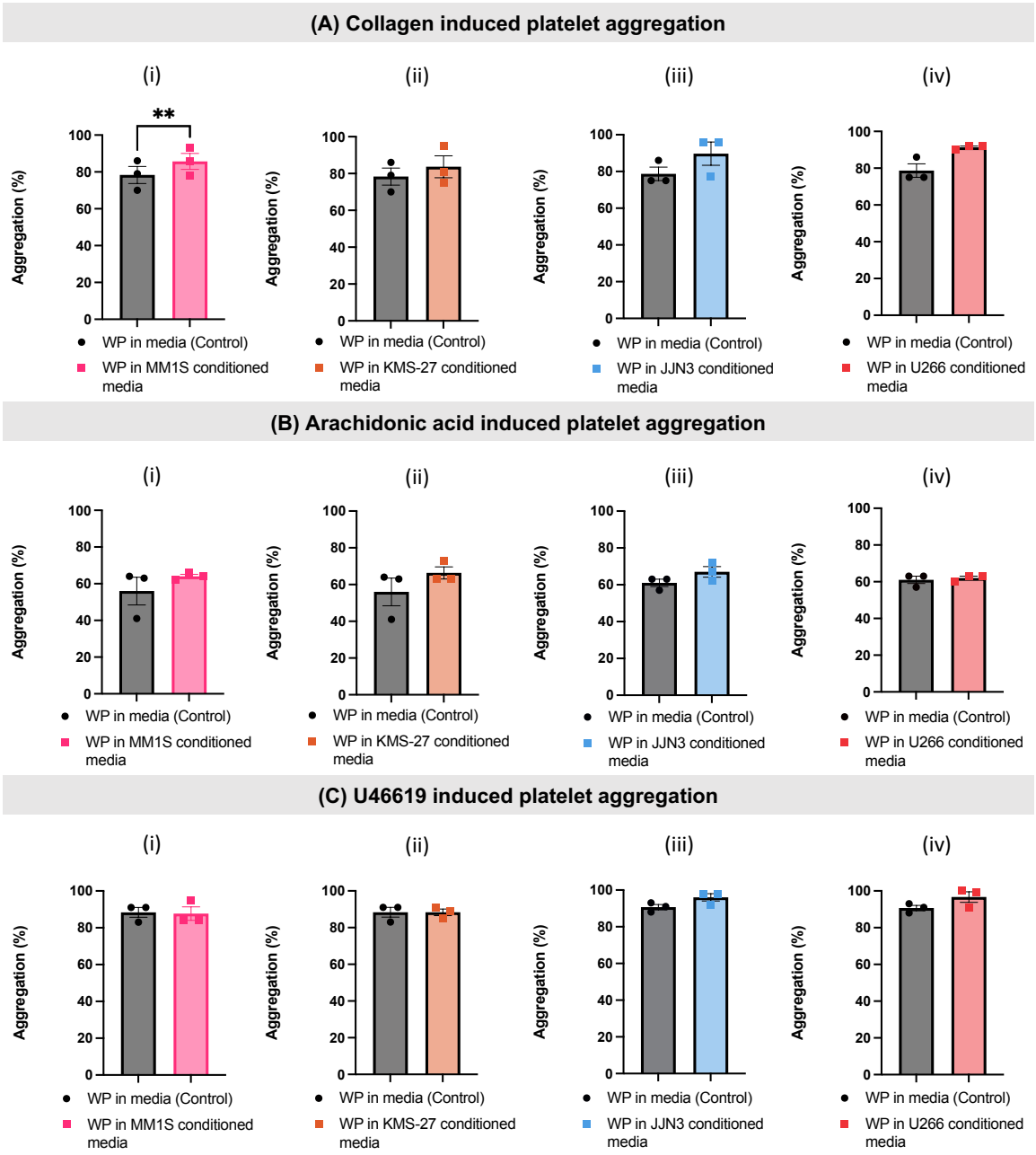

Figure 22 Aggregation of platelets resuspended in the conditioned media from MM.1S, KMS-27, U266 and JJN-3 cells in the presence of A) Collagen (2µg/mL) B) Arachidonic acid (500 µg/mL) C) U46619 (1 µM). Data is presented as mean ± SEM; n=3; unpaired t-test carried out using GraphPad Prism 9; **p<0.01.

3.3.2 Proteomics

Proteomic data was analysed using log-transformed LFQ intensity values generated by MaxQuant for each condition mentioned (**Table 3**) across samples from three independent platelet donors. Fold change and p-values were calculated in Microsoft Excel.

Table 3 Samples collected for proteomics analysis and terms used throughout the thesis

Sample number	Description	Term used
1	Supernatant collected from MM cells incubated in serum free media	Cell secretome
2	Supernatant collected from MM cells co-incubated with WP in serum free media	Cell-platelet secretome
3	Supernatant collected after inducing platelet aggregation with collagen	Platelet releasate
4	Supernatant collected after incubating MM cells with platelet releasate	Cell-platelet releasate secretome

Analysis of the data was done in these conditions:

1. Proteins expressed only in the cell-platelet secretome. These proteins were neither found in the cell secretome or the platelet releasate
2. Proteins increased in abundance in the cell-platelet secretome compared to both the cell secretome and platelet releasate. Proteins enriched only in the cell-platelet secreteomes were excluded from this. For this purpose, fold changes and p-values were calculated and compared between (a) cell-platelet secretome and cell secretome (b) cell-platelet secretome and platelet releasate. Out of these, fold change values only greater than or equal to 1.5 and p-values less than or equal to 0.05 were considered significant.
3. Proteins increased in abundance in the cell-platelet releasate secretome compared to the cell secretome and the cell-platelet secretome.

3.3.2.1 MM.1S Proteomics Data

3.3.2.1.1 Proteins that were enriched only in MM.1S cells- platelet secretome

A total of 211 proteins were enriched across all samples (MM.1S cell secretome, MM.1S cell-platelet secretome and platelet releasate). Out of these proteins, 78 proteins were enriched only in the MM.1S cell-platelet secretome. **Figure 23** shows the string data connections visualising protein interactions as a graph, where nodes represent proteins and edges represent interactions. The majority of the proteins present only in the MM.1S cell-platelet secretome are associated with metabolism, particularly carbon metabolism, pentose phosphate pathway,

glutathione metabolism, and antigen processing and presentation (**Figure 24**). **Table 4** enlists all these proteins with their biological role.

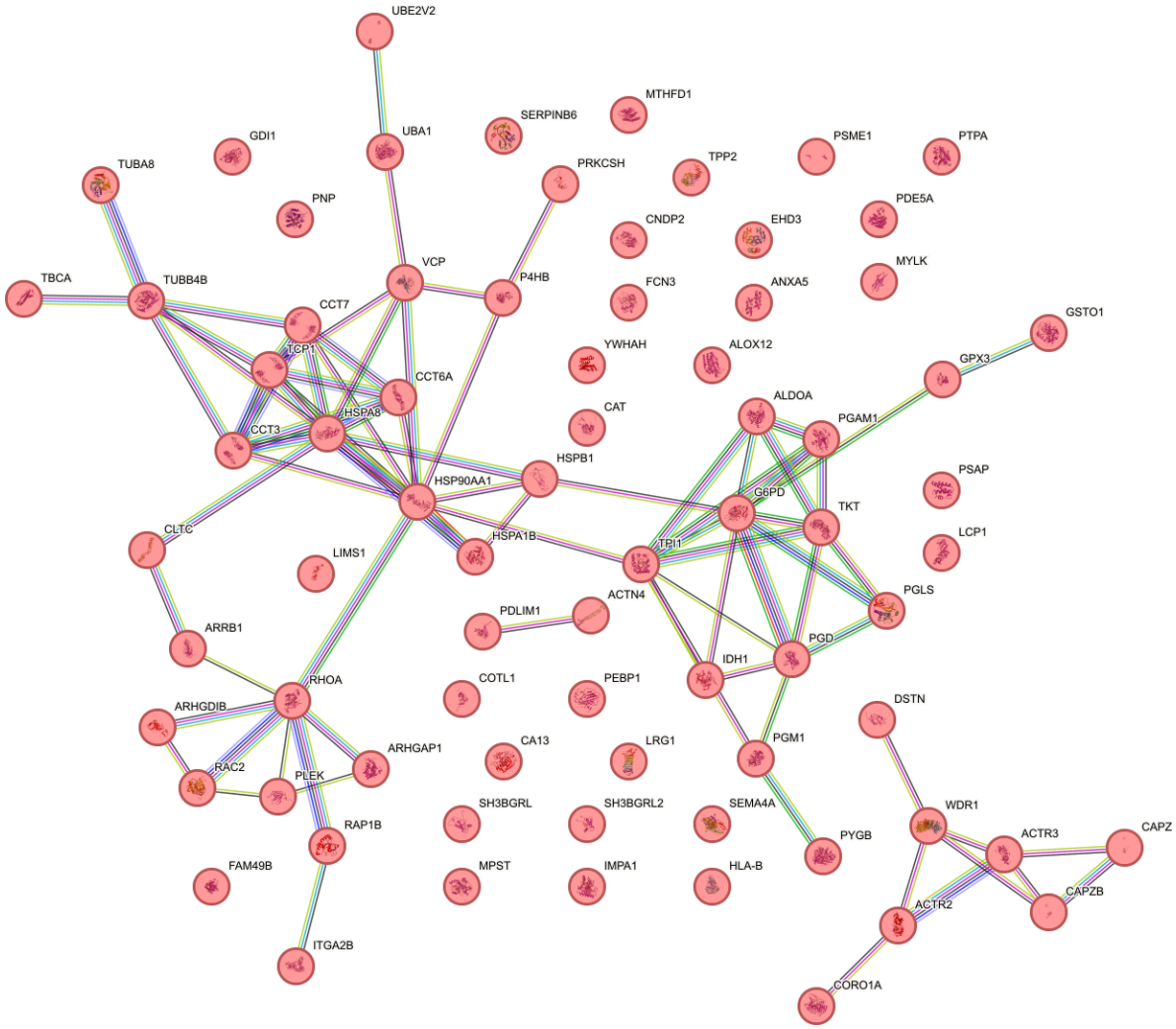

Figure 23 STRING protein interaction map depicting all the proteins expressed only in the MM.1S-platelet secretome. The nodes represents the proteins and the lines indicate the interaction. More number of lines indicate a stronger interaction.

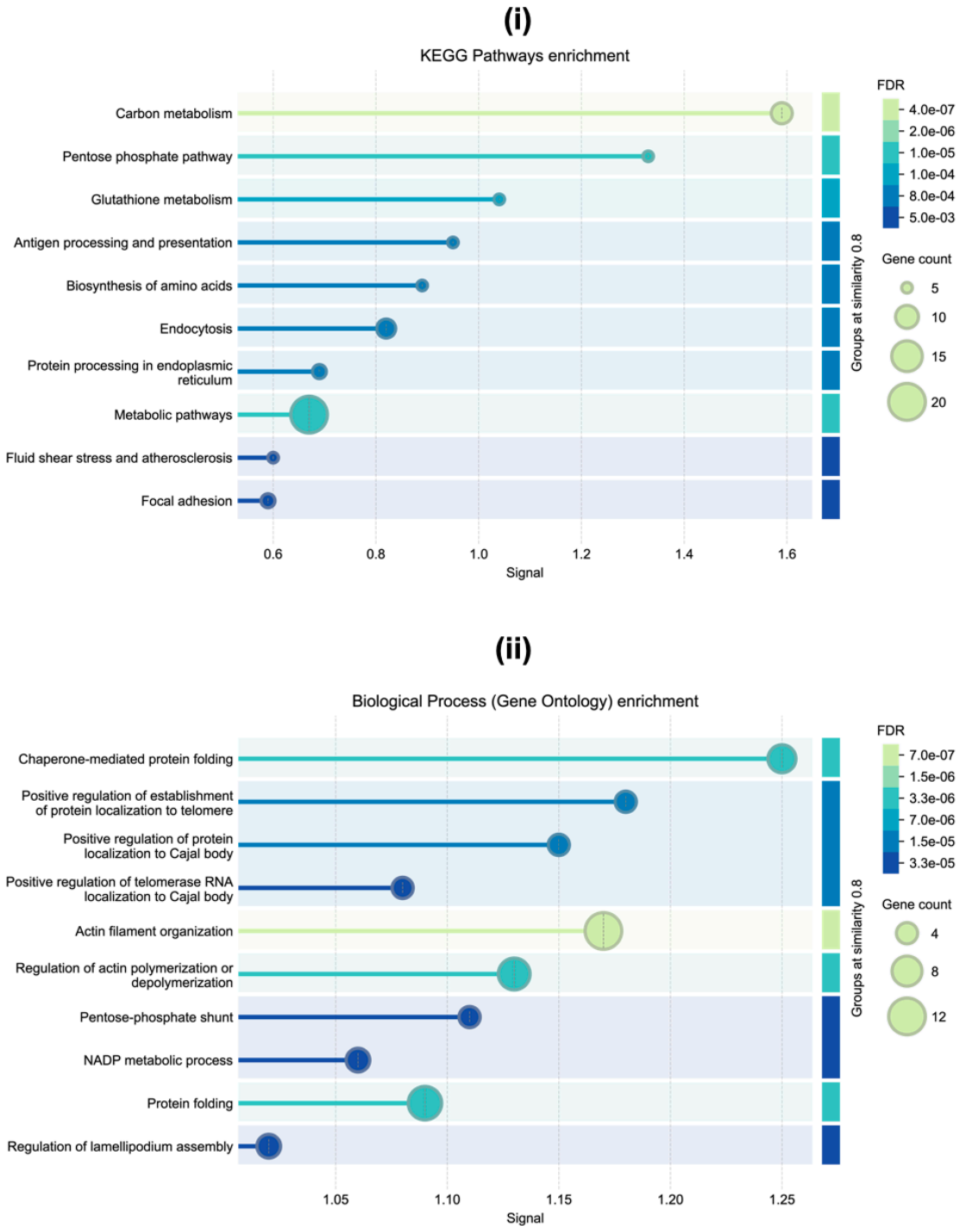

Figure 24 The enrichment analysis of proteins present exclusively in the presence of platelets and MM.1S cells based on (i) KEGG pathway, (ii) biology process (gene ontology), provided by the STRING database.

Table 4 Proteins present only in MM.1S cell-platelet secretome, along with their biological role

Protein ID	Biological Role
Metabolic and Catabolic proteins	
TPIS	Glycolytic enzyme catalysing reversible isomerization of triose phosphates
TKT	Key enzyme of pentose phosphate pathway; NADPH production
ALDOA	Glycolysis; fructose-1,6-bisphosphate cleavage
PGAM1	Glycolytic enzyme; interconversion of phosphoglycerates
G6PD	Rate-limiting enzyme of pentose phosphate pathway; cellular redox homeostasis
6PGD	Pentose phosphate pathway enzyme generating NADPH
IDHC (IDH1)	Cytosolic NADP-dependent isocitrate dehydrogenase; lipid synthesis, redox control
GPX1	Intracellular antioxidant enzyme; H_2O_2 detoxification
GPX3	Extracellular antioxidant defence
CATA	Hydrogen peroxide detoxification
LOX12 (ALOX12)	Arachidonic acid metabolism; inflammatory lipid mediators
PDIA1 (P4HB)	Protein folding and disulphide bond formation in ER
GSTO1	Detoxification and redox regulation
6PGL	Hydrolyzes 6-phosphogluconolactone in the pentose phosphate pathway
GLU2B	Cleaves glucose residues from immature glycoproteins in the ER
MDHC	Catalyzes the reversible oxidation of malate to oxaloacetate
PGM1	Interconverts glucose-1-phosphate and glucose-6-phosphate

PNPH	Essential enzyme for the purine salvage pathway
PYGB	Breaks down glycogen to provide energy
THTM	Cysteine catabolism and sulfur trafficking
TPP2	Large exopeptidase that degrades polypeptides into tripeptides
Structural & Cytoskeletal Proteins	
ARP2 / ARP3	Actin nucleation; branched filament assembly
ACTN4	Actin crosslinking; cell motility and adhesion
PLSL (L-plastin)	Actin bundling in immune cells
CAPZB	Regulation of actin filament elongation
TBCA	Tubulin folding and microtubule assembly
TBB4B	Microtubule structural component
TBA8	Microtubule assembly
CFL1	Actin depolymerization
LIMS1	Integrin-mediated signalling and adhesion
COR1A	Actin cytoskeleton regulation in immune cells
ARP3	Part of the Arp2/3 complex; initiates actin filament branching
COTL1	Binds to F-actin; regulates cytoskeleton and leukotriene synthesis
DEST	Depolymerizes actin filaments to promote turnover
ITA2B	Integrin subunit; mediates cell-matrix and cell-cell adhesion
PDLI1	Anchors proteins to the cytoskeleton via PDZ and LIM domains
WDR1	Enhances cofilin-mediated severing of actin filaments
Chaperones & Heat Shock Proteins	
HSP7C	Protein folding; stress response

HSPB1	Cytoskeletal stabilization; apoptosis regulation
HSP71	Stress-induced protein folding
HS90A	Stabilization of signalling proteins
TCPA/G/H/Z	TRiC/CCT complex; folding of actin and tubulin
PSME1	Proteasome activation; antigen processing
TERA	ATPase that extracts misfolded proteins for degradation (VCP)
C1TC	Assists in complex assembly/C1-THF synthase activity
Signalling & Regulatory Proteins	
GDIR2	Regulation of Rho GTPases
RAP1B	Cell adhesion and platelet activation
RAC2	Actin remodelling; immune cell migration
RHOA	Cytoskeletal dynamics; contractility
GDIA	Rho GTPase inhibition
MYLK	Myosin phosphorylation; cell motility
PDE5A	cGMP hydrolysis; smooth muscle signalling
PTPA	Activation of protein phosphatase 2A
1433F (YWHAZ)	Signal transduction and apoptosis regulation
SH3L1 / SH3L2	Adaptor proteins in cytoskeletal signalling
SEM4A	Immune regulation and axon guidance
A2GL	Promotes cell proliferation and TGF-beta signaling
CAH13	Regulates pH balance and ion transport
CAZA1	Binds to the ends of actin filaments to stop growth (capping)
CNDP2	Hydrolyzes dipeptides; involved in mucosal immune regulation

EHD3	Controls endocytic vesicle trafficking and recycling
IMPA1	Regulates inositol levels for cell signaling
PEBP1	Inhibits the Raf-1 signaling pathway
PLEK	Major protein kinase C substrate; triggers platelet activation
RHG01	Regulates Rho GTPases
Immune & Stress-Response Proteins	
UBA1	Ubiquitin-activating enzyme (E1)
UBE2V2	Ubiquitin conjugation; DNA damage response
SAP (APCS)	Innate immunity; amyloid binding
FCN3	Lectin pathway of complement activation
ANXA5	Apoptosis marker; membrane repair
CLH1	Clathrin-mediated endocytosis
ARRB1	GPCR signalling regulation
1B46	MHC Class I molecule; presents antigens to T-cells
FA49B	Suppresses Macropinocytosis; involved in T-cell activation
SPB6	Protease inhibitor that prevents cell death from internal enzymes

3.3.2.1.2 Proteins increased in abundance in MM.1S cells-platelet secretome (fold change ≥ 1.5 and p value ≤ 0.05) compared to both, MM.1S cell secretome and platelet releasate

To better understand the interaction network of proteins increased in abundance in the MM.1S–platelet secretome, a STRING protein–protein interaction (PPI) analysis was performed. The resulting network is illustrated in **Figure 25**, which highlights the connectivity and interaction strength among the proteins.

As shown in **Figure 26,** KEGG pathway and Gene Ontology (GO) biological process enrichment analysis revealed that the proteins increased in abundance

upon platelet–MM.1S cell co-incubation were predominantly associated with pathways involved in platelet aggregation, focal adhesion, actin cytoskeletal regulation, and leukocyte trans-endothelial migration.

Differential protein expression between the MM.1S cell-platelet secretome and MM.1S cell secretome was visualised using a volcano plot using a threshold fold change value ≥ 1.5 and p-value ≤ 0.05 **[Figure 27(A)].** This visualisation highlights proteins that are significantly increased or decreased in abundance upon platelet interaction, indicating platelet-driven modulation of the MM.1S proteome. A second volcano plot **[Figure 27 (B)],** compares the proteomic profile of the MM.1S cell-platelet secretome with that of the platelet releasate.

Table 5 and
Table 6 list all the top proteins that were increased in abundance in the MM.1S cell-platelet secretome when compared to the MM.1S cell secretome and platelet releasate, respectively.

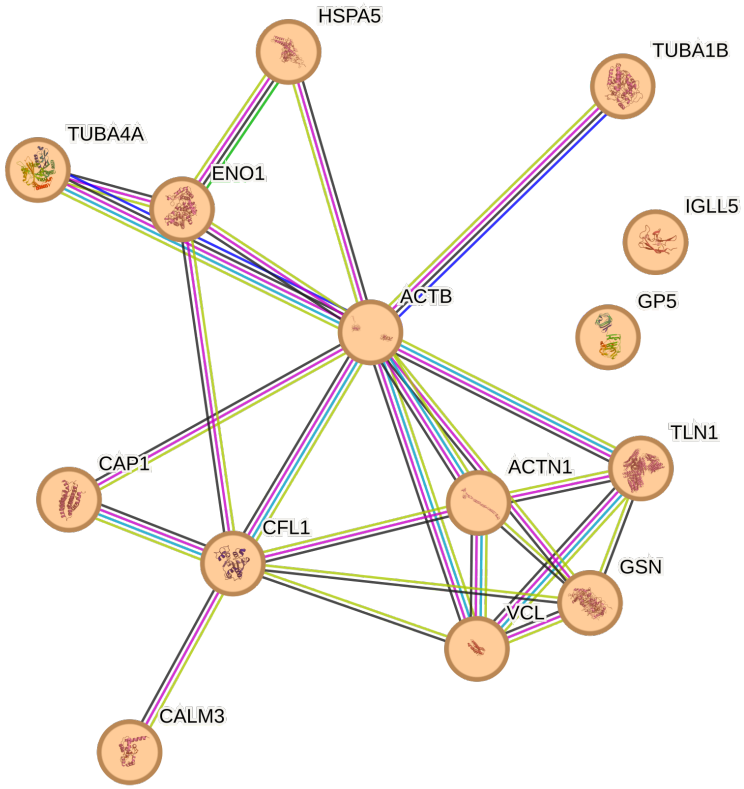

Figure 25 STRING protein interaction map depicting all the proteins increased in abundance in the MM.1S cell-platelet secretome. The nodes represents the proteins and the lines indicate the interaction. More number of lines indicate a stronger interaction.

(i)

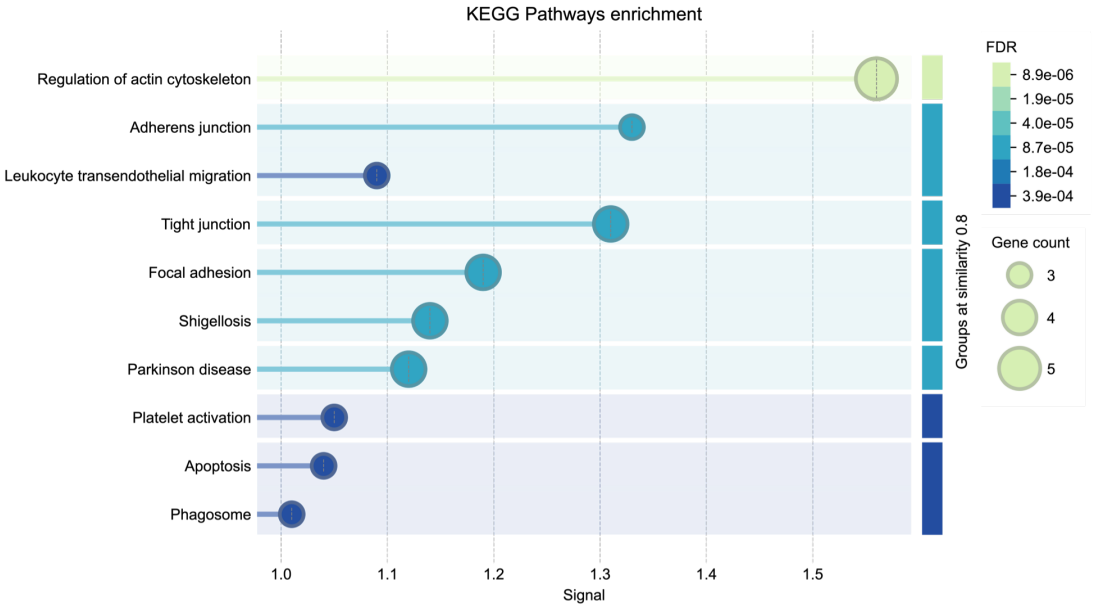

(ii)

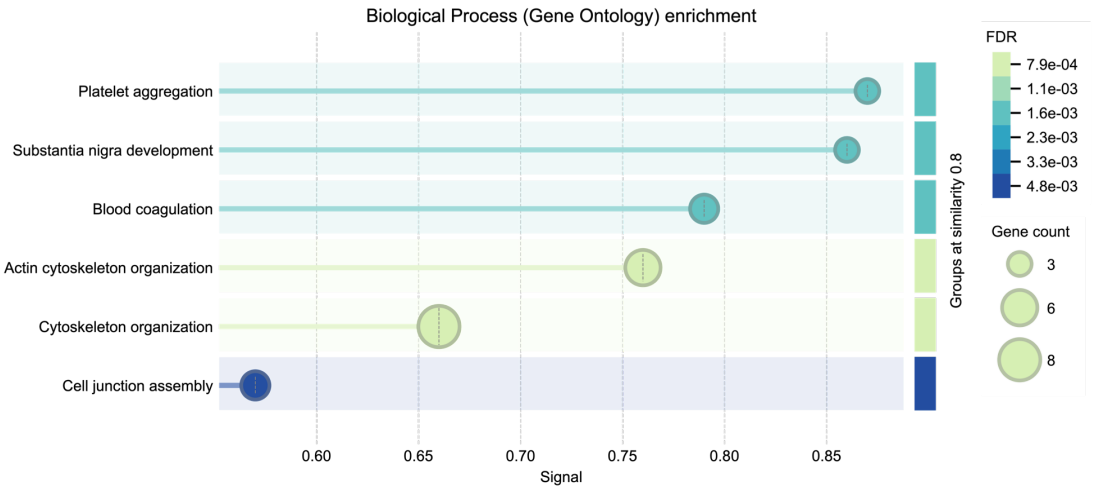

Figure 26 The enrichment analysis of proteins increased in abundance by the co-incubation of MM.1S cells with platelets, based on (i) KEGG pathway and, (ii) biological process (Gene Ontology), provided by the STRING database.

(i) Proteins in MM.1S cell-platelet secretome vs MM.1S cell secretome

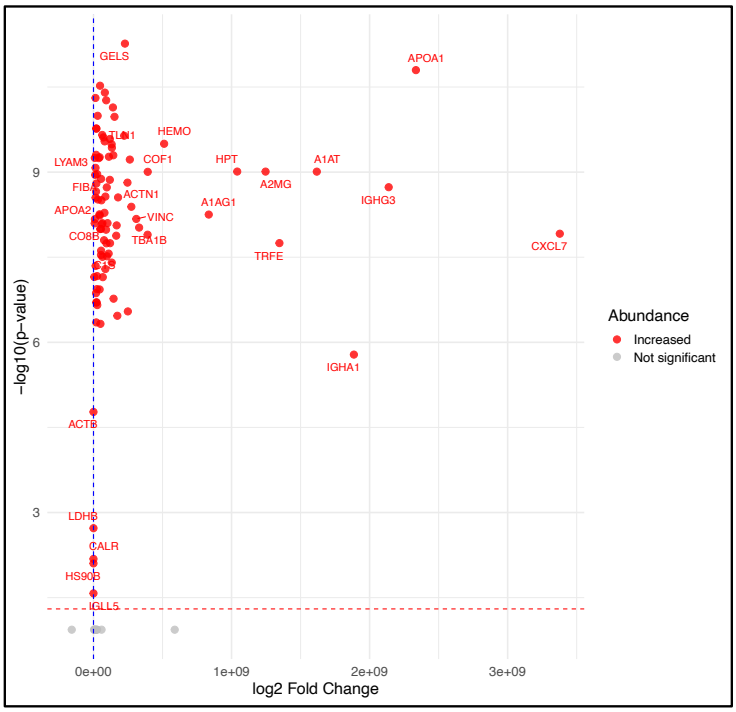

(ii) Proteins in MM.1S cell-platelet secretome vs platelet releasate

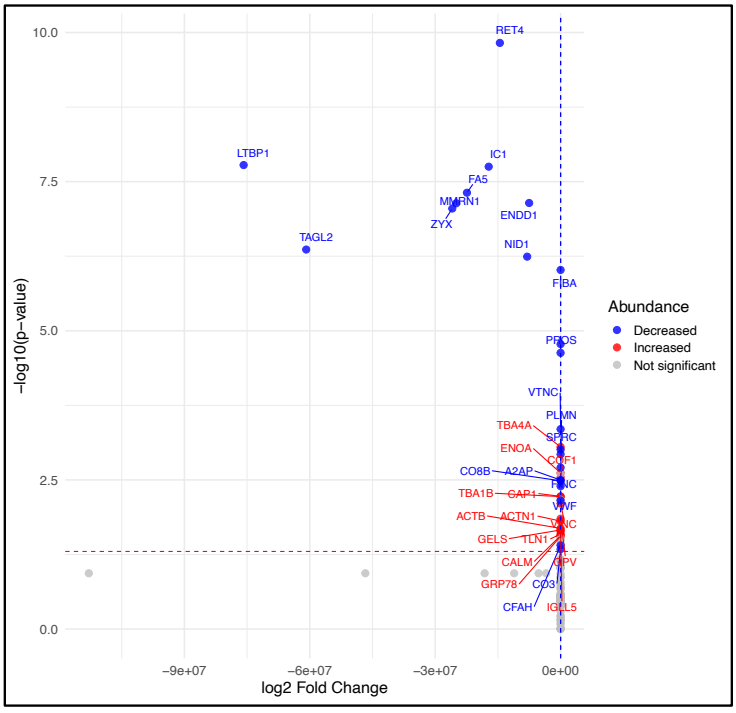

Figure 27 Differential Protein Abundance in the MM.1S cell-platelet secretome. Volcano plot illustrating significantly altered proteins when comparing i) MM.1S cell-platelets secretomes to MM.1S cell secretomes ii) MM.1S cell-platelets secretomes to platelet releasate. Proteins are plotted by Log2 fold change and –log10(p-value). Proteins exceeding the significance thresholds (fold change > 1.5, $p < 0.05$) are labelled in either red (increased in abundance) or blue (decreased in abundance). Created using R studio (version 2023.06.2+561).

Table 5 Top 10 proteins increased in abundance in MM.1S cell-platelet secretome compared to MM.1S cell secretome

Protein IDs	Fold change	p-value	Biological Role
COF1	3.93×10^{8}	9.87×10^{-10}	Actin depolymerization
TBA1B	3.31×10^{8}	9.49×10^{-9}	Microtubule component
VINC	2.63×10^{8}	6.68×10^{-9}	Focal adhesion linker
ACTN1	3.10×10^{8}	4.08×10^{-9}	Actin filament crosslinking
TBA4A	2.74×10^{8}	6×10^{-10}	Microtubule component
GELS	2.27×10^{8}	5.43×10^{-12}	Actin filament severing
CAP1	1.68×10^{8}	8.69×10^{-9}	Actin turnover regulation
ENOA	1.33×10^{8}	5.02×10^{-10}	Glycolysis enzyme
TLN1	1.33×10^{8}	3.72×10^{-10}	Actin filament crosslinking
GPV	8.62×10^{7}	2.69×10^{-9}	Platelet adhesion

Table 6 Top 10 proteins increased in abundance in MM.1S cell-platelet secretome compared to platelet releasate

Protein IDs	Fold change	p- value	Biological role
CAP1	7.48	0.0060	Actin turnover regulation
VINC	6.35	0.0079	Focal adhesion linker
ENOA	5.95	0.0024	Glycolysis enzyme
TBA4A	5.77	0.0009	Microtubule component

TBA1B	5.59	0.0060	Microtubule component
COF1	5.13	0.0029	Actin depolymerization
IGLL5	4.13	0.0229	B-cell development
CALM	4.12	0.0271	Calcium signalling
TLN1	3.55	0.0256	Actin filament crosslinking
ACTN1	3.36	0.0155	Actin filament crosslinking

3.3.2.1.3 Proteins increased in abundance in MM.1S cell-platelet releasate secretome (fold change ≥ 1.5 and p value ≤ 0.05)

When the MM.1S cells were incubated with platelet releasate, a total of 101 proteins were expressed in the cell-platelet releasate samples. Out of those proteins, only 4 proteins were found to be increased in abundance (fold change ≥ 1.5 and p value ≤ 0.05) compared to both the cell secretome and platelet releasate. These proteins were A1AT (Alpha-1-antitrypsin), PLSL (Plastin-2), UB2V2 (Ubiquitin-conjugating enzyme E2 variant 2), and LDHA (L-lactate dehydrogenase A chain).

3.3.2.2 JJN-3 Proteomics Data

3.3.2.2.1 Proteins enriched only in the JJN-3 cell-platelet secretome

Out of the total 203 proteins enriched across samples, 63 proteins were uniquely expressed in the presence of platelets. Their STRING data mapping is shown in **Figure 28**. The KEGG and GO enrichment analyses of the proteins shown in **Figure 29** indicate that most of the proteins are associated with carbon metabolism and participate in platelet activation, tight junctions, and focal adhesions.

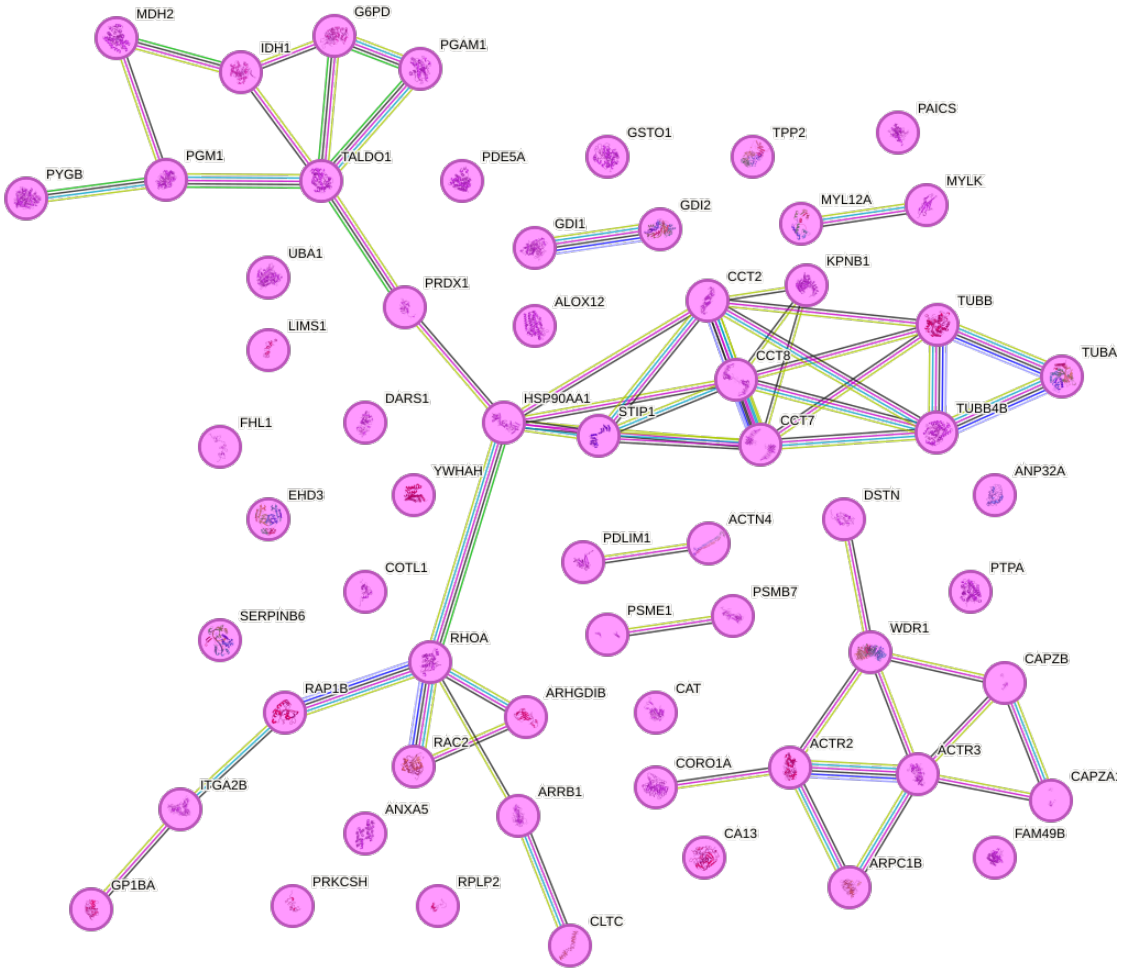

Figure 28 STRING protein interaction map depicting all the proteins enriched only by JJN-3 cell-platelet secretome. More number of lines indicate a stronger interaction.

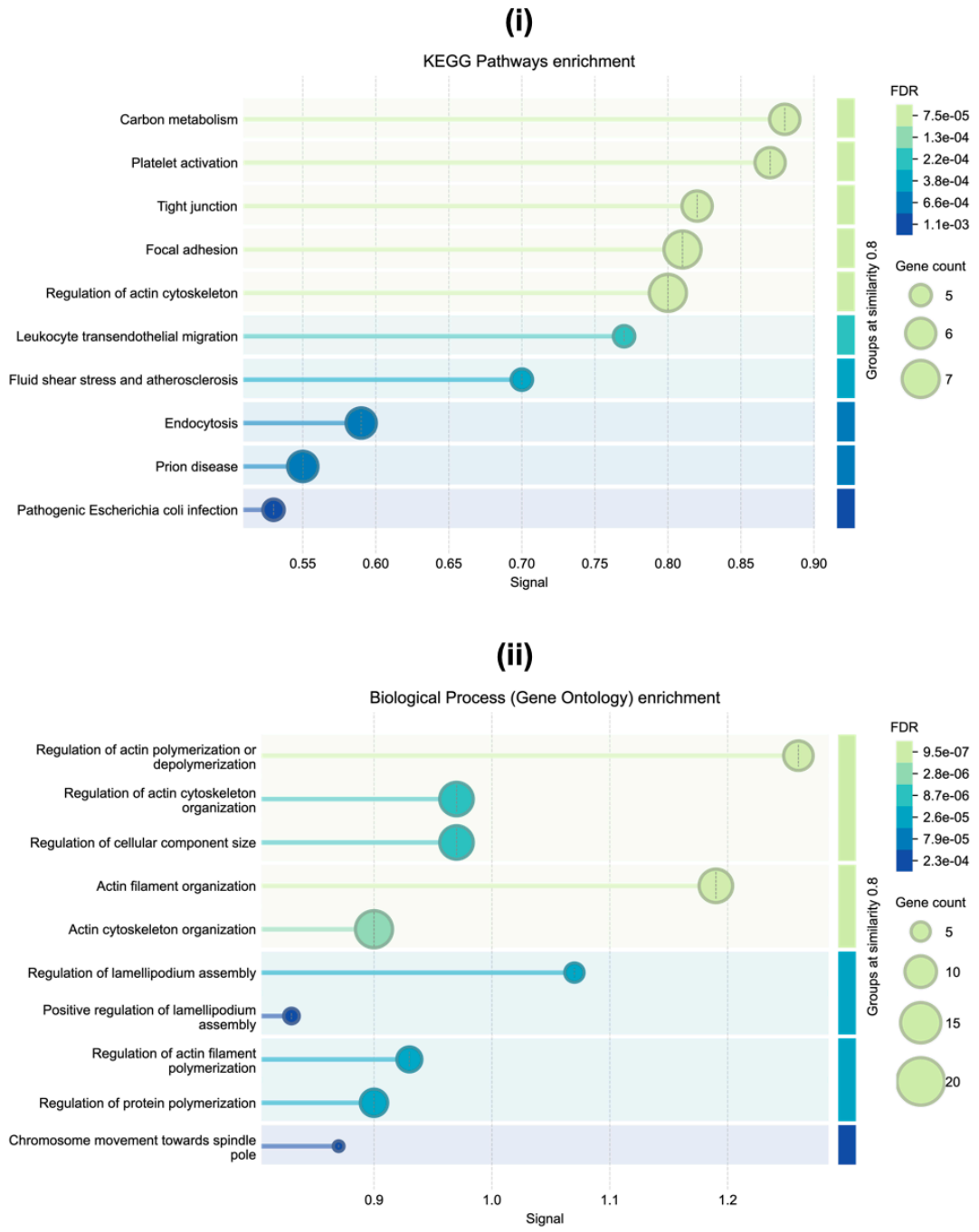

Figure 29 The enrichment analysis of proteins expressed only by the co-incubation of platelets and JJN-3 cells, based on (i) KEGG pathway and (ii) biological process (Gene Ontology), provided by the STRING database

Table 7 List of all the proteins enriched only in JJN-3 cell-platelet secretome along with their biological role

Protein ID	Biological Role
CYTOSKELETON AND ADHESION	
ARP2 / ARP3	Actin nucleation (Arp2/3 complex)
ACTN4	Actin crosslinking
CAPZB	Actin filament capping
COR1A	Actin-binding / Immune cytoskeleton
DEST	Actin depolymerization
TBA8 / TBB5	Microtubule structural proteins
CLH1	Endocytosis / Vesicle formation
LIMS1	Focal adhesion signalling
TBB4B	Microtubule structural proteins
WDR1	actin filament disassembly
ML12A	Non-muscle myosin II structural component
ITA2B	cell-cell adhesion and clotting.
COTL1	actin cytoskeleton organization
PDLI1	Scaffold to anchor proteins
CAZA1	Actin capping
ARC1B	Branches actin filaments
METABOLISM	
G6PD	Pentose phosphate pathway / NADPH production
PGM1	Carbohydrate metabolism
TALDO	Pentose phosphate pathway
IDHC	TCA cycle / NADPH production
CATA	Antioxidant defence (catalase)

PRDX1	Peroxide detoxification
LOX12	Lipid oxidation / Eicosanoid synthesis
GSTO1	Glutathione-dependent detoxification
PDE5A	cGMP signalling regulation
PGAM1	glycolysis (converts 3-PG to 2-PG)
PYGB	glycogenolysis
MDHM	TCA cycle for ATP production
GLU2B	Trims glucose from glycoproteins
TPP2	Protein turnover
SYDC	Protein translation
PUR6	Purine nucleotides biosynthesis
STRESS RESPONSE AND PROTEASOMES	
HS90A	Molecular chaperone (Hsp90)
HSP77	Heat shock protein
TCPB / TCPQ / TCPH	Chaperonin complex (CCT/TRiC)
STIP1	Hsp70–Hsp90 co-chaperone
PSME1 / PSB7	Proteasome regulation
RLA2	Protein synthesis and ribosomal stability
AN32A	mRNA transport
UBA1	Ubiquitin-Proteasome system
SPB6	Inhibits intracellular proteases
SMALL GTPASES AND SIGNALLING	
RAP1B	Small GTPase / Integrin activation
RHOA / RAC2	Actin cytoskeleton regulation
GP1BA	Platelet adhesion receptor

GDIR2 / GDIA	Rho/Rab GTPase regulation
ANXA5	Phospholipid binding / Anticoagulation
ARRB1	GPCR signalling regulation
FHL1	Muscle development and assembly signaling.
GDIB	Regulates Rho GTPases
EHD3	Vesicle trafficking
MYLK	Myosin contraction.
FA49B	Suppresses Macropinocytosis; involved in T-cell activation
1433F	Signal transduction and apoptosis regulation
PTPA	Activates PP2A phosphatase
IMB1	Nuclear transport
CAH13	Regulates cellular pH

3.3.2.2.2 Proteins increased in abundance in JJN-3 cell-platelet secretome compared to both JJN-3 cell secretome and platelet releasate (fold change ≥ 1.5 and p value ≤ 0.05)

To characterise how the proteins increased in abundance within the JJN-3 cell–platelet secretome functionally relate to one another, a STRING protein–protein interaction analysis was performed as depicted in **Figure 30**. **Figure 31** maps out the KEGG and GO enrichment analysis based on the biological process, respectively. Similar to the proteins increased in abundance in the MM.1S cell-platelet secretome, the majority of these proteins are associated with focal adhesion, regulation of actin-cytoskeleton, platelet aggregation, blood coagulation, and cell morphogenesis.

Differential protein expression between the JJN-3 cell-platelet secretome and JJN-3 cell secretome was visualised using a volcano plot using a threshold fold change value ≥ 1.5 and p-value ≤ 0.05 [**Figure 32** (i)]. This visualisation highlights proteins that are significantly increased or decreased in abundance upon platelet interaction, indicating platelet-driven modulation of the JJN-3 cell secretome. A

second volcano plot [**Figure 32** (ii)], compares the proteomic profile of the JJN-3 cell-platelet secretome with that of the platelet releasate.

Table 8 and **Table 9** list the top 10 proteins increased in abundance in the JJN-3 cell-platelet secretome compared to the JJN-3 cell secretome and the JJN-3 cell-platelet secretome compared to the platelet releasate, respectively.

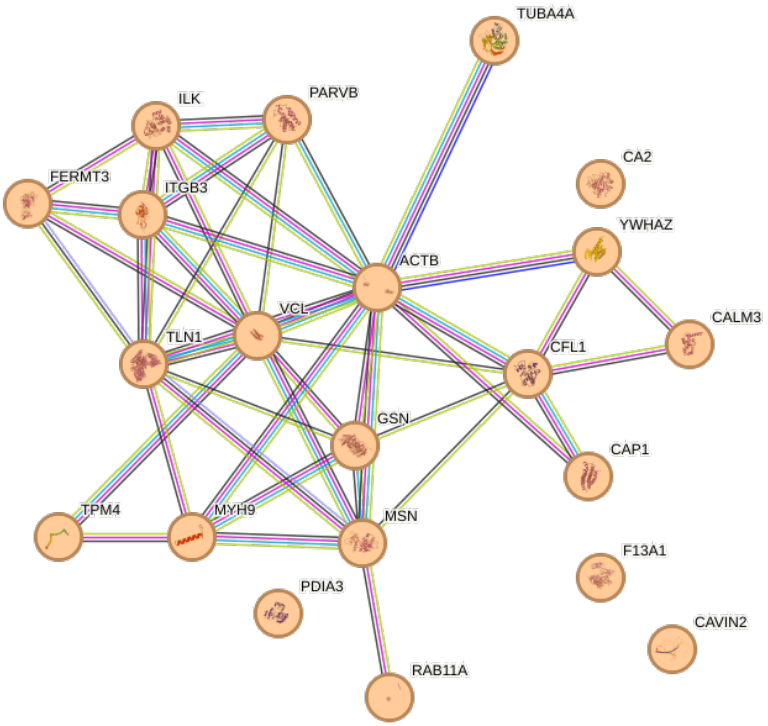

Figure 30 STRING protein interaction map depicting proteins increased in abundance in JJN-3 cell-platelet secretome (fold change ≥ 1.5 and p value ≤ 0.05)

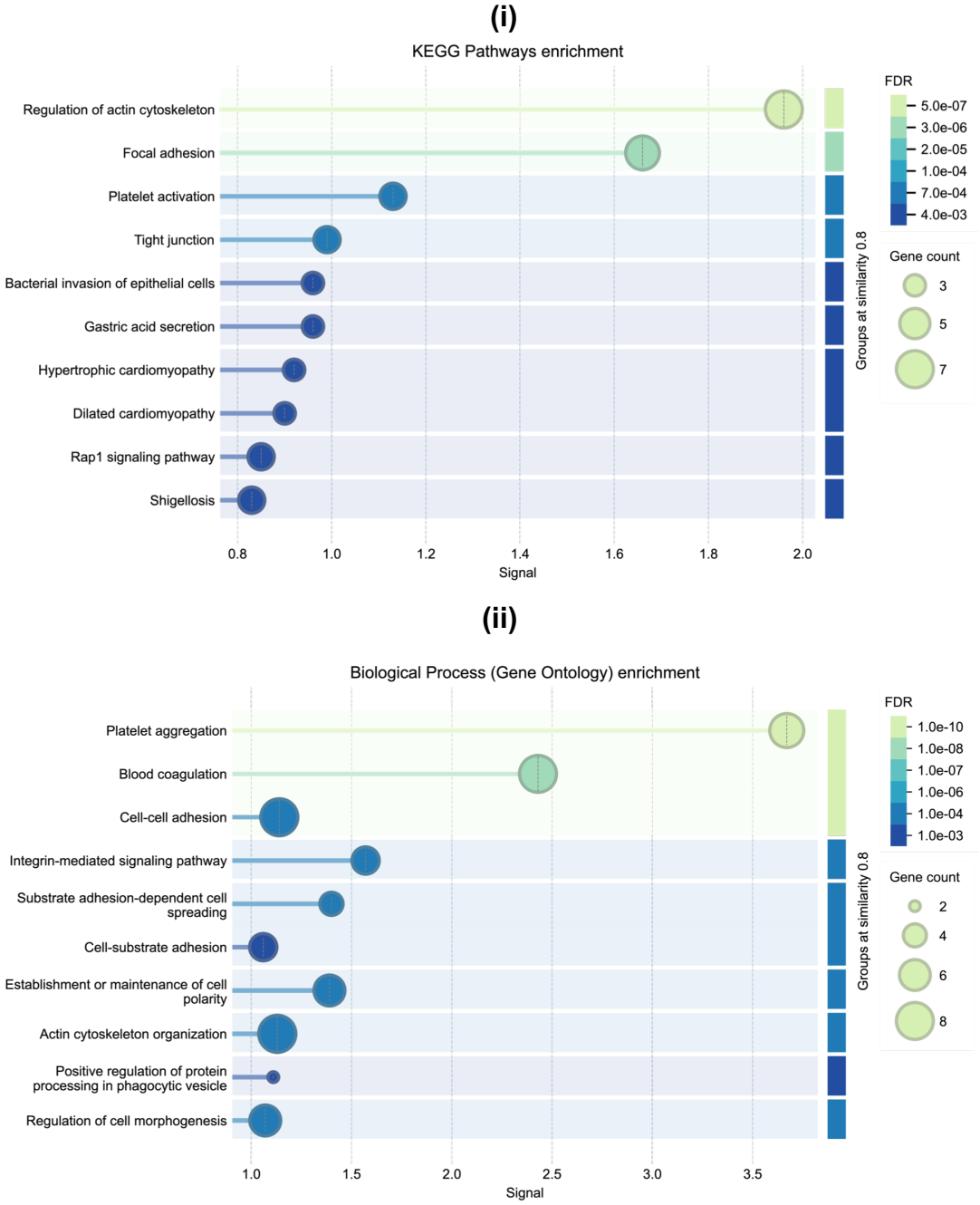

Figure 31 The enrichment analysis of proteins increased in abundance in the presence of JJN-3 cells and platelets, based on (i) KEGG pathway and (ii) biological process (Gene Ontology), provided by the STRING database.

(i) Proteins in JJN-3 cell-platelet secretome vs JJN-3 cell secretome

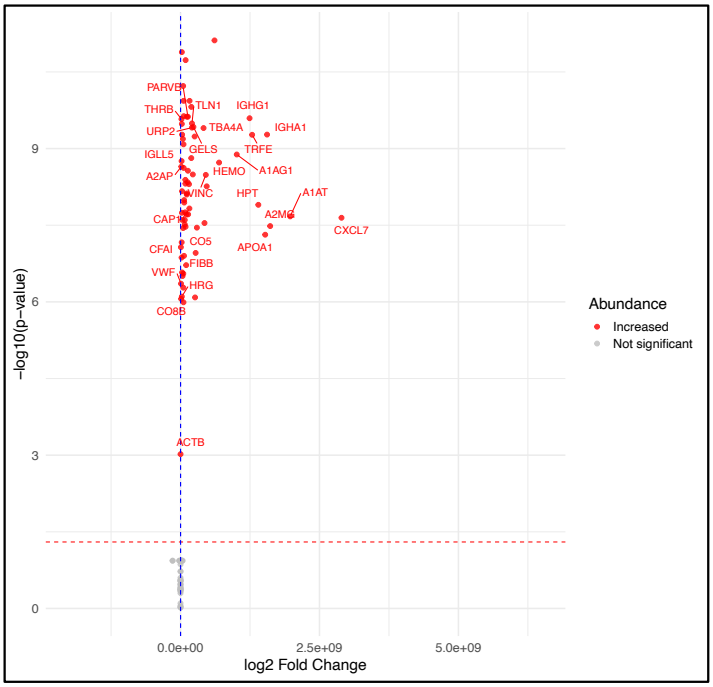

(ii) Proteins in JJN-3 cell-platelet secretome vs platelet releasate

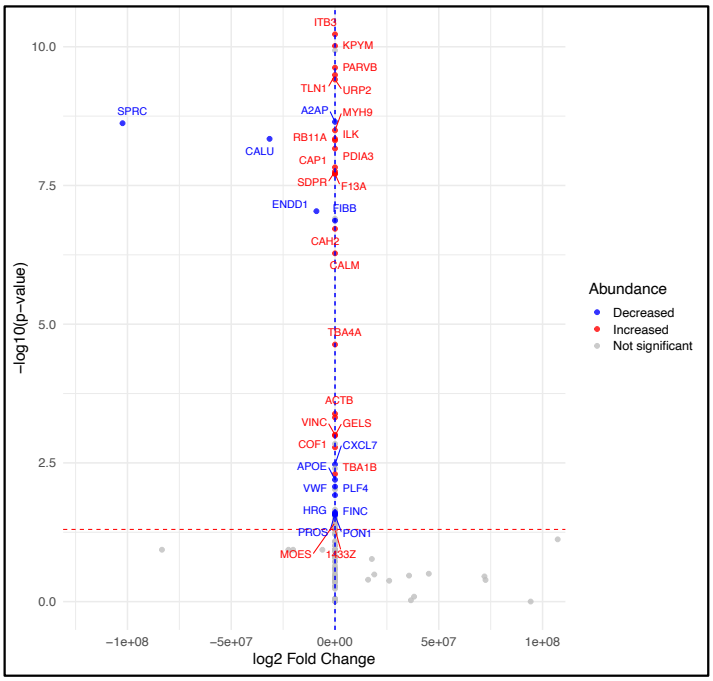

Figure 32 Differential Protein Abundance in the JJN-3 cell-platelet secretome. Volcano plot illustrating significantly altered proteins comparing i) JJN-3 cell-platelet secretome to JJN-3 cell secretome ii) JJN-3 cell-platelet secretome to platelet releasate. Proteins are plotted by Log2 fold change and –log10(p-value). Proteins exceeding the significance thresholds (fold change > 1.5, $p < 0.05$) are labelled in either red (increased in abundance) or blue (decreased in abundance). Created using R studio (version 2023.06.2+561).

Table 8 Top 10 proteins increased in abundance in JJN-3 cell-platelet secretome vs JJN-3 cells alone

Protein ID	Fold Change	p -value	Biological Role
COF1	6.11×10^{8}	7.63×10^{-12}	Actin depolymerization
VINC	4.54×10^{8}	3.27×10^{-9}	Focal adhesion linker
TBA4A	4.14×10^{8}	3.96×10^{-10}	Microtubule component
GELS	2.32×10^{8}	3.78×10^{-10}	Actin filament severing
MYH9	2.21×10^{8}	3.21×10^{-9}	Actomyosin contractility
TLN1	2.06×10^{8}	3.22×10^{-10}	Integrin activation
URP2	2.05×10^{8}	3.89×10^{-10}	Actin cytoskeleton regulation
CAP1	1.59×10^{8}	1.48×10^{-8}	Actin turnover regulation
TPM4	1.37×10^{8}	1.94×10^{-8}	Actin filament stabilization
PARVB	132244577.8	2.38×10^{-10}	Actin cytoskeleton / Focal adhesion

Table 9 Top 10 proteins increased in abundance in JJN-3 cell-platelet secretome compared to releasate control

Protein ID	Fold Change	p- value	Biological Role
VINC	8.65	0.00098	Focal adhesion linker
TBA4A	8.28	2.33×10^{-5}	Microtubule component

MYH9	7.36	3.21×10^{-9}	Actomyosin contractility
1433Z	6.19	0.049	Signal transduction / Cell cycle regulation
COF1	5.95	0.0016	Actin depolymerization
CAP1	5.89	1.49×10^{-8}	Actin turnover regulation
ITB3	5.29	5.96×10^{-11}	Cell adhesion / Cell–matrix interaction
TLN1	4.96	3.22×10^{-10}	Integrin activation
ILK	4.67	4.56×10^{-9}	Cell adhesion signalling
PARVB	3.93	2.38×10^{-10}	Actin cytoskeleton / Focal adhesion

3.3.2.2.3 Proteins increased in abundance in JJN-3 cells-platelet releasate secretome (fold change ≥ 1.5 and p value ≤ 0.05)

Out of the 106 proteins expressed in the cell-platelet releasate secretome, only SDC2 (syndecan-2) was increased in abundance compared to both the cell secretome and the platelet releasate. Expression of proteins associated with metabolism did not differ significantly from the cell secretome.

3.3.2.3 KMS-27 Proteomics Data

3.3.2.3.1 Proteins expressed only in the KMS-27 cell-platelet secretome

A total of 781 proteins were expressed across all samples, out of which 91 proteins were only expressed in the KMS-27 cell-platelet secretome. A protein-protein interaction map is depicted in **Figure 33**. The biological function of these proteins is presented in **Table 10.** **Figure 34** presents enrichment analyses of these

proteins for biological processes (GO) and KEGG pathways. The majority of the proteins are associated with metabolic pathways, blood coagulation and platelet development.

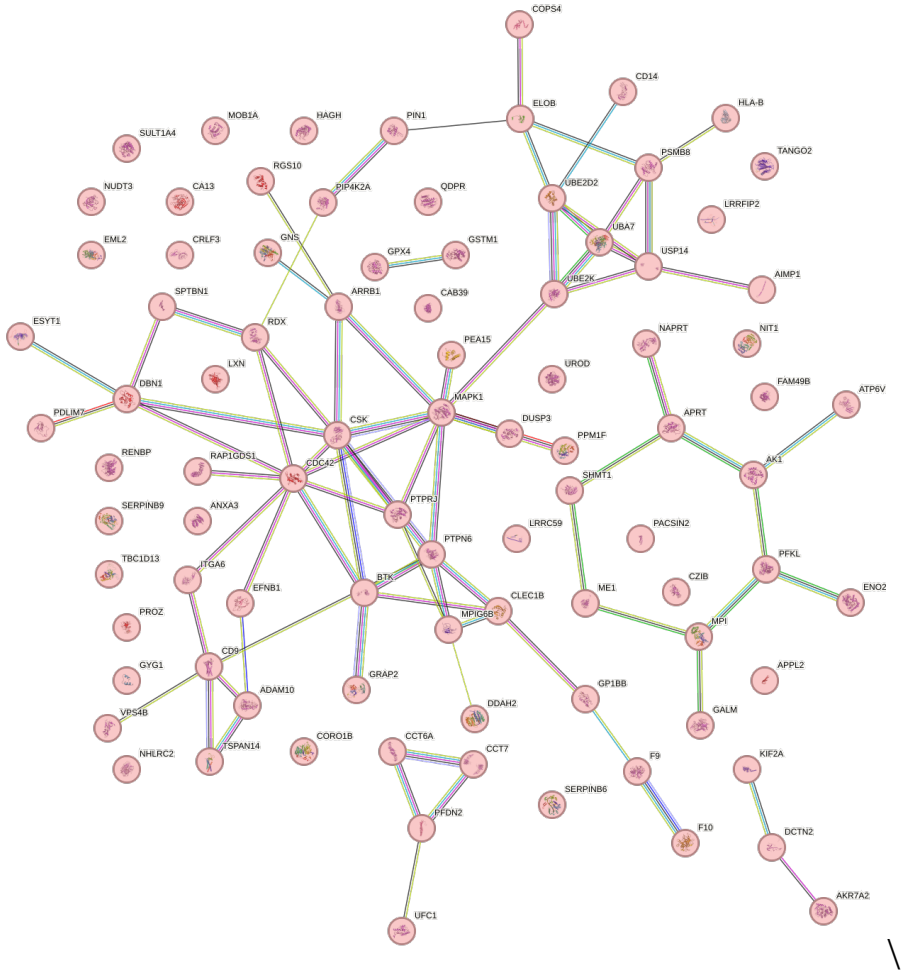

Figure 33 STRING protein interaction map depicting all the proteins enriched only by the KMS-27- platelet interaction

Table 10 Biological function of all the proteins expressed only in the KMS-27 cell- platelet secretome

Protein ID	Biological Role
METABOLISM	
KAD1	Nucleotide metabolism
APT	Purine salvage
GPX1	Response to oxidative stress, peroxide metabolism
GPX4	Lipid peroxide metabolism

ENOG	Glycolysis
GSTM1	Glutathione-dependent detoxification
PFKAL	Glycolysis
GLYC	One-carbon metabolism
MPI	Mannose metabolism
MAOX	Malate metabolism, NADPH production
ARK72	Aldehyde detoxification
DDAH2	Arginine metabolism, nitric oxide regulation
NUDT3	Polyphosphate hydrolysis
DCUP	Heme biosynthesis
DHPR	Tetrahydrobiopterin regeneration
GNS	Glycosaminoglycan catabolism
ST1A3	Sulfation of small molecules
RENBP	Sialic acid biosynthesis
GLO2	Methylglyoxal detoxification
PNCB	NAD+ biosynthesis
NIT1	Nitrogen compound metabolism
CAH13	Carbon dioxide hydration
GALM	Galactose metabolism
VATA	ATP-driven proton pump component
GLYG	Glycogen biosynthesis
PROTEIN HOMEOSTASIS AND MODIFICATION	
ADA10	Cleaves membrane proteins
VPS4B	Endosomal sorting

PSB8	Proteasomal degradation
SPB6	Protease inhibition
TCPZ	Protein folding
UBA7	Ubiquitination
SPB9	Protease inhibition
UBP14	Deubiquitination
UB2D2	Ubiquitin conjugation
UBE2K	Ubiquitin conjugation
TCPH	Protein folding
PFD2	Protein folding
UFC1	Ubiquitin-like modification
TNG2	Golgi trafficking
PACN2	Endocytic trafficking
ESYT1	Lipid transfer, membrane trafficking
CELLULAR SIGNALLING AND REGULATION	
KIF2A	Microtubule-based motor, regulates dynamics
RGS10	Modulates G-protein signalling
GRAP2	Immune signalling adapter
MK01	MAPK signalling
PTN6	Dephosphorylation in signalling
CSK	Src kinase regulation
ARRB1	GPCR signalling regulation
PPM1F	Protein dephosphorylation
DUS3	MAPK dephosphorylation

CDC42	Rho GTPase signalling
GDS1	Rap1 signalling regulation
EFNB1	Eph receptor signalling
BTK	B-cell receptor signalling
PTPRJ	Receptor signalling regulation
PIN1	Protein conformation regulation
PEA15	Apoptosis signalling regulation
MOB1A	Hippo pathway regulation
CSN4	Signalosome-mediated regulation
DP13B	Adapter in signalling pathways
CAB39	Regulates AMPK signalling
CELL STRUCTURE AND ORGANIZATION	
EMAL2	Microtubule organization
RADI	Actin-membrane linkage
SPTB2	Cytoskeletal organization
DCTN2	Microtubule-based transport
DREB	Actin cytoskeleton organization
COR1B	Actin cytoskeleton regulation
IMMUNE RESPONSE AND CELL COMMUNICATION	
FA9	Blood coagulation
FA10	Blood coagulation
KV105	Immune response (immunoglobulin component)
CD14	Innate immune response
ANXA3	Immune modulation, phagocytosis

GP1BB	Platelet activation
CD9	Cell adhesion, immune signalling
PROZ	Coagulation regulation
ITA6	Cell adhesion
1B44	Antigen presentation (MHC class I)
G6B	Platelet signalling; immune receptor on platelets
TSN14	Cell surface organization, signalling
CLC1B	Innate immune response
CRLF3	Cytokine-mediated signalling
AIMP1	Cytokine activity
LXN	Protease inhibition, immune modulation
PDLI7	Cell adhesion, signalling
LRC59	ER-membrane protein, potential immune role
LRRF2	Innate immune regulation
NHLC2	Potential immune signalling
FA49B	Immune cell regulation
TBC13	GTPase regulation, potential immune signalling
CA123	mitochondrial oxidative phosphorylation

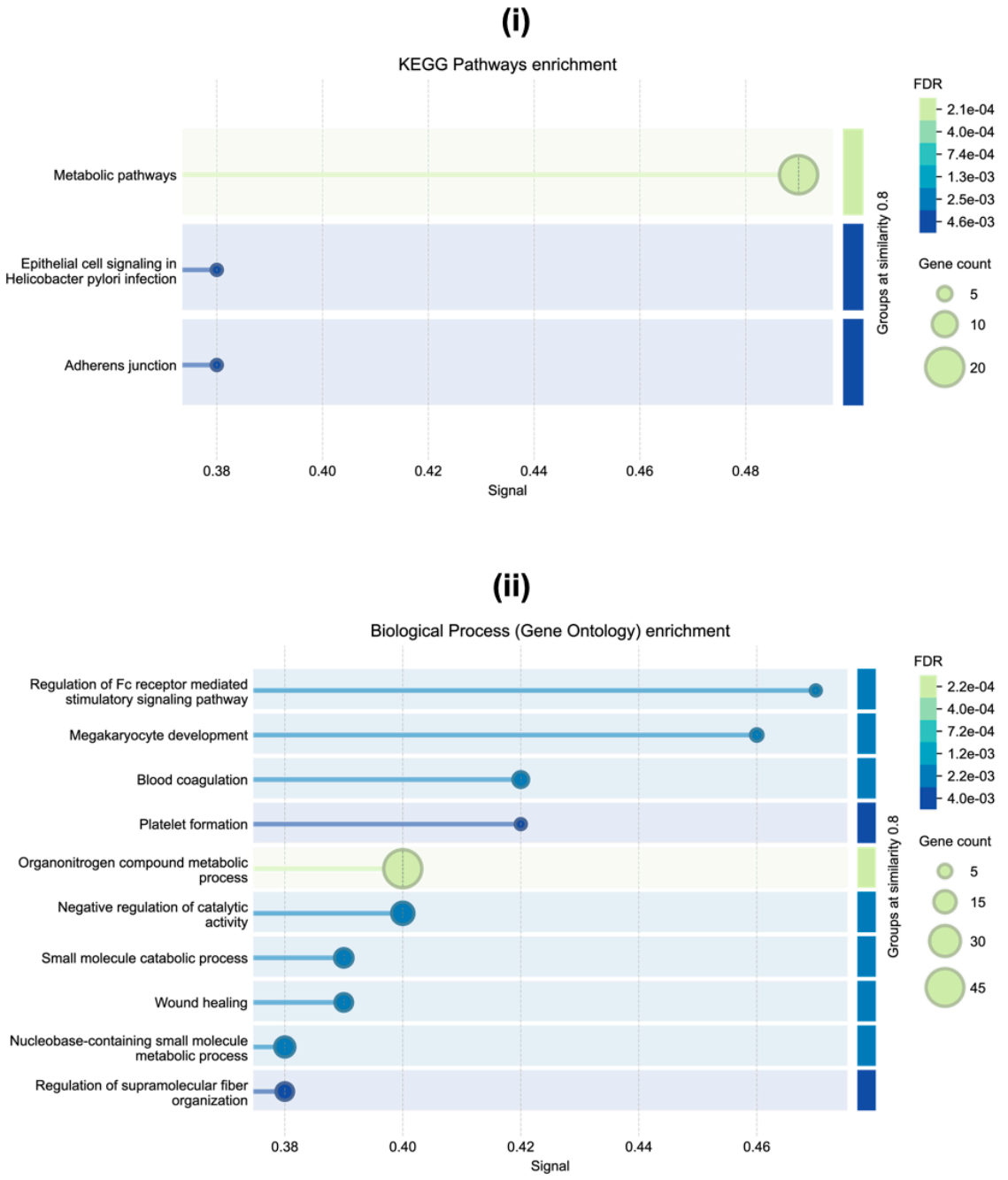

Figure 34 The enrichment analysis of proteins expressed by the co-incubation of platelets and KMS-27 cells, based on the biological process (GO) pathway, provided by the STRING database

3.3.2.3.2 Proteins increased in abundance in KMS-27 cell-platelet secretome compared to both, KMS-27 cell secretome and platelet releasate (fold change ≥ 1.5 and p value ≤ 0.05)

A STRING protein interaction map is presented in **Figure 35.** Similarly, protein enrichment is analysed using KEGG pathways and biological functions (GO) (**Figure 36**). The majority of these abundant proteins were associated with

glutathione and carbon metabolism, as well as glycogenesis. In addition, there are pathways related to actin–cytoskeletal organisation, suggesting changes in cell shape, adhesion, and motility.

A volcano plot illustrating proteins that are differentially increased or decreased in abundance during KMS-27 cell–platelet co-incubation is shown in **Figure 37**, comparing (A) co-incubated cells with untreated cells and (B) co-incubated cells with platelet releasate. Out of these, the top 10 proteins increased in abundance along with their fold change and p-values are presented in **Table 11** and **Table 12**.

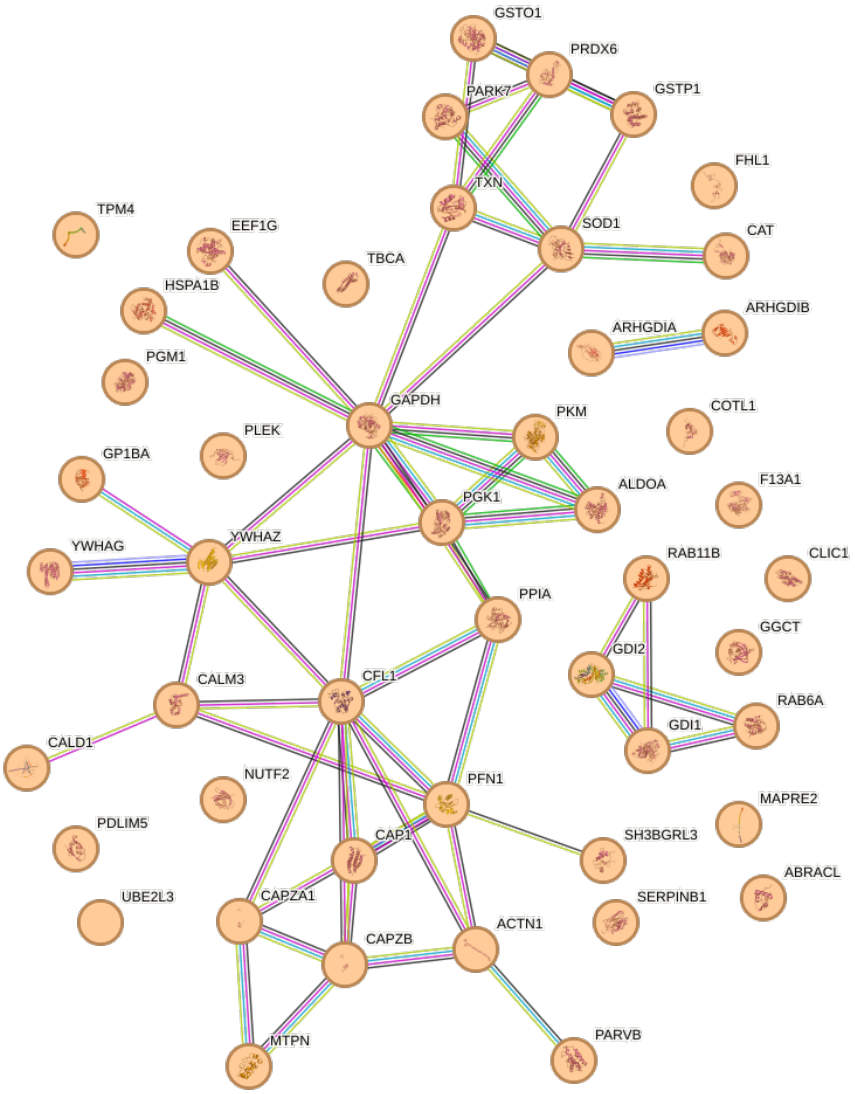

Figure 35 STRING protein interaction map depicting proteins increased in abundance in KM2-27 cell- platelet secretome (fold change ≥ 1.5 and p value ≤ to 0.05)

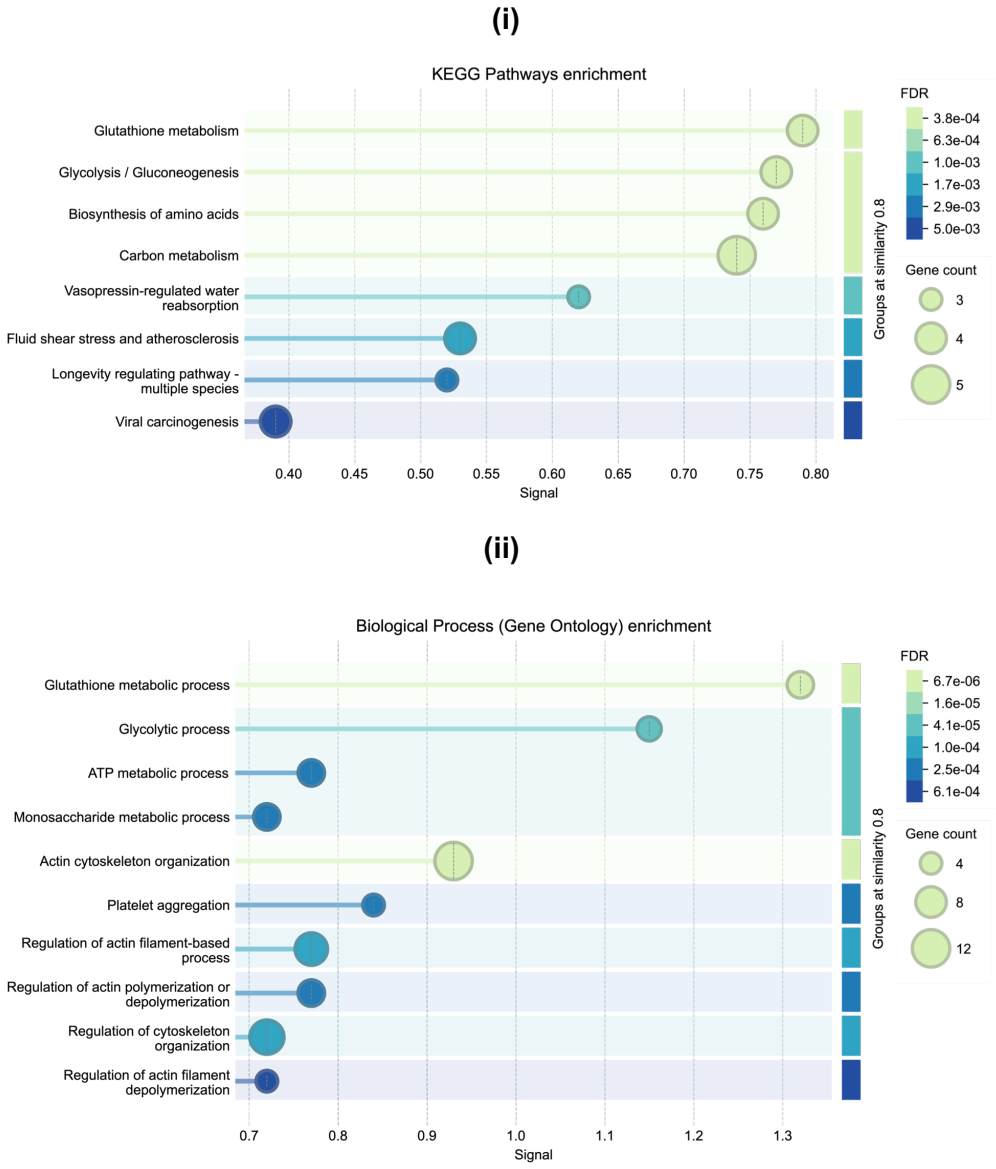

Figure 36 The enrichment analysis of proteins increased in abundance in KMS-27 cell-platelet secretomes, based on (i) KEGG pathway and (ii) biological process (GO), provided by the STRING database

(i) Proteins in KMS-27 cell-platelet secretome vs KMS-27 cell secretome

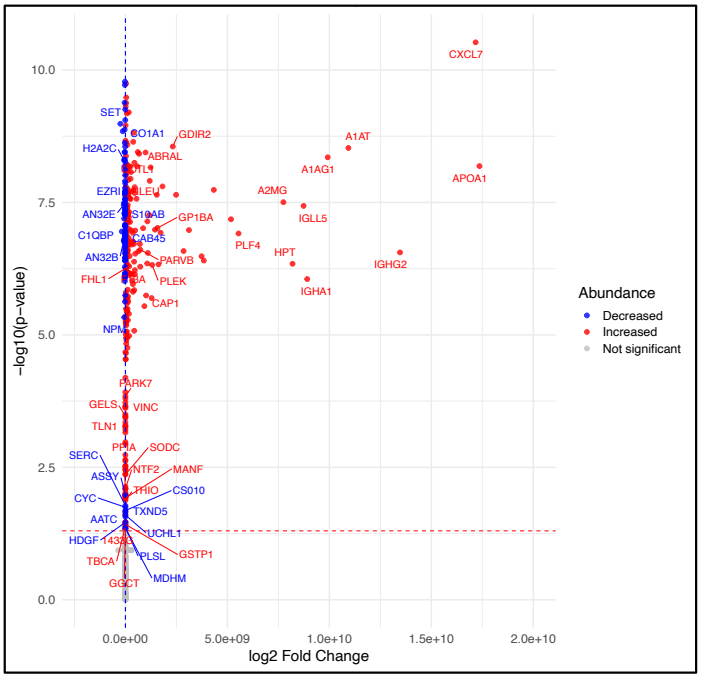

(ii) Proteins in KMS-27 cell-platelet secretome vs platelet releasate

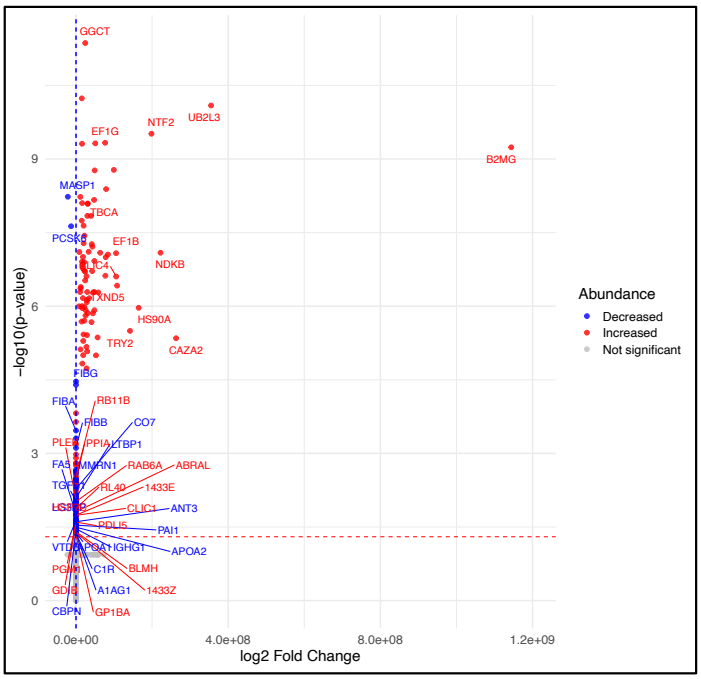

Figure 37 Differential protein abundance in the KMS-27 cell-platelet secretome. Volcano plot illustrating significantly altered proteins after comparing i) KMS-27 cell-platelet secretomes to KMS-27 cell secretomes ii) KMS-27 cell- platelet secretomes to platelet releasate. Proteins are plotted by Log2 fold change and –log10(p-value). Proteins exceeding the significance thresholds (fold change > 1.5, $p < 0.05$) are labelled in either red (increased in abundance) or blue (decreased in abundance). Created using R studio (version 2023.06.2+561).

Table 11 Top 10 proteins increased in abundance in the KMS-27 cell-platelet secretome when compared to the KMS-27 cell secretome

Protein ID	Fold Change	p-value	Biological Role
GDIR2	2.32×10^{9}	2.78×10^{-9}	Rho GTPase regulation
GP1BA	1.57×10^{9}	9.57×10^{-8}	Platelet adhesion receptor
PLEK	1.31×10^{9}	4.78×10^{-7}	Cytoskeletal signalling; involved in platelet activation
ABRAL	1.23×10^{9}	6.89×10^{-9}	Actin cytoskeleton regulator
CAP1	9.31×10^{8}	2.87×10^{-6}	Actin turnover regulation
PARVB	7.3×10^{8}	2.46×10^{-7}	Focal adhesion and actin binding
F13A	7.29×10^{8}	5.16×10^{-7}	Blood coagulation factor
COTL1	2.52×10^{8}	1.13×10^{-8}	Actin filament binding
FHL1	1.79×10^{8}	5.07×10^{-7}	Muscle signalling scaffold
ILEU	1.51×10^{8}	2.18×10^{-8}	Inhibits neutrophil elastase

Table 12 Top 10 proteins increased in abundance in the KMS-27 cell-platelet secretome when compared to the platelet releasate

Protein ID	Fold Change	p-value	Biological Role
UB2L3	3.55×10^{8}	8.1241×10^{-11}	Ubiquitination / Protein degradation

NTF2	1.98×10^{8}	3.06×10^{-10}	Nuclear transport
EF1G	5.07×10^{7}	4.79×10^{-10}	Protein synthesis (translation)
TBCA	4.77×10^{7}	6.82×10^{-9}	Cytoskeleton assembly (microtubule biogenesis)
GGCT	2.44×10^{7}	4.33×10^{-12}	Glutathione metabolism
PGM1	9.42	0.026	Carbohydrate metabolism
PLEK	8.83	0.0088	Signal transduction / Cytoskeleton regulation
RB11B	7.87	0.0029	Vesicle trafficking (endosomal recycling)
CLIC1	7.28	0.018	Ion transport / Redox regulation
GDIB	7.12	0.027	Vesicle trafficking regulation

3.3.2.4 U266 Proteomics Data

3.3.2.4.1 Proteins enriched only in U266 cell-platelet secretome

A total of 690 proteins were detected across all U266 samples, of which 266 were uniquely expressed when U266 cells were co-incubated with platelets (**Table 13**). A protein–protein interaction map of these proteins is shown in **Figure 38**, and the enriched pathways based on biological function (GO) and KEGG pathway are depicted in **Figure 39**. The majority of these proteins are associated with key metabolic and biosynthetic pathways. Several proteins were linked to the proteasome, metabolic pathways, particularly carbon metabolism, and tRNA aminoacylation.

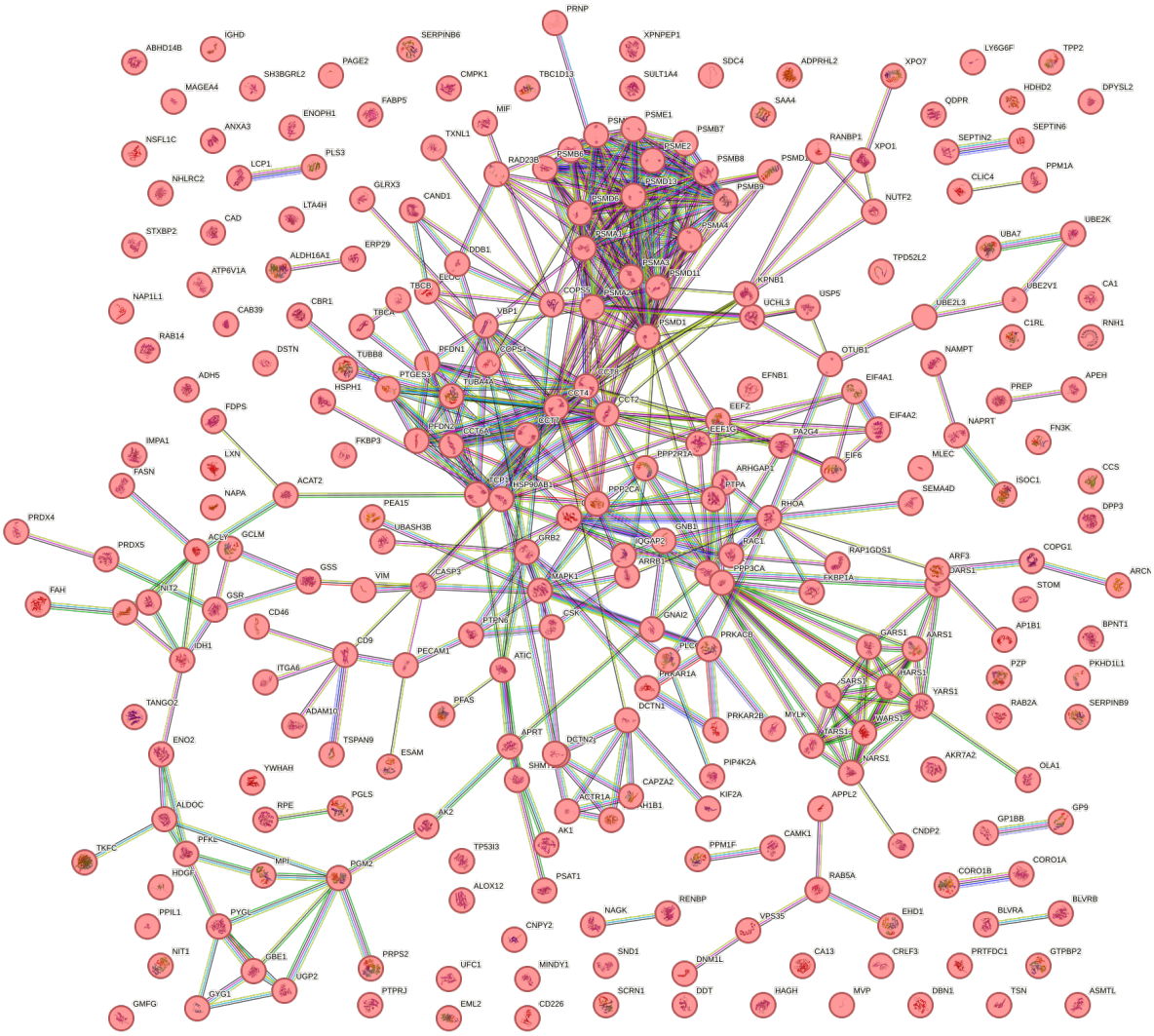

Figure 38 STRING protein interaction map depicting proteins enriched in the U266 cells- platelet secretome

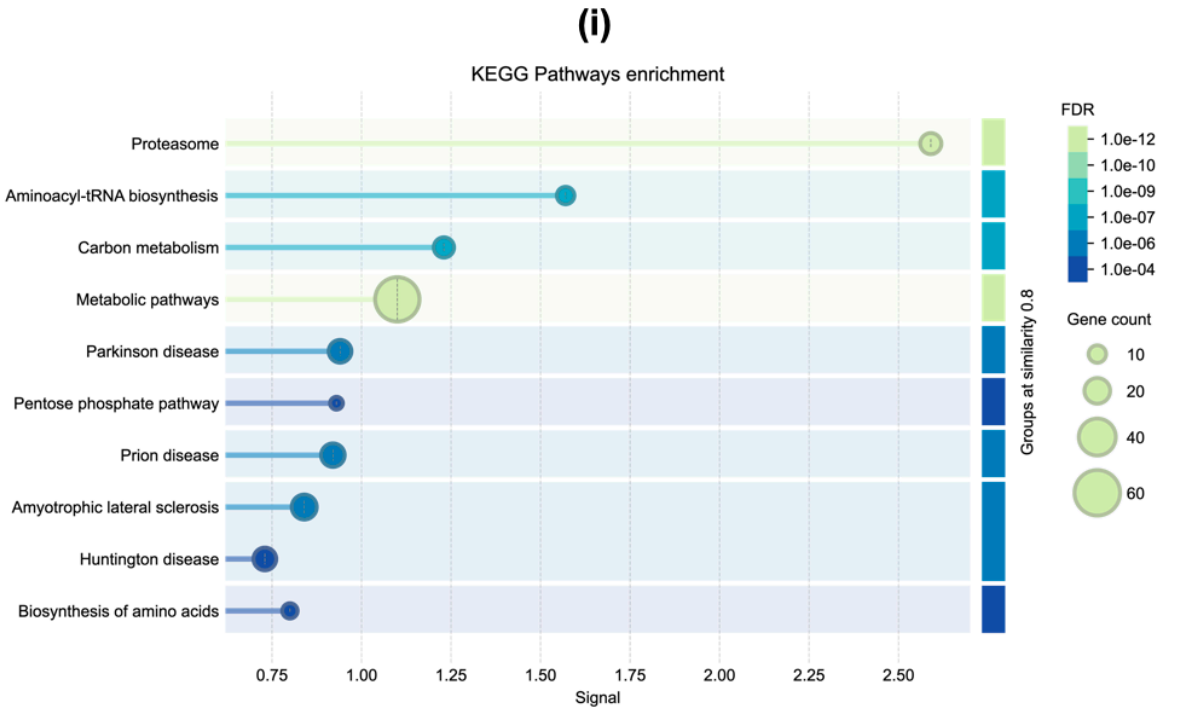

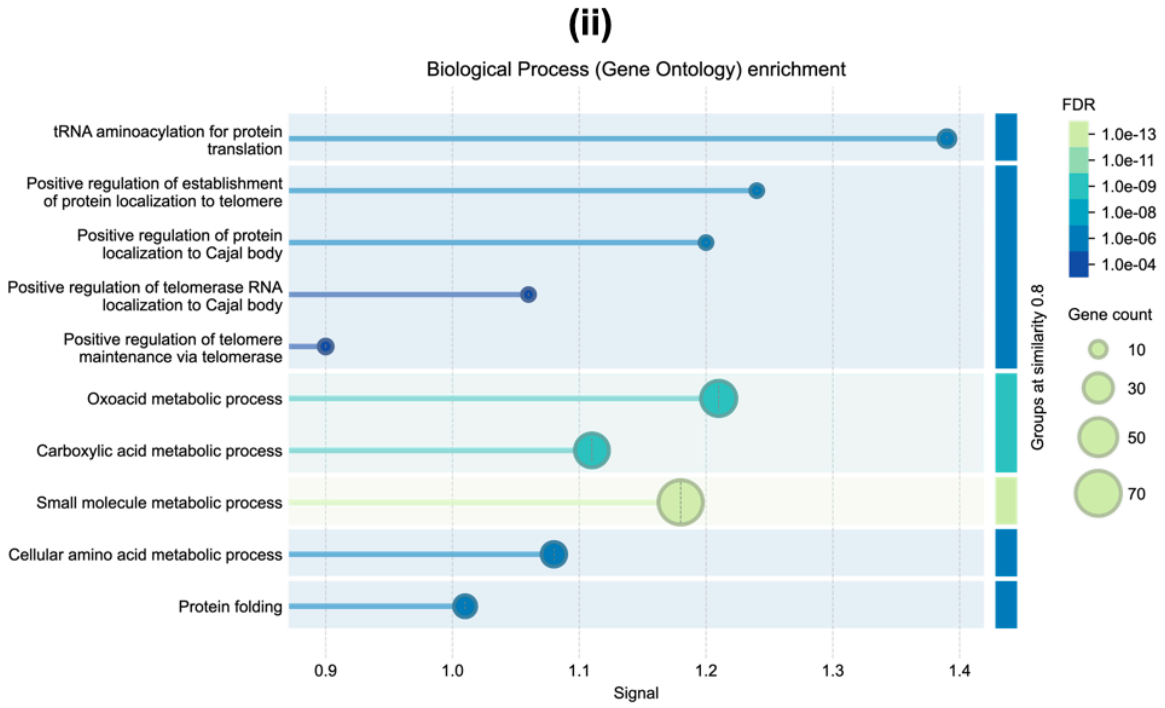

Figure 39 The enrichment analysis of proteins expressed by the co-incubation of platelets and U266 cells, based on (i) KEGG pathway and (ii) biological process (GO) pathway, provided by the STRING database

Table 13 Proteins enriched only in the U266 cell-platelet secretome along with their biological role

Protein ID	Biological Role
ACLY	Links glucose to lipid synthesis
ADHX	Formaldehyde/alcohol detoxification
ALDOC / ENOG / PFKAL	Core enzymes of the glycolysis pathway
ARK72	Aldehyde detoxification
ASML	Sphingolipid metabolism
BPNT1	Sulfur metabolism; scavenging
CAH1 / CAH13	Carbon dioxide hydration
DHPR	Cofactor regeneration for metabolism
DOPD	D-amino-acid oxidase; amino acid metabolism
FAAA	Tyrosine degradation
FUMH	Citric acid cycle (TCA) component

GLGB / GLYG	Glycogen synthesis
GLO2	Detoxification of methylglyoxal
GLYC	Carbon metabolism
GSHR / GSH0 / GSHB	Glutathione production and recycling
GPX1 / PRDX4	Antioxidants; peroxide neutralization
IDHC / 6PGL / RPE	Pentose phosphate pathway; NADPH production
IMPA1	Inositol signalling and metabolism
KAD1 / KAD2 / PRPS2	Nucleotide/Adenylate metabolism
MPI / UGPA	Mannose and sugar interconversion
NAGK	Amino sugar metabolism
NAMPT	NAD+ biosynthesis
PGM2 / PYGL	Glycogen and glucose-1-P conversion
ST1A3	Sulfation of small molecules.
SYAC/ SYDC/ SYEP/SYHC/SYWC	tRNA synthetases; amino acid charging for synthesis.
VATA	ATP-driven proton pump component
ENOPH	Methionine salvage pathway; amino acid metabolism
FN3K	Repairs glycated proteins (deglycation)
DHAK	Carbohydrate metabolism; phosphorylates dihydroxyacetone
QORX	Detoxification
GLRX3	Iron homeostasis and redox regulation
LOX12	Lipid metabolism
FABP5	Intracellular fatty acid transport and lipid signalling
PUR4/PUR9	First step in de novo purine nucleotide synthesis
NIT1/NIT2	Nitrogen compound metabolism
LKHA4	Leukotriene metabolism; inflammation

FPPS	Cholesterol/isoprenoid biosynthesis
CBR1	Drug/xenobiotic metabolism
SYTC	tRNA synthetase; protein synthesis
PYR1	Proline biosynthesis
APT	Purine salvage pathway
SERC	Serine biosynthesis
TNG2	ER–Golgi trafficking; metabolism
KCY	Nucleic acid synthesis
ISOC1	Kreb's cycle enzyme
PNCB	Preiss-Handler pathway
HDHD2	Metabolic hydrolase
A16A1	Alcohol metabolism
CAND1, CSN4, CSN5	Regulate the assembly of E3 ubiquitin ligases
ERP29	Protein folding and disulfide bond formation in the ER
HS90B, HS105	Heat-shock chaperones; protect proteins from stress
OTUB1, UCHL3, UBP5	Deubiquitinating enzymes; recycle ubiquitin tags
PFD1, PFD2, PFD3	Prefoldin complex; delivers proteins for folding
PSB2, PSB4, PSB6, PSB7, PSB8, PSB9	20S Proteasome core; breaks down proteins
PSD10, PSD11, PSD13	Proteasome regulatory subunits (19S lid)
PSMD1, PSMD6	Regulatory subunits of the degradation machinery.
PSA1/ PSA 2/ PSA 3/ PSA 4	Proteasome alpha subunits
TBA4A / TBB8	Tubulin subunits (building blocks)
TBCA/ TBCB/ TBC13	Tubulin-specific folding cofactors
TCPA/TCPB/TCPD/TCPH/TCPQ/ TCPZ)	CCT/TRiC complex; folds actin and tubulin
UBA7	E1 enzymes; start the ubiquitination process

UB2L3 / UBE2K / UB2V1	E2 enzymes; conjugate ubiquitin to targets
UFC1	UFM1-conjugating enzyme (ubiquitin-like)
EF2	Translation elongation
EF1G	Protein synthesis
IF6/IF4A1/IF4A2	Ribosome biogenesis & translation initiation
PPIL1	RNA splicing
PSME1/2	Protein degradation
RENBP	Sialic acid biosynthesis
ADA10	Cleaves membrane proteins
SPB6	Proteasome subunit; protein degradation
MLEC	ER protein folding; glycoprotein quality control
FA63A	Deubiquitination-associated protein
1433F	Signalling adapter; binds phosphoproteins
ARRB1	GPCR signalling regulation
CASP3	Main protease executing apoptosis
CDC42 / RAC1 / RHOA	Rho GTPases; regulate shape and growth signals
CSK	Inhibitor of Src-family kinases
DUS3	MAPK dephosphorylation/inactivation
EFNB1	Ephrin signalling; cell-to-cell communication
GNAI2 / GBB1	G-protein subunits for transmembrane signalling
GRB2	Adapter for growth factor receptor signalling
MK01	Essential kinase for growth and division signals
PEA15	Regulates MAPK signalling and blocks cell death
PLCG2	Phospholipase C; triggers calcium signalling
PP2AA / PP2BA	Phosphatases that turn off signalling cascades

PPM1A / PPM1F	Serine/threonine phosphatases for regulation
PTPRJ	Tyrosine phosphatases; regulate receptor activity
RAB2A/RAB5A/RAB14	Endosomal/vesicular trafficking
ARF3	Vesicle formation (Golgi)
TEBP	Telomere maintenance
KAP0	cAMP signalling regulation
SCRN1	Exocytosis regulation
2AAA	Serine/threonine dephosphorylation
ACPH	Tyrosine phosphatase; signaling regulation
RINI	Ras signaling; receptor endocytosis
PRIO	Prion protein; neuronal signaling/protection
SDC4	Cell adhesion; signaling
RHG01	Rho GTPase regulation
CRLF3	Cytokine receptor-like signaling
AP1B1 / COPG1 / COPD	Vesicle coating and cargo packaging
CAZA2	Regulate actin filament ends and recycling
COR1A / COR1B	Actin-binding for cell migration
DCTN1 / DCTN2	Dynactin motor helpers for vesicle transport
DEST	Actin-depolymerizing factor (ADF)
EHD1 / NSF1C	Endocytic recycling and membrane fusion
IMB1 / NTF2 / XPO1 / XPO7	Nuclear import/export of proteins and RNA
KIF2A / KAP3 / KAPCB	Microtubule-based motor, regulates dynamics
LIS1	Regulates dynein motor activity
MYLK	Myosin light chain kinase; contraction
RAB2A/ RAB 5A/ RAB 14	Small GTPases; manage vesicle docking/traffic

STOM / MVP	Membrane/vault proteins involved in transport
VIME	Intermediate filament; provides mechanical strength
STXB2	Vesicle trafficking & exocytosis
SND1	RNA regulation & gene expression
CNPY2	Protein folding & signalling modulation
RANG	Nuclear transport
PLSL	Actin bundling protein
PLST	Actin crosslinking in immune cells
EMAL2	Microtubule stabilization (EML family)
SYNC	Muscle cytoskeletal structural protein
GMFG	Actin remodeling; immune cell migration
ACTZ	Actin cytoskeleton component
IQGA2	Cytoskeleton scaffold; signaling integration
ARHL2	Small GTPase; microtubule dynamics
DREB	Actin-binding protein; neuronal growth
ANXA3	Membrane repair and immune modulation
CD9 / CD226	Cell adhesion and signalling in immune cells
CLIC4	Chloride ion channels for volume regulation
ESAM / ITA6	Endothelial/Integrin adhesion molecules
GP1BB / GPIX	Platelet receptors for clotting at wound sites
MIF	Pro-inflammatory immune cytokine
PECA1	Mediates leukocyte migration through vessels
PZP / IGHD	Plasma proteins; immunity and pregnancy
SAA4	Acute-phase protein in inflammation.
MCP	Regulates complement system; protects cells from immune damage

C1RL	Involved in complement activation and immune response
HDGF	Promotes cell growth, proliferation, and angiogenesis
TSN9	RNA binding; involved in RNA processing and regulation
DP13B	Intracellular peptide degradation
DPYL2	Neuronal development and axon guidance
BIEA	Converts biliverdin to bilirubin
LXN	Carboxypeptidase inhibitor; regulates cell growth
PKHL1	Structural protein in lens fiber cells of the eye
DNM1L	Mitochondrial fission and membrane remodelling
OLA1	Stress response and protein translation regulation
BLVRB	Heme metabolism and redox regulation
DPP3	Protein and peptide degradation
CNDP2	Dipeptide metabolism and cellular detoxification
TXNL1	Redox regulation; oxidative stress response
CCS	Copper chaperone for SOD1; antioxidant defense
TPD54	Vesicle trafficking; cell proliferation (TPD52 family)
TPP2	Cytosolic peptidase; protein turnover
PTN6	Tyrosine phosphatase; immune signaling
PRDX5	Antioxidant enzyme
PPCE	Propionyl-CoA metabolism
PI42A	Phosphoinositide signaling (likely PI4KA)
KCC1A	Potassium/chloride transport
LY66F	Immune-related surface protein (LY6 family)
SH3L2	Endocytosis; vesicle recycling
PA2G4	Cell growth & transcription regulation

CAB39	Kinase scaffold; LKB1 signaling pathway
FAS	Apoptosis receptor
SYSC	tRNA synthetase (serine)
SPB9	Serine protease inhibitor; immune protection
GDS1	Small GTPase signaling regulator
SYYC	Likely RNA-binding protein
RD23B	DNA repair; nucleotide excision repair
SNAA	Vesicle fusion; membrane trafficking
NP1L1	RNA splicing factor
FKB1A	Immunophilin; protein folding
FKBP3	Nuclear chaperone; transcription regulation
PTPA	PP2A phosphatase activator
ELOC	Transcription elongation; ubiquitin ligase complex
TSN	RNA binding; DNA repair
DDB1	DNA damage recognition; repair
NHLC2	Protein quality control; cytoskeleton
UBS3B	negative regulator of receptor-mediated signaling in immune cells
SEM4D	Immune signaling; axon guidance
ABHEB	Protein-lysine deacylase
VPS35	Endosomal protein sorting
THIC	Fatty acid oxidation
XPP1	Aminopeptidase; protein processing
PAGE2	Testis antigen; role in cancer
LV104	Antigen recognition
HV206	Antigen recognition

3.3.2.5 Proteins increased in abundance in U266 cell-platelet secretome compared to both, U266 cell secretome and platelet releasate (fold change ≥ 1.5 and p value ≤ 0.05)

STRING mapping of all the proteins increased in abundance is depicted in **Figure 40** and enrichment analysis of those proteins based on KEGG pathways and biological processes is shown in **Figure 41**. The majority of the proteins are associated with the phagosome, focal adhesion, platelet aggregation and regulation of cytoskeletal organisation. **Figure 42** presents volcano plots of proteins differentially regulated in the U266 cell-platelet secretome, with comparisons to (i) the U266 cell secretome and (ii) the platelet releasate. The proteins showing the highest increases in abundance, together with their fold-change values and statistical significance, are listed in **Table 14** and **Table 15.**

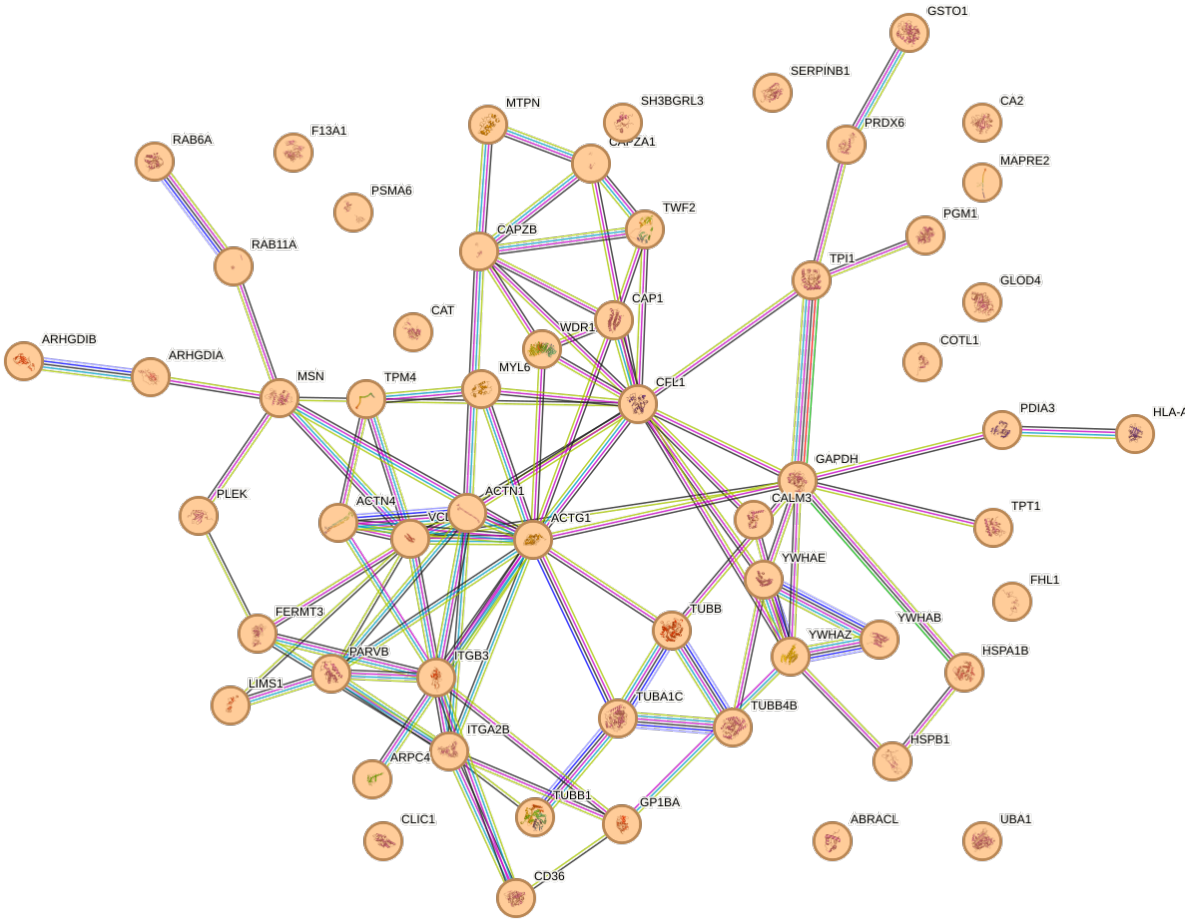

Figure 40 STRING protein interaction map depicting proteins increased in abundance in the U266 cells- platelet secretome (fold change ≥ 1.5 and p value ≤ 0.05)

(i)

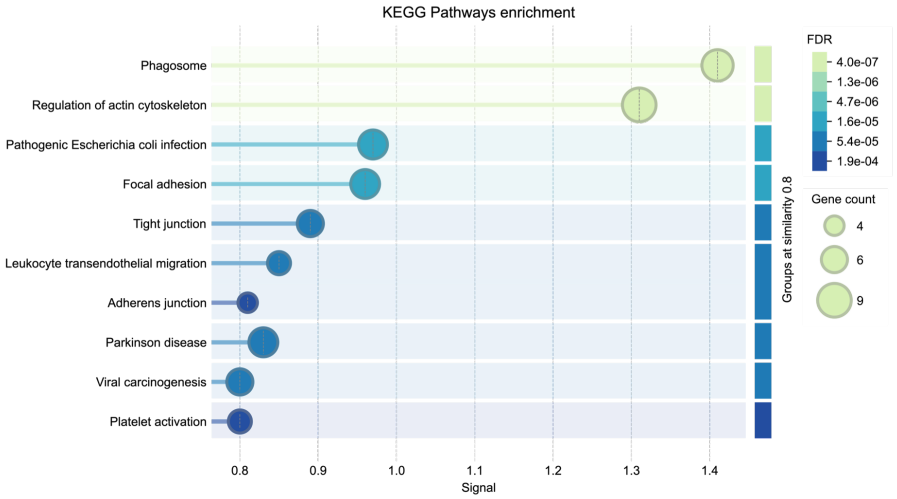

(ii)

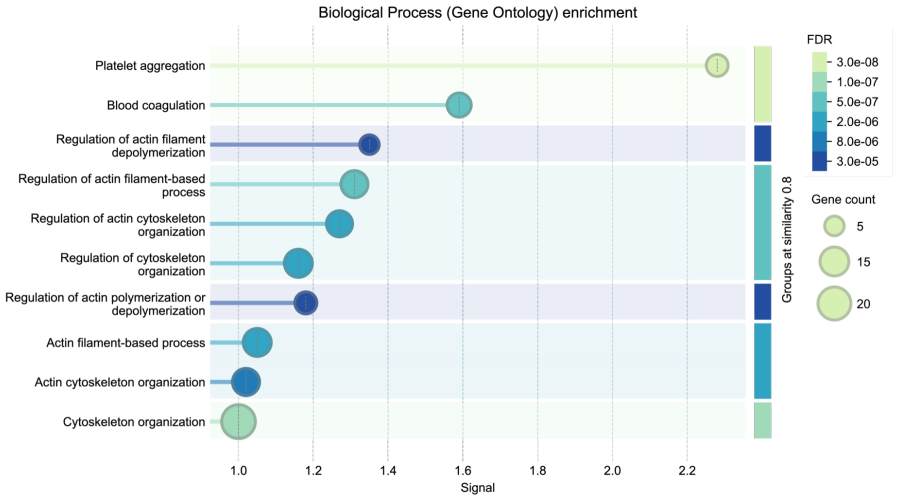

Figure 41 The enrichment analysis of proteins increased in abundance in the U266 cell-platelet secretome, based on (i) KEGG pathway and (ii) biological process (GO), provided by the STRING database

(i) Proteins in U266 cell-platelet secretome vs U266 cell secretome

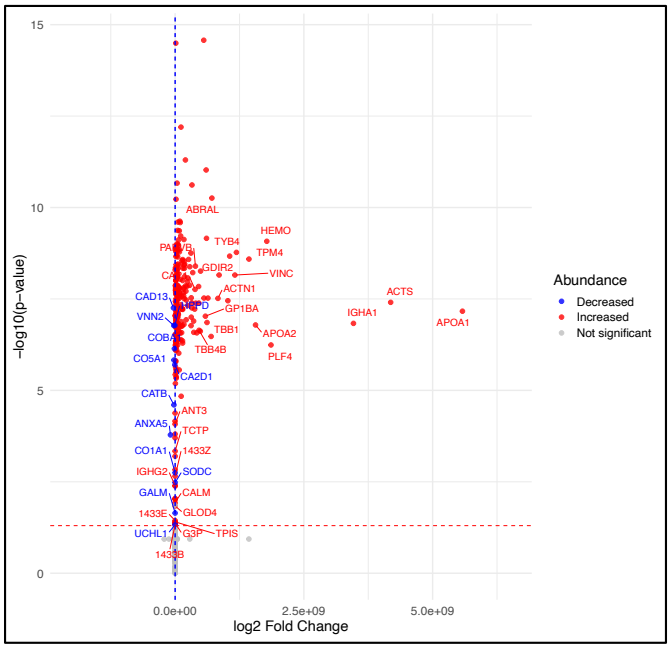

(ii) Proteins in U266 cell-platelet secretome vs platelet releasate

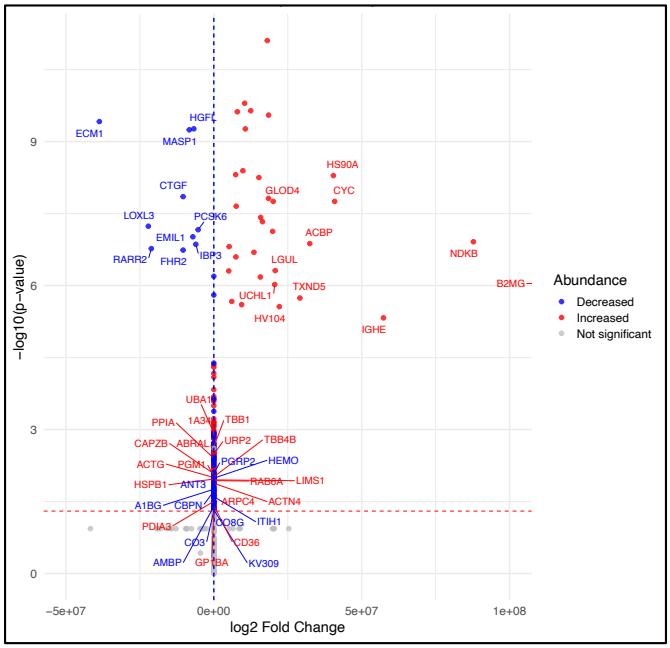

Figure 42 Differential protein abundance in the U266 cell-platelet secretomes. Volcano plots showing differentially expressed proteins after comparing (i) U266 cell-platelet secretomes to U266 cell secretomes. (ii) U266 cell-platelet secretomes to platelet releasate. Proteins are plotted by Log2 fold change and –log10(p-value). Proteins exceeding the significance thresholds (fold change > 1.5, $p < 0.05$) are labelled in either red (increased in abundance) or blue (decreased in abundance). Created using R studio (version 2023.06.2+561)

Table 14 Top 10 proteins increased in abundance in the U266 cell-platelet secretome when compared to the U266 cell secretome

Protein ID	Fold Change	p-value	Biological Role
TPM4	1.43×10^{9}	2.57×10^{-9}	Actin filament stabilization
VINC	1.16×10^{9}	7.02×10^{-9}	Focal adhesion linker
GDIR2	1.06×10^{9}	2.13×10^{-9}	Rho GTPase regulation
ACTN1	8.31×10^{8}	3.05×10^{-8}	Actin filament crosslinking
ABRAL	7.14×10^{8}	5.51×10^{-11}	Actin cytoskeleton regulator
TBB1	6.19×10^{8}	1.39×10^{-7}	Microtubule component
GP1BA	5.88×10^{8}	9.36×10^{-8}	Platelet adhesion receptor
TBB4B	4.65×10^{8}	2.27×10^{-7}	Microtubule component
PARVB	3.94×10^{8}	4.01×10^{-9}	Focal adhesion and actin binding
CAP1	3.87×10^{8}	1.73×10^{-8}	Actin turnover regulation

Table 15 Top 10 proteins increased in abundance in the U266 cell-platelet secretome when compared to the platelet releasate

Protein ID	Fold Change	p-value	Biological Role
GLOD4	2×10^{7}	1.76×10^{-8}	Detoxification/ Oxidative stress response
LIMS1	11.14	0.011	Cell adhesion & signalling
PGM1	10.16	0.0092	Carbohydrate metabolism

TBB1	9.59	0.0023	Cytoskeleton (microtubules)
CAPZB	8.92	0.0083	Actin cytoskeleton regulation
PRDX6	8.76	0.0063	Antioxidant defence
PDIA3	8.35	0.031	Protein folding (ER stress response)
HSPB1	7.88	0.011	Molecular chaperone / Stress response
UBA1	7.8	0.0012	Ubiquitination / Protein degradation
TBB4B	7.1	0.0097	Cytoskeleton (microtubules)

3.3.2.6 Identification of a common proteins signature across MM cell-platelet secretomes

The proteomic landscape of the four MM cell lines revealed a conserved secretome signature. The degree of proteomic overlap and the specific number of common proteins among the four lineages are depicted in the Venn diagram in **Figure 43**. Proteins consistently identified across all lines—comprising those exclusively enriched or significantly increased in abundance within the cell-platelet secretome—are detailed in **Table 16**.

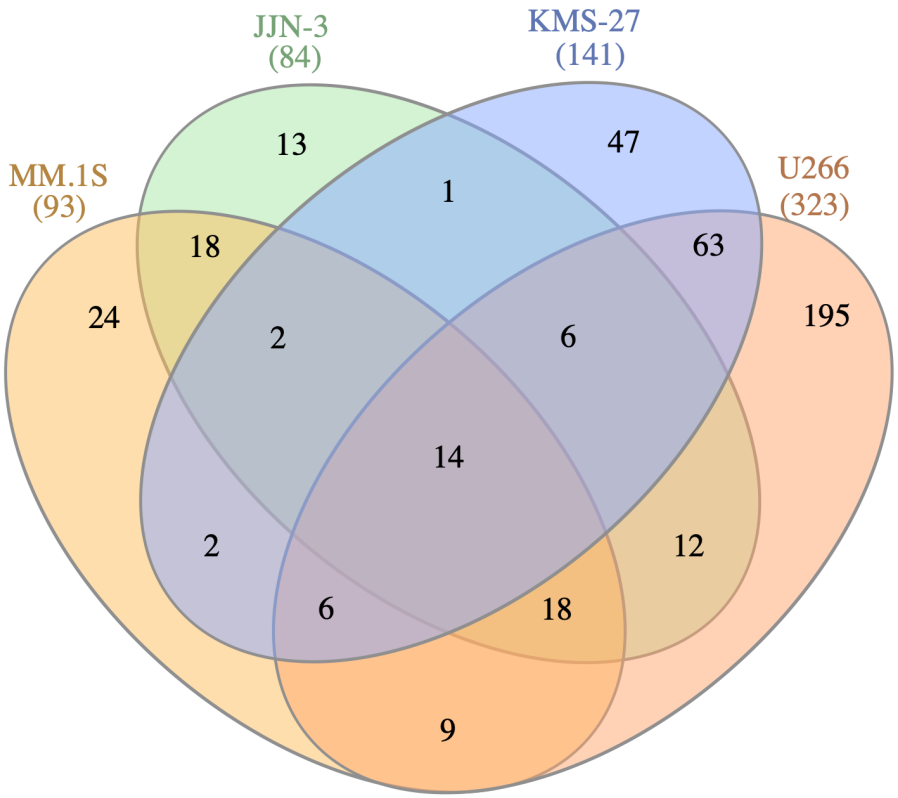

Figure 43 Comparative proteomic analysis of cell-platelet secretomes. Venn diagram illustrating the distribution of unique and overlapping proteins across all MM cell lines. Data includes proteins exclusively detected in MM cell-platelet secretomes ("enriched") and those demonstrating a statistically significant increase in abundance compared to cell-secretomes and platelet releasate (fold change ≥ 1.5 and p value < 0.05). Overlapping regions represent a shared proteomic signature induced by platelet interaction. *Created using InteractiVenn* [250] .

Table 16 MM cell-platelet secretome proteins consistently regulated across four cell lines. Selection criteria included proteins either exclusively enriched in the cell-platelet secretome or demonstrating a statistically significant increase in abundance compared to both cell secretomes and platelet releasate ($p<0.05$; fold change ≥ 1.5).

Enriched only in the cell-platelet secretomes
Increased in abundance in the cell-platelet secretomes

Protein ID	MM.1S	JJN-3	KMS-27	U266
SPB6				
ARRB1				
CAH13				
TCPH				
PGM1				

CAPZB				
COF1				
CAP1				
CATA				
CAZA1				
COTL1				
GSTO1				
CALM				
GDIR2				

3.4 DISCUSSION

Platelets play an increasingly recognised role in cancer biology, influencing tumour progression, immune modulation, and therapeutic response. Previous studies in our lab (unpublished data) using solid tumour cell lines demonstrated that tumour-cell secretome can differentially modulate platelet function. Specifically, platelets resuspended in cell secretome from a human breast cancer cell line (HCC-1954) underwent immediate aggregation, whereas platelets resuspended in cell secretome from a human lung adenocarcinoma cell line (A549) were inhibited from aggregating in response to platelet agonists. These findings suggest that cancer cell–derived soluble factors can either promote or suppress platelet activation depending on the tumour cell type.

In the present study, cell secretome from MM.1S, KMS-27, U266, and JJN-3 cells did not induce platelet aggregation, nor did inhibit collagen-, arachidonic acid–, or U46619-induced aggregation. However, when platelets were resuspended in the MM.1S cell secretome and stimulated with collagen (2 µg/mL), a significant increase in platelet aggregation was observed compared with the control (**Figure 22**). This effect was not observed with cell secretome from KMS-27, U266, or JJN-3 cells. Although no significant difference was observed with arachidonic acid stimulation, the collagen-specific enhancement suggests that MM.1S conditioned media may contain pro-aggregatory mediators that sensitise platelets to certain agonists. Therefore, future studies could investigate platelet response to sub-optimal concentrations of agonists Unfortunately, using our approach, very few

proteins were detected in the MM.1S cell secretome, and none are known to have a platelet-aggregatory effect.

Various samples were prepared for proteomic analysis as outlined in **Table 3**. Although the inclusion of a resting platelet sample as a standalone control might be considered, this was deemed neither feasible from the experimental point of view (as per our ethics application, only 36mL of whole blood could be taken per donor), nor analytically informative within the scope of the present study. Indeed, a resting platelet control would not yield meaningful comparative data, as the objective of the present analysis was not to characterise the secretome of non-activated platelets, but rather to investigate and compare the proteomic profile of secretomes under conditions of platelet aggregation and tumour cell-platelet crosstalk.

Proteomic analysis of the MM cell secretome revealed proteins associated with tumour progression, immune modulation and platelet interaction. Among these were HSP90 (MM.1S, KMS-27), CCL3 (MM.1S, U266), thrombospondin-1 (TSP1; U266, KMS-27), CXCL7 (U266), and cathepsin L1 (CTSL1; U266).

CCL3, a chemokine elevated in bone marrow plasma of MM patients, has been shown to inhibit erythropoiesis [251]. CXCL7, expressed by both platelets and tumour cells, promotes bone destruction and MM proliferation. In a mouse xenograft tumour model, CXCL7 reduced bone mineral density, thereby contributing to femoral fractures, and promoted MM cell proliferation [252]. Similarly, cathepsin L (CTSL1) has been shown to drive tumour expansion as antisense RNA targeting cathepsin L significantly reduced tumour growth in mouse models [253].

Thrombospondin 1 (TSP1), a major extracellular matrix glycoprotein, mediates cell adhesion, angiogenesis, and platelet interactions. While platelets are a major source of TSP1, multiple studies have shown that cancer cells themselves, including breast, ovarian, glioma, and plasma cell malignancies [254], actively express and secrete TSP-1 into their microenvironment. In MM, TSP1 has been detected in patient bone marrow serum and proteomic samples [255]. Functionally, TSP1 binds to platelet receptors such as CD36 (glycoprotein IV) and CD47 (integrin-

associated protein), amplifying platelet aggregation and promoting a prothrombotic phenotype [256]. Its presence in MM cell lines highlights that myeloma cells may actively contribute to tumour-associated platelet activation and heightened thrombotic risk.

In parallel, several platelet-inhibitory or anti-aggregatory proteins were also identified in the cell secretome, including annexin A5 (ANXA5; U266) [257], alpha-1 antitrypsin (A1AT; U266, KMS-27), gelsolin (GELS; KMS-27) [258], and apolipoprotein A4 (APOA4; KMS-27) [259]. The coexistence of both platelet-activating and inhibitory factors underscores the intricately balanced and context-dependent regulation of platelet function by MM cells.

Metabolic Adaptations and Enzyme Dysregulation

Metabolic reprogramming is a hallmark of malignant cells. While many cancers rely primarily on glycolysis (the *Warburg* effect) [260], MM cells exhibit dual dependency on glycolysis and oxidative phosphorylation (OXPHOS), reflecting metabolic flexibility [261].

Several metabolic enzymes were enriched exclusively in the MM.1S and JJN-3 cell–platelet secretome, including glucose 6 phosphate dehydrogenase (G6PD), a rate-limiting enzyme of the pentose phosphate pathway. G6PD is known to enhance MM proliferation and dexamethasone resistance in vitro. In the same study, researchers also conducted metabolomic analysis and found that elevated G6PD levels correlate with a poor prognosis in MM patients [262]. Similarly, aldolase A (ALDOA), expressed in MM.1S and JJN-3 cell-platelet secretomes, is a glycolytic enzyme found to be upregulated across many tumour types [263–265], contributes to tumour progression via metabolic reprogramming, cytoskeletal remodelling, EMT induction and DNA repair. Pan-cancer analysis showed that ALDOA is a highly expressed in myeloma cancer and its correlation is usually associated with poor prognosis in patients as found in brain, skin, breast cancer, and lung adenocarcinoma [266]. These findings suggest that the presence of ALDOA in the MM cell-platelet secretome may similarly reflect a clinically relevant role in MM, warranting further investigation in patient-derived samples.

α-Enolase (ENO1), another key glycolytic enzyme, was also increased in abundance in the MM.1S cell-platelet secretome. Beyond glycolysis, ENO1 functions as a cell-surface plasminogen receptor, facilitating extracellular matrix degradation and migration. ENO1 is frequently overexpressed in MM and correlates with poor survival across disease stages. Mechanistically, ENO1 enhances glycolysis, supports immune evasion, and drives chemoresistance by stabilising YWHAZ and activating mitophagy, making it an attractive therapeutic target [267,268].

Lactate dehydrogenase (LDH) serves as a classic prognostic marker of aggressive disease; elevated serum LDH levels predict poorer outcomes in MM [269]. Although LDH was not elevated in the cell-platelet secretome, it was found to be significantly increased in abundance in the cell-platelet releasate secretome.

Structural, cytoskeletal and adhesion proteins

The MM cell–platelet secretome was also enriched with cytoskeletal and adhesion-molecules linked to tumour invasiveness, migration, and drug resistance. Analysis of CoMMpass database data revealed that high levels of cofilin 1 (CFL1) and vimentin (VIM) gene expression were associated with a worse prognosis in MM patients, among other proteins [270]. CFL1 was exclusively enriched in the MM.1S cell–platelet secretome.

Among key adhesion regulators, talin-1 (TLN1) and vinculin (VINC) were markedly elevated in the MM.1S and JJN-3cell–platelet secretomes, with VINC additionally showing increased abundance in the U266 cell–platelet secretome.

TLN1 has emerged as an upstream regulator of STAT3, a critical oncogenic transcription factor in MM, regulating proliferation, cell cycle progression, and apoptosis [271]. In pancreatic β-cells, TLN1 prevented STAT3 ubiquitination by interacting with the E3 ligase Smad ubiquitination regulatory factor 1 (Smurf1) [272], whereas in colorectal cancer cells, TLN1 knockdown reduced STAT3 phosphorylation and inhibited proliferation and migration [273]. Similarly, TLN1 overexpression has been associated with increased AKT-mediated migration and invasion in pancreatic cancer cells [274]. These findings collectively suggest that

increased TLN1 abundance in the MM–platelet secretome may contribute to STAT3-dependent survival and proliferation.

VINC interacts directly with TLN1 to stabilize integrin–actin linkages, reinforcing focal adhesions and promoting downstream survival signalling [275]. This interaction between VINC and TLN1 is crucial for integrin-mediated cell adhesion and migration. In MM, integrin-dependent cell-adhesion–mediated drug resistance (CAM-DR) is a well-recognised mechanism that reduces responsiveness to therapy. While BTZ can partially overcome CAM-DR by downregulating VLA-4, recent proteomic studies have shown increased TLN1 and VINC expression in serum from MM patients least responsive to BTZ, implicating focal adhesion signalling with poor therapeutic outcomes [238]. Notably, TLN1 is also required for EC–mediated angiogenesis [276] and facilitates MM cell adhesion to the bone marrow vasculature, thereby promoting dissemination. Silencing TLN1 increases susceptibility to BTZ-induced apoptosis, further supporting its role in drug resistance [277,278].

Among the proteins increased in the MM.1S and JJN-3 cell-platelet secretome was gelsolin (GELS), an actin-severing protein that mediates platelet shape change upon Ca^{2+} influx and regulates cell motility, division, and apoptosis in cancer cells [277]. In cancer cells, it serves a crucial role as a regulator of cell activity, division, and death. Gelsolin has had varied outcomes in different types of solid cancers. In colon carcinoma, its overexpression is associated with reduced invasion; in oral carcinoma, it is associated with increased proliferation and invasion [279–281]. Finally, overexpression of GELS, TLN1, and VINC has been observed in the serum of MM patients who were least sensitive to BTZ [238].

Annexin A2 (ANXA2), a calcium-dependent phospholipid-binding protein that acts as a multifunctional regulator of cell membrane processes including endocytosis, exocytosis, and membrane repair [282], was enriched only in the MM.1S cell-platelet releasate secretome. ANXA2 is responsible for cell development and angiogenesis. In addition, ANXA2 expression showed a significant negative correlation with disease-free and overall survival in MM patients, and ANXA2 knockdown can inhibit MM cell proliferation and induce MM cell apoptosis [15].

Transforming protein RhoA (Ras homolog family member A) is a small GTPase that functions as a molecular switch, primarily regulating the actin cytoskeleton [283]. In our data, it was enriched in the MM.1S, JJN-3, and U266 cell-platelet secretome. RHOA-mediated signalling is implicated in regulating MM cell interactions within the bone marrow microenvironment, further supporting its relevance in disease progression and as a potential therapeutic target [284]. Its inhibition via PTX-100, a first-in-class agent targeting geranylgeranyl transferase-1 (GGT-1) activity, prevents the necessary lipid modification of RHOA. It is currently in a Phase 2a clinical trial for refractory/relapsed cutaneous T-cell lymphoma (CTCL) and has received orphan drug designation from the US FDA [285,286].

Coordinating with other Rho family members like cell division cycle 42 (CDC42 ; enriched in the U266 and KMS-27 cell-platelet secretomes), RHOA facilitates the structural reorganisation necessary for cell shape changes, adhesion, and motility. CDC42 activity is elevated in melphalan- and BTZ-resistant MM cells, and pharmacological inhibition using CASIN restored drug sensitivity and induced MM cell death in vivo [287]. Along with Rac-1, CDC42 plays a central role in MM cell growth and survival [288].

LIMS1 (also known an PINCH1; enriched in the MM.1S and JJN-3 cell-platelet secretome and increased in abundance in the U266 cell-platelet secretomes), and PARVB (increased in abundance in JJN-3, KMS-27 and U266 cell-platelet secretome) form part of the PINCH-ILK-parvin ternary complex [289]. This complex plays an important role in cancer cell–extracellular matrix adhesion-mediated cell behaviour[290] , while in platelets, it interacts with β integrin cytoplasmic domains of αIIbβ3 in response to agonists and is also responsible for the formation of stable thrombus [291,292] . Increased expression of these proteins could either mean increased cell migratory behaviour or increased platelet activation.

Heat Shock Proteins and Proteostasis Regulation

Heat shock proteins (HSPs) and protein-folding machinery play key roles in MM pathogenesis and therapeutic resistance.

HSP90 (enriched in the MM.1S, JJN-3 and U266 cell-platelet secretomes), a molecular chaperone, stabilises numerous oncoproteins, and its inhibition can disrupt multiple signalling pathways essential for MM cell survival, making it a promising therapeutic target [293]. Similarly, HSPB1 (HSP27), increased in abundance in the U266 cell-platelet secretome, has shown to contribute to MM cell survival and dexamethasone resistance, suggesting that targeting HSPB1 may enhance the efficacy of existing therapies [294,295].

HSP7C (HSC70/HSPA8), expressed only in the MM.1S cell-platelet secretome, is a constitutive chaperone that assists in protein folding and prevents aggregation. In a study by Zhang et al., HSC70 knockdown in MM cell lines led to MM cell death. Furthermore, in the same study, HSC70 knockdown led to reduced Ig secretion, followed by reduced ubiquitinated proteins, suggesting that it increases the proteasomal load [296]. Platelets also express HSC70, which serves as a signalling scaffold, facilitating molecular events in platelet integrin αIIbβ3 activation, granule secretion, and aggregation [297]. Enrichment of this protein only in the presence of the MM cell-platelet secretome indicates a synergistic increase.

The E2 ubiquitin-conjugating enzyme, UB2L3 (enriched in the U266 cell-platelet secretome and increased in abundance in the KMS-27 cell-platelet secretome) participates in protein degradation pathways. Although it has not been established as an MM biomarker, it is linked to drug resistance and prognosis in AML [298].

Proteasome activator complex subunit 1 (PSME1; enriched only in the MM.1S JJN-3 and U266 cell-platelet secretome) enhances proteasome activity and supports MM cell survival. While downregulation of PSME1 reduces proteasome load and increases resistance to BTZ [299], its increased abundance following platelet co-incubation may, paradoxically, sensitise cells to proteasome inhibition.

Cellular signalling

Several signalling proteins were identified in MM cell -platelet co-cultures.

Bruton's tyrosine kinase (BTK; enriched in the KM-27 cell-platelet secretome) is preferentially expressed in the hematopoietic cells, including MM. In vivo models with xenograft MM cells demonstrated that BTK knockdown promoted MM cell growth and proliferation while inhibiting metastasis, suggesting its role in MM cell adhesion and migration [300]. For this reason, BTK inhibitors have promise in the MM landscape. At present, Ibrutinib is an FDA-approved drug (BTK inhibitor) for its use in refractory CLL and mantle cell lymphoma (MCL)[301].

Peptidyl-prolyl cis-trans isomerase NIMA-interacting 1 (Pin1; enriched in the KMS-27 cell-platelet secretome), playing a role in cell proliferation, motility, and apoptosis, is implicated in many cancers [302]. Analysis of existing MM patient datasets by Zhang et al. revealed that Pin1 was overexpressed in patients at relapse compared to those at baseline. Furthermore, patients who responded to BTZ had significantly lower Pin1 expression than non-responders, suggesting a role for Pin1 in BTZ resistance [303].

Chloride intracellular channel protein (CLIC1; enriched in U266 cell-platelets secretome and increased in abundance in the KMS-27 cell-platelet secretome) has proven to participate in the proliferation, invasion and migration of several solid tumour cell lines [304,305] and may exhibit analogous roles in MM.

Caspase-3 (CASP3), enriched in the U266 cell–platelet secretome, is a key executioner of apoptosis and has been shown to be activated by BTZ in U266 cells in a dose-dependent manner. Notably, exposure to platelet factor 4 (PF4) further increases caspase-3 activity by 2.6 fold in U266 cells and 3.2 fold in OPM2 cells, indicating that platelet-derived factors can enhance apoptotic signalling under specific MM contexts [306].

Exportin-1 (XPO1), enriched in the U266 cell–platelet secretome, is a critical nuclear export protein that mediates the transport of proteins and RNA from the nucleus to the cytoplasm. XPO1 is overexpressed in MM, where it facilitates the nuclear export of key tumour suppressors such as p53 and regulators of NF-κB signalling. Pharmacological inhibition of XPO1 with selinexor has demonstrated clinical efficacy in patients with relapsed or refractory MM [307,308].

Macrophage migration inhibitory factor (MIF; enriched only in the U266 cell-platelet secretome) is an inflammatory cytokine and its expression inversely correlates with overall survival in MM patients. In addition, gene profiling data has showed an inverse correlation between its expression levels and patient's response to proteasome (such as BTZ) inhibition suggesting its role drug resistance [309]. Furthermore, MIF secreted from MM cells was found to regulate PD-L1 expression on CD14+ cells and MDSC in mice bearing MM cells and its knockdown reduced the PD-LI expression, suggesting that MIF may play a paramount role in T-cell exhaustion in MM[310].

Identification of a common proteins signature across MM cell-platelet secretomes

The intersection of the secretome profiles across all four MM cell lines reveals a core set of 14 conserved proteins solely enriched or increased in response to platelet interaction. Among those, ARRB1, CAP1 and CALM have shown to play a role in MM progression.

Beta-Arrestin 1 (ARRB1) plays a pivotal role in immune system regulation, cell proliferation and metabolic reprogramming. In paraffin-embedded gastric cancer specimens, immunohistochemical (IHC) staining revealed that higher ARRB1 expression was associated with worse patient outcomes. Furthermore, the same study found that ARRB1 knockdown in organoid cells obtained from patients led to decreased proliferation [311]. In a study investigating the role of ARRB1 in MM immune landscape using a syngeneic murine MM model, researchers found that ARRB1 knockout mice exhibited increased T-cell infiltration along with markedly decreased programmed cell death protein-1 (PD-1) on both, myeloid derived suppressor cells and T cells, indicating decreased immune exhaustion [312].

Cyclase-associated protein 1 (CAP1), another actin-regulatory molecule, was also upregulated across all four MM cell lines. CAP1 modulates actin turnover through cofilin regulation and influences cell motility, adhesion, and signal transduction. It is dysregulated in several cancers, including MM, where its expression is significantly higher in malignant plasma cells than in normal counterparts, contributing to disease progression [313–315].

Calmodulin (CALM) is a calcium sensing protein, and responsible for mediating the intracellular calcium levels. In a study by Yokokura et al, CALM antagonists reduced MM tumour burden in murine MM model. In the same study, they also reduced MM cell proliferation in vitro [316].

Coactosin-like protein 1 (COTL1) is a known stabilizer of actin filaments, its specific role in MM remains under-researched. However, its documented influence on migration in various solid tumour cell lines suggests that it may play a similar role in the progression of haematological malignancies [317,318].

Limitations

It is important to acknowledge the limitations of this study. The proteomics analysis cannot distinguish between platelet-derived and MM cell-derived proteins in the MM cell-platelet secretomes However, since platelets lack nuclei and cannot synthesize proteins *de novo*, all the proteins stored are released upon aggregation. Therefore, the increased abundance of proteins in cell-platelet secretomes are likely derived from MM cells. Furthermore, results from proteomic analysis cannot be correlated with each cell line's platelet aggregation ability as the observed protein profiles reflect effects arising from prolonged co-incubation (24 hours) rather than the short-term dynamics captured in the 60-min LTA experiments. They may incorporate stress responses, EVs exchange, and bidirectional signalling that require a longer exposure or interaction time. Additionally, platelets in LTA assays experience shear stress from stirring, whereas co-incubation experiments are relatively static, allowing extended receptor-mediated interactions, sustained release of platelet cargo, and changes in the MM cell proteome.

3.5 CONCLUSIONS

Platelet functional studies demonstrated that the secretomes derived from MM.1S, KMS-27, U266, and JJN-3 cell lines do not independently induce platelet aggregation, nor do they significantly inhibit collagen-, arachidonic acid–, or U46619-mediated aggregation under the experimental conditions employed. However, a significant increase in platelet aggregation was observed when WP resuspended in MM.1S cell secretome were stimulated using collagen. This suggests the presence of potential aggregatory substances. Future studies

should employ sub-optimal agonist concentrations to investigate the role of MM sceretome in inducing platelet aggregation.

Proteomic analyses across the MM.1S, KMS-27, U266, and JJN-3 cell lines demonstrate that platelet–tumour cell interactions profoundly remodel the protein landscape when compared to myeloma cells cultured alone. Across all cell lines, co-incubation with platelets led to a marked increase in secreted protein abundance, underscoring the active role of platelets in modulating tumour cell behaviour and secretory output. Although the proteomic approach cannot definitively distinguish whether these proteins originate from myeloma cells or platelets, their selective increase in abundance under co-culture conditions indicates that they arise from tumour cells since platelets cannot synthesize new proteins de novo.

A consistent and prominent feature across all MM cell lines was the enrichment of metabolic enzymes, particularly those involved in carbon metabolism. This finding suggests that platelet interaction induces metabolic reprogramming in myeloma cells, likely supporting increased energy production and biosynthetic demands associated with survival, proliferation, and stress adaptation. This metabolic shift was accompanied by the enrichment of proteins previously linked to therapeutic resistance, including BTZ resistance, highlighting a potential role for platelets in shaping drug-refractory phenotypes. Notably, several cytoskeletal and adhesion-related proteins, most prominently VINC, TLN1, and GELS, were recurrently enriched in the cell–platelet secretomes, although in a cell–line–dependent manner. In MM.1S and JJN-3 cells, these proteins showed pronounced increases in abundance following platelet co-incubation, while in U266 cells, VINC abundance increased specifically in the presence of platelets, with TLN1 and GELS enriched but not significantly upregulated. In contrast, KMS-27 cells exhibited enrichment of VINC and TLN1 even in the absence of platelets, suggesting an intrinsic adhesion- and cytoskeleton-oriented phenotype. The presence of these proteins indicates that platelet interactions may promote structural reorganisation, enhanced motility, and adhesion-mediated survival signalling in myeloma cells. These pathways are well recognized contributors to cell adhesion–mediated drug resistance, tumour dissemination, and reduced therapeutic responsiveness in MM. Furthermore, the observation that these same proteins have been identified in serum from patients with poor responses to BTZ [238]

underscores the clinical relevance of platelet-driven modulation of cytoskeletal and adhesion machinery.

Importantly, the data also reveal substantial heterogeneity in platelet responsiveness among MM cell lines. While MM.1S cells rapidly induced platelet aggregation in LTA, JJN-3 cells showed delayed or less aggressive platelet aggregation, suggesting that prolonged interaction during extended co-culture may contribute to the observed proteomic changes. Differences in experimental conditions, including shear stress during aggregometry versus static long-term incubation, further emphasise that platelet–tumour interactions are dynamic and context-dependent.

Collectively, these findings demonstrate that platelets are not passive bystanders but active modulators of the myeloma microenvironment. MM–platelet interactions reshape the tumour secretome, driving adaptive programs that may promote proliferation, immune modulation, and drug resistance. Targeting these pathways may offering novel therapeutic strategies to disrupt tumour–microenvironment crosstalk and overcome drug resistance. Building on these proteomic insights, subsequent experimental chapters will evaluate the functional consequences of platelet–MM interactions on BTZ resistance, cellular migration, and invasion, to directly assess how platelet-induced proteomic changes translate into altered tumour behaviour.

Chapter 4

Platelets–multiple myeloma cell interactions driving invasion and migration of myeloma cells

4.1 INTRODUCTION

Cancer metastasis is a complex, multistep process involving the dissemination of malignant cells from a primary tumour to distant organs, primarily mediated by cell migration and invasion. These cellular behaviours are essential hallmarks of cancer progression and represent major challenges to successful treatment and long-term remission [319]. While solid tumours have traditionally been the focus of metastasis research, haematological malignancies such as MM also exhibit invasive and migratory behaviour that facilitates disease progression and therapeutic resistance [320].

In advanced stages, MM can progress to extramedullary multiple myeloma (EMM), where MM cells become independent of the bone marrow microenvironment. In EMM, cells infiltrate soft tissues or distant organs, including the liver, lymph nodes, and the central nervous system. These aggressive behaviours are orchestrated through complex interactions with the extracellular matrix (ECM), stromal cells, and signalling pathways that promote cellular motility and tissue invasion [321].

Platelets release a wide range of pro-invasive factors, including TGF-β, VEGF, PDGF, platelet-derived microvesicles, and chemokines (e.g., CCL5), which can directly stimulate tumour cell motility [322]. They also interact with selectins and integrins on tumour cells, forming aggregates that enhance adhesion to the endothelium and facilitate migration through the vascular wall [323].

Direct contact between platelets and tumour cells activates TGFβ1 and NF-κB signalling in tumour cells, inducing epithelial–mesenchymal transition and promoting metastasis [324]. Platelets release MMPs, TGF-β, and heparanase, all of which are upregulated in advanced disease and contribute to ECM degradation, bone destruction and poorer prognosis [325,326]. Notably, heparanase, which is released by both MM cells and platelets, can promote dissemination by causing shedding of syndecan-1 from MM cells, which can bind to the ECM layer and cause extramedullary spread in addition to promoting angiogenesis, osteolysis and enhanced drug resistance in MM [327]. The impact of platelets on the invasive capacity of solid cancers has also been demonstrated in solid cancer models. For

instance, studies on colorectal cancer cell lines (Caco-2 and HT29) have shown that platelets presence significantly increases invasion. This is driven by an upregulation of MMP-9 expression, a process mediated by the p38MAPK signalling pathway [328].

Extracellular communication is also mediated by microvesicles. Platelet-derived microvesicles (PMVs) have been shown to transfer pro-migratory signals to tumour cells, in particular lung and breast cancer cells, potentially contributing to metastatic spread [329,330]. MM-derived microvesicles (MVs) have been shown to contain angiogenic and coagulation factors. These MVs also increased endothelial cell and mesenchymal cell migration, whereas MVs obtained from BTZ-treated cells showed decreased migration [331].

Finally, in vivo evidence suggests that platelet-tumour contact using a mouse model of lung cancer induces the secretion of chemokines like CXCL5 and CXCL7. These recruit granulocytes to form "early metastatic niches," providing a fertile environment for tumour progression [332].

In light of the above literature, the aim of this chapter is to understand how direct platelet-MM cell contact and platelet releasate may modulate the invasive and migratory potential of myeloma cells.

4.2 METHODS

4.2.1 Cell lines employed in this chapter

For invasion assays, the MM.1S and JJN-3 cell lines were used. Migration studies were performed using MM.1S, JJN-3, KMS-27, and U266 cell lines.

4.2.2 Washed platelets and platelet releaseate preparation

Briefly, blood was collected from healthy, consenting volunteers in accordance with the Declaration of Helsinki. PRP was obtained by centrifugation of whole blood at 250 × g for 20 min. Washed platelets were prepared by centrifuging PRP at 900 × g for 10 min in the presence of prostacyclin, followed by resuspension in serum-free RPMI 1640 with 1% antibiotic–antimycotic to a final concentration of 250,000 platelets/μL. Platelet releasate (PR, mixture of biologically active compounds

released by platelets upon activation) was prepared by inducing platelet aggregation with 4 μg/mL collagen using the LTA.

4.2.3 Invasion Studies

Transwell invasion assays were performed using 24-well plate culture inserts with 8 μm pores according to the manufacturer's protocol (BioCoat™ Matrigel™ Invasion Chamber with Corning™ Matrigel Matrix, Corning, USA) (**Figure 44 A**). The Matrigel layer was allowed to rehydrate for 2 hours at room temperature. MM.1S and JJN-3 cells (2,000,000 cells/mL) were suspended in serum-free RPMI medium and co-incubated with and without platelets in the upper chamber of the Transwell inserts. The lower chamber contained 750 μL of RPMI medium supplemented with 10% FBS, which served as the chemoattractant [**Figure 44 (A)].** After 48 hours, a sample from the upper chamber was collected, cytospinned and visualised using an Olympus BX51M reflection epi-fluorescence microscope (Mason Technology, Ireland). Images were captured using the digital camera attached to it (using the Soft Imaging System, SIS, GmbH, Münster, Germany). Media from the upper chamber were also collected, centrifuged at 13,000 rpm for 5 min, and stored at -80 °C for further zymography analysis. The cells that were attached to the upper chamber were removed by scrubbing with a cotton swab and the cells attached to the bottom surface of the membrane were stained with Diff-Quick (Sigma-Aldrich, Ireland) and counted under an Olympus IX81 inverted microscope.

4.2.4 Gelatin Zymography

Gelatin zymography was performed on supernatant collected from the upper chamber of the Transwell insert after centrifugation as previously described (add reference or previous section). The gels were incubated for 7 days in the enzyme buffer. The gelatinolytic activity was visualised as clear bands on a Coomassie blue–stained background and quantified using a Gel Doc XR+ system (Bio-Rad, USA). Conditioned media from human fibrosarcoma cell line HT1080 stimulated with phorbol 12-myristate 13-acetate (PMA) served as a positive control for MMP-2 (72 kDa) and MMP-9 (92 kDa).

4.2.5 Migration Studies

Transwell migration assays were performed using 24-well plate culture inserts with 8 μm pores (Corning, Costar Corporation, USA) (**Figure 44B**). For these experiments, MM cells were cultured for 24 hours in serum-free RPMI. 5,000,000 cells/mL were suspended in serum-free RPMI media and co-incubated with 250,000 platelets/μL in the upper chamber of the Transwell inserts. RPMI medium supplemented with 10% FBS (500 μL) was used as the chemoattractant. MM.1S and U266 cell migration was quantified after 24 hours using trypan blue and JJN-3 and KMS-27 using the IncuCyte system (Sartorius AG, Germany). PR and WP were also used as chemoattractants [**Figure 44 (B)**].

4.2.6 Quantification of cell migration using IncuCyte system

IncuCyte® live-cell imaging system is an automated, incubator-based platform that enables real-time, non-invasive imaging of live cells under physiological culture conditions (37 °C, 5% CO_2). The system captures high-resolution phase-contrast images at predefined locations within each well without disturbing the cultures. Phase-contrast images of the lower chamber of the Transwell inserts were acquired after 24 hours. Images were acquired at 20x magnification from 16 non-overlapping images per well using the IncuCyte image viewer, and the mean number of cells/well was calculated.

4.2.7 Statistical Analysis

GraphPad Prism version 9.0 (GraphPad Software, La Jolla, CA, USA) was used for statistical analyses. Cell migration and invasion in the absence of platelets were set as 1, and the corresponding fold change values in the presence of platelets were calculated relative to this baseline. Data is presented as the mean ± standard error of mean (SEM) from at least three independent experiments. Statistical significance between groups was assessed using an unpaired Student's t-test, and differences were considered significant at $p < 0.05$.

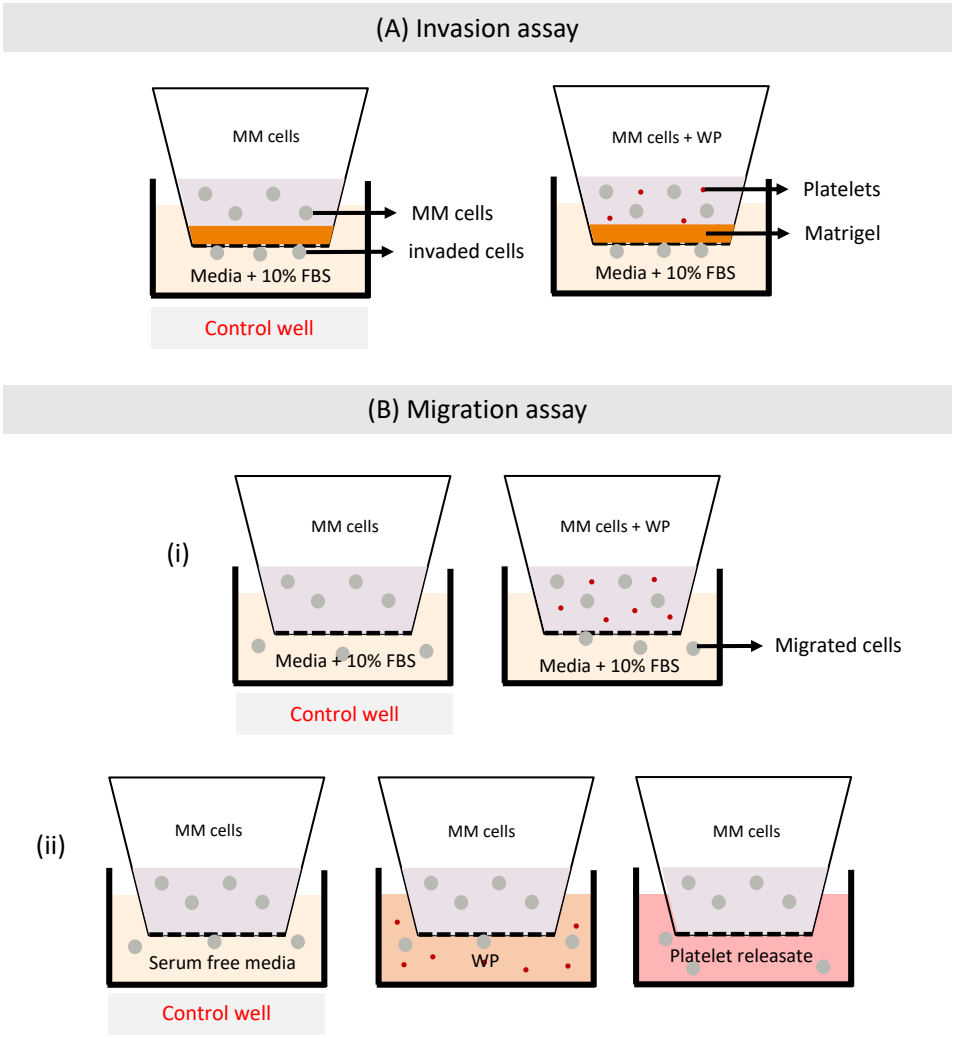

Figure 44 Schematic overview of the experimental design utilised for (A) invasion and (B) migration studies.

4.3 RESULTS

4.3.1 Invasion Studies

Incubation of MM.1S and JJN-3 cells with platelets resulted in a significant reduction in the number of invading cells compared with the control [**Figure 45 (i-ii)**, **Figure 46 (i-ii)**]. The contents of the inserts were collected and prepared for optical microscopy. As shown in **Figure 45 (iv)** and **Figure 46 (iv),** platelet aggregation was observed in the presence of MM.1S cells and JJN-3 cells, respectively.

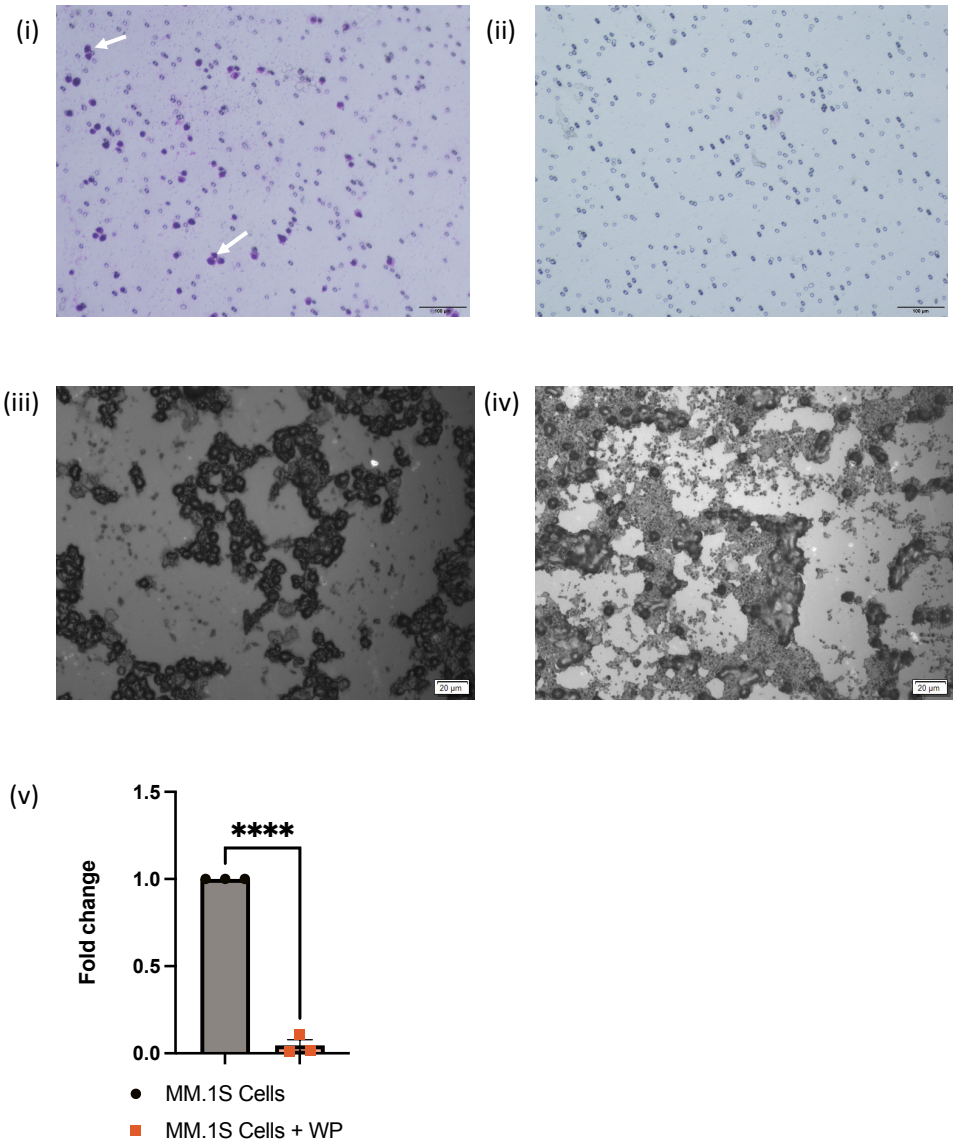

Figure 45 Matrigel invasion assays of MM.1S. Representative optical microscopy image of (i) invading MM.1S cells (ii) invading MM.1S cells incubated with platelets; Scale bar 100 µm. White arrows represent cell cytoplasm and nuclei stained in violet with Diff-Quik reagent. Note that violet dots are pores. Optical microscopy image of (iii) MM.1S cells (iv) MM.1S cells incubated with washed platelets taken from the upper chamber showing big aggregates; Scale bare 20 µm (v) Statistical analysis. Data is represented using fold change values analysed using unpaired student t-test (n=3) carried out using GraphPad Prism 9; **** $p<0.0001$.

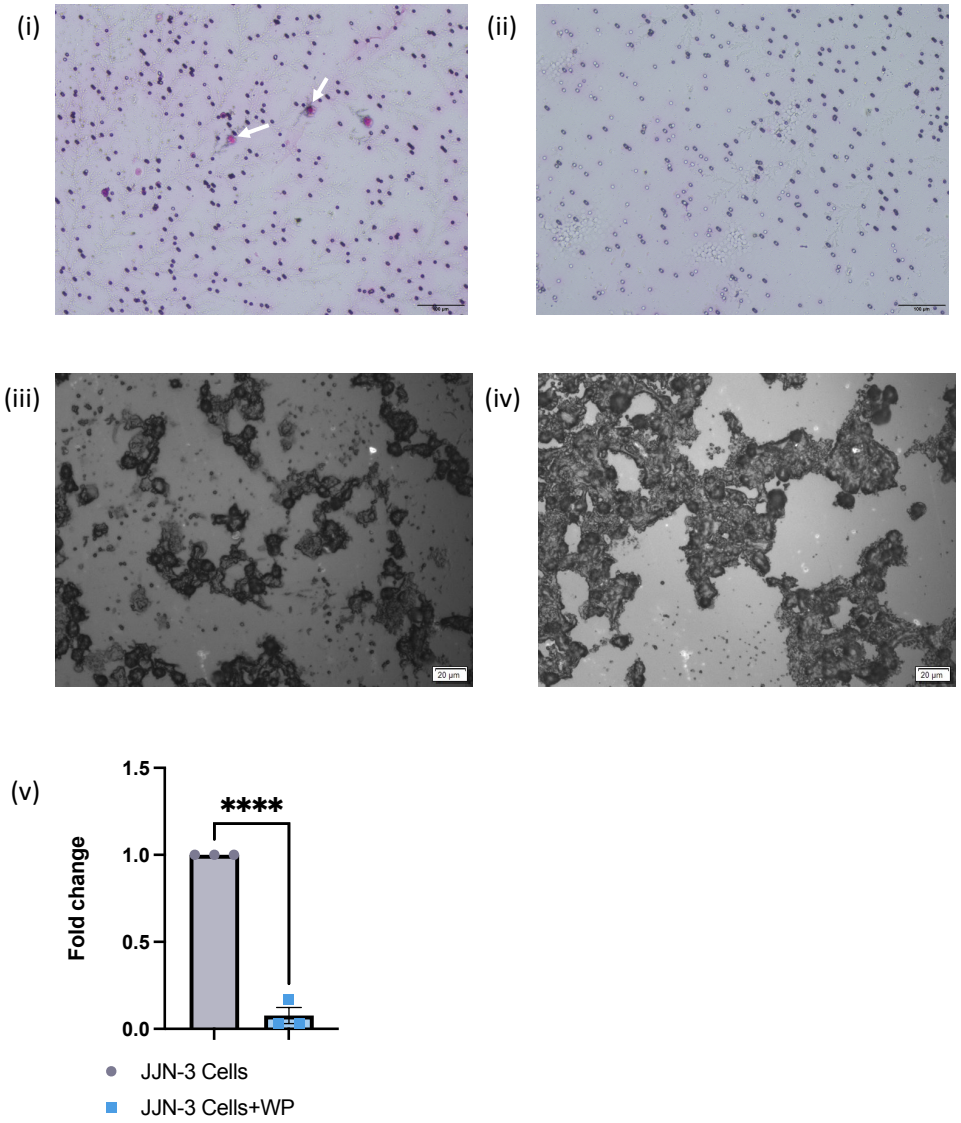

Figure 46 Matrigel invasion assays of JJN-3. Representative optical microscopy image of (i) invading JJN-3 cells (ii) invading JJN-3 cells incubated with platelets. White arrows point towards MM cells with stained cytoplasm and nucleus. Note that violet dots are pores. Scale bar 100 µm; Optical microscopy image of (iii) JJN-3 cells (iv) JJN-3 cells incubated with washed platelets taken from the upper chamber showing big cell-platelets aggregates. (v) Statistical analysis. Data is represented using fold change values analysed using unpaired student t-test (n=3) carried out using GraphPad Prism 9; **** $p<0.0001$.

4.3.2 Gelatin zymography on supernatant collected from the upper chambers of the Transwell inserts

Gelatin zymography of insert contents revealed a significant increase in MMP-2 and MMP-9 activity following co-incubation of JJN-3 cells with platelets. In MM.1S cells co-incubated with platelets, a trend toward increased MMP-2 activity was

observed, while MMP-9 activity was significantly elevated compared with the control (MM.1S cells alone) (**Figure 47**).

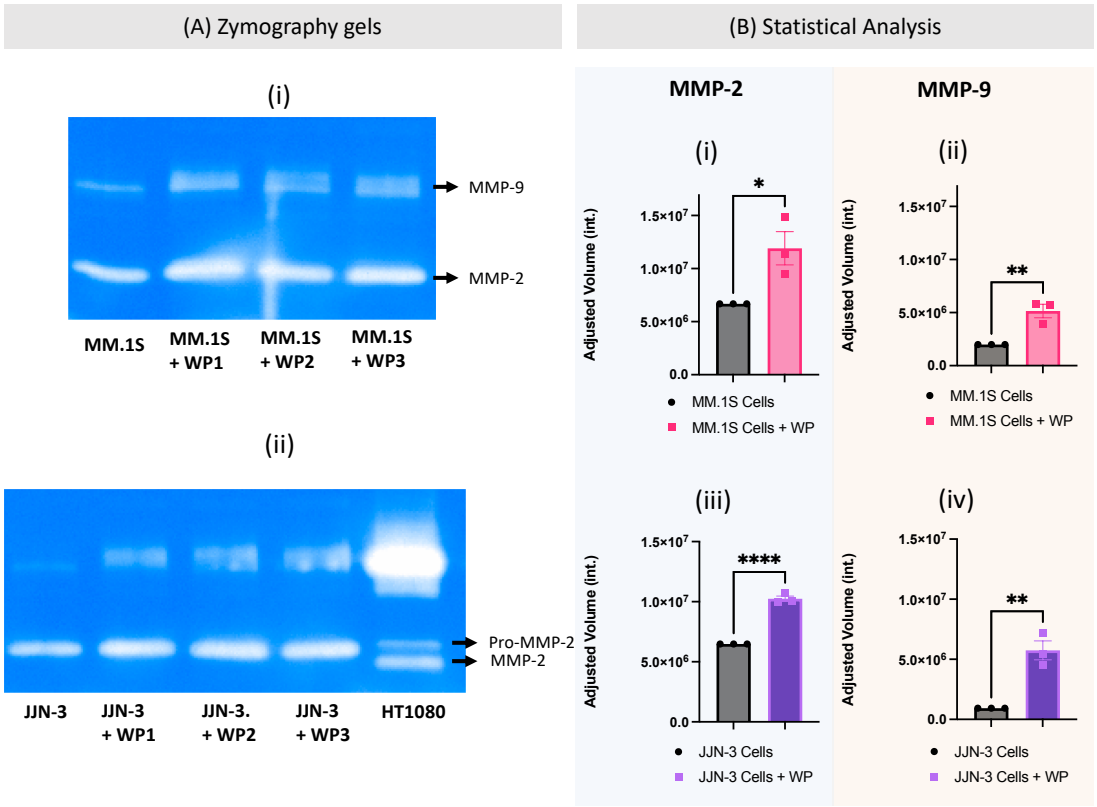

Figure 47 MMP activity during MM.1S and JJN-3 invasion was assessed by gelatin zymography. (A) Zymography gels depicting MMP-2 and MMP-9 activities in (i) MM.1S cells alone and MM.1S cells incubated with WP, and (ii) JJN-3 cells alone and JJN-3 cells incubated with WP. Conditioned media from PMA induced HT1080 (fibrosarcoma) cells were used as a positive control for gelatinase identification. (B) Statistical analysis. MMP levels were quantified by densitometric analysis using adjusted volume intensity. Data are presented as mean ± SEM (n = 3). Statistical significance was determined using Student's t-test carried out using GraphPad Prism; *p<0.05 **p<0.01 **** p<0.0001; WP- washed platelets, MMP- matrix metalloproteinases

4.3.3 Migration Studies

4.3.3.1 MM cells co-incubated with platelets

When MM cells were co-incubated with platelets in Transwell inserts, the number of migrating cells increased. **Figure 48** and **Figure 49** depicts representative pictograms showing MM cells that migrated to the bottom chamber in the presence and absence of platelets. The bottom surface of the inserts was also examined under a microscope, and no cells were observed attached to them.

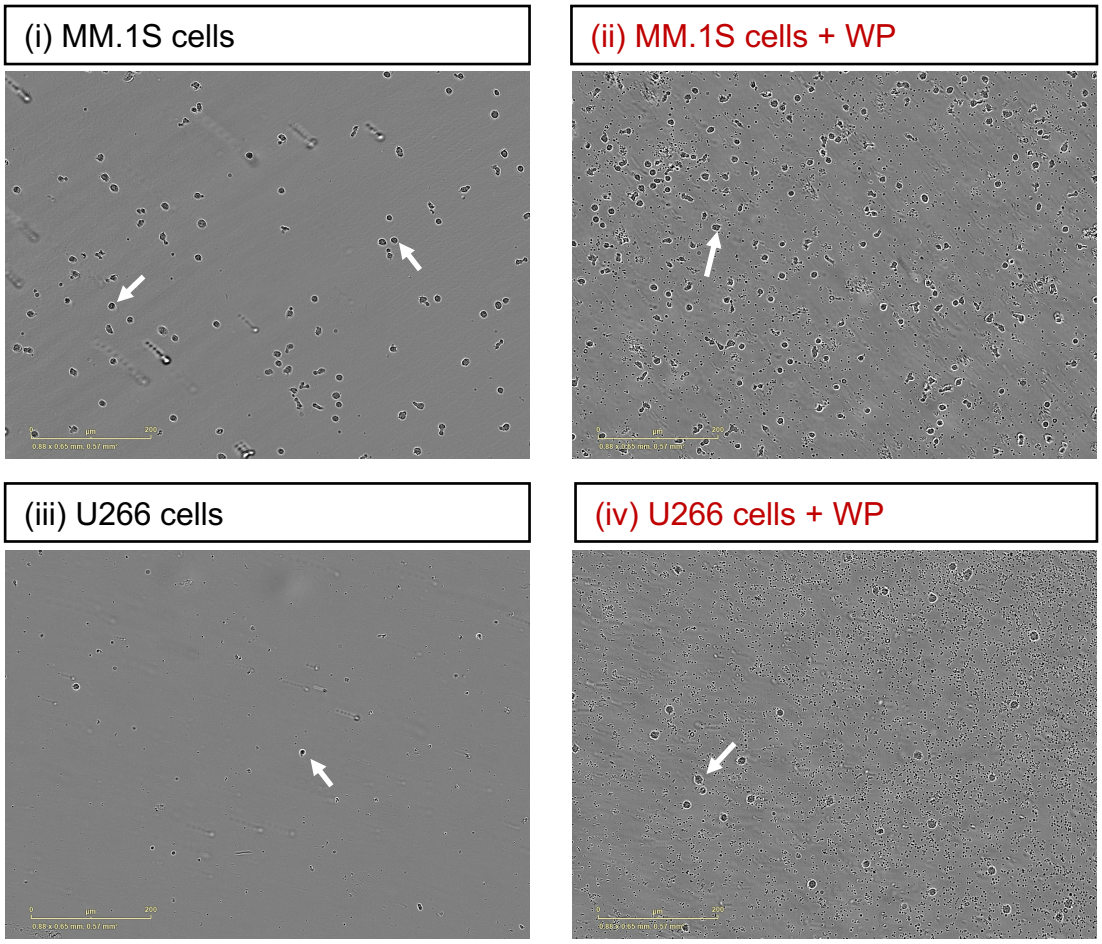

Figure 48 Migration of MM.1S and U266 cells in the presence or absence of platelets. Representative images taken using IncuCyte depicting migration of (i) MM.1S cells alone (ii) MM.1S cells co-incubated with WP (iii) U266 cells alone (iv) U266 cells co-incubated with WP. White arrows point towards the cells (biggest black dots), while the smallest dark dots correspond with platelets. Magnification- 20X. WP-washed platelets

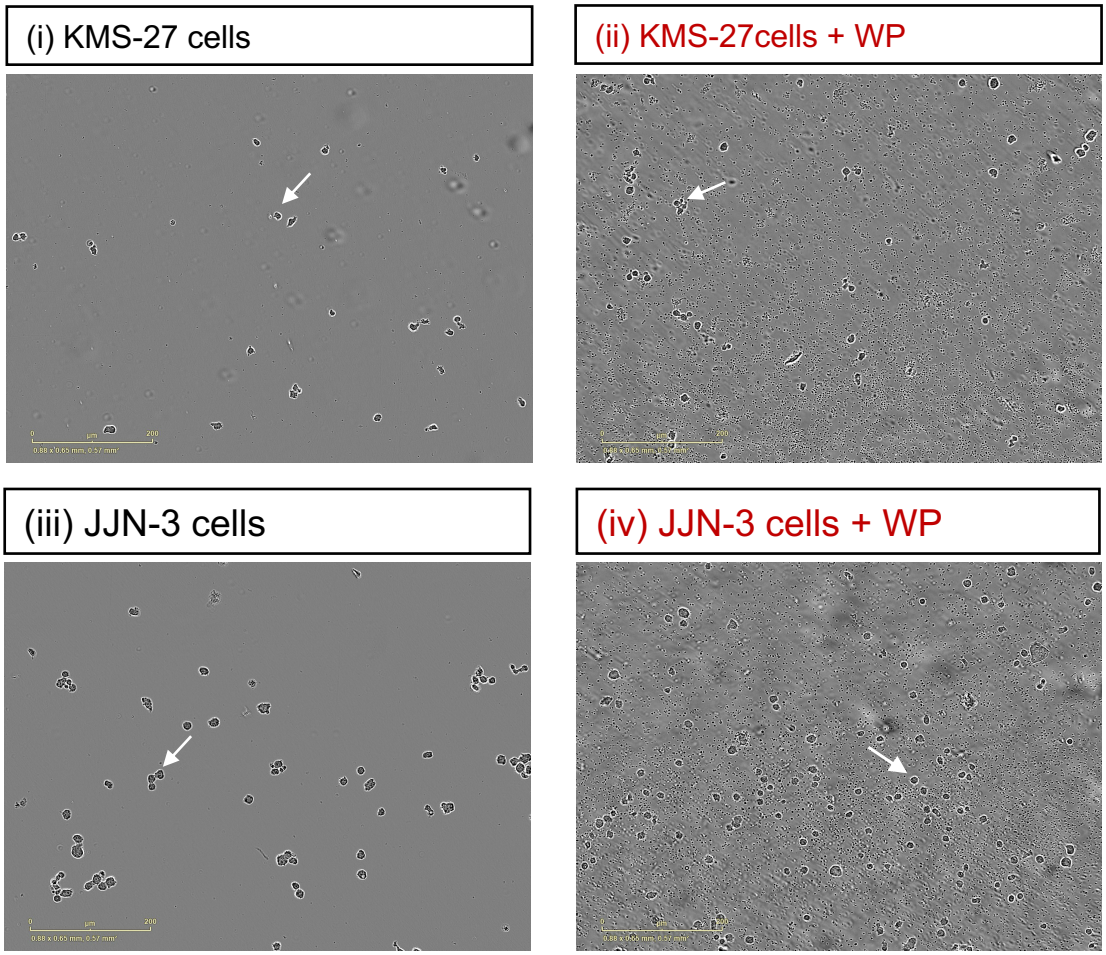

Figure 49 Migration of KMS-27 and JJN-3 cells in the presence or absence of platelets. Representative images taken using IncuCyte depicting migration of (v) KMS-27 cells alone (vi) KMS-27 cells co-incubated with WP vii) JJN-3 cells alone viii) JJN-3 cells co-incubated with WP . White arrows point towards the cells (biggest black dots), while the smallest dark dots correspond with platelets. Magnification- 20X. WP-washed platelets

As shown in **Figure 50,** there was a significant increase in the number of MM.1S and U266 migrating cells in the presence of WP, with a mean of 1.86x and 2.50x cells, respectively, compared to the control (taken as 1x in the absence of WP). This data is from 4 independent experiments with different platelet donors. While there was no significant increase in the number of JJN-3 and KMS-27 migrating cells in the presence of WP, an increasing trend compared to the control is observed. Out of the 6 donors employed for the migration assays with the JJN-3 cells, and the 7 donors with the KMS-27 cells, platelets from two donors decreased the migration of MM cells in both cases.

4.3.3.2 Platelets and platelet releasate used as a chemoattractant

Cell migration assays were performed using the MM.1S and U266 cell lines, with WP and PR as chemoattractants in the lower compartment. After 24 hours, a significant decrease in migration of MM.1S and U266 cells when platelets were used as chemoattractant was observed [**Figure 50 (v-vi)**]. When PR was used as a chemoattractant, a significant increase in MM.1S migration was observed (**Figure 50 vii**), whereas a significant decrease in U266 migration was observed (**Figure 50 viii**).

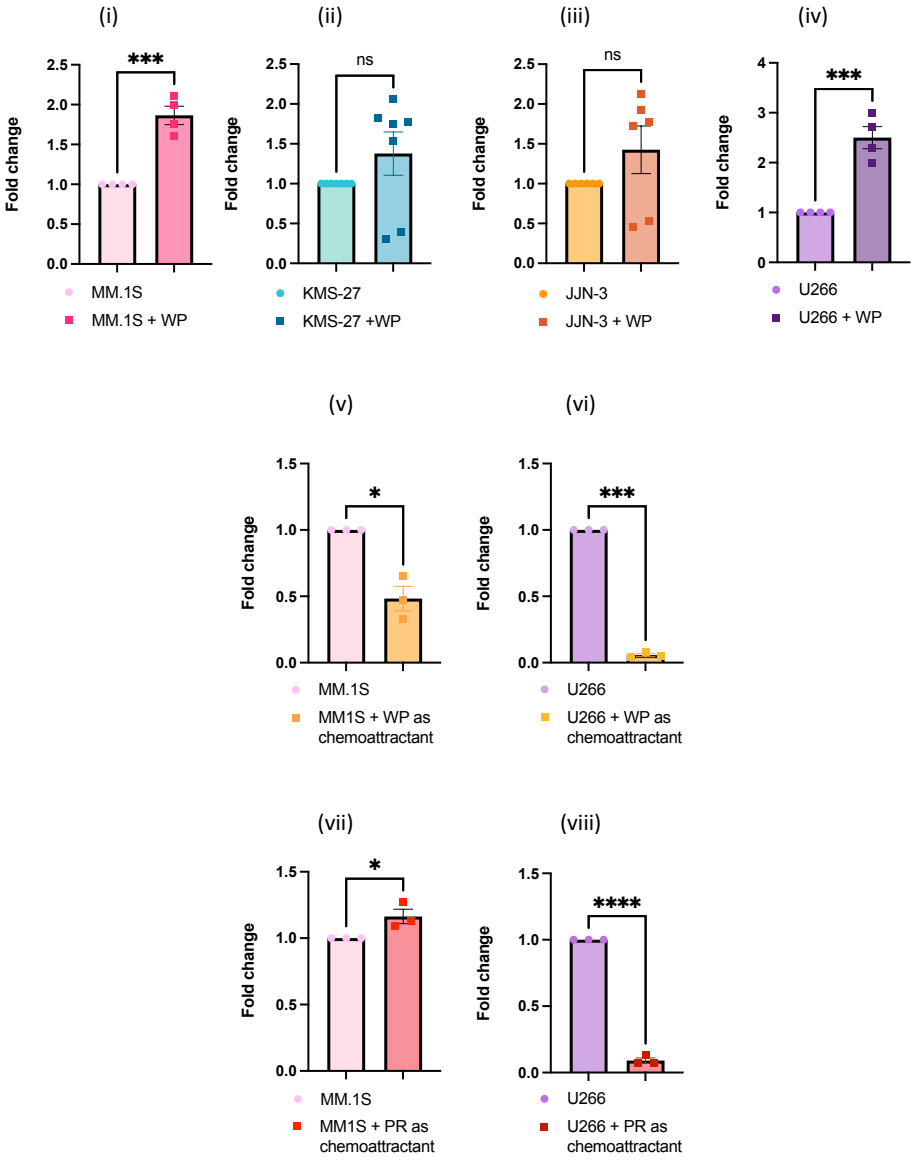

Figure 50 Migration assay of multiple myeloma cells with and without platelets. Statistical analysis carried out using GraphPad prism; unpaired student t-test; Data are represented as fold change values. (i-iv) MM migration with and without co-incubating WP; (v-vi) MM migration when WP were used as chemoattractant; and, (vii-viii) MM migration when PR was used as chemoattractant; Experiments were performed with n ≥ 3 independent platelet donors in duplicates. Statistical significance is indicated as follows: *p < 0.05, ***p < 0.001, ****p < 0.0001.WP- washed platelets; PR- platelet releasate

4.4 DISCUSSION

Matrix metalloproteinases (MMPs), particularly the gelatinases MMP-2 and MMP-9, are essential mediators of cancer cell invasion. Their primary role involves the proteolytic degradation of the extracellular matrix (ECM), specifically Type IV collagen, which dismantles the physical barriers of the basement membrane and allows tumour cells to migrate into the surrounding stroma and vasculature [152].

In the tumour microenvironment, platelets are a significant source of these proteases. Upon activation, platelets release pre-synthesised MMP-2 and MMP-9 from their α-granules, which locally amplify ECM remodelling and facilitate tumour cell intravasation. Interestingly, this relationship is bidirectional, as MMP-2 can reciprocally modulate platelet activity through a non-canonical pathway. Specifically, MMP-2 interacts with the platelet surface by binding to GPIIb/IIIa via its C-terminal hemopexin-like domain . This integrin acts as a cofactor or docking scaffold, anchoring MMP-2 to the membrane to facilitate its role in "priming" platelets for aggregation and amplifying the signalling of other receptors like PAR-1 [218,333].

A previous study carried out by Que et al. utilised the U266 cell line to investigate the mechanisms of MM invasion, finding that doxorubicin treatment significantly reduces cellular invasiveness [334]. However, invasion assays have not been well characterised for MM.1S and JJN-3 cell lines. In our study, the addition of WP significantly reduced invasion by both cell lines through Matrigel. This observation contrasts with gelatin zymography data demonstrating a significant increase in MMP-2 and MMP-9 activity when MM.1S and JJN-3 cells were co-cultured with WP. As MMP-2 and MMP-9 are key regulators of ECM degradation known to promote tumour cell migration and invasion across a range of cancers, their upregulation typically correlates with increased invasiveness [335]. In MM specifically, malignant plasma cells rely on MMP-9 activity to invade toward CXCL12, a requirement further supported by the reduction in invasion seen upon targeted MMP-9 inhibition [336,337].

The findings in this chapter indicate that platelets promote a proteolytic phenotype in MM.1S and JJN-3 cells, as demonstrated by the significant upregulation of MMP-2 and MMP-9 activity. However, the lack of measurable invasion is likely attributable to fundamental differences between suspension and adherent invasion models. Unlike solid tumour models, where adherent cancer cells attach to the membrane prior to platelet exposure, MM.1S and JJN-3 cells remain non-adherent. As a result, WP are likely to contact the Matrigel matrix before forming stable interactions with tumour cells. In fact, Matrigel contains extracellular matrix proteins such as laminin, collagen IV, entactin, and perlecan, which can interact with platelet receptors and facilitate platelet adhesion and aggregation, potentially influencing tumour cell invasion in our in vitro assays. This phenomenon differs fundamentally from invasion assays performed with adherent solid tumour cells, in which early tumour cell attachment limits platelet–Matrigel contact and allows platelet–tumour cell signalling to predominate. Multiple studies in solid tumours have demonstrated that platelets enhance cancer cell invasion in Transwell and Matrigel assays. For example, Radziwon-Balicka et al. showed that platelets significantly increased colon cancer cell invasion through Matrigel by activating the p38 MAPK pathway and upregulating MMP-9 expression, while inhibition of p38 MAPK or MMP-9 reduced platelet-stimulated invasion [328]. Similar platelet-driven increases in invasion have been reported in breast, ovarian, melanoma, and hepatocellular carcinoma models, in which platelets or platelet-derived factors enhance invasion and epithelial–mesenchymal transition via increased MMP-2 and MMP-9 activity [338–340]. These findings highlight the limitations of using Matrigel invasion assays to study platelet–tumour interactions in haematological malignancies and suggest that alternative assay formats may be necessary to accurately assess invasive behaviour in MM. Such alternative assay formats could employ synthetic polyethylene glycol (PEG) -based hydrogels functionalised with Arg-Gly-Asp (cell-adhesion motifs) and/or MMP-cleavable peptide crosslinks [341]. However, there is a slight possibility that the cell adhesion motifs could still activate the platelets. In addition, the PEG hydrogel would not mimic physiological conditions, as with Matrigel. Therefore, per se, there isn't any suitable comparable method available.

Several studies have reported that platelets enhance cancer cell migration. For example, co-incubation of platelets with breast cancer cells increased trans

endothelial migration [342,343], while platelet co-culture with melanoma (B16F10-C3) and breast cancer (231-GFP) cells enhanced both migration and proliferation [344]. However, platelet-mediated effects on migration are not uniform across tumour types. Canine osteosarcoma cell lines co-incubated with platelets led to a decrease in migration as measured by Bulla et al. [343]. Yoon et al. further demonstrated that human and murine carcinoma cells generally exhibit increased migration and invasion after human and murine platelet exposure respectively, whereas murine sarcoma cell lines displayed inhibited migration/invasion as measure by scratch migration/invasion assays. Migration of human sarcoma cell lines remained unaffected to platelet exposure [345].

It is worth highlighting that, despite the fact that all osteosarcoma cell lines examined by Bulla et al. and the carcinoma cell lines analysed by Yoon et al. successfully induced platelet aggregation in vitro using LTA [346–348], their behaviour in migration assays diverged substantially. These observations reinforce the notion that platelet–tumour cell interactions are multifactorial, influenced not only by the propensity of tumour cells to activate and aggregate platelets but also by inherent biological properties unique to each tumour type.

A similar pattern was observed for migration assay results for all the cell lines in this chapter. Direct co-incubation with platelets significantly increased migration of MM.1S and U266 cells. While KMS-27 and JJN-3 cells exhibited a similar trend, this did not reach statistical significance. This is most likely due to donor-dependent effects as platelets from two independent donors prevented cell migration. Such variability is consistent with known heterogeneity in platelet activation profiles between donors [349]. Interestingly, these results show that a cell line's ability to aggregate platelets does not always predict its potential to migrate. For instance, KMS-27 was highly effective at triggering aggregation, yet this did not translate into a significant increase in migration. In contrast, U266 cells hardly triggered aggregation at all, yet showed a strong migratory response in the presence of platelets. Furthermore, even though the proteomics data showed an increased abundance of proteins linked to cytoskeletal reorganization and focal adhesion across all four cell lines, they still differ in their migratory ability. In other words, the proteomics data reveal a universal potential for migration, but the migration assays show that the final 'decision' to move is cell-line specific and likely

regulated by internal signalling pathways downstream of the initial platelet contact.

When WP or PR were used as a chemoattractant in the lower chamber, MM cell migration was reduced rather than enhanced, except in MM.1S where a significant increase in migrated cells was observed in presence of PR as chemoattractant. In previous studies using solid tumours such as ovarian adenocarcinoma, platelets placed in the lower chamber acted as a potent chemoattractant for adherent cells such as SKOV3 and UCI101 [350]. Similarly, in breast cancer cell lines, PR when used as a chemoattractant, increased the invasion of cells [342]. In contrast, no prior studies have reported reduced migration or invasion in response to platelets used as chemoattractant, suggesting that this phenomenon may be specific to suspension cell lines. The decreased migration could result from platelet aggregation or physical obstruction at the membrane, ineffective formation of a soluble chemotactic gradient, or inherent differences in how MM cells respond to platelet-derived signals compared with adherent solid tumour cells.

As described in 3:68, interactions between platelets and tumour cells trigger the release of a wide variety of factors that, in multiple cancer models, have been shown to promote migration and invasion. These factors include, but are not limited to, RAC1, RAP1B (notably implicated in chronic lymphocytic leukaemia and potentially in MM), ITGA2 in gastric cancer, and PDLIM1 in both gastric and breast cancer, ITGA2 in gastric cancer, PDLIM1 in gastric and breast cancer, etc [351–356]. Furthermore, co-incubation with platelets led to upregulation of cytoskeletal and adhesion-associated proteins, including VINC, TLN1, GELS, TPM4, ACTN1, and PARVB. Many of these proteins were absent or minimally expressed in the MM cell secretome, indicating that their induction requires direct platelet–cell contact rather than exposure to soluble platelet-derived factors alone (present in the releasate used as chemoattractant in our experiments but not in direct contact with the cells). Additional studies are needed to investigate the effects of MM cell-platelet secretomes on the migration of MM cells and effectively determine whether soluble factors released by platelets modulate MM cell migration independently of direct cell-platelet contact.

4.5 CONCLUSIONS

This study demonstrates that platelets exert complex and context-dependent effects on MM cell invasion and migration. While platelet co-culture significantly increased MMP-2 and MMP-9 expression in the presence of MM.1S and JJN-3 cells, this biochemical change did not translate into increased invasion in Matrigel-based assays. Instead, platelet presence was associated with reduced measurable invasion, highlighting important limitations of conventional invasion models when applied to suspension cancer cell lines. These findings suggest that protease induction is insufficient to drive invasion when platelet–matrix interactions physically restrict cell motility. In contrast, direct platelet–MM cell co-incubation significantly enhanced migration of MM.1S and U266 cells; similar effects were observed in KMS-27 and JJN-3 cells, although donor-dependent variability was observed. This variability is consistent with known heterogeneity in platelet activation and secretion profiles and underscores the influence of platelet intrinsic properties on tumour cell behaviour [349].

Notably, the use of platelets or platelet releasate as chemoattractants decreased MM cell migration, except for MM-1S, where releasate was used, resulting in a significant increase. This finding contradicts reports in adherent solid tumour models and suggests fundamental differences in how suspension myeloma cells respond to platelet-derived cues in the absence of direct contact. Collectively, these findings indicate that platelet-mediated regulation of MM cell invasion and migration might be dependent on direct cell–platelet interaction and assay context. Further studies exploring the migration of MM cells co-incubated with platelet releasate are warranted. In addition, these findings highlight key biological distinctions between haematological malignancies and solid tumours in platelet–tumour crosstalk. Importantly, this work emphasises the need for alternative or adapted experimental models, such as microfluidic chips, to more accurately assess platelet-driven chemotaxis in MM. A microfluidic chip maintains a stable, linear gradient. This would allow you to investigate whether MM cells truly migrate toward or away from platelet factors, a finding that could significantly improve our current understanding of MM progression.

Chapter 5

Evaluating platelet involvement in multiple myeloma: contributors to resistance mechanisms or innocent bystanders

5.1 INTRODUCTION

BTZ is a proteasome inhibitor that remains a cornerstone in MM treatment. It blocks the 26S proteasome, resulting in the accumulation of misfolded or ubiquitinated proteins, activation of endoplasmic reticulum stress pathways, and, consequently, apoptosis of malignant myeloma cells (**Figure 51**) [357]. Despite improved outcomes in patients, patient relapses are common and related to both intrinsic and acquired drug resistance [358].

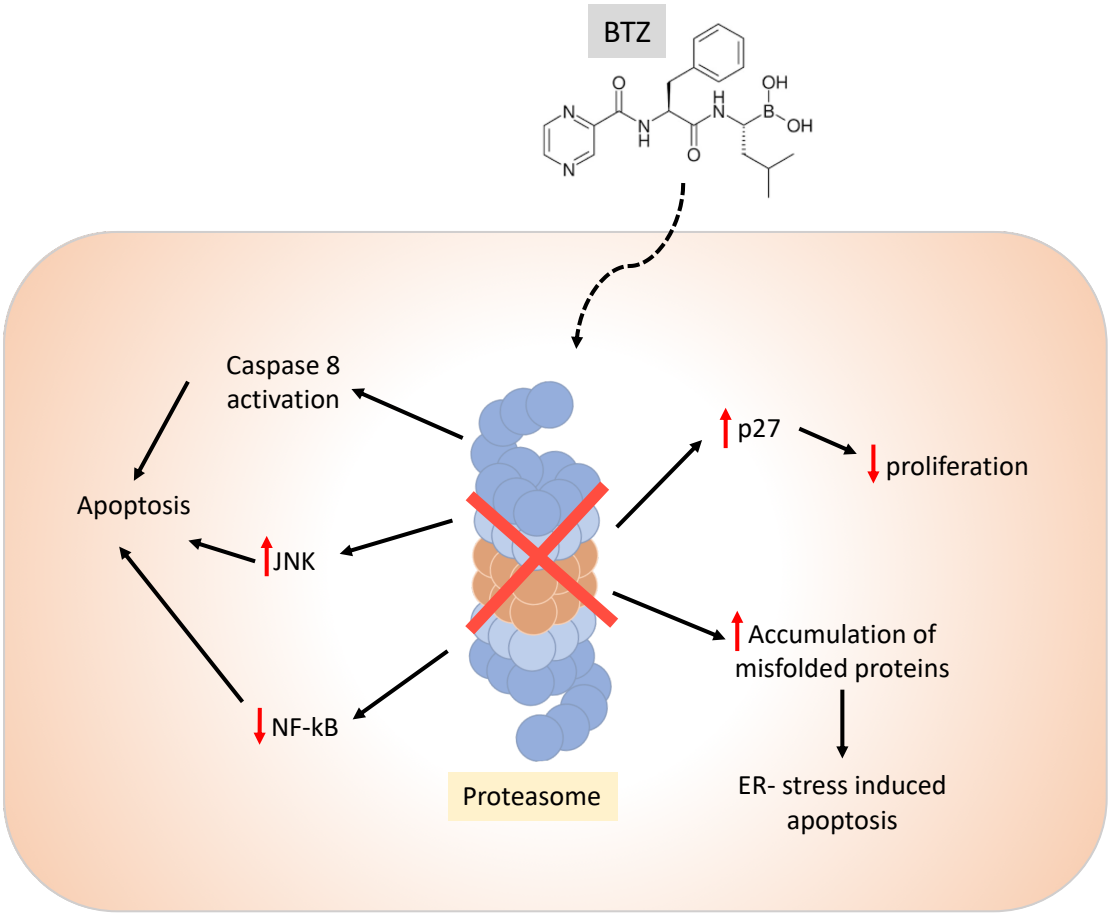

Figure 51 Mechanism of action of bortezomib (BTZ). BTZ targets the 26S proteasome in MM. BTZ prevents the degradation of IκB, the inhibitory partner of NF-κB, leading to decreased nuclear translocation of NF-κB and a reduction in its downstream anti-apoptotic and proliferative signalling. Proteasome blockade also leads to the direct activation of caspase-8 and the upregulation of the c-Jun N-terminal kinase (JNK) pathway, both of which serve as potent drivers of apoptosis. Furthermore, the accumulation of the cyclin-dependent kinase inhibitor p27, which would otherwise be degraded by the proteasome, leads to a significant decrease in cell proliferation. Finally, the buildup of polyubiquitinated, misfolded proteins triggers a terminal unfolded protein response (UPR), resulting in endoplasmic reticulum (ER) stress-induced apoptosis. *Figure created using Microsoft PowerPoint*

The development of BTZ resistance in MM is multifactorial, arising from both tumour microenvironment–dependent influences and intrinsic myeloma cell–associated factors.

a) Tumour microenvironment- associated BTZ resistance

Multiple components and factors within the tumour microenvironment have been associated with BTZ resistance. Stromal cells derived cytokines such as IL-6 and IGF-1 have been shown to protect MM cells from dexamethasone-induced apoptosis by activating pro-survival pathways including PI3K/Akt, NF-κB, and JAK/STAT3 [359,360]. Bone marrow stromal cells (BMSCs) also secrete, among other factors, growth differentiation factor 15 (GDF15), which confers resistance to BTZ and higher plasma levels in MM patients negatively correlated to overall survival 30 months after diagnosis [361,362]. CCL3 is increased in bone marrow plasma of MM patients, and in vitro studies have shown that co-culture of MM cells and THP-1-derived M2 macrophages significantly increased MM cells' proliferation and protected cells from BTZ-induced apoptosis via the CCL3-CXCR5 axis and activating PI3K/AKT/RhoA signalling [363]. Furthermore, hypoxia induced the secretion of small extracellular vesicles (sEVs) from BMSCs, which reduced the BTZ sensitivity of MM cells. These sEV contained miR-140-5p and miR-28-3p that targeted SPRED1, regulating the MAPK pathway [364].

b) Myeloma-cell associated BTZ resistance

Since BTZ targets the 26S proteasome, particularly the proteasome β5 subunit (PSMB5), mutations in PSMB5 or overexpression of PSMB5 have been shown to reduce BTZ binding and efficacy [365]. The MAPK-HSP27 pathway has been found to confer BTZ resistance in MM cells. In fact, HSP27 blockade overcomes BTZ resistance [366]. This finding was also supported by analyses of peripheral blood samples from MM patients, which showed reduced HSP27 levels after BTZ treatment in BTZ-sensitive patients, whereas levels remained unchanged in patients with low BTZ sensitivity [367]. Furthermore, other pathway activities, such as the NF-κB pathway activity, are also increased in BTZ-resistant MM cells compared to sensitive ones [316], and these cells undergo profound metabolic programming, leading to high cellular metabolism, oxidative phosphorylation with increased protein folding and sphingomyelin synthesis [368,369]. Notably, LDHA is overexpressed in BTZ-resistant MM cell lines and its knockdown restores BTZ

sensitivity in MM [370]. Consistent with these observations of metabolic adaptation, we demonstrate in Chapter 3 that MM cells exhibit a significant upregulation of key metabolic proteins in the presence of WP, suggesting that WP may further drive this resistant metabolic phenotype.

Platelets and drug resistance

In solid tumours, platelets have been shown to increase the survival of adenocarcinoma cells treated with 5-fluorouracil and paclitaxel by upregulating anti-apoptotic and downregulating pro-apoptotic genes and promoting cell proliferation and survival [371]. It has also been demonstrated that the presence of platelet aggregates in biopsy samples of breast cancer patients was associated with increased chemotherapeutic resistance [372]. In haematological malignancies, platelets also play a significant role in AML patients, as platelet-leukaemia cell aggregates are positively correlated with disease severity, with relapsed patients exhibiting increased aggregates. Furthermore, cells co-cultured with platelets exhibited increased resistance to doxorubicin [373]. Despite such progress, a significant gap in our understanding of how platelets influence therapeutic responses in MM remains.

We demonstrated that platelets promote myeloma cell migration. Our proteomic analysis revealed a repertoire of proteins upregulated in conditioned media from myeloma cells co-cultured with platelets, many of which are implicated in focal adhesion dynamics and cytoskeletal remodelling. Notably, these included proteins such as VINC, TLN1, and GELS, which were found to be increased in abundance in serum of MM patients least sensitive to bortezomib [238] . Therefore, in this chapter, we aim to examine whether platelet–myeloma interactions may contribute to MM cell resistance to proteasome inhibition, particularly to BTZ.

5.2 METHODS

5.2.1 WP preparation

Blood was obtained from healthy volunteers following consent. Whole blood in 3.15% of sodium citrate was centrifuged, and washed platelets were prepared from PRP in the presence of prostacyclin to prevent platelet aggregation. The pellet containing the platelets was resuspended in serum-free RPMI 1640 and 1% Antibiotic-Antimycotic.

5.2.2 Cell lines used

MM.1S cell line was used and cultured in RPMI supplemented with 10% Foetal Bovine Serum (FBS) [Sigma-Aldrich, Ireland)] and 1% Antibiotic-Antimycotic (100X) [Fisher Scientific Ltd., Ireland] and maintained at 37 °C in a 5% CO_2 atmosphere using a 170 L CO_2 cell culture incubator (GS Biotech, Medical Supply Company Ltd., Ireland).

5.2.3 BTZ EC_{50}

MM.1S cells were seeded in a 96-well plate at a concentration of 20,000 cells/well using RPMI 1640 + 8% FBS. They were allowed to attach and settle for 24 hours. Then, BTZ (Bio-Techne Ireland Limited, Ireland) was added in concentrations ranging from 2-50 nM (by duplicate and in 4 independent experiments) and cell death was quantified, after 48 hours, in real time using propidium iodide (PI) fluorescence with the IncuCyte live-cell imaging system. BTZ EC_{50} value was calculated from the ratio of PI-positive cells (red dots) to total cells/well (referred to as % PI positive cells) using the IncuCyte S3 software, and the data fitted using the Hill equation or non-linear regression analysis in GraphPad Prism 9 version 9.0 (GraphPad Software, La Jolla, CA, USA).

5.2.4 Effect of BTZ on MM cells co-incubated in the presence and absence of platelets

MM.1S cells were seeded in triplicate at a density of 20,000 cells/well in a 96-well plate. After 12 hours, platelets were added to the wells at a final concentration of 250,000/µL and co-cultured with the MM.1S cells for 24 hours. Cells were then treated with 6 nM BTZ and maintained for an additional 48 hours. % PI-positive cells were quantified in real time using propidium iodide (PI) fluorescence with the IncuCyte live-cell imaging system.

5.2.5 Effect of BTZ on MM cells co-incubated in the presence of MM cell secretome and MM cell-platelet secretome

For these experiments, MM.1S cells were cultured to 70–80% confluence in two flasks and then incubated in serum-free medium and WP. Following 24 hours of incubation, the supernatant from the flasks was collected (hereafter referred to as

the MM.1S cell secretome or MM.1S cell–platelet secretome), centrifuged, filtered through a 0.22 µm membrane, and stored at –80 °C until further use.

For subsequent experiments, 20,000 MM.1S cells were resuspended in either MM.1S cell secretome or MM cell–platelet secretome and seeded in triplicate into a 96-well plate. After 24 hours, cells were treated with BTZ (6 nM) and incubated for an additional 48 hours (**Figure 52**). % PI-positive cells were quantified in real time using propidium iodide (PI) fluorescence with the IncuCyte live-cell imaging system (Sartorius, UK).

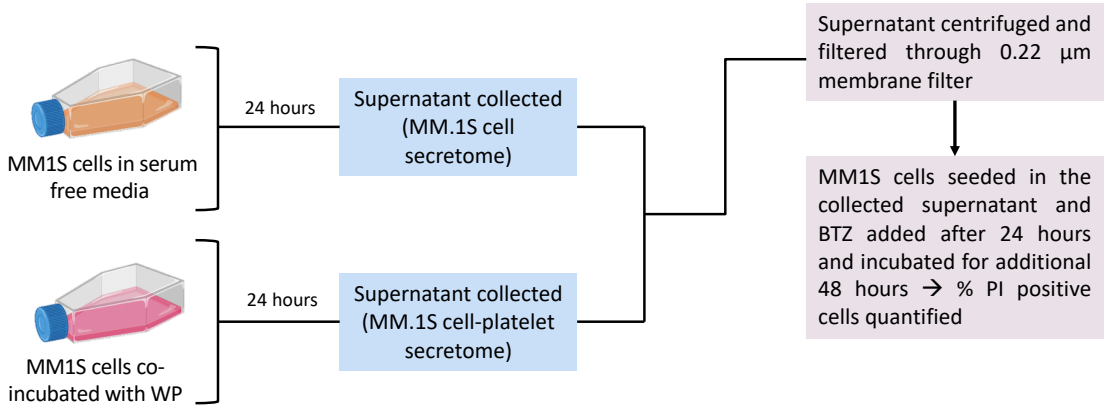

Figure 52 Procedure followed to study the effect of Bortezomib (BTZ) on cell death of MM cells co-incubated with and without MM cell-platelet secretome. Figure prepared using Microsoft Powerpoint.

5.3 RESULTS

5.3.1 Calculation of EC_{50} value of BTZ

The half-maximal effective concentration (EC_{50}) of BTZ in the MM.1S cell line was determined to be 6 nM, with a 95% confidence interval of 5.75 to 6.47 nM (**Figure 53**).

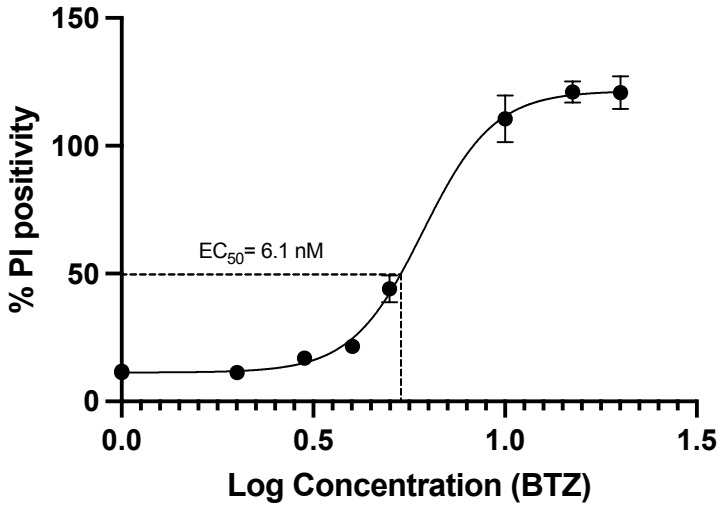

Figure 53 Half-maximal effective concentration (EC50) curve of BTZ in MM.1S cell line. Results are presented as % PI positive cells ± SEM from 4 independent experiments; EC50 6.1 nM; 95% CI (5.75, 6.47nM). Figure prepared in GraphPad prism 9.

5.3.2 Effect of BTZ on MM cells co-incubated in the presence and absence of platelets

As shown in **Figure 54 A (i-ii)**, co-incubation of MM.1S cells with platelets resulted in complete coverage of cells by platelets. Quantitative analysis therefore could not be performed.

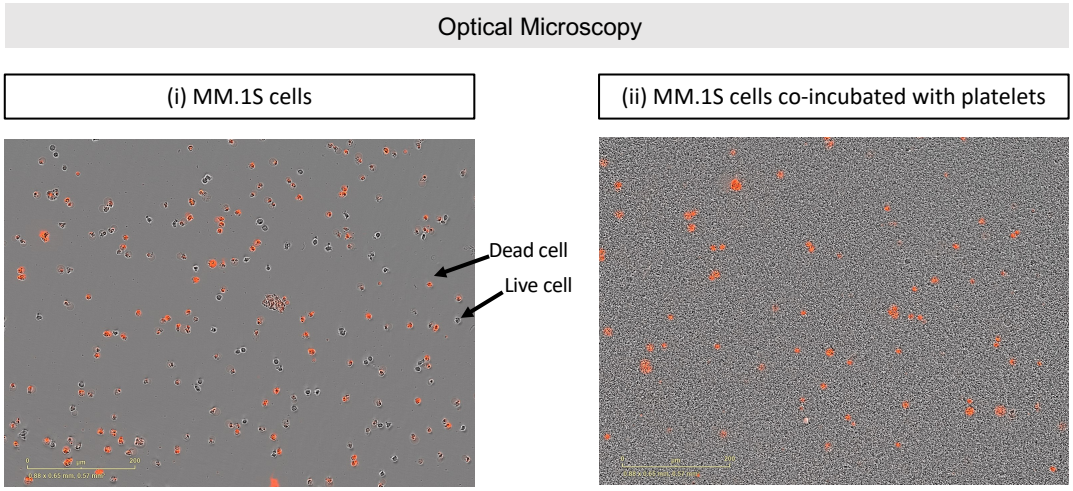

Figure 54 Effect of bortezomib on cell death of MM cells co-incubated in the presence and absence of platelets. Representative images of (i) MM.1S cells cultured alone or (ii) co-incubated with platelets demonstrating complete coverage of tumour cells by platelets following co-culture. Images captured with IncuCyte live imaging system.

5.3.3 Effect of BTZ on MM cells co-incubated in the presence of MM.1S cell secretome and MM.1S cell-platelet secretome

When MM.1S cells were resuspended in either MM.1S cell secretome or MM.1S cell-platelet secretome and subsequently treated with BTZ for 48 hours, no statistically significant difference in cell death was detected between the two conditions (**Figure 55 i-ii**). However, when compared to the control (MM.1S cells resuspended in 8% FBS+ BTZ), both conditions, MM.1S cell secretome and MM.1S cell-platelet secretome, significantly prevented cell death in the presence of BTZ (**Figure 55 ii**).

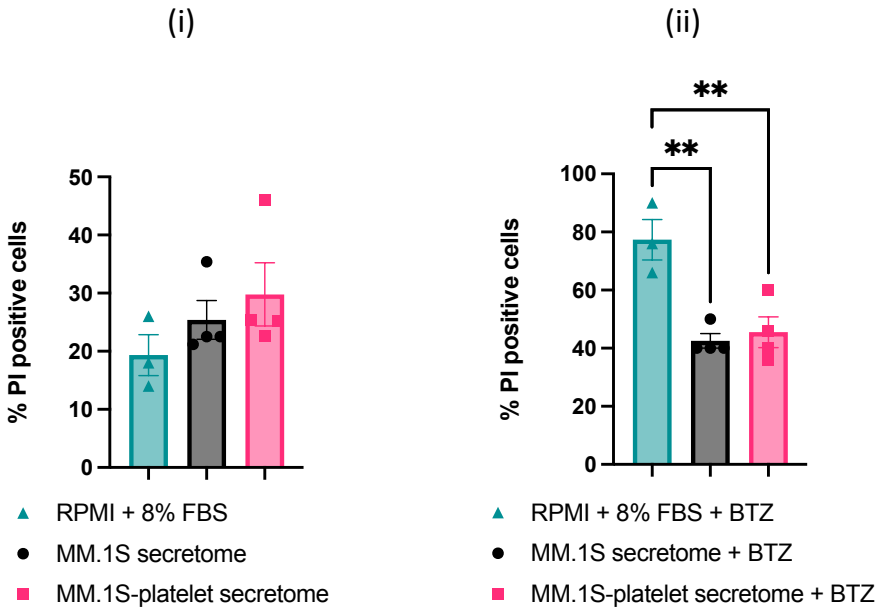

Figure 55 Effect of BTZ on MM.1S cells resuspended in MM.1S cell secretome and MM.1S cell-platelet secretome. (i) Cells incubated without BTZ. (ii) cells incubated with BTZ. Cells were counted using IncuCyte S3 software. Data is presented as mean ± SEM; n=4; one-way ANOVA and Dunnett's post-test; ** $p \leq 0.005$

5.4 DISCUSSION

Platelet–tumour cell interactions are increasingly recognised as modulators of cancer cell survival and therapeutic response. In chapter 3, we found proteins such as vinculin, talin-1, and gelsolin that were increased in abundance in the presence of platelets. These proteins were also found to be increased in MM patients who were least sensitive to BTZ, according to a study by Tierney et al. [238]. Driven by these proteomic insights, we sought to determine if platelets could directly confer

a protective advantage to MM.1S cells against BTZ. To establish a robust baseline for these experiments, we first determined the EC_{50} of BTZ in our MM.1S model. Our calculated value of 6.1 nM is within the 4–11.25 nM range reported in previous studies [374,375].

Unfortunately, the direct effect of platelets on BTZ-induced cell death could not be evaluated due to technical limitations in the experimental conditions. Platelets completely covered the cell surface, as confirmed by microscopy, and thus, the IncuCyte software could not count the total number of cells in the well. In addition, although red dots representing dead cells were visible, they could not be relied upon, leading to inconsistent readings and, consequently, inaccurate analysis. Alternative colourimetric and luminescent viability assays (Cell Counting Kit-8 and RealTime-MT Glo; Promega, UK) were also tested, but they also produced confounding signals because their reagents reacted with platelets. As a consequence, reliable quantification of MM.1S cell death under these conditions was not feasible. Therefore, although reduced apparent cell death was observed visually in co-culture conditions, these findings could not be quantified and therefore cannot be interpreted as evidence of platelet-mediated protection, as tumour cell viability could not be accurately assessed. Importantly, this represents a technical limitation rather than a biological absence of effect.

The potential impact of soluble factors was examined by resuspending MM.1S cells in MM.1S cell secretome and MM.1S cell–platelet secretome prior to BTZ treatment. Although both secretomes prevented cell death in the presence of BTZ, no statistically significant difference was detected between them, indicating that the inclusion of platelet-derived soluble mediators is insufficient to confer protection against BTZ-induced cytotoxicity in MM.1S cells. These data suggest that, if platelet-mediated protection occurs in MM, it is unlikely to be driven solely by platelet-secreted factors and may require direct cell–platelet contact.

In contrast, evidence from solid tumour models has demonstrated that platelets can protect adherent cancer cells from cytotoxic therapies through direct physical interactions and aggregation. A study in HER2-negative breast cancer patients demonstrated that those patients whose diagnostic biopsy samples had platelet cell aggregates in more than 10% of tumour cells prior to treatment were more likely to

have persistent residual disease after completion of the chemotherapy regimen [372]. Similarly, an in vitro study involving the co-incubation of colonic and ovarian adenocarcinoma cell lines with platelets showed that platelets increased the survival of those cells in response to 5-fluorouracil and paclitaxel, as measured by flow cytometry [371]. In such adherent tumour systems, platelets can be experimentally removed prior to cell viability assessment, enabling clear attribution of protective effects to platelet contact. However, such separation is not readily achievable in suspension cultures, including this MM model.

This distinction highlights a critical methodological difference between adherent and suspension tumour models in the investigation of platelet-mediated drug resistance. Consequently, the absence of demonstrable platelet-mediated protection in MM.1S suspension cultures should not be interpreted as biological evidence that platelets lack protective capacity in MM, but rather as a limitation of the current experimental approaches. To overcome these technical hurdles, future work should employ multi-parameter methods capable of distinguishing cell populations within dense aggregates. By using a CD41-specific antibody to identify the platelet population, and a constitutive marker (e.g., Green Fluorescent Protein) to identify MM cells, the MM cell population could be separated for analysis. Combined with PI, this would enable precise quantification of MM cell death within aggregates, thereby bypassing the optical and biochemical interference caused by platelets in standard assays.

5.5 CONCLUSIONS

This study investigated whether platelets influence the sensitivity of MM.1S cells to the proteasome inhibitor BTZ, and whether any such effect is mediated by soluble factors or requires direct platelet–tumour cell contact. The EC_{50} of BTZ in MM.1S cells was consistent with previously reported values, confirming the expected drug sensitivity of this cell line to this proteasome inhibitor. While qualitative observations suggested that platelet co-culture reduced MM.1S cell death, technical interferences prevented an accurate quantification. In fact, platelet coverage of MM.1S cells interfered with image-based cell counting, while commonly used metabolic and luminescent viability assays generated confounding signals due to platelet reactivity. As a result, the direct effect of platelets on BTZ-induced cytotoxicity could not be conclusively assessed. Importantly, this limitation reflects

methodological challenges rather than a definitive absence of platelet-mediated protection. Experiments using secretome indicated that although both MM.1S cell secretome and MM.1S cell-platelet secretome confer protection against BTZ, this effect, however, cannot be attributed to soluble factors released only by platelets. Together, these findings suggest that any potential platelet-mediated protection in MM likely requires direct cell–platelet contact. Importantly, the inability to detect such effects in MM.1S suspension cultures was due to methodological limitations rather than a definitive biological absence of platelet-mediated protection. To resolve this, future studies may focus on single-cell techniques, such as multi-parameter flow cytometry or mass cytometry (CyTOF), which can distinguish viable MM cells from associated platelets within dense aggregates.

DISCUSSION

The present study investigated whether multiple myeloma cells were able to induce platelet aggregation. This phenomenon is called as tumour cell-induced platelet aggregation (TCIPA). Four myeloma cell lines, MM.1S, KMS-27, JJN-3, and U266, and examined how soluble and contact-dependent platelet interactions modulate myeloma cell behaviour, including migration, invasion, and resistance to bortezomib. Collectively, the findings reveal that myeloma cells engage platelets through heterogeneous, cell-line-specific mechanisms and that these interactions have broader implications for tumour progression.

MM.1S and KMS-27 cell lines consistently induced platelet aggregation across all concentrations tested, whereas JJN-3 and U266 did not and even when they did induce, they did so only at the highest cell concentrations. MM.1S cells were more aggressive in their ability to aggregate platelets than KMS-27, inducing aggregation in a shorter timeframe. Phenanthroline could not inhibit platelet aggregation in response to MM.1S cells, an effect not observed for KMS-27. This suggests that MM.1S cells may secrete higher levels of MMP-2. Apyrase, which scavenges ADP, had no effect on MM.1S-induced TCIPA but marginally inhibited KMS-27-induced aggregation, pointing to differential reliance on ADP-mediated signalling. Similarly, aspirin inhibited KMS-27 but not MM.1S-induced aggregation, suggesting that thromboxane A_2-dependent pathways contribute more substantially to KMS-27 TCIPA. EDTA and prostacyclin completely inhibited aggregation in both cell lines, underscoring calcium dependency and the central role of cAMP-mediated signalling in MM TCIPA, consistent with prior literature on solid tumour lines.

While MM.1S and KMS-27, both expressing wild-type p53, consistently induced aggregation using the LTA, their behaviour in the ultrasound wave trap diverged markedly: MM.1S induced platelet aggregation, whereas KMS-27 did not, likely due to the substantially lower cell numbers used in the trap compared to LTA or the potential release of platelet-inhibitory factors under cluster conditions. These results collectively imply that p53 status, solely, is not a deterministic factor governing TCIPA in MM.

Proteomic analysis of MM cell–platelet co-culture secretomes revealed a rich landscape of proteins implicated in tumour progression, immune evasion, and

drug resistance. Metabolic enzymes such as G6PD, ALDOA, and ENO1 were enriched in MM.1S and JJN-3 secretomes, reflecting the metabolic reprogramming characteristic of aggressive MM. Notably, ENO1 also functions as a plasminogen receptor, linking metabolic adaptation to invasive capacity. Structural and adhesion proteins, including talin-1, vinculin, gelsolin, and cofilin-1, were elevated in multiple cell line secretomes, consistent with their known roles in integrin-mediated adhesion and drug resistance. Importantly, increased abundance of talin-1 and vinculin has been reported in serum from MM patients least responsive to bortezomib [238], suggesting that platelet-driven upregulation of these proteins may contribute to a drug-resistant phenotype in vivo. A core set of 14 proteins conserved across all four MM cell–platelet secretomes, including Beta arrestin 1, cyclase associated protein 1, and calmodulin, further highlights shared platelet-responsive mechanisms that may represent novel therapeutic targets.

Notably, one of the most biologically relevant findings was that co-incubation of MM cells with platelets significantly increased the migration of MM.1S and U266 cells. KMS-27 and JJN-3 demonstrated similar directional trends, though these did not achieve statistical significance, potentially reflecting inter-donor variability in platelet reactivity. Strikingly, a cell line's capacity to aggregate platelets did not predict its migratory response: KMS-27 was a potent aggregator yet showed no significant platelet-enhanced migration, whereas U266 was a weak aggregator yet demonstrated a robust migratory response in the presence of platelets. Gelatinase zymography confirmed that co-incubation with platelets significantly upregulated MMP-2 and MMP-9 activity in MM.1S and JJN-3 cells, indicative of enhanced proteolytic capacity. However, this did not translate into increased invasion through Matrigel, most likely because myeloma suspension cells do not adhere to the membrane before platelet contact, allowing platelets to interact with the Matrigel components, get activated and potentially block the membrane pores via formation of cell-platelet aggregates as confirmed by optical microscopy after fixation of co-incubated samples. This demonstrates a fundamental methodological limitation of Transwell-based assays for non-adherent tumour cell lines.

Several other limitations must be also considered when interpreting these findings. First, the proteomic analysis of MM cell–platelet co-culture secretomes cannot discriminate between platelet-derived and MM cell-derived proteins. However, platelets cannot synthesise proteins de novo and release all the proteins that are

stored within them,, attributing the increase in abundance of proteins in cell-platelet secretomes to myeloma cells themselves rather than platelets. As an experimental control, platelet releasate (proteins releasate by platelets upon activation by collagen) was used . Second, the temporal discrepancy between the short-term LTA experiments (60 minutes) and the extended co-incubation conditions applied for proteomic profiling (24 hours) limits the capacity to draw direct associations between a cell line's ability to aggregate and its proteomic profile. The prolonged co-incubation in cell culture flasks may capture stress responses, extracellular vesicle exchange, and bidirectional signalling that do not reflect the short term dynamics of TCIPA using the LTA. Furthermore, LTA assays involve shear stress from continuous stirring, whereas co-incubation conditions in cell culture flasks are largely static, introducing additional mechanistic differences between the two experimental contexts.

Third, the inability to quantify platelet-mediated protection against BTZ represents a significant technical limitation. Direct co-culture experiments were confounded by platelet coverage of MM.1S cells, which prevented accurate cell counting by the IncuCyte system, while alternative viability assays (CCK-8 and RealTime-Glo) produced misleading signals due to platelet reactivity with assay reagents. Although visual inspection suggested reduced cell death in co-culture conditions, these observations could not be quantitavely measured. Future studies could employ fluorescent cell tracking strategies, such as GFP-labelled MM cells combined with CD41 antibody staining to exclude platelets, alongside with propidium iodide viability gating to enable accurate quantification of MM cell death within mixed aggregates.

Finally, donor-dependent variability in platelet reactivity was a recurring source of experimental noise across aggregation, migration, and secretome studies. Sex-related differences, age, and individual genetic variation are known to influence platelet responsiveness.

CONCLUSIONS AND FUTURE DIRECTIONS

The present study demonstrated for the first time that MM.1S and KMS-27 cell line consistently induced platelet aggregation that could be modulated using different inhibitors of platelet aggregation whereas JJN-3 and U266 did not, suggesting that multiple myeloma cell induced platelet aggregation is cell line specific and may vary between patients based on disease biology and risk profile. To more closely replicate the clinical context, future investigations should employ platelets and plasma cells derived directly from myeloma patients, enabling assessment of whether cancer-associated alterations in platelet phenotype meaningfully influence platelet–tumour cell interactions. It is well established that platelets in myeloma patients exist within a delicate equilibrium between hyporeactivity, attributable to chronic activation and exhaustion, and hyperreactivity arising from a pro-tumourigenic microenvironment. Systematic evaluation of how patient-derived or healthy donor platelets respond to established myeloma cell lines and/or primary plasma cells in vitro would yield important mechanistic insights into how disease-state platelets contribute to TCIPA. Quantitative assessment of platelet reactivity states could further be accomplished using Quartz Crystal Microbalance with Dissipation (QCM-D), which offers a sensitive, label-free approach to characterising platelet adhesion and activation dynamics.

Platelet aggregation was not inhibited when platelets resuspended in myeloma cell secretomes were stimulated using agonists. Rather, a significant increase in platelet aggregation was observed when platelets resuspended in MM.1S cell secretome were stimulated with collagen, suggesting the presence of pro-aggregatory soluble mediators within the myeloma cell secretome. This finding warrants further investigation, specifically, future studies could employ sub-threshold concentrations of agonists to stimulate platelet aggregation in the presence of myeloma secretomes, which may provide greater sensitivity in detecting secretome-driven modulatory effects that are masked at standard agonist concentrations.

Proteomic analysis of myeloma cell–platelet co-culture secretomes revealed an enrichment of proteins associated with carbon metabolism, cytoskeletal reorganisation, and focal adhesion pathways. A critical priority for subsequent

work is the validation of proteins consistently identified across all cell lines, followed by targeted functional modulation of candidate proteins to determine their specific contributions to TCIPA, and in progression of MM.

Perhaps the most clinically significant finding of the present study is the demonstration that platelets promote the migration of multiple myeloma cells, with statistically significant increases observed in MM.1S and U266 cell lines. This finding raises the important possibility that platelets may actively facilitate extramedullary dissemination of myeloma cells, a process of particular relevance given that extramedullary multiple myeloma represents a highly aggressive, treatment-refractory disease manifestation. However, it remains unclear whether this effect is mediated by physical contact or by soluble factors released from activated platelets or from MM cells specifically during this interaction. To disambiguate these mechanisms, future studies should incorporate myeloma cells-platelet releasate co-incubation assays, enabling direct comparison of the pro-migratory effects attributable to secreted mediators alone versus those requiring cell–cell contact.

Finally, investigating the role of platelets in bortezomib resistance of myeloma cells revealed that myeloma cell-platelet secretome alone did not protect the myeloma cells from bortezomib induced cell death. This result implies that any platelet-mediated chemoresistance in MM is likely contingent upon direct cell–platelet contact rather than paracrine signalling alone. To rigorously test this hypothesis, future studies should develop a multi-parameter flow cytometric platform incorporating a CD41-specific antibody to delineate the platelet population, a constitutively expressed fluorescent marker such as Green Fluorescent Protein (GFP) to identify myeloma cells, and propidium iodide to discriminate viable from non-viable cells.

In summary, this data suggests that platelets are not passive bystanders in myeloma. They actively reshape the microenviroment, promote migration and may promote drug resistance through direct cell-platelet contact rather than souble factors which needs further investigation, which opens up avenues for future work.

REFERENCES

1. *Cancer statistics | Irish Cancer Society*. https://www.cancer.ie/cancer-information-and-support/cancer-information/about-cancer/cancer-statistics (accessed 2023-11-16).
2. *Living with blood cancer after diagnosis - Health News*. https://www.healthnews.ie/haematology/living-blood-cancer/# (accessed 2023-11-16).
3. *Multiple myeloma | Irish Cancer Society*. https://www.cancer.ie/cancer-information/cancer-types/multiple-myeloma (accessed 2026-02-26).
4. Durie, B. G. M.; Salmon, S. E. A Clinical Staging System for Multiple Myeloma Correlation of Measured Myeloma Cell Mass with Presenting Clinical Features, Response to Treatment, and Survival. *Cancer* **1975**, *36* (3), 842–854. https://doi.org/10.1002/1097-0142(197509)36:3<842::AID-CNCR2820360303>3.0.CO;2-U.
5. Dima, D.; Jiang, D.; Singh, D. J.; Hasipek, M.; Shah, H. S.; Ullah, F.; Khouri, J.; Maciejewski, J. P.; Jha, B. K. Multiple Myeloma Therapy: Emerging Trends and Challenges. *Cancers 2022, Vol. 14, Page 4082* **2022**, *14* (17), 4082. https://doi.org/10.3390/CANCERS14174082.
6. Fonseca, R.; Bergsagel, P. L.; Drach, J.; Shaughnessy, J.; Gutierrez, N.; Stewart, A. K.; Morgan, G.; Van Ness, B.; Chesi, M.; Minvielle, S.; Neri, A.; Barlogie, B.; Kuehl, W. M.; Liebisch, P.; Davies, F.; Chen-Kiang, S.; Durie, B. G. M.; Carrasco, R.; Sezer, O.; Reiman, T.; Pilarski, L.; Avet-Loiseau, H. International Myeloma Working Group Molecular Classification of Multiple Myeloma: Spotlight Review. *Leukemia 2009 23:12* **2009**, *23* (12), 2210–2221. https://doi.org/10.1038/leu.2009.174.
7. Hale, D. A.; Krause, J. R. Plasma Cell Myeloma with Lymphoplasmacytic Morphology and Cyclin D1 Expression, an Uncommon Variant. *Proc. (Bayl. Univ. Med. Cent).* **2017**, *30* (2), 192. https://doi.org/10.1080/08998280.2017.11929581.
8. Bergsagel, P. L.; Kuehl, W. M. Molecular Pathogenesis and a Consequent Classification of Multiple Myeloma. *Journal of Clinical Oncology* **2005**, *23* (26), 6333–6338. https://doi.org/10.1200/JCO.2005.05.021/ASSET/A43AF7D0-1BEF-4B9D-86C0-8860A6ED64A7/ASSETS/GRAPHIC/JCO05021F02.JPEG.
9. Chesi, M.; Nardini, E.; Brents, L. A.; Schrock, E.; Ried, T.; Kuehl, W. M.; Bergsagel, P. L. Frequent Translocation t(4;14)(P16.3;Q32.3) in Multiple Myeloma Is Associated with Increased Expression and Activating Mutations of Fibroblast Growth Factor Receptor 3. *Nat. Genet.* **1997**, *16* (3), 260–264. https://doi.org/10.1038/NG0797-260.
10. Kuo, A. J.; Cheung, P.; Chen, K.; Zee, B. M.; Kioi, M.; Lauring, J.; Xi, Y.; Park, B. H.; Shi, X.; Garcia, B. A.; Li, W.; Gozani, O. NSD2 Links Dimethylation of Histone H3 at Lysine 36 to Oncogenic Programming. *Mol. Cell* **2011**, *44* (4), 609. https://doi.org/10.1016/J.MOLCEL.2011.08.042.
11. Hurt, E. M.; Wiestner, A.; Rosenwald, A.; Shaffer, A. L.; Campo, E.; Grogan, T.; Bergsagel, P. L.; Kuehl, W. M.; Staudt, L. M. Overexpression of C-Maf Is a Frequent Oncogenic Event in Multiple Myeloma That Promotes Proliferation and Pathological Interactions with Bone Marrow Stroma. *Cancer Cell* **2004**, *5* (2), 191–199. https://doi.org/10.1016/S1535-6108(04)00019-4.

12. Ram, M.; Fraser, M. R.; Dos Santos, J. V.; Tasakis, R.; Islam, A.; Abo-Donia, J. U.; Parekh, S.; Lagana, A. The Genetic and Molecular Drivers of Multiple Myeloma: Current Insights, Clinical Implications, and the Path Forward. *Pharmgenomics. Pers. Med.* **2024**, *17*, 573. https://doi.org/10.2147/PGPM.S350238.
13. Aubrey, B. J.; Strasser, A.; Kelly, G. L. Tumor-Suppressor Functions of the TP53 Pathway. *Cold Spring Harb. Perspect. Med.* **2016**, *6* (5), a026062. https://doi.org/10.1101/cshperspect.a026062.
14. Malkin, D.; Li, F. P.; Strong, L. C.; Fraumeni, J. F.; Nelson, C. E.; Kim, D. H.; Kassel, J.; Gryka, M. A.; Bischoff, F. Z.; Tainsky, M. A.; Friend, S. H. Germ Line P53 Mutations in a Familial Syndrome of Breast Cancer, Sarcomas, and Other Neoplasms. *Science* **1990**, *250* (4985), 1233–1238. https://doi.org/10.1126/SCIENCE.1978757.
15. Ding, L.; Getz, G.; Wheeler, D. A.; Mardis, E. R.; McLellan, M. D.; Cibulskis, K.; Sougnez, C.; Greulich, H.; Muzny, D. M.; Morgan, M. B.; Fulton, L.; Fulton, R. S.; Zhang, Q.; Wendl, M. C.; Lawrence, M. S.; Larson, D. E.; Chen, K.; Dooling, D. J.; Sabo, A.; Hawes, A. C.; Shen, H.; Jhangiani, S. N.; Lewis, L. R.; Hall, O.; Zhu, Y.; Mathew, T.; Ren, Y.; Yao, J.; Scherer, S. E.; Clerc, K.; Metcalf, G. A.; Ng, B.; Milosavljevic, A.; Gonzalez-Garay, M. L.; Osborne, J. R.; Meyer, R.; Shi, X.; Tang, Y.; Koboldt, D. C.; Lin, L.; Abbott, R.; Miner, T. L.; Pohl, C.; Fewell, G.; Haipek, C.; Schmidt, H.; Dunford-Shore, B. H.; Kraja, A.; Crosby, S. D.; Sawyer, C. S.; Vickery, T.; Sander, S.; Robinson, J.; Winckler, W.; Baldwin, J.; Chirieac, L. R.; Dutt, A.; Fennell, T.; Hanna, M.; Johnson, B. E.; Onofrio, R. C.; Thomas, R. K.; Tonon, G.; Weir, B. A.; Zhao, X.; Ziaugra, L.; Zody, M. C.; Giordano, T.; Orringer, M. B.; Roth, J. A.; Spitz, M. R.; Wistuba, I. I.; Ozenberger, B.; Good, P. J.; Chang, A. C.; Beer, D. G.; Watson, M. A.; Ladanyi, M.; Broderick, S.; Yoshizawa, A.; Travis, W. D.; Pao, W.; Province, M. A.; Weinstock, G. M.; Varmus, H. E.; Gabriel, S. B.; Lander, E. S.; Gibbs, R. A.; Meyerson, M.; Wilson, R. K. Somatic Mutations Affect Key Pathways in Lung Adenocarcinoma. *Nature* **2008**, *455* (7216), 1069–1075. https://doi.org/10.1038/NATURE07423.
16. Flynt, E.; Bisht, K.; Sridharan, V.; Ortiz, M.; Towfic, F.; Thakurta, A. Prognosis, Biology, and Targeting of TP53 Dysregulation in Multiple Myeloma. *Cells* **2020**, *9* (2). https://doi.org/10.3390/CELLS9020287.
17. Drach, J.; Ackermann, J.; Fritz, E.; Krömer, E.; Schuster, R.; Gisslinger, H.; DeSantis, M.; Zojer, N.; Fiegl, M.; Roka, S.; Schuster, J.; Heinz, R.; Ludwig, H.; Huber, H. Presence of a P53 Gene Deletion in Patients with Multiple Myeloma Predicts for Short Survival after Conventional-Dose Chemotherapy. *Blood* **1998**, *92* (3), 802–809.
18. Gaballa, S.; Saliba, R. M.; Srour, S.; Lu, G.; Brammer, J. E.; Shah, N.; Bashir, Q.; Patel, K.; Bock, F.; Parmar, S.; Hosing, C.; Popat, U.; Delgado, R.; Rondon, G.; Shah, J. J.; Manasanch, E. E.; Orlowski, R. Z.; Champlin, R.; Qazilbash, M. H. Outcomes in Patients with Multiple Myeloma with TP53 Deletion after Autologous Hematopoietic Stem Cell Transplant. *Am. J. Hematol.* **2016**, *91* (10), E442. https://doi.org/10.1002/AJH.24487.
19. Rojas, E. A.; Corchete, L. A.; De Ramón, C.; Krzeminski, P.; Quwaider, D.; García-Sanz, R.; Martínez-López, J.; Oriol, A.; Rosiñol, L.; Bladé, J.; Lahuerta, J. J.; San Miguel, J. F.; González, M.; Mateos, M. V.; Bourdon, J. C.; Misiewicz-Krzeminska, I.; Gutiérrez, N. C. Expression of P53 Protein Isoforms Predicts Survival in Patients with Multiple Myeloma. *Am. J. Hematol.* **2022**, *97* (6), 700. https://doi.org/10.1002/AJH.26507.
20. Lohr, J. G.; Stojanov, P.; Carter, S. L.; Cruz-Gordillo, P.; Lawrence, M. S.; Auclair, D.; Sougnez, C.; Knoechel, B.; Gould, J.; Saksena, G.; Cibulskis, K.; McKenna, A.; Chapman, M. A.; Straussman, R.; Levy, J.; Perkins, L. M.; Keats, J. J.; Schumacher, S. E.;

Rosenberg, M.; Getz, G.; Golub, T. R. Widespread Genetic Heterogeneity in Multiple Myeloma: Implications for Targeted Therapy. *Cancer Cell* **2014**, *25* (1), 91. https://doi.org/10.1016/J.CCR.2013.12.015.

21. Chapman, M. A.; Lawrence, M. S.; Keats, J. J.; Cibulskis, K.; Sougnez, C.; Schinzel, A. C.; Harview, C. L.; Brunet, J. P.; Ahmann, G. J.; Adli, M.; Anderson, K. C.; Ardlie, K. G.; Auclair, D.; Baker, A.; Bergsagel, P. L.; Bernstein, B. E.; Drier, Y.; Fonseca, R.; Gabriel, S. B.; Hofmeister, C. C.; Jagannath, S.; Jakubowiak, A. J.; Krishnan, A.; Levy, J.; Liefeld, T.; Lonial, S.; Mahan, S.; Mfuko, B.; Monti, S.; Perkins, L. M.; Onofrio, R.; Pugh, T. J.; Rajkumar, S. V.; Ramos, A. H.; Siegel, D. S.; Sivachenko, A.; Stewart, A. K.; Trudel, S.; Vij, R.; Voet, D.; Winckler, W.; Zimmerman, T.; Carpten, J.; Trent, J.; Hahn, W. C.; Garraway, L. A.; Meyerson, M.; Lander, E. S.; Getz, G.; Golub, T. R. Initial Genome Sequencing and Analysis of Multiple Myeloma. *Nature* **2011**, *471* (7339), 467. https://doi.org/10.1038/NATURE09837.
22. Bolli, N.; Avet-Loiseau, H.; Wedge, D. C.; Van Loo, P.; Alexandrov, L. B.; Martincorena, I.; Dawson, K. J.; Iorio, F.; Nik-Zainal, S.; Bignell, G. R.; Hinton, J. W.; Li, Y.; Tubio, J. M. C.; McLaren, S.; O'Meara, S.; Butler, A. P.; Teague, J. W.; Mudie, L.; Anderson, E.; Rashid, N.; Tai, Y. T.; Shammas, M. A.; Sperling, A. S.; Fulciniti, M.; Richardson, P. G.; Parmigiani, G.; Magrangeas, F.; Minvielle, S.; Moreau, P.; Attal, M.; Facon, T.; Futreal, P. A.; Anderson, K. C.; Campbell, P. J.; Munshi, N. C. Heterogeneity of Genomic Evolution and Mutational Profiles in Multiple Myeloma. *Nature Communications 2014 5:1* **2014**, *5* (1), 1–13. https://doi.org/10.1038/ncomms3997.
23. Kyle, R. A.; Therneau, T. M.; Rajkumar, S. V.; Offord, J. R.; Larson, D. R.; Plevak, M. F.; Melton, L. J. A Long-Term Study of Prognosis in Monoclonal Gammopathy of Undetermined Significance. *New England Journal of Medicine* **2002**, *346* (8), 564–569. https://doi.org/10.1056/NEJMOA01133202/ASSET/4B58620B-2EEC-4A03-B72A-8DDBD3749B28/ASSETS/IMAGES/LARGE/NEJMOA01133202_T3.JPG.
24. Rajkumar, S. V.; Peter, ; Bergsagel, L.; Reece, D. E. MGUS and Smoldering Multiple Myeloma: Update on Pathogenesis, Natural History, and Management. *Hematology* **2005**, *2005* (1), 340–345. https://doi.org/10.1182/ASHEDUCATION-2005.1.340.
25. Rajkumar, S. V.; Kumar, S.; Lonial, S.; Mateos, M. V. Smoldering Multiple Myeloma Current Treatment Algorithms. *Blood Cancer J.* **2022**, *12* (9), 129. https://doi.org/10.1038/S41408-022-00719-0.
26. Manier, S.; Salem, K. Z.; Park, J.; Landau, D. A.; Getz, G.; Ghobrial, I. M. Genomic Complexity of Multiple Myeloma and Its Clinical Implications. *Nat. Rev. Clin. Oncol.* **2017**, *14* (2), 100–113. https://doi.org/10.1038/NRCLINONC.2016.122.
27. Ho, M.; Patel, A.; Goh, C. Y.; Moscvin, M.; Zhang, L.; Bianchi, G. Changing Paradigms in Diagnosis and Treatment of Monoclonal Gammopathy of Undetermined Significance (MGUS) and Smoldering Multiple Myeloma (SMM). *Leukemia* **2020**, *34* (12), 3111–3125. https://doi.org/10.1038/S41375-020-01051-X.
28. Givi, J. P.; Williams, N.; Hass, R.; Tacker, D. H.; Goswami, A.; Randall, C. Educational Case: Multiple Myeloma. *Acad. Pathol.* **2024**, *11* (2), 100117. https://doi.org/10.1016/J.ACPATH.2024.100117.
29. Wang, H.; Chen, J. Immunoparesis in Multiple Myeloma: A Current Overview. *Front. Oncol.* **2025**, *15*, 1628144. https://doi.org/10.3389/FONC.2025.1628144.
30. De Stefano, V.; Larocca, A.; Carpenedo, M.; Cavo, M.; Di Raimondo, F.; Falanga, A.; Offidani, M.; Petrucci, M. T.; Ruggeri, M.; Santi, R. M.; Barosi, G. Thrombosis in Multiple Myeloma: Risk Stratification, Antithrombotic Prophylaxis, and Management

of Acute Events. A Consensus-Based Position Paper from an *Ad Hoc* Expert Panel. *Haematologica* **2022**, *107* (11), 2536–2547. https://doi.org/10.3324/HAEMATOL.2022.280893.

31. Dispenzieri, A.; Kyle, R. A. Neurological Aspects of Multiple Myeloma and Related Disorders. *Best Pract. Res. Clin. Haematol.* **2005**, *18* (4), 673–688. https://doi.org/10.1016/J.BEHA.2005.01.024.
32. *International Staging System for Multiple Myeloma | The IMF*. https://www.myeloma.org/international-staging-system-iss-reivised-iss-r-iss (accessed 2023-05-14).
33. *Multiple Myeloma Treatment Overview | Int'l Myeloma Foundation*. https://www.myeloma.org/multiple-myeloma-treatment (accessed 2023-09-01).
34. Dimopoulos, M. A.; Moreau, P.; Terpos, E.; Mateos, M. V; Zweegman, S.; Cook, G.; Delforge, M.; Hájek, R.; Schjesvold, F.; Cavo, M.; Goldschmidt, H.; Facon, T.; Einsele, H.; Boccadoro, M.; San-Miguel, J.; Sonneveld, P. Multiple Myeloma: EHA-ESMO Clinical Practice Guidelines for Diagnosis, Treatment and Follow-up y Behalf of the EHA Guidelines Committee * and ESMO Guidelines Committee. **2021**, *17*. https://doi.org/10.1016/j.annonc.2020.11.014.
35. Usmani, S. Z.; Facon, T.; Hungria, V.; Bahlis, N. J.; Venner, C. P.; Braunstein, M.; Pour, L.; Martí, J. M.; Basu, S.; Cohen, Y. C.; Matsumoto, M.; Suzuki, K.; Hulin, C.; Grosicki, S.; Legiec, W.; Beksac, M.; Maiolino, A.; Takamatsu, H.; Perrot, A.; Turgut, M.; Ahmadi, T.; Liu, W.; Wang, J.; Chastain, K.; Vermeulen, J.; Krevvata, M.; Lopez-Masi, L.; Carey, J.; Rowe, M.; Carson, R.; Zweegman, S. Daratumumab plus Bortezomib, Lenalidomide and Dexamethasone for Transplant-Ineligible or Transplant-Deferred Newly Diagnosed Multiple Myeloma: The Randomized Phase 3 CEPHEUS Trial. *Nature Medicine 2025 31:4* **2025**, *31* (4), 1195–1202. https://doi.org/10.1038/s41591-024-03485-7.
36. Goldman-Mazur, S.; Visram, A.; Rajkumar, S. V.; Kapoor, P.; Dispenzieri, A.; Lacy, M. Q.; Gertz, M. A.; Buadi, F. K.; Hayman, S. R.; Dingli, D.; Kourelis, T.; Gonsalves, W. I.; Warsame, R. M.; Muchtar, E.; Leung, N.; Kyle, R. A.; Kumar, S. Second Line Treatment Strategies in Multiple Myeloma: A Referral-Center Experience. *Blood* **2021**, *138* (Supplement 1), 819. https://doi.org/10.1182/BLOOD-2021-151466.
37. Comprehensive Cancer Network, N. NCCN Guidelines for Patients: Multiple Myeloma.
38. Arastu-Kapur, S.; Anderl, J. L.; Kraus, M.; Parlati, F.; Shenk, K. D.; Lee, S. J.; Muchamuel, T.; Bennett, M. K.; Driessen, C.; Ball, A. J.; Kirk, C. J. Nonproteasomal Targets of the Proteasome Inhibitors Bortezomib and Carfilzomib: A Link to Clinical Adverse Events. *Clinical Cancer Research* **2011**, *17* (9), 2734–2743. https://doi.org/10.1158/1078-0432.CCR-10-1950/83727/AM/NON-PROTEASOMAL-TARGETS-OF-THE-PROTEASOME.
39. Sorgiovanni, I.; Del Giudice, M. L.; Galimberti, S.; Buda, G. Monoclonal Antibodies in Relapsed-Refractory Multiple Myeloma. *Pharmaceuticals 2025, Vol. 18,* **2025**, *18* (2). https://doi.org/10.3390/PH18020145.
40. Ma, J.; Mo, Y.; Tang, M.; Shen, J.; Qi, Y.; Zhao, W.; Huang, Y.; Xu, Y.; Qian, C. Bispecific Antibodies: From Research to Clinical Application. *Front. Immunol.* **2021**, *12*, 626616. https://doi.org/10.3389/FIMMU.2021.626616/BIBTEX.
41. *A Study of Talquetamab in Participants With Relapsed or Refractory Multiple Myeloma - Full Text View - ClinicalTrials.gov*. https://classic.clinicaltrials.gov/ct2/show/NCT04634552 (accessed 2023-08-28).

42. *MagnetisMM-3: Study Of Elranatamab (PF-06863135) Monotherapy in Participants With Multiple Myeloma Who Are Refractory to at Least One PI, One IMiD and One Anti-CD38 mAb - Full Text View - ClinicalTrials.gov*. https://classic.clinicaltrials.gov/ct2/show/NCT04649359 (accessed 2023-08-30).
43. Moreau, P.; Garfall, A. L.; van de Donk, N. W. C. J.; Nahi, H.; San-Miguel, J. F.; Oriol, A.; Nooka, A. K.; Martin, T.; Rosinol, L.; Chari, A.; Karlin, L.; Benboubker, L.; Mateos, M.-V.; Bahlis, N.; Popat, R.; Besemer, B.; Martínez-López, J.; Sidana, S.; Delforge, M.; Pei, L.; Trancucci, D.; Verona, R.; Girgis, S.; Lin, S. X. W.; Olyslager, Y.; Jaffe, M.; Uhlar, C.; Stephenson, T.; Van Rampelbergh, R.; Banerjee, A.; Goldberg, J. D.; Kobos, R.; Krishnan, A.; Usmani, S. Z. Teclistamab in Relapsed or Refractory Multiple Myeloma. *New England Journal of Medicine* **2022**, *387* (6), 495–505. https://doi.org/10.1056/NEJMOA2203478/SUPPL_FILE/NEJMOA2203478_DATA-SHARING.PDF.
44. Bieliński, K.; Puła, B. Bispecific Antibodies in Multiple Myeloma. *Acta Haematol. Pol.* **2025**, *56* (1), 39–47. https://doi.org/10.5603/AHP.104091.
45. *Early results from Johnson & Johnson's trispecific antibody show promising response in heavily pretreated multiple myeloma patients*. https://www.prnewswire.com/news-releases/early-results-from-johnson--johnsons-trispecific-antibody-show-promising-response-in-heavily-pretreated-multiple-myeloma-patients-302471267.html (accessed 2026-05-12).
46. *Impressive Results of Trispecific Antibody in Myeloma Presented at EHA 2025 Congress | Targeted Oncology - Immunotherapy, Biomarkers, and Cancer Pathways*. https://www.targetedonc.com/view/impressive-results-of-trispecific-antibody-in-myeloma-presented-at-eha-2025-congress (accessed 2026-05-12).
47. Zhang, Q.; Song, Y.; Zhou, K.; Lin, Q. Emerging Therapeutic Agents in Multiple Myeloma: Highlights from the 2024 ASH Annual Meeting. *Biomark. Res.* **2025**, *13* (1), 90. https://doi.org/10.1186/S40364-025-00803-0.
48. Tsai, D. Y.; Hung, K. H.; Chang, C. W.; Lin, K. I. Regulatory Mechanisms of B Cell Responses and the Implication in B Cell-Related Diseases. *Journal of Biomedical Science 2019 26:1* **2019**, *26* (1), 64-. https://doi.org/10.1186/S12929-019-0558-1.
49. García-Ortiz, A.; Rodríguez-García, Y.; Encinas, J.; Maroto-Martín, E.; Castellano, E.; Teixidó, J.; Martínez-López, J. The Role of Tumor Microenvironment in Multiple Myeloma Development and Progression. *Cancers 2021, Vol. 13, Page 217* **2021**, *13* (2), 217. https://doi.org/10.3390/CANCERS13020217.
50. Roccaro, A. M.; Sacco, A.; Maiso, P.; Azab, A. K.; Tai, Y. T.; Reagan, M.; Azab, F.; Flores, L. M.; Campigotto, F.; Weller, E.; Anderson, K. C.; Scadden, D. T.; Ghobrial, I. M. BM Mesenchymal Stromal Cell-Derived Exosomes Facilitate Multiple Myeloma Progression. *J. Clin. Invest.* **2013**, *123* (4), 1542–1555. https://doi.org/10.1172/JCI66517.
51. Dadzie, T. G.; Green, A. C. The Role of the Bone Microenvironment in Regulating Myeloma Residual Disease and Treatment. *Front. Oncol.* **2022**, *12*, 999939. https://doi.org/10.3389/FONC.2022.999939.
52. Hao, M.; Zhang, L.; An, G.; Meng, H.; Han, Y.; Xie, Z.; Xu, Y.; Li, C.; Yu, Z.; Chang, H.; Qiu, L. Bone Marrow Stromal Cells Protect Myeloma Cells from Bortezomib Induced Apoptosis by Suppressing MicroRNA-15a Expression. *Leuk. Lymphoma* **2011**, *52* (9), 1787–1794. https://doi.org/10.3109/10428194.2011.576791.

53. Markovina, S.; Callander, N. S.; O'Connor, S. L.; Xu, G.; Shi, Y.; Leith, C. P.; Kim, K. M.; Trivedi, P.; Kim, J.; Hematti, P.; Miyamoto, S. Bone Marrow Stromal Cells from Multiple Myeloma Patients Uniquely Induce Bortezomib Resistant NF-KB Activity in Myeloma Cells. *Mol. Cancer* **2010**, *9*, 176. https://doi.org/10.1186/1476-4598-9-176.
54. Ghamlouch, H.; Gagler, D. C.; Blaney, P.; Boyle, E. M.; Wang, Y.; Avigan, J.; Choi, J.; Landgren, O.; Tsirigos, A.; Maura, F.; Morgan, G. J.; Davies, F. E. A Proinflammatory Response and Polarized Differentiation of Stromal Elements Characterizes the Murine Myeloma Bone Marrow Niche. *Exp. Hematol. Oncol.* **2025**, *14* (1), 1–14. https://doi.org/10.1186/S40164-025-00606-X/FIGURES/7.
55. Vacca, A.; Ria, R.; Semeraro, F.; Merchionne, F.; Coluccia, M.; Boccarelli, A.; Scavelli, C.; Nico, B.; Gernone, A.; Battelli, F.; Tabilio, A.; Guidolin, D.; Petrucci, M. T.; Ribatti, D.; Dammacco, F. Endothelial Cells in the Bone Marrow of Patients with Multiple Myeloma. *Blood* **2003**, *102* (9), 3340–3348. https://doi.org/10.1182/BLOOD-2003-04-1338.
56. Pellegrino, A.; Ria, R.; Di Pietro, G.; Cirulli, T.; Surico, G.; Pennisi, A.; Morabito, F.; Ribatti, D.; Vacca, A. Bone Marrow Endothelial Cells in Multiple Myeloma Secrete CXC-Chemokines That Mediate Interactions with Plasma Cells. *Br. J. Haematol.* **2005**, *129* (2), 248–256. https://doi.org/10.1111/J.1365-2141.2005.05443.X.
57. Ria, R.; Vacca, A. Bone Marrow Stromal Cells-Induced Drug Resistance in Multiple Myeloma. *Int. J. Mol. Sci.* **2020**, *21* (2), 613. https://doi.org/10.3390/IJMS21020613.
58. Wang, Z.; Zhang, L.; Wang, H.; Xiong, S.; Li, Y.; Tao, Q.; Xiao, W.; Qin, H.; Wang, Y.; Zhai, Z. Tumor-Induced CD14+HLA-DR (-/Low) Myeloid-Derived Suppressor Cells Correlate with Tumor Progression and Outcome of Therapy in Multiple Myeloma Patients. *Cancer Immunol. Immunother.* **2015**, *64* (3), 389–399. https://doi.org/10.1007/S00262-014-1646-4.
59. Nakamura, K.; Kassem, S.; Cleynen, A.; Chrétien, M. L.; Guillerey, C.; Putz, E. M.; Bald, T.; Förster, I.; Vuckovic, S.; Hill, G. R.; Masters, S. L.; Chesi, M.; Bergsagel, P. L.; Avet-Loiseau, H.; Martinet, L.; Smyth, M. J. Dysregulated IL-18 Is a Key Driver of Immunosuppression and a Possible Therapeutic Target in the Multiple Myeloma Microenvironment. *Cancer Cell* **2018**, *33* (4), 634-648.e5. https://doi.org/10.1016/J.CCELL.2018.02.007.
60. Berardi, S.; Ria, R.; Reale, A.; De Luisi, A.; Catacchio, I.; Moschetta, M.; Vacca, A. Multiple Myeloma Macrophages: Pivotal Players in the Tumor Microenvironment. *J. Oncol.* **2013**, *2013* (1), 183602. https://doi.org/10.1155/2013/183602.
61. Lopes, R.; Caetano, J.; Ferreira, B.; Barahona, F.; Carneiro, E. A.; João, C. The Immune Microenvironment in Multiple Myeloma: Friend or Foe? *Cancers (Basel).* **2021**, *13* (4), 1–16. https://doi.org/10.3390/CANCERS13040625.
62. Arandi, N.; Dehghani, M. Immune Microenvironment in Hematologic Malignancies. *Iran. J. Med. Sci.* **2023**, *48* (1), 1. https://doi.org/10.30476/IJMS.2023.48937.
63. Sklavenitis-Pistofidis, R.; Bustoros, M.; Ghobrial, I. M. Bone Marrow Niche in Multiple Myeloma and Its Precursor States. *Hemasphere* **2019**, *3* (Suppl), 121–123. https://doi.org/10.1097/HS9.0000000000000246.
64. Rodríguez, P. C.; Ochoa, A. C. Arginine Regulation by Myeloid Derived Suppressor Cells and Tolerance in Cancer: Mechanisms and Therapeutic Perspectives. *Immunol. Rev.* **2008**, *222* (1), 180. https://doi.org/10.1111/J.1600-065X.2008.00608.X.
65. Brown, R. D.; Pope, B.; Murray, A.; Esdale, W.; Sze, D. M.; Gibson, J.; Joy Ho, P.; Hart, D.; Joshua, D. Dendritic Cells from Patients with Myeloma Are Numerically Normal

but Functionally Defective as They Fail to Up-Regulate CD80 (B7-1) Expression after HuCD40LT Stimulation Because of Inhibition by Transforming Growth Factor-Beta1 and Interleukin-10. *Blood* **2001**, *98* (10), 2992–2998. https://doi.org/10.1182/BLOOD.V98.10.2992.

66. Barillé, S.; Akhoundi, C.; Collette, M.; Mellerin, M. P.; Rapp, M. J.; Harousseau, J. L.; Bataille, R.; Amiot, M. Metalloproteinases in Multiple Myeloma: Production of Matrix Metalloproteinase-9 (MMP-9), Activation of ProMMP-2, and Induction of MMP-1 by Myeloma Cells. *Blood* **1997**, *90* (4), 1649–1655. https://doi.org/10.1182/BLOOD.V90.4.1649.
67. Kelly, T.; Børset, M.; Abe, E.; Gaddy-Kurten, D.; Sanderson, R. D. Matrix Metalloproteinases in Multiple Myeloma. *Leuk. Lymphoma* **2000**, *37* (3–4), 273–281. https://doi.org/10.3109/10428190009089428.
68. Vincent, T.; Mechti, N. Extracellular Matrix in Bone Marrow Can Mediate Drug Resistance in Myeloma. *Leuk. Lymphoma* **2005**, *46* (6), 803–811. https://doi.org/10.1080/10428190500051448/ASSET//CMS/ASSET/78CBA03D-05F0-4869-AB7E-0970D1E5C84C/10428190500051448.FP.PNG.
69. Hideshima, T.; Nakamura, N.; Chauhan, D.; Anderson, K. C. Biologic Sequelae of Interleukin-6 Induced PI3-K/Akt Signaling in Multiple Myeloma. *Oncogene* **2001**, *20* (42), 5991–6000. https://doi.org/10.1038/SJ.ONC.1204833.
70. Hideshima, T.; Mitsiades, C.; Tonon, G.; Richardson, P. G.; Anderson, K. C. Understanding Multiple Myeloma Pathogenesis in the Bone Marrow to Identify New Therapeutic Targets. *Nat. Rev. Cancer* **2007**, *7* (8), 585–598. https://doi.org/10.1038/NRC2189.
71. De Bruyne, E.; Bos, T. J.; Schuit, F.; Van Valckenborgh, E.; Menu, E.; Thorrez, L.; Atadja, P.; Jernberg-Wiklund, H.; Vanderkerken, K. IGF-1 Suppresses Bim Expression in Multiple Myeloma via Epigenetic and Posttranslational Mechanisms. *Blood* **2010**, *115* (12), 2430–2440. https://doi.org/10.1182/BLOOD-2009-07-232801.
72. Emile, C.; Fermand, J. P.; Danon, F. Interleukin-6 Serum Levels in Patients with Multiple Myeloma. *Br. J. Haematol.* **1994**, *86* (2), 439–440. https://doi.org/10.1111/j.1365-2141.1994.tb04765.x.
73. Wang, J.; Faict, S.; Maes, K.; De Bruyne, E.; Van Valckenborgh, E.; Schots, R.; Vanderkerken, K.; Menu, E. Extracellular Vesicle Cross-Talk in the Bone Marrow Microenvironment: Implications in Multiple Myeloma. *Oncotarget* **2016**, *7* (25), 38927. https://doi.org/10.18632/ONCOTARGET.7792.
74. Bucci-Muñoz, M.; Gola, A. M.; Rigalli, J. P.; Ceballos, M. P.; Ruiz, M. L. Extracellular Vesicles and Cancer Multidrug Resistance: Undesirable Intercellular Messengers? . **2023**, *13* (8). https://doi.org/10.3390/LIFE13081633.
75. Li, B.; Xu, H.; Han, H.; Song, S.; Zhang, X.; Ouyang, L.; Qian, C.; Hong, Y.; Qiu, Y.; Zhou, W.; Huang, M.; Zhuang, W. Exosome-Mediated Transfer of LncRUNX2-AS1 from Multiple Myeloma Cells to MSCs Contributes to Osteogenesis. *Oncogene* **2018**, *37* (41), 5508–5519. https://doi.org/10.1038/S41388-018-0359-0.
76. Soncini, D.; Marimpietri, D.; Ladisa, F.; Lai, F.; Airoldi, I.; Gramignoli, R.; Cea, M.; Morandi, F. Bone Marrow-Derived Extracellular Vesicles from Multiple Myeloma Patients Promote Adaptive Immune Dysfunction via HLA-G, PD-1, and PD-L1. *Front. Immunol.* **2025**, *16*, 1640168. https://doi.org/10.3389/FIMMU.2025.1640168/FULL.
77. Yang, X.; Lin, Z.; Liu, H.; Wang, X.; Liu, H. Multiple Myeloma Side Population Cells Promote Dexamethasone Resistance of Main Population Cells through Exosome

Metastasis of LncRNA SNHG16. *J. Oncol.* **2023**, *2023*. https://doi.org/10.1155/2023/5135445.
78. Yamamoto, T.; Nakayama, J.; Yamamoto, Y.; Kuroda, M.; Hattori, Y.; Ochiya, T. SORT1/LAMP2-Mediated Extracellular Vesicle Secretion and Cell Adhesion Are Linked to Lenalidomide Resistance in Multiple Myeloma. *Blood Adv.* **2022**, *6* (8), 2480–2495. https://doi.org/10.1182/BLOODADVANCES.2021005772.
79. Williams, O.; Sergent, S. R. Histology, Platelets. *StatPearls* **2022**.
80. Chaudhry, R.; Killeen, R. B.; Babiker, H. M. Physiology, Coagulation Pathways. *StatPearls* **2025**.
81. Green, D. Coagulation Cascade. *Hemodial. Int.* **2006**, *10 Suppl 2* (SUPPL. 2). https://doi.org/10.1111/J.1542-4758.2006.00119.X.
82. Ho-Tin-Noé, B.; Demers, M.; Wagner, D. D. How Platelets Safeguard Vascular Integrity. *J. Thromb. Haemost.* **2011**, *9* (Suppl 1), 56. https://doi.org/10.1111/J.1538-7836.2011.04317.X.
83. Saba, S. R.; Mason, R. G. Effects of Platelets and Certain Platelet Components on Growth of Cultured Human Endothelial Cells. *Thromb. Res.* **1975**, *7* (5), 807–812. https://doi.org/10.1016/0049-3848(75)90205-4.
84. Thurston, G.; Rudge, J. S.; Ioffe, E.; Zhou, H.; Ross, L.; Croll, S. D.; Glazer, N.; Holash, J.; McDonald, D. M.; Yancopoulos, G. D. Angiopoietin-1 Protects the Adult Vasculature against Plasma Leakage. *Nat. Med.* **2000**, *6* (4), 460–463. https://doi.org/10.1038/74725.
85. Schaphorst, K. L.; Chiang, E.; Jacobs, K. N.; Zaiman, A.; Natarajan, V.; Wigley, F.; Garcia, J. G. N. Role of Sphingosine-1 Phosphate in the Enhancement of Endothelial Barrier Integrity by Platelet-Released Products. *Am. J. Physiol. Lung Cell. Mol. Physiol.* **2003**, *285* (1). https://doi.org/10.1152/AJPLUNG.00311.2002.
86. Minnear, F. L.; Patil, S.; Bell, D.; Gainor, J. P.; Morton, C. A. Platelet Lipid(s) Bound to Albumin Increases Endothelial Electrical Resistance: Mimicked by LPA. *Am. J. Physiol. Lung Cell. Mol. Physiol.* **2001**, *281* (6). https://doi.org/10.1152/AJPLUNG.2001.281.6.L1337.
87. Rhee, J. S.; Black, M.; Schubert, U.; Fischer, S.; Morgenstern, E.; Hammes, H. P.; Preissner, K. T. The Functional Role of Blood Platelet Components in Angiogenesis. *Thromb. Haemost.* **2004**, *92* (2), 394–402. https://doi.org/10.1160/TH03-04-0213.
88. Brill, A.; Dashevsky, O.; Rivo, J.; Gozal, Y.; Varon, D. Platelet-Derived Microparticles Induce Angiogenesis and Stimulate Post-Ischemic Revascularization. *Cardiovasc. Res.* **2005**, *67* (1), 30–38. https://doi.org/10.1016/J.CARDIORES.2005.04.007.
89. Goerge, T.; Ho-Tin-Noe, B.; Carbo, C.; Benarafa, C.; Remold-O'Donnell, E.; Zhao, B. Q.; Cifuni, S. M.; Wagner, D. D. Inflammation Induces Hemorrhage in Thrombocytopenia. *Blood* **2008**, *111* (10), 4958–4964. https://doi.org/10.1182/BLOOD-2007-11-123620.
90. Sonmez, O.; Sonmez, M. Role of Platelets in Immune System and Inflammation. *Porto Biomed. J.* **2017**, *2* (6), 311. https://doi.org/10.1016/J.PBJ.2017.05.005.
91. Jiang, K.; Lim, S. Bin; Xiao, J.; Jokhun, D. S.; Shang, M.; Song, X.; Zhang, P.; Liang, L.; Low, B. C.; Shivashankar, G. V.; Lim, C. T. Deleterious Mechanical Deformation Selects Mechanoresilient Cancer Cells with Enhanced Proliferation and Chemoresistance. *Adv. Sci. (Weinh).* **2023**, *10* (22). https://doi.org/10.1002/ADVS.202201663.
92. WOOD, S. Pathogenesis of Metastasis Formation Observed in Vivo in the Rabbit Ear Chamber. *AMA Arch. Pathol.* **1958**, *66* (4), 550–568.

93. Philippe, C.; Philippe, B.; Fouqueray, B.; Perez, J.; Lebret, M.; Baud, L. Protection from Tumor Necrosis Factor-Mediated Cytolysis by Platelets. *Am. J. Pathol.* **1993**, *143* (6), 1713–1723.
94. Egan, K.; Cooke, N.; Kenny, D. Living in Shear: Platelets Protect Cancer Cells from Shear Induced Damage. *Clin. Exp. Metastasis* **2014**, *31* (6), 697–704. https://doi.org/10.1007/S10585-014-9660-7.
95. Lian, L.; Li, W.; Li, Z. Y.; Mao, Y. X.; Zhang, Y. T.; Zhao, Y. M.; Chen, K.; Duan, W. M.; Tao, M. Inhibition of MCF-7 Breast Cancer Cell-Induced Platelet Aggregation Using a Combination of Antiplatelet Drugs. *Oncol. Lett.* **2013**, *5* (2), 675–680. https://doi.org/10.3892/OL.2012.1074/HTML.
96. Drabsch, Y.; Ten Dijke, P. TGF-β Signaling in Breast Cancer Cell Invasion and Bone Metastasis. *J. Mammary Gland Biol. Neoplasia* **2011**, *16* (2), 97. https://doi.org/10.1007/S10911-011-9217-1.
97. Wang, F. qiang; Ariztia, E. V.; Boyd, L. R.; Horton, F. R.; Smicun, Y.; Hetherington, J. A.; Smith, P. J.; Fishman, D. A. Lysophosphatidic Acid (LPA) Effects on Endometrial Carcinoma in Vitro Proliferation, Invasion, and Matrix Metalloproteinase Activity. *Gynecol. Oncol.* **2010**, *117* (1), 88–95. https://doi.org/10.1016/J.YGYNO.2009.12.012.
98. Jurasz, P.; North, S.; Venner, P.; Radomski, M. W. Matrix Metalloproteinase-2 Contributes to Increased Platelet Reactivity in Patients with Metastatic Prostate Cancer: A Preliminary Study. *Thromb. Res.* **2003**, *112* (1–2), 59–64. https://doi.org/10.1016/j.thromres.2003.10.012.
99. Andersen, H.; Greenberg, D. L.; Fujikawa, K.; Xu, W.; Chung, D. W.; Davie, E. W. Protease-Activated Receptor 1 Is the Primary Mediator of Thrombin-Stimulated Platelet Procoagulant Activity. *Proc. Natl. Acad. Sci. U. S. A.* **1999**, *96* (20), 11189. https://doi.org/10.1073/PNAS.96.20.11189.
100. Cole, M.; Bromberg, M. Tissue Factor as a Novel Target for Treatment of Breast Cancer. *Oncologist* **2013**, *18* (1), 14. https://doi.org/10.1634/THEONCOLOGIST.2012-0322.
101. Minamiya, Y.; Matsuzaki, I.; Sageshima, M.; Saito, H.; Taguchi, K.; Nakagawa, T.; Ogawa, J. I. Expression of Tissue Factor MRNA and Invasion of Blood Vessels by Tumor Cells in Non-Small Cell Lung Cancer. *Surg. Today* **2004**, *34* (1), 1–5. https://doi.org/10.1007/s00595-003-2643-y.
102. Akashi, T.; Furuya, Y.; Ohta, S.; Fuse, H. Tissue Factor Expression and Prognosis in Patients with Metastatic Prostate Cancer. *Urology* **2003**, *62* (6), 1078–1082. https://doi.org/10.1016/S0090-4295(03)00768-4.
103. Fillmann, L. S.; Fillmann, L. P.; Zarpelon De Oliveira, L.; Fillmann, H. S.; Carvalhal, G. F. Tissue Factor Expression in Colorectal Adenocarcinoma: Association with Angiogenesis and Clinical and Pathological Aspects. *J Coloproctol* **2022**, *42* (1), 54–58. https://doi.org/10.1055/s-0041-1739453.
104. Jiang, X.; Bailly, M. A.; Panetti, T. S.; Cappello, M.; Konigsberg, W. H.; Bromberg, M. E. Formation of Tissue Factor-Factor VIIa-Factor Xa Complex Promotes Cellular Signaling and Migration of Human Breast Cancer Cells. *J. Thromb. Haemost.* **2004**, *2* (1), 93–101. https://doi.org/10.1111/J.1538-7836.2004.00545.X.
105. Bluff, J. E.; Brown, N. J.; Reed, M. W. R.; Staton, C. A. Tissue Factor, Angiogenesis and Tumour Progression. *Breast Cancer Res.* **2008**, *10* (2), 204. https://doi.org/10.1186/BCR1871.

106. Rucińska, M.; Furman, M.; Skrzydlewski, Z.; Zaremba, E. Activity of Cancer Procoagulant (CP) in Serum of Patients with Cancer of Lung, Breast, Oesophagus and Colorectum. *Acta Biochim. Pol.* **1997**, *44* (1), 109–112.
107. Kee, N. L. A.; Naudé, R. J.; Blatch, G. L.; Frost, C. L. The Effect of Cancer Procoagulant on Expression of Metastatic and Angiogenic Markers in Breast Cancer and Embryonic Stem Cell Lines. *Biol. Chem.* **2012**, *393* (3), 113–121. https://doi.org/10.1515/HSZ-2011-0177/MACHINEREADABLECITATION/RIS.
108. Oleksowicz, L.; Mrowiec, Z.; Schwartz, E.; Khorshidi, M.; Dutcher, J. P.; Puszkin, E. Characterization of Tumor-Induced Platelet Aggregation: The Role of Immunorelated GPIb and GPIIb/IIIa Expression by MCF-7 Breast Cancer Cells. *Thromb. Res.* **1995**, *79* (3), 261–274. https://doi.org/10.1016/0049-3848(95)00113-6.
109. Huong, P. T.; Nguyen, L. T.; Nguyen, X. B.; Lee, S. K.; Bach, D. H. The Role of Platelets in the Tumor-Microenvironment and the Drug Resistance of Cancer Cells. *Cancers (Basel).* **2019**, *11* (2). https://doi.org/10.3390/CANCERS11020240.
110. Terraube, V.; Pendu, R.; Baruch, D.; Gebbink, M. F. B. G.; Meyer, D.; Lenting, P. J.; Denis, C. V. Increased Metastatic Potential of Tumor Cells in von Willebrand Factor-Deficient Mice. *J. Thromb. Haemost.* **2006**, *4* (3), 519–526. https://doi.org/10.1111/J.1538-7836.2005.01770.X.
111. Andrade, S. S.; Gouvea, I. E.; Silva, M. C. C.; Castro, E. D.; de Paula, C. A. A.; Okamoto, D.; Oliveira, L.; Peres, G. B.; Ottaiano, T.; Facina, G.; Nazário, A. C. P.; Campos, A. H. J. F. M.; Paredes-Gamero, E. J.; Juliano, M.; da Silva, I. D. C. G.; Oliva, M. L. V.; Girão, M. J. B. C. Cathepsin K Induces Platelet Dysfunction and Affects Cell Signaling in Breast Cancer - Molecularly Distinct Behavior of Cathepsin K in Breast Cancer. *BMC Cancer* **2016**, *16* (1), 1–19. https://doi.org/10.1186/S12885-016-2203-7/FIGURES/7.
112. Khan, M.; Carmona, S.; Sukhumalchandra, P.; Roszik, J.; Philips, A.; Perakis, A. A.; Kerros, C.; Zhang, M.; Qiao, N.; St. John, L. S.; Zope, M.; Goldberg, J.; Qazilbash, M.; Jakher, H.; Clise-Dwyer, K.; Qiu, Y.; Mittendorf, E. A.; Molldrem, J. J.; Kornblau, S. M.; Alatrash, G. Cathepsin G Is Expressed by Acute Lymphoblastic Leukemia and Is a Potential Immunotherapeutic Target. *Front. Immunol.* **2018**, *8* (JAN), 314888. https://doi.org/10.3389/FIMMU.2017.01975/BIBTEX.
113. Qiu, X.; Zhu, X.; Zhang, L.; Mao, Y.; Zhang, J.; Hao, P.; Li, G.; Lv, P.; Li, Z.; Sun, X.; Wu, L.; Zheng, J.; Deng, Y.; Hou, C.; Tang, P.; Zhang, S.; Zhang, Y. Human Epithelial Cancers Secrete Immunoglobulin g with Unidentified Specificity to Promote Growth and Survival of Tumor Cells. *Cancer Res.* **2003**, *63* (19), 6488–6495.
114. Miao, S.; Shu, D.; Zhu, Y.; Lu, M.; Zhang, Q.; Pei, Y.; He, A. Di; Ma, R.; Zhang, B.; Ming, Z. Y. Cancer Cell-Derived Immunoglobulin G Activates Platelets by Binding to Platelet FcγRIIa. *Cell Death & Disease 2019 10:2* **2019**, *10* (2), 1–13. https://doi.org/10.1038/s41419-019-1367-x.
115. Boukerche, H.; Berthier-Vergnes, O.; Penin, F.; Tabone, E.; Lizard, G.; Bailly, M.; McGregor, J. L. Human Melanoma Cell Lines Differ in Their Capacity to Release ADP and Aggregate Platelets. *Br. J. Haematol.* **1994**, *87* (4), 763–772. https://doi.org/10.1111/J.1365-2141.1994.TB06736.X.
116. Mocellin, S.; Bronte, V.; Nitti, D. Nitric Oxide, a Double Edged Sword in Cancer Biology: Searching for Therapeutic Opportunities. *Med. Res. Rev.* **2007**, *27* (3), 317–352. https://doi.org/10.1002/MED.20092.
117. Loibl, S.; Von Minckwitz, G.; Weber, S.; Sinn, H. P.; Schini-Kerth, V. B.; Lobysheva, I.; Nepveu, F.; Wolf, G.; Strebhardt, K.; Kaufmann, M. Expression of Endothelial and

Inducible Nitric Oxide Synthase in Benign and Malignant Lesions of the Breast and Measurement of Nitric Oxide Using Electron Paramagnetic Resonance Spectroscopy. *Cancer* **2002**, *95* (6), 1191–1198. https://doi.org/10.1002/CNCR.10817.

118. Vakkala, M.; Kahlos, K.; Lakari, E.; Pääkkö, P.; Kinnula, V.; Soini, Y. Inducible Nitric Oxide Synthase Expression, Apoptosis, and Angiogenesis in in Situ and Invasive Breast Carcinomas. *Clin. Cancer Res.* **2000**, *6* (6), 2408–2416.
119. Ambs, S.; Merriam, W. G.; Bennett, W.; Felley-Bosco, E.; Ogunfusika, M. O.; Oser, S.; Klein, S.; Shields, P.; Billiar, T.; Harris, C. Frequent Nitric Oxide Synthase-2 Expression in Human Colon Adenomas: Implication for Tumor Angiogenesis and Colon Cancer Progression. *Cancer Res.* **1998**.
120. Ambs, S.; Bennett, W. P.; Merriam, W. G.; Ogunfusika, M. O.; Oser, S. M.; Khan, M. A.; Jones, R. T.; Harris, C. C. Vascular Endothelial Growth Factor and Nitric Oxide Synthase Expression in Human Lung Cancer and the Relation to P53. *British Journal of Cancer 1998 78:2* **1998**, *78* (2), 233–239. https://doi.org/10.1038/bjc.1998.470.
121. Swana, H. S.; Smith, S. D.; Perrotta, P. L.; Saito, N.; Wheeler, M. A.; Weiss, R. M. INDUCIBLE NITRIC OXIDE SYNTHASE WITH TRANSITIONAL CELL CARCINOMA OF THE BLADDER. *J. Urol.* **1999**, *161* (2), 630–634. https://doi.org/10.1016/S0022-5347(01)61985-2.
122. Selective Expression of Inducible Nitric Oxide Synthase in Human Prostate Carcinoma BACKGROUND. Nitric Oxide (NO) Is Synthesized by Inducible Nitric Oxide Synthase. https://doi.org/10.1002/(SICI)1097-0142(19980515)82:10.
123. Bergamin, L. S.; Braganhol, E.; Zanin, R. F.; Edelweiss, M. I. A.; Battastini, A. M. O. Ectonucleotidases in Tumor Cells and Tumor-Associated Immune Cells: An Overview. *J. Biomed. Biotechnol.* **2012**, *2012*, 959848. https://doi.org/10.1155/2012/959848.
124. Pulte, D.; Olson, K. E.; Johan, M. J.; Islam, N.; Ballard, H. S.; Furman, R. R.; Olson, A. E.; Marcus, A. J. CD39 Activity Correlates with Stage and Inhibits Platelet Reactivity in Chronic Lymphocytic Leukemia. *J. Transl. Med.* **2007**, *5*, 23. https://doi.org/10.1186/1479-5876-5-23.
125. Ning, Z.; Liu, K.; Zhang, H.; Dong, G.; Wang, X.; Xiong, H. Platelets Induce CD39 Expression in Tumor Cells to Facilitate Tumor Metastasis. *Br. J. Cancer* **2024**, *130* (9), 1542–1551. https://doi.org/10.1038/S41416-024-02640-8.
126. Netsch, P.; Elvers-Hornung, S.; Uhlig, S.; Klüter, H.; Huck, V.; Kirschhöfer, F.; Brenner-Weiß, G.; Janetzko, K.; Solz, H.; Wuchter, P.; Bugert, P.; Bieback, K. Human Mesenchymal Stromal Cells Inhibit Platelet Activation and Aggregation Involving CD73-Converted Adenosine. *Stem Cell Res. Ther.* **2018**, *9* (1), 184. https://doi.org/10.1186/S13287-018-0936-8.
127. Mehta, P.; Lawson, D.; Ward, M. B.; Kimura, A.; Gee, A. Effect of Human Tumor Cells on Platelet Aggregation: Potential Relevance to Pattern of Metastasis. *Cancer Res.* **1987**, *47* (12), 3115–3117.
128. Takagi, S.; Tsukamoto, S.; Park, J.; Johnson, K. E.; Kawano, Y.; Moschetta, M.; Liu, C. J.; Mishima, Y.; Kokubun, K.; Manier, S.; Salem, K. Z.; Huynh, D.; Sacco, A.; Forward, J.; Roccaro, A. M.; Battinelli, E. M.; Ghobrial, I. M. Platelets Enhance Multiple Myeloma Progression via Il-1b Upregulation. *Clinical Cancer Research* **2018**, *24* (10), 2430–2439. https://doi.org/10.1158/1078-0432.CCR-17-2003/87519/AM/PLATELETS-ENHANCE-MULTIPLE-MYELOMA-PROGRESSION-VIA.
129. Tsubaki, M.; Komai, M.; Itoh, T.; Imano, M.; Sakamoto, K.; Shimaoka, H.; Ogawa, N.; Mashimo, K.; Fujiwara, D.; Takeda, T.; Mukai, J.; Sakaguchi, K.; Satou, T.; Nishida, S.

Inhibition of the Tumour Necrosis Factor-Alpha Autocrine Loop Enhances the Sensitivity of Multiple Myeloma Cells to Anticancer Drugs. *Eur. J. Cancer* **2013**, *49* (17), 3708–3717. https://doi.org/10.1016/J.EJCA.2013.07.010.

130. Pignatelli, P.; De Biase, L.; Lenti, L.; Tocci, G.; Brunelli, A.; Cangemi, R.; Riondino, S.; Grego, S.; Volpe, M.; Violi, F. Tumor Necrosis Factor-α as Trigger of Platelet Activation in Patients with Heart Failure. *Blood* **2005**, *106* (6), 1992–1994. https://doi.org/10.1182/BLOOD-2005-03-1247.
131. Jourdan, M.; Tarte, K.; Legouffe, É.; Brochier, J.; Rossi, J. F.; Klein, B. Tumor Necrosis Factor Is a Survival and Proliferation Factor for Human Myeloma Cells. *Eur. Cytokine Netw.* **1999**, *10* (1), 65.
132. Gazitt, Y.; Shaughnessy, P.; Montgomery, W. Apoptosis-Induced by TRAIL AND TNF-Alpha in Human Multiple Myeloma Cells Is Not Blocked by BCL-2. *Cytokine* **1999**, *11* (12), 1010–1019. https://doi.org/10.1006/CYTO.1999.0536.
133. Egan, K.; Cooke, N.; Dunne, E.; Murphy, P.; Quinn, J.; Kenny, D. Platelet Hyporeactivity in Active Myeloma. *Thromb. Res.* **2014**, *134* (3), 747–749. https://doi.org/10.1016/j.thromres.2014.06.018.
134. Gibbins, J.; Rana, R.; Khan, D.; Shapiro, S.; Grech, H.; Ramasamy, K. Multiple Myeloma Treatment Is Associated with Enhanced Platelet Reactivity. *Blood* **2018**, *132* (Supplement 1), 3300. https://doi.org/10.1182/BLOOD-2018-99-116006.
135. Kawano, M.; Hirano, T.; Matsuda, T.; Taga, T.; Horii, Y.; Iwato, K.; Asaoku, H.; Tang, B.; Tanabe, O.; Tanaka, H.; Kuramoto, A.; Kishimoto, T. Autocrine Generation and Requirement of BSF-2/IL-6 for Human Multiple Myelomas. *Nature* **1988**, *332* (6159), 83–85. https://doi.org/10.1038/332083A0.
136. Gadó, K.; Domján, G.; Hegyesi, H.; Falus, A. Role of INTERLEUKIN-6 in the Pathogenesis of Multiple Myeloma. *Cell Biol. Int.* **2000**, *24* (4), 195–209. https://doi.org/10.1006/CBIR.2000.0497.
137. Steeve, K. T.; Marc, P.; Sandrine, T.; Dominique, H.; Yannick, F. IL-6, RANKL, TNF-Alpha/IL-1: Interrelations in Bone Resorption Pathophysiology. *Cytokine Growth Factor Rev.* **2004**, *15* (1), 49–60. https://doi.org/10.1016/J.CYTOGFR.2003.10.005.
138. Kaser, A.; Brandacher, G.; Steurer, W.; Kaser, S.; Offner, F. A.; Zoller, H.; Theurl, I.; Widder, W.; Molnar, C.; Ludwiczek, O.; Atkins, M. B.; Mier, J. W.; Tilg, H. Interleukin-6 Stimulates Thrombopoiesis through Thrombopoietin: Role in Inflammatory Thrombocytosis. *Blood* **2001**, *98* (9), 2720–2725. https://doi.org/10.1182/BLOOD.V98.9.2720.
139. O'Sullivan, L. R.; Meade-Murphy, G.; Gilligan, O. M.; Mykytiv, V.; Young, P. W.; Cahill, M. R. Platelet Hyperactivation in Multiple Myeloma Is Also Evident in Patients with Premalignant Monoclonal Gammopathy of Undetermined Significance. *Br. J. Haematol.* **2021**, *192* (2), 322–332. https://doi.org/10.1111/BJH.16774.
140. Mitchell, J. L.; Khan, D.; Rana, R. H.; Kriek, N.; Unsworth, A. J.; Sage, T.; Bye, A. P.; Laffan, M.; Shapiro, S.; Thakurta, A.; Grech, H.; Ramasamy, K.; Gibbins, J. M. Multiple Myeloma and Its Treatment Contribute to Increased Platelet Reactivity. *Platelets* **2023**, *34* (1). https://doi.org/10.1080/09537104.2023.2264940.
141. Mera Azaín, C. A.; Vargas Pasquel, J. L.; Quijano Gómez, S. M.; Rodríguez-Pardo, V. M. Mesenchymal Stem Cells and Reticulated Platelets: New Horizons in Multiple Myeloma. *Hematology Reports 2024, Vol. 16, Pages 732-741* **2024**, *16* (4), 732–741. https://doi.org/10.3390/HEMATOLREP16040070.

142. Robak, M.; Treliński, J.; Chojnowski, K. Hemostatic Changes after 1 Month of Thalidomide and Dexamethasone Therapy in Patients with Multiple Myeloma. *Medical Oncology* **2012**, *29* (5), 3574–3580. https://doi.org/10.1007/S12032-012-0290-0/TABLES/4.
143. Sarfraz, H.; Anand, K.; Liu, S.; Shah, S. Multiple Myeloma with Concurrent Immune Thrombocytopenic Purpura. *Ecancermedicalscience* **2020**, *14*. https://doi.org/10.3332/ECANCER.2020.1012.
144. O'Sullivan, L.; Meade-Murphy, G.; Gilligan, O.; Mykytiv, V.; Young, P.; Cahill, M. MM-080: Platelet Hyperactivation in Multiple Myeloma Is Also Evident in Premalignant MGUS Patients and Persists During Treatment Initiation. *Clin. Lymphoma Myeloma Leuk.* **2020**, *20*, S290. https://doi.org/10.1016/S2152-2650(20)30921-6.
145. Swieringa, F.; Sang, Y.; Remijn, J. A.; Fijnheer, R.; Korporaal, S. J. A.; Urbanus, R. T.; Huskens, D.; Konings, J.; Li, L.; De Laat, B.; Roest, M. High Prevalence of Acquired Platelet Secretion Defects in Multiple Myeloma. *Hamostaseologie* **2025**. https://doi.org/10.1055/A-2418-5664.
146. Rahman, S.; Veeraballi, S.; Chan, K. H.; Shaaban, H. S. Bleeding Diathesis in Multiple Myeloma: A Rare Presentation of a Dreadful Emergency With Management Nightmare. *Cureus* **2021**, *13* (3). https://doi.org/10.7759/CUREUS.13990.
147. Siddiq, N.; Bergstrom, C.; Anderson, L. D.; Nagalla, S. Bleeding Due to Acquired Dysfibrinogenemia as the Initial Presentation of Multiple Myeloma. *BMJ Case Reports CP* **2019**, *12* (7), e229312. https://doi.org/10.1136/BCR-2019-229312.
148. Shinagawa, A.; Kojima, H.; Berndt, M. C.; Kaneko, S.; Suzukawa, K.; Hasegawa, Y.; Shigeta, O.; Nagasawa, T. Characterization of a Myeloma Patient with a Life-Threatening Hemorrhagic Diathesis: Presence of a Lambda Dimer Protein Inhibiting Shear-Induced Platelet Aggregation by Binding to the A1 Domain of von Willebrand Factor. *Thromb. Haemost.* **2005**, *93* (5), 889–896. https://doi.org/10.1160/TH04-03-0193.
149. Saif, M. W.; Allegra, C. J.; Greenberg, B. Bleeding Diathesis in Multiple Myeloma. *J. Hematother. Stem Cell Res.* **2001**, *10* (5), 657–660. https://doi.org/10.1089/152581601753193869.
150. DiMinno, G.; Coraggio, F.; Cerbone, A. M.; Capitanio, A. M.; Manzo, C.; Spina, M.; Scarpato, P.; Dattoli, G. M.; Mattioli, P. L.; Mancini, M. A Myeloma Paraprotein with Specificity for Platelet Glycoprotein IIIa in a Patient with a Fatal Bleeding Disorder. *J. Clin. Invest.* **1986**, *77* (1), 157–164. https://doi.org/10.1172/JCI112270.
151. Li, L.; Roest, M.; Sang, Y.; Remijn, J. A.; Fijnheer, R.; Smit, K.; Huskens, D.; Wan, J.; de Laat, B.; Konings, J. Patients With Multiple Myeloma Have a Disbalanced Whole Blood Thrombin Generation Profile. *Front. Cardiovasc. Med.* **2022**, *9*, 919495. https://doi.org/10.3389/FCVM.2022.919495/FULL.
152. Laronha, H.; Caldeira, J. Structure and Function of Human Matrix Metalloproteinases. *Cells* **2020**, *9* (5), 1076. https://doi.org/10.3390/CELLS9051076.
153. Whittaker, M.; Floyd, C. D.; Brown, P.; Gearing, A. J. H. Design and Therapeutic Application of Matrix Metalloproteinase Inhibitors. *Chem. Rev.* **1999**, *99* (9), 2735–2776. https://doi.org/10.1021/CR9804543.
154. Nagase, H.; Murphy, G. Metalloproteinases, Matrix. *Encyclopedia of Biological Chemistry: Second Edition* **2013**, 90–97. https://doi.org/10.1016/B978-0-12-378630-2.00475-8.

155. Li, H.; Qiu, Z.; Li, F.; Wang, C. The Relationship between MMP-2 and MMP-9 Expression Levels with Breast Cancer Incidence and Prognosis. *Oncol. Lett.* **2017**, *14* (5), 5865–5870. https://doi.org/10.3892/OL.2017.6924.
156. Jiang, H.; Li, H. Prognostic Values of Tumoral MMP2 and MMP9 Overexpression in Breast Cancer: A Systematic Review and Meta-Analysis. *BMC Cancer* **2021**, *21* (1), 149-. https://doi.org/10.1186/S12885-021-07860-2/FIGURES/5.
157. Mudatsir; Labeda, I.; Uwuratuw, J. A.; Hendarto, J.; Warsinggih; Lusikooy, R. E.; Mappincara; Sampetoding, S.; Kusuma, M. I.; Syarifuddin, E.; Arsyad, A.; Faruk, M. Relationship between Metalloproteinase-9 (MMP-9) Expression and Clinicopathology in Colorectal Cancer: A Cross-Sectional Study. *Annals of Medicine and Surgery* **2023**, *85* (9), 4277. https://doi.org/10.1097/MS9.0000000000000892.
158. Mazor, R.; Alsaigh, T.; Shaked, H.; Altshuler, A. E.; Pocock, E. S.; Kistler, E. B.; Karin, M.; Schmid-Schönbein, G. W. Matrix Metalloproteinase-1-Mediated up-Regulation of Vascular Endothelial Growth Factor-2 in Endothelial Cells. *J. Biol. Chem.* **2013**, *288* (1), 598–607. https://doi.org/10.1074/JBC.M112.417451.
159. Li, A.; Dubey, S.; Varney, M. L.; Dave, B. J.; Singh, R. K. IL-8 Directly Enhanced Endothelial Cell Survival, Proliferation, and Matrix Metalloproteinases Production and Regulated Angiogenesis. *J. Immunol.* **2003**, *170* (6), 3369–3376. https://doi.org/10.4049/JIMMUNOL.170.6.3369.
160. Yu, Q.; Stamenkovic, I. Cell Surface-Localized Matrix Metalloproteinase-9 Proteolytically Activates TGF-β and Promotes Tumor Invasion and Angiogenesis. *Genes Dev.* **2000**, *14* (2), 163. https://doi.org/10.1101/gad.14.2.163.
161. Han, Y. P.; Tuan, T. L.; Wu, H.; Hughes, M.; Garner, W. L. TNF-Alpha Stimulates Activation of pro-MMP2 in Human Skin through NF-(Kappa)B Mediated Induction of MT1-MMP. *J. Cell Sci.* **2001**, *114* (Pt 1), 131–139. https://doi.org/10.1242/JCS.114.1.131.
162. Lynch, C. C.; Hikosaka, A.; Acuff, H. B.; Martin, M. D.; Kawai, N.; Singh, R. K.; Vargo-Gogola, T. C.; Begtrup, J. L.; Peterson, T. E.; Fingleton, B.; Shirai, T.; Matrisian, L. M.; Futakuchi, M. MMP-7 Promotes Prostate Cancer-Induced Osteolysis via the Solubilization of RANKL. *Cancer Cell* **2005**, *7* (5), 485–496. https://doi.org/10.1016/J.CCR.2005.04.013.
163. Choi, J.-Y. ; Kim, Y. ; Kuo, H.-D. ; Chang, H.-H. ; Kim, Y.-C. ; Park, J.-Y.; Choi, Y.; Kim, H.-D.; Kuo, H.-H.; Chang, Y.-C.; Kim, C.-H. Matrix Metalloproteinases and Their Inhibitors in the Pathogenesis of Epithelial Differentiation, Vascular Disease, Endometriosis, and Ocular Fibrotic Pterygium. *International Journal of Molecular Sciences 2025, Vol. 26, Page 5553* **2025**, *26* (12), 5553. https://doi.org/10.3390/IJMS26125553.
164. Verhulst, E.; Garnier, D.; De Meester, I.; Bauvois, B. Validating Cell Surface Proteases as Drug Targets for Cancer Therapy: What Do We Know, and Where Do We Go? *Cancers (Basel).* **2022**, *14* (3), 624. https://doi.org/10.3390/CANCERS14030624/S1.
165. Barillé, S.; Akhoundi, C.; Collette, M.; Mellerin, M. P.; Rapp, M. J.; Harousseau, J. L.; Bataille, R.; Amiot, M. Metalloproteinases in Multiple Myeloma: Production of Matrix Metalloproteinase-9 (MMP-9), Activation of ProMMP-2, and Induction of MMP-1 by Myeloma Cells. *Blood* **1997**, *90* (4), 1649–1655. https://doi.org/10.1182/BLOOD.V90.4.1649.
166. Urbaniak-Kujda, D.; Kapelko-Slowik, K.; Prajs, I.; Dybko, J.; Wolowiec, D.; Biernat, M.; Slowik, M.; Kuliczkowski, K. Increased Expression of Metalloproteinase-2 and -9 (MMP-2, MMP-9), Tissue Inhibitor of Metalloproteinase-1 and -2 (TIMP-1, TIMP-2),

and EMMPRIN (CD147) in Multiple Myeloma. *Hematology* **2016**, *21* (1), 26–33. https://doi.org/10.1179/1607845415Y.0000000043.
167. Van Valckenborgh, E.; Croucher, P. I.; De Raeve, H.; Carron, C.; De Leenheer, E.; Blacher, S.; Devy, L.; Noël, A.; De Bruyne, E.; Asosingh, K.; Van Riet, I.; Van Camp, B.; Vanderkerken, K. Multifunctional Role of Matrix Metalloproteinases in Multiple Myeloma: A Study in the 5T2MM Mouse Model. *American Journal of Pathology* **2004**, *165* (3), 869–878. https://doi.org/10.1016/S0002-9440(10)63349-4.
168. Pais, A. S.; Gonçalves, A. C.; Geraldes, C.; Nascimento-Costa, J. M.; Sarmento-Ribeiro, A. B. Metalloproteinase Inhibitors as a Potential Therapeutic Approach in Multiple Myeloma: A Preliminary Study. *BMC Proc.* **2010**, *4* (Suppl 2), P50.
169. Shay, G.; Tauro, M.; Loiodice, F.; Tortorella, P.; Sullivan, D. M.; Hazlehurst, L. A.; Lynch, C. C. Selective Inhibition of Matrix Metalloproteinase-2 in the Multiple Myeloma-Bone Microenvironment. *Oncotarget* **2017**, *8* (26), 41827–41840. https://doi.org/10.18632/ONCOTARGET.18103.
170. Fakhari, S.; Jalili, A.; Nikkhoo, B.; Ghaderi, B.; Boshagh, M. A.; Mirzaie, S.; Moradzad, M. MT2-MMP Is Differentially Expressed in Multiple Myeloma Cells and Mediates Their Growth and Progression. *Cell. Signal.* **2022**, *92*. https://doi.org/10.1016/J.CELLSIG.2022.110248.
171. Cooke, N. M.; Egan, K.; Mcfadden, S.; Grogan, L.; Breathnach, O. S.; O'Leary, J.; Hennessy, B. T.; Kenny, D. Increased Platelet Reactivity in Patients with Late-Stage Metastatic Cancer. *Cancer Med.* **2013**, *2* (4), 564–570. https://doi.org/10.1002/CAM4.86.
172. Hoffman, R.; Haim, N.; Brenner, B. Cancer and Thrombosis Revisited. *Blood Rev.* **2001**, *15* (2), 61–67. https://doi.org/10.1054/BLRE.2001.0149.
173. Hvas, A. M.; Favaloro, E. J. Platelet Function Analyzed by Light Transmission Aggregometry. *Methods Mol. Biol.* **2017**, *1646*, 321–331. https://doi.org/10.1007/978-1-4939-7196-1_25.
174. Bazou, D.; Santos-Martinez, M. J.; Medina, C.; Radomski, M. W. Elucidation of Flow-Mediated Tumour Cell-Induced Platelet Aggregation Using an Ultrasound Standing Wave Trap. *Br. J. Pharmacol.* **2011**, *162* (7), 1577–1589. https://doi.org/10.1111/J.1476-5381.2010.01182.X.
175. Grignani, G.; Jamieson, G. A. Platelets in Tumor Metastasis: Generation of Adenosine Diphosphate by Tumor Cells Is Specific but Unrelated to Metastatic Potential. *Blood* **1988**, *71* (4), 844–849.
176. Zucchella, M.; Dezza, L.; Pacchiarini, L.; Meloni, F.; Tacconi, F.; Bonomi, E.; Grignani, G.; Notario, A. Human Tumor Cells Cultured "in Vitro" Activate Platelet Function by Producing ADP or Thrombin. *Haematologica* **1989**, *74* (6), 541–545.
177. Heinmöller, E.; Weinel, R. J.; Heidtmann, H. H.; Salge, U.; Seitz, R.; Schmitz, I.; Müller, K. M.; Zirngibl, H. Studies on Tumor-Cell-Induced Platelet Aggregation in Human Lung Cancer Cell Lines. *J. Cancer Res. Clin. Oncol.* **1996**, *122* (12), 735–744. https://doi.org/10.1007/BF01209121.
178. Crunkhorn, S. Engineered Apyrase Averts Clot Formation. *Nature Reviews Drug Discovery 2014 13:10* **2014**, *13* (10), 725–725. https://doi.org/10.1038/nrd4444.
179. Alonso-Escolano, D.; Strongin, A. Y.; Chung, A. W.; Deryugina, E. I.; Radomski, M. W. Membrane Type-1 Matrix Metalloproteinase Stimulates Tumour Cell-Induced Platelet Aggregation: Role of Receptor Glycoproteins. *Br. J. Pharmacol.* **2004**, *141* (2), 241–252. https://doi.org/10.1038/SJ.BJP.0705606.

180. Lian, L.; Li, W.; Li, Z. Y.; Mao, Y. X.; Zhang, Y. T.; Zhao, Y. M.; Chen, K.; Duan, W. M.; Tao, M. Inhibition of MCF-7 Breast Cancer Cell-Induced Platelet Aggregation Using a Combination of Antiplatelet Drugs. *Oncol. Lett.* **2013**, *5* (2), 675–680. https://doi.org/10.3892/OL.2012.1074.
181. Sheu, J. R.; Lin, C. H.; Peng, H. C.; Teng, C. M.; Huang, T. F. Triflavin, an Arg-Gly-Asp-Containing Peptide, Inhibits Tumor Cell-Induced Platelet Aggregation. *Jpn. J. Cancer Res.* **1993**, *84* (10), 1062–1071. https://doi.org/10.1111/J.1349-7006.1993.TB02802.X.
182. Alonso-Escolano, D.; Strongin, A. Y.; Chung, A. W.; Deryugina, E. I.; Radomski, M. W. Membrane Type-1 Matrix Metalloproteinase Stimulates Tumour Cell-Induced Platelet Aggregation: Role of Receptor Glycoproteins. *Br. J. Pharmacol.* **2004**, *141* (2), 241. https://doi.org/10.1038/SJ.BJP.0705606.
183. Li, H.; Qiu, Z.; Li, F.; Wang, C. The Relationship between MMP-2 and MMP-9 Expression Levels with Breast Cancer Incidence and Prognosis. *Oncol. Lett.* **2017**, *14* (5), 5865–5870. https://doi.org/10.3892/OL.2017.6924.
184. Liu, S. C.; Yang, S. F.; Yeh, K. T.; Yeh, C. M.; Chiou, H. L.; Lee, C. Y.; Chou, M. C.; Hsieh, Y. S. Relationships between the Level of Matrix Metalloproteinase-2 and Tumor Size of Breast Cancer. *Clinica Chimica Acta* **2006**, *371* (1–2), 92–96. https://doi.org/10.1016/J.CCA.2006.02.026.
185. Jurasz, P.; Sawicki, G.; Duszyk, M.; Sawicka, J.; Miranda, C.; Mayers, I.; Radomski, M. W. Matrix Metalloproteinase 2 in Tumor Cell-Induced Platelet Aggregation: Regulation by Nitric Oxide. *Cancer Res.* **2001**, *61* (1), 376–382.
186. Li, H.; Lee, M.-H.; Liu, K.; Wang, T.; Song, M.; Han, Y.; Yao, K.; Xie, H.; Zhu, F.; Grossmann, M.; Cleary, M. P.; Chen, W.; Bode, A. M.; Dong, Z. Inhibiting Breast Cancer by Targeting the Thromboxane A2 Pathway. *npj Precision Oncology 2017 1:1* **2017**, *1* (1), 1–8. https://doi.org/10.1038/s41698-017-0011-4.
187. Aitokallio-Tallberg, A. M.; Viinikka, L. U.; Ylikorkala, R. O. Increased Synthesis of Prostacyclin and Thromboxane in Human Ovarian Malignancy. *Cancer Res.* **1988**, *48* (9), 2396–2398.
188. Ashton, A. W.; Zhang, Y.; Cazzolli, R.; Honn, K. V. The Role and Regulation of Thromboxane A2 Signaling in Cancer-Trojan Horses and Misdirection. *Molecules* **2022**, *27* (19). https://doi.org/10.3390/MOLECULES27196234.
189. Nie, D.; Che, M.; Zacharek, A.; Qiao, Y.; Li, L.; Li, X.; Lamberti, M.; Tang, K.; Cai, Y.; Guo, Y.; Grignon, D.; Honn, K. V. Differential Expression of Thromboxane Synthase in Prostate Carcinoma: Role in Tumor Cell Motility. *Am. J. Pathol.* **2004**, *164* (2), 429–439. https://doi.org/10.1016/S0002-9440(10)63133-1.
190. Giese, A.; Hagel, C.; Kim, E. L.; Zapf, S.; Djawaheri, J.; Berens, M. E.; Westphal, M. Thromboxane Synthase Regulates the Migratory Phenotype of Human Glioma. *Neuro. Oncol.* **1999**, *1* (1), 3–13. https://doi.org/10.1093/NEUONC/1.1.3.
191. Medina, C.; Harmon, S.; Inkielewicz, I.; Santos-Martinez, M. J.; Jones, M.; Cantwell, P.; Bazou, D.; Ledwidge, M.; Radomski, M. W.; Gilmer, J. F. Differential Inhibition of Tumour Cell-Induced Platelet Aggregation by the Nicotinate Aspirin Prodrug (ST0702) and Aspirin. *Br. J. Pharmacol.* **2012**, *166* (3), 938–949. https://doi.org/10.1111/J.1476-5381.2011.01794.X.
192. Guillem-Llobat, P.; Dovizio, M.; Bruno, A.; Ricciotti, E.; Cufino, V.; Sacco, A.; Grande, R.; Alberti, S.; Arena, V.; Cirillo, M.; Patrono, C.; FitzGerald, G. A.; Steinhilber, D.; Sgambato, A.; Patrignani, P. Aspirin Prevents Colorectal Cancer Metastasis in Mice by

Splitting the Crosstalk between Platelets and Tumor Cells. *Oncotarget* **2016**, *7* (22), 32462. https://doi.org/10.18632/ONCOTARGET.8655.
193. SACKER, L. S.; SAUNDERS, K. E.; PAGE, B.; GOODFELLOW, M. Dilithium Sequestrene as an Anticoagulant. *J. Clin. Pathol.* **1959**, *12* (3), 254–257. https://doi.org/10.1136/jcp.12.3.254.
194. Moncada, S.; Vane, J. R. The Role of Prostacyclin in Vascular Tissue. *Fed. Proc.* **1979**, *38* (1), 66–71.
195. Menter, D. G.; Onoda, J. M.; Taylor, J. D.; Honn, K. V. Effects of Prostacyclin on Tumor Cell-Induced Platelet Aggregation. *Cancer Res.* **1984**, *44* (2), 450–456.
196. Sogo, N.; Magid, K. S.; Shaw, C. A.; Webb, D. J.; Megson, I. L. Inhibition of Human Platelet Aggregation by Nitric Oxide Donor Drugs: Relative Contribution of CGMP-Independent Mechanisms. *Biochem. Biophys. Res. Commun.* **2000**, *279* (2), 412–419. https://doi.org/10.1006/bbrc.2000.3976.
197. Jurasz, P.; Alonso-Escolano, D.; Radomski, M. W. Platelet–Cancer Interactions: Mechanisms and Pharmacology of Tumour Cell-Induced Platelet Aggregation. *Br. J. Pharmacol.* **2004**, *143* (7), 819. https://doi.org/10.1038/SJ.BJP.0706013.
198. Frederick Woessner, J. Quantification of Matrix Metalloproteinases in Tissue Samples. *Methods Enzymol.* **1995**, *248* (C), 510–528. https://doi.org/10.1016/0076-6879(95)48033-1.
199. Bazou, D.; Kuznetsova, L. A.; Coakley, W. T. Physical Enviroment of 2-D Animal Cell Aggregates Formed in a Short Pathlength Ultrasound Standing Wave Trap. *Ultrasound Med. Biol.* **2005**, *31* (3), 423–430. https://doi.org/10.1016/J.ULTRASMEDBIO.2004.12.007.
200. Roomi, M. W.; Kalinovsky, T.; Monterrey, J.; Rath, M.; Niedzwiecki, A. In Vitro Modulation of MMP-2 and MMP-9 in Adult Human Sarcoma Cell Lines by Cytokines, Inducers and Inhibitors. *Int. J. Oncol.* **2013**, *43* (6), 1787–1798. https://doi.org/10.3892/IJO.2013.2113.
201. *MM.1S - CRL-2974 | ATCC*. https://www.atcc.org/products/crl-2974 (accessed 2024-02-10).
202. Kleiner, D. E.; Stetler-Stevenson, W. G. Matrix Metalloproteinases and Metastasis. *Cancer Chemother. Pharmacol.* **1999**, *43 Suppl*. https://doi.org/10.1007/S002800051097.
203. Larkin, C. M.; Hante, N. K.; Breen, E. P.; Tomaszewski, K. A.; Eisele, S.; Radomski, M. W.; Ryan, T. A.; Santos-Martinez, M.-J. Role of Matrix Metalloproteinases 2 and 9, Toll-like Receptor 4 and Platelet-Leukocyte Aggregate Formation in Sepsis-Associated Thrombocytopenia. *PLoS One* **2018**, *13* (5), e0196478. https://doi.org/10.1371/journal.pone.0196478.
204. Jurasz, P.; Alonso-Escolano, D.; Radomski, M. W. Platelet–Cancer Interactions: Mechanisms and Pharmacology of Tumour Cell-Induced Platelet Aggregation. *Br. J. Pharmacol.* **2004**, *143* (7), 819. https://doi.org/10.1038/SJ.BJP.0706013.
205. Carazo, A.; Hrubša, M.; Konečný, L.; Skořepa, P.; Paclíková, M.; Musil, F.; Karlíčková, J.; Javorská, L.; Matoušová, K.; Krčmová, L. K.; Parvin, M. S.; Šmahelová, A.; Blaha, V.; Mladěnka, P. Sex-Related Differences in Platelet Aggregation: A Literature Review Supplemented with Local Data from a Group of Generally Healthy Individuals. *Semin. Thromb. Hemost.* **2023**, *49* (5), 488–506. https://doi.org/10.1055/S-0042-1756703.
206. Garner, S. F.; Furnell, A.; Kahan, B. C.; Jones, C. I.; Attwood, A.; Harrison, P.; Kelly, A. M.; Goodall, A. H.; Cardigan, R.; Ouwehand, W. H. Platelet Responses to Agonists in a

Cohort of Highly Characterised Platelet Donors Are Consistent over Time. *Vox Sang.* **2017**, *112* (1), 18–24. https://doi.org/10.1111/VOX.12468.
207. Hisada, Y.; Mackman, N. Cancer Cell-Derived Tissue Factor Positive Extracellular Vesicles: Biomarkers of Thrombosis and Survival. *Curr. Opin. Hematol.* **2019**, *26* (5), 349. https://doi.org/10.1097/MOH.0000000000000521.
208. Davila, M.; Amirkhosravi, A.; Coll, E.; Desai, H.; Robles, L.; Colon, J.; Baker, C. H.; Francis, J. L. Tissue Factor-Bearing Microparticles Derived from Tumor Cells: Impact on Coagulation Activation. *J. Thromb. Haemost.* **2008**, *6* (9), 1517–1524. https://doi.org/10.1111/J.1538-7836.2008.02987.X.
209. Papageorgiou, L.; Alhaj Hussen, K.; Thouroude, S.; Mbemba, E.; Cost, H.; Garderet, L.; Elalamy, I.; Larsen, A.; Van Dreden, P.; Dimopoulos, M. A.; Mohty, M.; Gerotziafas, G. T. Modelization of Blood-Borne Hypercoagulability in Myeloma: A Tissue-Factor-Bearing Microparticle-Driven Process. *TH Open* **2019**, *3* (4), e340. https://doi.org/10.1055/S-0039-1700885.
210. Menter, D. G.; Onoda, J. M.; Taylor, J. D.; Honn2, K. V. Effects of Prostacyclin on Tumor Cell-Induced Platelet Aggregation1. *Cancer Res.* **1984**, *44*, 450–456.
211. Jurasz, P.; Stewart, M. W.; Radomski, A.; Khadour, F.; Duszyk, M.; Radomski, M. W. Role of von Willebrand Factor in Tumour Cell-Induced Platelet Aggregation: Differential Regulation by NO and Prostacyclin. *Br. J. Pharmacol.* **2001**, *134* (5), 1104. https://doi.org/10.1038/SJ.BJP.0704343.
212. Mitchell, J. A.; Ali, F.; Bailey, L.; Moreno, L.; Harrington, L. S. Role of Nitric Oxide and Prostacyclin as Vasoactive Hormones Released by the Endothelium. *Exp. Physiol.* **2008**, *93* (1), 141–147. https://doi.org/10.1113/EXPPHYSIOL.2007.038588.
213. Cheung, P. Y.; Salas, E.; Schulz, R.; Radomski, M. W. Nitric Oxide and Platelet Function: Implications for Neonatology. *Semin. Perinatol.* **1997**, *21* (5), 409–417. https://doi.org/10.1016/S0146-0005(97)80006-7.
214. Fukumura, D.; Kashiwagi, S.; Jain, R. K. The Role of Nitric Oxide in Tumour Progression. *Nat. Rev. Cancer* **2006**, *6* (7), 521–534. https://doi.org/10.1038/NRC1910.
215. Khan, F. H.; Dervan, E.; Bhattacharyya, D. D.; McAuliffe, J. D.; Miranda, K. M.; Glynn, S. A. The Role of Nitric Oxide in Cancer: Master Regulator or NOt? *Int. J. Mol. Sci.* **2020**, *21* (24), 1–30. https://doi.org/10.3390/IJMS21249393.
216. White, J. G.; Krumwiede, M. D.; Escolar, G. EDTA Induced Changes in Platelet Structure and Function: Influence on Particle Uptake. *Platelets* **1999**, *10* (5), 327–337. https://doi.org/10.1080/09537109975979.
217. Doolan, P. D.; Schwartz, S. L.; Hayes, J. R.; Mullen, J. C.; Cummings, N. B. An Evaluation of the Nephrotoxicity of Ethylenediaminetetraacetate and Diethylenetriaminepentaacetate in the Rat. *Toxicol. Appl. Pharmacol.* **1967**, *10* (3), 481–500. https://doi.org/10.1016/0041-008X(67)90088-9.
218. Choi, W. S.; Jeon, O. H.; Kim, H. H.; Kim, D. S. MMP-2 Regulates Human Platelet Activation by Interacting with Integrin AlphaIIbbeta3. *J. Thromb. Haemost.* **2008**, *6* (3), 517–523. https://doi.org/10.1111/J.1538-7836.2007.02871.X.
219. Fernandez-Patron, C.; Martinez-Cuesta, M. A.; Salas, E.; Sawicki, G.; Wozniak, M.; Radomski, M. W.; Davidge, S. T. Differential Regulation of Platelet Aggregation by Matrix Metalloproteinases-9 and -2. *Thromb. Haemost.* **1999**, *82* (6), 1730–1735. https://doi.org/10.1055/S-0037-1614906.

220. Medina, C.; Jurasz, P.; Santos-Martinez, M. J.; Soon, S. J.; Mitsky, T.; Chen, R.; Radomski, M. W. Platelet Aggregation-Induced by Caco-2 Cells: Regulation by Matrix Metalloproteinase-2 and Adenosine Diphosphate. *J. Pharmacol. Exp. Ther.* **2006**, *317* (2), 739–745. https://doi.org/10.1124/JPET.105.098384.
221. Trivedi, V.; Boire, A.; Tchernychev, B.; Kaneider, N. C.; Leger, A. J.; O'Callaghan, K.; Covic, L.; Kuliopulos, A. Platelet Matrix Metalloprotease-1 Mediates Thrombogenesis by Activating PAR1 at a Cryptic Ligand Site. *Cell* **2009**, *137* (2), 332–343. https://doi.org/10.1016/J.CELL.2009.02.018.
222. Santos-Martinez, M. J.; Medina, C.; Gilmer, J. F.; Radomski, M. W. Matrix Metalloproteinases in Platelet Function: Coming of Age. *Journal of Thrombosis and Haemostasis* **2008**, *6* (3), 514–516. https://doi.org/10.1111/j.1538-7836.2007.02876.x.
223. Parmo-Cabañas, M.; Molina-Ortiz, I.; Matías-Román, S.; García-Bernal, D.; Carvajal-Vergara, X.; Valle, I.; Pandiella, A.; Arroyo, A. G.; Teixidó, J. Role of Metalloproteinases MMP-9 and MT1-MMP in CXCL12-Promoted Myeloma Cell Invasion across Basement Membranes. *J. Pathol.* **2006**, *208* (1), 108–118. https://doi.org/10.1002/PATH.1876.
224. Woulfe, D.; Yang, J.; Brass, L. ADP and Platelets: The End of the Beginning. *Journal of Clinical Investigation* **2001**, *107* (12), 1503. https://doi.org/10.1172/JCI13361.
225. Alonso-Escolano, D.; Strongin, A. Y.; Chung, A. W.; Deryugina, E. I.; Radomski, M. W. Membrane Type-1 Matrix Metalloproteinase Stimulates Tumour Cell-Induced Platelet Aggregation: Role of Receptor Glycoproteins. *Br. J. Pharmacol.* **2004**, *141* (2), 241–252. https://doi.org/10.1038/SJ.BJP.0705606.
226. Chauhan, M.; Thomas, A.; Goodall, A.; Wright, J.; Adlam, D. Aspirin and Ticagrelor for the Prevention of Tumour Cell Induced Platelet Aggregation. *Annals of Oncology* **2019**, *30*, v792. https://doi.org/10.1093/ANNONC/MDZ268.097.
227. Lian, L.; Li, W.; Li, Z. Y.; Mao, Y. X.; Zhang, Y. T.; Zhao, Y. M.; Chen, K.; Duan, W. M.; Tao, M. Inhibition of MCF-7 Breast Cancer Cell-Induced Platelet Aggregation Using a Combination of Antiplatelet Drugs. *Oncol. Lett.* **2013**, *5* (2), 675–680. https://doi.org/10.3892/OL.2012.1074/HTML.
228. Yang, J.; Yamashita-Kanemaru, Y.; Morris, B. I.; Contursi, A.; Trajkovski, D.; Xu, J.; Patrascan, I.; Benson, J.; Evans, A. C.; Conti, A. G.; Al-Deka, A.; Dahmani, L.; Avdic-Belltheus, A.; Zhang, B.; Okkenhaug, H.; Whiteside, S. K.; Imianowski, C. J.; Wesolowski, A. J.; Webb, L. V.; Puccio, S.; Tacconelli, S.; Bruno, A.; Di Berardino, S.; De Michele, A.; Welch, H. C. E.; Yu, I. S.; Lin, S. W.; Mitra, S.; Lugli, E.; van der Weyden, L.; Okkenhaug, K.; Saeb-Parsy, K.; Patrignani, P.; Adams, D. J.; Roychoudhuri, R. Aspirin Prevents Metastasis by Limiting Platelet TXA2 Suppression of T Cell Immunity. *Nature 2025 640:8060* **2025**, *640* (8060), 1052–1061. https://doi.org/10.1038/s41586-025-08626-7.
229. Palumbo, A.; Cavo, M.; Bringhen, S.; Zamagni, E.; Romano, A.; Patriarca, F.; Rossi, D.; Gentilini, F.; Crippa, C.; Galli, M.; Nozzoli, C.; Ria, R.; Marasca, R.; Montefusco, V.; Baldini, L.; Elice, F.; Callea, V.; Pulini, S.; Carella, A. M.; Zambello, R.; Benevolo, G.; Magarotto, V.; Tacchetti, P.; Pescosta, N.; Cellini, C.; Polloni, C.; Evangelista, A.; Caravita, T.; Morabito, F.; Offidani, M.; Tosi, P.; Boccadoro, M. Aspirin, Warfarin, or Enoxaparin Thromboprophylaxis in Patients with Multiple Myeloma Treated with Thalidomide: A Phase III, Open-Label, Randomized Trial. *J. Clin. Oncol.* **2011**, *29* (8), 986–993. https://doi.org/10.1200/JCO.2010.31.6844.

230. Aspirin May Be Inadequate Thromboprophylaxis in Multiple Myeloma. *Blood* **2017**, *130*, 3419. https://doi.org/10.1182/BLOOD.V130.SUPPL_1.3419.3419.
231. Birmann, B. M.; Giovannucci, E. L.; Rosner, B. A.; Colditz, G. A. Regular Aspirin Use and Risk of Multiple Myeloma: A Prospective Analysis in the Health Professionals Follow-up Study and Nurses' Health Study. *Cancer Prev. Res. (Phila).* **2013**, *7* (1), 33. https://doi.org/10.1158/1940-6207.CAPR-13-0224.
232. Marinac, C. R.; Lee, D. H.; Colditz, G. A.; Rebbeck, T. R.; Rosner, B.; Bustoros, M.; Ghobrial, I. M.; Birmann, B. M. Regular Aspirin Use and Mortality in Multiple Myeloma Patients. *Cancer Epidemiol. Biomarkers Prev.* **2021**, *31* (2), 479. https://doi.org/10.1158/1055-9965.EPI-21-0946.
233. Morello, S.; Caiazzo, E.; Turiello, R.; Cicala, C. Thrombo-Inflammation: A Focus on NTPDase1/CD39. *Cells 2021, Vol. 10, Page 2223* **2021**, *10* (9), 2223. https://doi.org/10.3390/CELLS10092223.
234. Hurt, E. M.; Thomas, S. B.; Peng, B.; Farrar, W. L. Reversal of P53 Epigenetic Silencing in Multiple Myeloma Permits Apoptosis by a P53 Activator. https://doi.org/10.4161/cbt.5.9.3001.
235. Teoh, P. J.; Chung, T. H.; Sebastian, S.; Choo, S. N.; Yan, J.; Ng, S. B.; Fonseca, R.; Chng, W. J. P53 Haploinsufficiency and Functional Abnormalities in Multiple Myeloma. *Leukemia* **2014**, *28* (10), 2066–2074. https://doi.org/10.1038/LEU.2014.102.
236. Hanash, S.; Taguchi, A. The Grand Challenge to Decipher the Cancer Proteome. *Nat. Rev. Cancer* **2010**, *10* (9), 652–660. https://doi.org/10.1038/NRC2918.
237. Hanash, S. M.; Pitteri, S. J.; Faca, V. M. Mining the Plasma Proteome for Cancer Biomarkers. *Nature* **2008**, *452* (7187), 571–579. https://doi.org/10.1038/NATURE06916.
238. Tierney, C.; Bazou, D.; Majumder, M. M.; Anttila, P.; Silvennoinen, R.; Heckman, C. A.; Dowling, P.; O'Gorman, P. Next Generation Proteomics with Drug Sensitivity Screening Identifies Sub-Clones Informing Therapeutic and Drug Development Strategies for Multiple Myeloma Patients. *Scientific Reports 2021 11:1* **2021**, *11* (1), 1–15. https://doi.org/10.1038/s41598-021-90149-y.
239. Kubicki, T.; Bednarek, K.; Kostrzewska-Poczekaj, M.; Luczak, M.; Visser, L.; Lodewijk, M.; Zyłka, K. ˙; Gil, L.; Jarmu˙ Z-Szymczak, M.; Dytfeld, D. Comparative Proteomic Profiling of Multiple Myeloma (MM) Cell Lines Identifies Mitochondrial Dysfunction As a Marker of Resistance to Proteasome Inhibitors (PIs) with Potential Therapeutic Implications for BH3-Mimetics. *Blood* **2024**, *144* (Supplement 1), 6821–6821. https://doi.org/10.1182/BLOOD-2024-203854.
240. Setayesh, S. M.; Ndacayisaba, L. J.; Rappard, K. E.; Hennes, V.; Rueda, L. Y. M.; Tang, G.; Lin, P.; Orlowski, R. Z.; Symer, D. E.; Manasanch, E. E.; Shishido, S. N.; Kuhn, P. Targeted Single-Cell Proteomic Analysis Identifies New Liquid Biopsy Biomarkers Associated with Multiple Myeloma. *npj Precision Oncology 2023 7:1* **2023**, *7* (1), 1–10. https://doi.org/10.1038/s41698-023-00446-0.
241. Dunphy, K.; Bazou, D.; Henry, M.; Meleady, P.; Miettinen, J. J.; Heckman, C. A.; Dowling, P.; O'Gorman, P. Proteomic and Metabolomic Analysis of Bone Marrow and Plasma from Patients with Extramedullary Multiple Myeloma Identifies Distinct Protein and Metabolite Signatures. *Cancers (Basel).* **2023**, *15* (15), 3764. https://doi.org/10.3390/CANCERS15153764/S1.
242. Papanota, A. M.; Karousi, P.; Kontos, C. K.; Ntanasis-Stathopoulos, I.; Scorilas, A.; Terpos, E. Multiple Myeloma Bone Disease: Implication of MicroRNAs in Its Molecular

Background. *Int. J. Mol. Sci.* **2021**, *22* (5), 2375. https://doi.org/10.3390/IJMS22052375.
243. Faict, S.; Muller, J.; De Veirman, K.; De Bruyne, E.; Maes, K.; Vrancken, L.; Heusschen, R.; De Raeve, H.; Schots, R.; Vanderkerken, K.; Caers, J.; Menu, E. Exosomes Play a Role in Multiple Myeloma Bone Disease and Tumor Development by Targeting Osteoclasts and Osteoblasts. *Blood Cancer Journal 2018 8:11* **2018**, *8* (11), 1–12. https://doi.org/10.1038/s41408-018-0139-7.
244. Wang, J.; Hendrix, A.; Hernot, S.; Lemaire, M.; De Bruyne, E.; Van Valckenborgh, E.; Lahoutte, T.; De Wever, O.; Vanderkerken, K.; Menu, E. Bone Marrow Stromal Cell–Derived Exosomes as Communicators in Drug Resistance in Multiple Myeloma Cells. *Blood* **2014**, *124* (4), 555–566. https://doi.org/10.1182/BLOOD-2014-03-562439.
245. Mendes, M. L.; Dittmar, G. Targeted Proteomics on Its Way to Discovery. *Proteomics* **2022**, *22* (15–16). https://doi.org/10.1002/PMIC.202100330.
246. Sinha, A.; Mann, M. A Beginner's Guide to Mass Spectrometry–Based Proteomics. *Biochem. (Lond).* **2020**, *42* (5), 64–69. https://doi.org/10.1042/BIO20200057.
247. Wang, M.; You, J.; Bemis, K. G.; Tegeler, T. J.; Brown, D. P. G. Label-Free Mass Spectrometry-Based Protein Quantification Technologies in Proteomic Analysis. *Brief. Funct. Genomic. Proteomic.* **2008**, *7* (5), 329–339. https://doi.org/10.1093/BFGP/ELN031.
248. Zhu, W.; Smith, J. W.; Huang, C. M. Mass Spectrometry-Based Label-Free Quantitative Proteomics. *J. Biomed. Biotechnol.* **2010**, *2010*. https://doi.org/10.1155/2010/840518.
249. *Getting started - STRING Help*. https://string-db.org/help/getting_started/?utm_source=chatgpt.com (accessed 2026-01-07).
250. Heberle, H.; Meirelles, V. G.; da Silva, F. R.; Telles, G. P.; Minghim, R. InteractiVenn: A Web-Based Tool for the Analysis of Sets through Venn Diagrams. *BMC Bioinformatics* **2015**, *16* (1), 169-. https://doi.org/10.1186/S12859-015-0611-3/FIGURES/4.
251. Liu, L.; Yu, Z.; Cheng, H.; Mao, X.; Sui, W.; Deng, S.; Wei, X.; Lv, J.; Du, C.; Xu, J.; Huang, W.; Xia, S.; An, G.; Zhou, W.; Ma, X.; Cheng, T.; Qiu, L.; Hao, M. Multiple Myeloma Hinders Erythropoiesis and Causes Anaemia Owing to High Levels of CCL3 in the Bone Marrow Microenvironment. *Scientific Reports 2020 10:1* **2020**, *10* (1), 20508-. https://doi.org/10.1038/s41598-020-77450-y.
252. Wang, Y.; Lan, T.; Zhang, Q.; Zhou, C.; Liu, P. Myeloma Cell-Derived CXCL7 Facilitates Proliferation of Tumor Cells and Occurrence of Osteolytic Lesions through JAK/STAT3 Pathway. *Cell Death & Disease 2025 16:1* **2025**, *16* (1), 74-. https://doi.org/10.1038/s41419-025-07413-6.
253. Kirschke, H.; Eerola, R.; Hopsu-Havu, V. K.; Brömme, D.; Vuorio, E. Antisense RNA Inhibition of Cathepsin L Expression Reduces Tumorigenicity of Malignant Cells. *Eur. J. Cancer* **2000**, *36* (6), 787–795. https://doi.org/10.1016/S0959-8049(00)00014-9.
254. Huang, T.; Sun, L.; Yuan, X.; Qiu, H.; Huang, T.; Sun, L.; Yuan, X.; Qiu, H. Thrombospondin-1 Is a Multifaceted Player in Tumor Progression. *Oncotarget* **2017**, *8* (48), 84546–84558. https://doi.org/10.18632/ONCOTARGET.19165.
255. Wu, X.; Guo, J.; Deng, H.; Chen, W. Serum Proteome Profiling Identified Thrombospondin-1 and Lactoferrin as Biomarkers of Relapsed Multiple Myeloma. *Front. Med. (Lausanne).* **2025**, *12*. https://doi.org/10.3389/FMED.2025.1640245.
256. Nergiz-Unal, R.; Lamers, M. M. E.; Van Kruchten, R.; Luiken, J. J.; Cosemans, J. M. E. M.; Glatz, J. F. C.; Kuijpers, M. J. E.; Heemskerk, J. W. M. Signaling Role of CD36 in

Platelet Activation and Thrombus Formation on Immobilized Thrombospondin or Oxidized Low-Density Lipoprotein. *J. Thromb. Haemost.* **2011**, *9* (9), 1835–1846. https://doi.org/10.1111/J.1538-7836.2011.04416.X.

257. Galán, A. M.; Van Heerde, W. L.; Escolar, G.; Ordinas, A.; Sixma, J.; De Groot, P. G. Antithrombotic Action of Annexin V Proved as Efficient as Direct Inhibition of Tissue Factor or Thrombin. *Eur. J. Clin. Invest.* **2006**, *36* (9), 633–639. https://doi.org/10.1111/J.1365-2362.2006.01698.X.
258. Vasconcellos, C. A.; Lind, S. E. Coordinated Inhibition of Actin-Induced Platelet Aggregation by Plasma Gelsolin and Vitamin D-Binding Protein. *Blood* **1993**, *82* (12), 3648–3657. https://doi.org/10.1182/BLOOD.V82.12.3648.3648.
259. Xu, X. R.; Wang, Y.; Adili, R.; Ju, L.; Spring, C. M.; Jin, J. W.; Yang, H.; Neves, M. A. D.; Chen, P.; Yang, Y.; Lei, X.; Chen, Y.; Gallant, R. C.; Xu, M.; Zhang, H.; Song, J.; Ke, P.; Zhang, D.; Carrim, N.; Yu, S. Y.; Zhu, G.; She, Y. M.; Cyr, T.; Fu, W.; Liu, G.; Connelly, P. W.; Rand, M. L.; Adeli, K.; Freedman, J.; Lee, J. E.; Tso, P.; Marchese, P.; Davidson, W. S.; Jackson, S. P.; Zhu, C.; Ruggeri, Z. M.; Ni, H. Apolipoprotein A-IV Binds AIIbβ3 Integrin and Inhibits Thrombosis. *Nat. Commun.* **2018**, *9* (1). https://doi.org/10.1038/S41467-018-05806-0.
260. Hammoudi, N.; Ahmed, K. B. R.; Garcia-Prieto, C.; Huang, P. Metabolic Alterations in Cancer Cells and Therapeutic Implications. *Chin. J. Cancer* **2011**, *30* (8), 508. https://doi.org/10.5732/CJC.011.10267.
261. Bloedjes, T. A.; de Wilde, G.; Khan, G. H.; Ashby, T. C.; Shaughnessy, J. D.; Zhan, F.; Houtkooper, R. H.; Bende, R. J.; van Noesel, C. J. M.; Spaargaren, M.; Guikema, J. E. J. AKT Supports the Metabolic Fitness of Multiple Myeloma Cells by Restricting FOXO Activity. *Blood Adv.* **2023**, *7* (9), 1697–1712. https://doi.org/10.1182/BLOODADVANCES.2022007383.
262. Li, R.; Ke, M.; Qi, M.; Han, Z.; Cao, Y.; Deng, Z.; Qian, J.; Yang, Y.; Gu, C. G6PD Promotes Cell Proliferation and Dexamethasone Resistance in Multiple Myeloma via Increasing Anti-Oxidant Production and Activating Wnt/β-Catenin Pathway. *Exp. Hematol. Oncol.* **2022**, *11* (1), 77-. https://doi.org/10.1186/S40164-022-00326-6/FIGURES/8.
263. Peng, Y.; Li, X.; Wu, M.; Yang, J.; Liu, M.; Zhang, W.; Xiang, B.; Wang, X.; Li, X.; Li, G.; Shen, S. New Prognosis Biomarkers Identified by Dynamic Proteomic Analysis of Colorectal Cancer. *Mol. Biosyst.* **2012**, *8* (11), 3077–3088. https://doi.org/10.1039/C2MB25286D.
264. Chen, X.; Yang, T. T.; Zhou, Y.; Wang, W.; Qiu, X. C.; Gao, J.; Li, C. X.; Long, H.; Ma, B. A.; Ma, Q.; Zhang, X. Z.; Yang, L. J.; Fan, Q. Y. Proteomic Profiling of Osteosarcoma Cells Identifies ALDOA and SULT1A3 as Negative Survival Markers of Human Osteosarcoma. *Mol. Carcinog.* **2014**, *53* (2), 138–144. https://doi.org/10.1002/MC.21957.
265. Du, S.; Guan, Z.; Hao, L.; Song, Y.; Wang, L.; Gong, L.; Liu, L.; Qi, X.; Hou, Z.; Shao, S. Fructose-Bisphosphate Aldolase A Is a Potential Metastasis-Associated Marker of Lung Squamous Cell Carcinoma and Promotes Lung Cell Tumorigenesis and Migration. *PLoS One* **2014**, *9* (1), e85804. https://doi.org/10.1371/JOURNAL.PONE.0085804.
266. Tian, W.; Zhou, J.; Chen, M.; Qiu, L.; Li, Y.; Zhang, W.; Guo, R.; Lei, N.; Chang, L. Bioinformatics Analysis of the Role of Aldolase A in Tumor Prognosis and Immunity. *Sci. Rep.* **2022**, *12* (1), 11632. https://doi.org/10.1038/S41598-022-15866-4.

267. Ray, A.; Song, Y.; Du, T.; Chauhan, D.; Anderson, K. C. Preclinical Validation of Alpha-Enolase (ENO1) as a Novel Immunometabolic Target in Multiple Myeloma. *Oncogene* **2020**, *39* (13), 2786–2796. https://doi.org/10.1038/S41388-020-1172-0.
268. Gao, X.; Feng, Q.; Zhang, Q.; Zhang, Y.; Hu, C.; Zhang, L.; Zhang, H.; Wang, G.; Hu, K.; Ma, M.; Wang, Z.; Liu, Y.; An, D.; Yi, H.; Peng, Y.; Wu, X.; Chen, G.; Jia, X.; Cai, H.; Shi, J. Targeting Enolase 1 Reverses Bortezomib Resistance in Multiple Myeloma through YWHAZ/Parkin Axis. *J. Biomed. Sci.* **2025**, *32* (1), 1–20. https://doi.org/10.1186/S12929-024-01101-X/FIGURES/9.
269. Gu, Y.; Yuan, Y. H.; Xu, J.; Shi, Q. L.; Qu, X. Y.; Guo, R.; Bai, H.; Xu, J. D.; Li, J. Y.; Chen, L. J. High Serum Lactate Dehydrogenase Predicts an Unfavorable Outcome in Chinese Elderly Patients with Multiple Myeloma. *Oncotarget* **2017**, *8* (29), 48350–48361. https://doi.org/10.18632/ONCOTARGET.16237.
270. Børset, M.; Elsaadi, S.; Vandsemb, E. N.; Hess, E. S.; Steiro, I. J.; Cocera Fernandez, M.; Sponaas, A. M.; Abdollahi, P. Highly Expressed Genes in Multiple Myeloma Cells – What Can They Tell Us about the Disease? *Eur. J. Haematol.* **2022**, *109* (1), 31. https://doi.org/10.1111/EJH.13766.
271. Zhou, J.; Chng, W. J. Biological Hallmarks and Emerging Strategies to Target STAT3 Signaling in Multiple Myeloma. *Cells* **2022**, *11* (6), 941. https://doi.org/10.3390/CELLS11060941.
272. Hou, X.; Chen, Y.; Zhou, B.; Tang, W.; Ding, Z.; Chen, L.; Wu, Y.; Yang, H.; Du, C.; Yang, D.; Ma, G.; Cao, H. Talin-1 Inhibits Smurf1-Mediated Stat3 Degradation to Modulate β-Cell Proliferation and Mass in Mice. *Cell Death & Disease 2023 14:10* **2023**, *14* (10), 1–15. https://doi.org/10.1038/s41419-023-06235-8.
273. Ji, L.; Jiang, F.; Cui, X.; Qin, C. Talin1 Knockdown Prohibits the Proliferation and Migration of Colorectal Cancer Cells via the EMT Signaling Pathway. *Oncol. Lett.* **2019**, *18* (5), 5408–5416. https://doi.org/10.3892/OL.2019.10902/HTML.
274. Sakamoto, S.; McCann, R. O.; Dhir, R.; Kyprianou, N. Talin1 Promotes Tumor Invasion and Metastasis via Focal Adhesion Signaling and Anoikis Resistance. *Cancer Res.* **2010**, *70* (5), 1885–1895. https://doi.org/10.1158/0008-5472.CAN-09-2833/655707/P/TALIN1-PROMOTES-TUMOR-INVASION-AND-METASTASIS-VIA.
275. Papagrigoriou, E.; Gingras, A. R.; Barsukov, I. L.; Bate, N.; Fillingham, I. J.; Patel, B.; Frank, R.; Ziegler, W. H.; Roberts, G. C. K.; Critchley, D. R.; Emsley, J. Activation of a Vinculin-Binding Site in the Talin Rod Involves Rearrangement of a Five-Helix Bundle. *EMBO Journal* **2004**, *23* (15), 2942–2951. https://doi.org/10.1038/SJ.EMBOJ.7600285/SUPPL_FILE/EMBJ7600285-SUP-0003.DOC.
276. Lim, I. R.; Joo, H. J.; Jeong, M.; Kim, J. H.; Choi, S. C.; Kim, C.; Jung, J. W.; Hong, S. J. Talin Modulation by a Synthetic N-Acylurea Derivative Reduces Angiogenesis in Human Endothelial Cells. *International Journal of Molecular Sciences 2017, Vol. 18, Page 221* **2017**, *18* (1), 221. https://doi.org/10.3390/IJMS18010221.
277. Martnez-Moreno, M.; Leiva, M.; Aguilera-Montilla, N.; Sevilla-Movilla, S.; Isern de Val, S.; Arellano-Snchez, N.; Gutiérrez, N. C.; Maldonado, R.; Martnez-López, J.; Buo, I.; Garca-Marco, J. A.; Snchez-Mateos, P.; Hidalgo, A.; Garca-Pardo, A.; Teixidó, J. In Vivo Adhesion of Malignant B Cells to Bone Marrow Microvasculature Is Regulated by A4β1 Cytoplasmic-Binding Proteins. *Leukemia* **2016**, *30* (4), 861–872. https://doi.org/10.1038/LEU.2015.332.

278. Li, S.; Chen, A.; Gui, J.; Zhou, H.; Zhu, L.; Mi, Y. TLN1: An Oncogene Associated with Tumorigenesis and Progression. *Discover Oncology* **2024**, *15* (1), 716. https://doi.org/10.1007/S12672-024-01593-X.
279. Deng, R.; Hao, J.; Han, W.; Ni, Y.; Huang, X.; Hu, Q. Gelsolin Regulates Proliferation, Apoptosis, Migration and Invasion in Human Oral Carcinoma Cells. *Oncol. Lett.* **2015**, *9* (5), 2129–2134. https://doi.org/10.3892/OL.2015.3002.
280. Li, W. X.; Yang, M. X.; Hong, X. Q.; Dong, T. G.; Yi, T.; Lin, S. L.; Qin, X. Y.; Niu, W. X. Overexpression of Gelsolin Reduces the Proliferation and Invasion of Colon Carcinoma Cells. *Mol. Med. Rep.* **2016**, *14* (4), 3059–3065. https://doi.org/10.3892/MMR.2016.5652.
281. Zhuo, J.; Tan, E. H.; Yan, B.; Tochhawng, L.; Jayapal, M.; Koh, S.; Tay, H. K.; Maciver, S. K.; Hooi, S. C.; Salto-Tellez, M.; Kumar, A. P.; Goh, Y. C.; Lim, Y. C.; Yap, C. T. Gelsolin Induces Colorectal Tumor Cell Invasion via Modulation of the Urokinase-Type Plasminogen Activator Cascade. *PLoS One* **2012**, *7* (8). https://doi.org/10.1371/JOURNAL.PONE.0043594.
282. Sharma, M. C. Annexin A2 (ANX A2): An Emerging Biomarker and Potential Therapeutic Target for Aggressive Cancers. *Int. J. Cancer* **2019**, *144* (9), 2074–2081. https://doi.org/10.1002/IJC.31817.
283. *RHOA (ras homolog gene family, member A)*. https://atlasgeneticsoncology.org/gene/42107/rhoa-(ras-homolog-gene-family-member-a) (accessed 2026-02-22).
284. Azab, A. K.; Azab, F.; Blotta, S.; Pitsillides, C. M.; Thompson, B.; Runnels, J. M.; Roccaro, A. M.; Ngo, H. T.; Melhem, M. R.; Sacco, A.; Jia, X.; Anderson, K. C.; Lin, C. P.; Rollins, B. J.; Ghobrial, I. M. RhoA and Rac1 GTPases Play Major and Differential Roles in Stromal Cell–Derived Factor-1–Induced Cell Adhesion and Chemotaxis in Multiple Myeloma. *Blood* **2009**, *114* (3), 619–629. https://doi.org/10.1182/BLOOD-2009-01-199281.
285. *Targeted Therapy: PTX-100 | Cutaneous Lymphoma Foundation*. https://www.clfoundation.org/ptx-100 (accessed 2026-02-12).
286. Santos, J. C.; Profitós-Pelejà, N.; Sánchez-Vinces, S.; Roué, G. RHOA Therapeutic Targeting in Hematological Cancers. *Cells 2023, Vol. 12,* **2023**, *12* (3). https://doi.org/10.3390/CELLS12030433.
287. Nguyen, P.; Chakrabarti, J.; Li, Y.; Kalim, K. W.; Zhang, M.; Zhang, L.; Zheng, Y.; Guo, F. Rational Targeting of Cdc42 Overcomes Drug Resistance of Multiple Myeloma. *Front. Oncol.* **2019**, *9*, 958. https://doi.org/10.3389/FONC.2019.00958/FULL.
288. Van De Donk, N. W. C. J.; Lokhorst, H. M.; Nijhuis, E. H. J.; Kamphuis, M. M. J.; Bloem, A. C. Geranylgeranylated Proteins Are Involved in the Regulation of Myeloma Cell Growth. *Clinical Cancer Research* **2005**, *11* (2), 429–439. https://doi.org/10.1158/1078-0432.429.11.2.
289. Legate, K. R.; Montañez, E.; Kudlacek, O.; Fässler, R. ILK, PINCH and Parvin: The TIPP of Integrin Signalling. *Nat. Rev. Mol. Cell Biol.* **2006**, *7* (1), 20–31. https://doi.org/10.1038/NRM1789.
290. Ito, S.; Takahara, Y.; Hyodo, T.; Hasegawa, H.; Asano, E.; Hamaguchi, M.; Senga, T. The Roles of Two Distinct Regions of PINCH-1 in the Regulation of Cell Attachment and Spreading. *Mol. Biol. Cell* **2010**, *21* (23), 4120–4129. https://doi.org/10.1091/MBC.E10-05-0459.

291. Honda, S.; Shirotani-Ikejima, H.; Tadokoro, S.; Maeda, Y.; Kinoshita, T.; Tomiyama, Y.; Miyata, T. Integrin-Linked Kinase Associated with Integrin Activation. *Blood* **2009**, *113* (21), 5304–5313. https://doi.org/10.1182/BLOOD-2008-07-169136.
292. Tucker, K. L.; Sage, T.; Stevens, J. M.; Jordan, P. A.; Jones, S.; Barrett, N. E.; St-Arnaud, R.; Frampton, J.; Dedhar, S.; Gibbins, J. M. A Dual Role for Integrin-Linked Kinase in Platelets: Regulating Integrin Function and α-Granule Secretion. *Blood* **2008**, *112* (12), 4523. https://doi.org/10.1182/BLOOD-2008-03-148502.
293. Liu, Y.; Li, C.; Liu, H.; Tan, S. Combination Therapy Involving HSP90 Inhibitors for Combating Cancer: An Overview of Clinical and Preclinical Progress. *Archives of Pharmacal Research 2024 47:5* **2024**, *47* (5), 442–464. https://doi.org/10.1007/S12272-024-01494-1.
294. Chauhan, D.; Li, G.; Auclair, D.; Hideshima, T.; Podar, K.; Mitsiades, N.; Mitsiades, C.; Chen, L. B.; Munshi, N.; Saxena, S.; Anderson, K. C. 2-Methoxyestardiol and Bortezomib/Proteasome-Inhibitor Overcome Dexamethasone-Resistance in Multiple Myeloma Cells by Modulating Heat Shock Protein-27. *Apoptosis* **2004**, *9* (2), 149–155. https://doi.org/10.1023/B:APPT.0000018797.66067.6C/METRICS.
295. Heinrich, J. C.; Donakonda, S.; Haupt, V. J.; Lennig, P.; Zhang, Y.; Schroeder, M. New HSP27 Inhibitors Efficiently Suppress Drug Resistance Development in Cancer Cells. *Oncotarget* **2016**, *7* (42), 68156. https://doi.org/10.18632/ONCOTARGET.11905.
296. Zhang, L.; Fok, J. J. L.; Mirabella, F.; Aronson, L. I.; Fryer, R. A.; Workman, P.; Morgan, G. J.; Davies, F. E. Hsp70 Inhibition Induces Myeloma Cell Death via the Intracellular Accumulation of Immunoglobulin and the Generation of Proteotoxic Stress. *Cancer Lett.* **2013**, *339* (1), 49–59. https://doi.org/10.1016/J.CANLET.2013.07.023.
297. Polanowska-Grabowska, R.; Gear, A. R. L. Heat-Shock Proteins and Platelet Function. *Platelets* **2000**, *11* (1), 6–22. https://doi.org/10.1080/09537100075742.
298. Ling, C.; Cao, N.; Wang, H.; Wan, Y.; Liang, X.; Guo, J.; Xiao, M.; Zhang, Q.; Zhai, Z. Systematic Analysis of E3 Ligase-Related Genes Identified UBE2L3 as a Prognostic Biomarker Associated With Drug Resistance in Acute Myeloid Leukemia. *Int. J. Gen. Med.* **2025**, *18*, 459–472. https://doi.org/10.2147/IJGM.S502644.
299. Gu, Y.; Barwick, B. G.; Shanmugam, M.; Hofmeister, C. C.; Kaufman, J.; Nooka, A.; Gupta, V.; Dhodapkar, M.; Boise, L. H.; Lonial, S. Downregulation of PA28α Induces Proteasome Remodeling and Results in Resistance to Proteasome Inhibitors in Multiple Myeloma. *Blood Cancer Journal 2020 10:12* **2020**, *10* (12), 1–10. https://doi.org/10.1038/s41408-020-00393-0.
300. Bam, R.; Venkateshaiah, S. U.; Khan, S.; Ling, W.; Randal, S. S.; Li, X.; Zhang, Q.; Van Rhee, F.; Barlogie, B.; Epstein, J.; Yaccoby, S. Role of Bruton's Tyrosine Kinase (BTK) in Growth and Metastasis of INA6 Myeloma Cells. *Blood Cancer J.* **2014**, *4* (8). https://doi.org/10.1038/BCJ.2014.54.
301. Pan, Z.; Scheerens, H.; Li, S. J.; Schultz, B. E.; Sprengeler, P. A.; Burrill, L. C.; Mendonca, R. V.; Sweeney, M. D.; Scott, K. C. K.; Grothaus, P. G.; Jeffery, D. A.; Spoerke, J. M.; Honigberg, L. A.; Young, P. R.; Dalrymple, S. A.; Palmer, J. T. Discovery of Selective Irreversible Inhibitors for Bruton's Tyrosine Kinase. *ChemMedChem* **2007**, *2* (1), 58–61. https://doi.org/10.1002/CMDC.200600221.
302. Chen, Y.; Wu, Y. ran; Yang, H. ying; Li, X. zhe; Jie, M. meng; Hu, C. jiang; Wu, Y. yun; Yang, S. ming; Yang, Y. bin. Prolyl Isomerase Pin1: A Promoter of Cancer and a Target for Therapy. *Cell Death Dis.* **2018**, *9* (9), 883. https://doi.org/10.1038/S41419-018-0844-Y.

303. Zhang, H.; Chen, J.; Meng, Y.; Cen, Q.; Wang, H.; Ding, X.; Ai, K.; Yang, Y.; Gao, Y.; Qiu, Y.; Hu, Y.; Li, M.; He, Y.; Li, Y. Overexpression of Pin1 Regulated by TOP2A, Which Subsequently Stabilizes Pyk2 to Promote Bortezomib Resistance in Multiple Myeloma. *Cancer Gene Therapy 2024 32:1* **2024**, *32* (1), 22–37. https://doi.org/10.1038/s41417-024-00845-w.
304. Li, B. P.; Mao, Y. T.; Wang, Z.; Chen, Y. Y.; Wang, Y.; Zhai, C. Y.; Shi, B.; Liu, S. Y.; Liu, J. L.; Chen, J. Q. CLIC1 Promotes the Progression of Gastric Cancer by Regulating the MAPK/AKT Pathways. *Cell. Physiol. Biochem.* **2018**, *46* (3), 907–924. https://doi.org/10.1159/000488822.
305. Ding, Q.; Li, M.; Wu, X.; Zhang, L.; Wu, W.; Ding, Q.; Weng, H.; Wang, X.; Liu, Y. CLIC1 Overexpression Is Associated with Poor Prognosis in Gallbladder Cancer. *Tumour Biol.* **2015**, *36* (1), 193–198. https://doi.org/10.1007/S13277-014-2606-5.
306. Liang, P.; Cheng, S. H.; Cheng, C. K.; Lau, K. M.; Lin, S. Y.; Chow, E. Y. D.; Chan, N. P. H.; Ip, R. K. L.; Wong, R. S. M.; Ng, M. H. L. Platelet Factor 4 Induces Cell Apoptosis by Inhibition of STAT3 via Up-Regulation of SOCS3 Expression in Multiple Myeloma. *Haematologica* **2013**, *98* (2), 288. https://doi.org/10.3324/HAEMATOL.2012.065607.
307. Chanukuppa, V.; Paul, D.; Taunk, K.; Chatterjee, T.; Sharma, S.; Kumar, S.; Santra, M. K.; Rapole, S. XPO1 Is a Critical Player for Bortezomib Resistance in Multiple Myeloma: A Quantitative Proteomic Approach. *J. Proteomics* **2019**, *209*. https://doi.org/10.1016/J.JPROT.2019.103504.
308. Gandhi, U. H.; Senapedis, W.; Baloglu, E.; Unger, T. J.; Chari, A.; Vogl, D.; Cornell, R. F. Clinical Implications of Targeting XPO1-Mediated Nuclear Export in Multiple Myeloma. *Clin. Lymphoma Myeloma Leuk.* **2018**, *18* (5), 335–345. https://doi.org/10.1016/J.CLML.2018.03.003.
309. Wang, Q.; Zhao, D.; Xian, M.; Wang, Z.; Bi, E.; Su, P.; Qian, J.; Ma, X.; Yang, M.; Liu, L.; Zu, Y.; Pingali, S. R.; Chen, K.; Cai, Z.; Yi, Q. MIF as a Biomarker and Therapeutic Target for Overcoming Resistance to Proteasome Inhibitors in Human Myeloma. *Blood* **2020**, *136* (22), 2557–2573. https://doi.org/10.1182/BLOOD.2020005795.
310. Gunes, M.; Rosen, S. T.; Gunes, E. G. The Role of Macrophage Migration Inhibitory Factor (MIF) in Regulation of T-Cell Activity in Multiple Myeloma. *Blood* **2023**, *142* (Supplement 1), 4669–4669. https://doi.org/10.1182/BLOOD-2023-180085.
311. Yu, H.; Wang, M.; Zhang, T.; Cao, L.; Li, Z.; Du, Y.; Hai, Y.; Gao, X.; Ji, J.; Wu, J. Dual Roles of β-Arrestin 1 in Mediating Cell Metabolism and Proliferation in Gastric Cancer. *Proc. Natl. Acad. Sci. U. S. A.* **2022**, *119* (40), e2123231119. https://doi.org/10.1073/PNAS.2123231119/SUPPL_FILE/PNAS.2123231119.SD03.XLSX.
312. Wu, J.; Wang, X.; Jabbar, S.; Ganesh, N.; Chu, E.; Math, V. T.; Rein, L.; Kang, Y. Beta-Arrestin 1 Deficiency Enhances Host Anti-Myeloma Immunity Through T Cell Activation and Checkpoint Modulation. *Int. J. Mol. Sci.* **2025**, *26* (23), 11478. https://doi.org/10.3390/IJMS262311478/S1.
313. Zhao, X. D.; Zhou, J. X.; Yao, J. R.; Shi, Q. M.; Su, J.; Hu, N. Single-Cell Transcriptome Analysis Reveals the Effect of MIF on Myeloid-Derived Suppressor Cells in Multiple Myeloma. *Int. J. Lab. Hematol.* **2025**. https://doi.org/10.1111/IJLH.14473.
314. Liu, X.; Yao, N.; Qian, J.; Huang, H. High Expression and Prognostic Role of CAP1 and CtBP2 in Breast Carcinoma: Associated with E-Cadherin and Cell Proliferation. *Med. Oncol.* **2014**, *31* (3). https://doi.org/10.1007/S12032-014-0878-7.

315. Liu, X.; Yao, N.; Qian, J.; Huang, H. High Expression and Prognostic Role of CAP1 and CtBP2 in Breast Carcinoma: Associated with E-Cadherin and Cell Proliferation. *Med. Oncol.* **2014**, *31* (3). https://doi.org/10.1007/S12032-014-0878-7.
316. Yokokura, S.; Yurimoto, S.; Matsuoka, A.; Imataki, O.; Dobashi, H.; Bandoh, S.; Matsunaga, T. Calmodulin Antagonists Induce Cell Cycle Arrest and Apoptosis in Vitro and Inhibit Tumor Growth in Vivo in Human Multiple Myeloma. *BMC Cancer* **2014**, *14* (1), 882. https://doi.org/10.1186/1471-2407-14-882.
317. Shishkin, S.; Eremina, L.; Pashintseva, N.; Kovalev, L.; Kovaleva, M. Cofilin-1 and Other ADF/Cofilin Superfamily Members in Human Malignant Cells. *International Journal of Molecular Sciences 2017, Vol. 18,* **2016**, *18* (1). https://doi.org/10.3390/IJMS18010010.
318. Poukkula, M.; Kremneva, E.; Serlachius, M.; Lappalainen, P. Actin-Depolymerizing Factor Homology Domain: A Conserved Fold Performing Diverse Roles in Cytoskeletal Dynamics. *Cytoskeleton* **2011**, *68* (9), 471–490. https://doi.org/10.1002/CM.20530.
319. Hanahan, D.; Weinberg, R. A. Hallmarks of Cancer: The next Generation. *Cell* **2011**, *144* (5), 646–674. https://doi.org/10.1016/J.CELL.2011.02.013.
320. Raab, M. S.; Podar, K.; Breitkreutz, I.; Richardson, P. G.; Anderson, K. C. Multiple Myeloma. *Lancet* **2009**, *374* (9686), 324–339. https://doi.org/10.1016/S0140-6736(09)60221-X.
321. Bianchi, G.; Kumar, S.; Ghobrial, I. M.; Roccaro, A. M. Cell Trafficking in Multiple Myeloma. *Open J. Hematol.* **2012**, *3* (Suppl 1), 1. https://doi.org/10.13055/OJHMT_3_S1_04.120221.
322. Li, N. Platelets in Cancer Metastasis: To Help the "Villain" to Do Evil. *Int. J. Cancer* **2016**, *138* (9), 2078–2087. https://doi.org/10.1002/IJC.29847.
323. Jurasz, P.; Alonso-Escolano, D.; Radomski, M. W. Platelet–Cancer Interactions: Mechanisms and Pharmacology of Tumour Cell-Induced Platelet Aggregation. *Br. J. Pharmacol.* **2004**, *143* (7), 819. https://doi.org/10.1038/SJ.BJP.0706013.
324. Labelle, M.; Begum, S.; Hynes, R. O. Direct Signaling between Platelets and Cancer Cells Induces an Epithelial-Mesenchymal-like Transition and Promotes Metastasis. *Cancer Cell* **2011**, *20* (5), 576–590. https://doi.org/10.1016/J.CCR.2011.09.009.
325. Masola, V.; Zaza, G.; Gambaro, G.; Franchi, M.; Onisto, M. Role of Heparanase in Tumor Progression: Molecular Aspects and Therapeutic Options. *Semin. Cancer Biol.* **2020**, *62*, 86–98. https://doi.org/10.1016/J.SEMCANCER.2019.07.014.
326. Santos-Martínez, M. J.; Medina, C.; Jurasz, P.; Radomski, M. W. Role of Metalloproteinases in Platelet Function. *Thromb. Res.* **2008**, *121* (4), 535–542. https://doi.org/10.1016/J.THROMRES.2007.06.002.
327. Purushothaman, A.; Sanderson, R. D. Heparanase: A Dynamic Promoter of Myeloma Progression. *Adv. Exp. Med. Biol.* **2020**, *1221*, 331. https://doi.org/10.1007/978-3-030-34521-1_12.
328. Radziwon-Balicka, A.; Santos-Martinez, M. J.; Corbalan, J. J.; O'Sullivan, S.; Treumann, A.; Gilmer, J. F.; Radomski, M. W.; Medina, C. Mechanisms of Platelet-Stimulated Colon Cancer Invasion: Role of Clusterin and Thrombospondin 1 in Regulation of the P38MAPK-MMP-9 Pathway. *Carcinogenesis* **2014**, *35* (2), 324–332. https://doi.org/10.1093/CARCIN/BGT332.
329. Vismara, M.; Negri, S.; Scolari, F.; Brunetti, V.; Trivigno, S. M. G.; Faris, P.; Galgano, L.; Soda, T.; Berra-Romani, R.; Canobbio, I.; Torti, M.; Guidetti, G. F.; Moccia, F. Platelet-Derived Extracellular Vesicles Stimulate Migration through Partial Remodelling of the

Ca2+ Handling Machinery in MDA-MB-231 Breast Cancer Cells. *Cells* **2022**, *11* (19). https://doi.org/10.3390/CELLS11193120.
330. Janowska-Wieczorek, A.; Wysoczynski, M.; Kijowski, J.; Marquez-Curtis, L.; Machalinski, B.; Ratajczak, J.; Ratajczak, M. Z. Microvesicles Derived from Activated Platelets Induce Metastasis and Angiogenesis in Lung Cancer. *Int. J. Cancer* **2005**, *113* (5), 752–760. https://doi.org/10.1002/IJC.20657.
331. Zarfati, M.; Katz, T.; Avivi, I.; Brenner, B.; Aharon, A. PO-45 - The Role of Microvesicles in Multiple Myeloma Progression. *Thromb. Res.* **2016**, *140*, S193. https://doi.org/10.1016/s0049-3848(16)30178-5.
332. Labelle, M.; Begum, S.; Hynes, R. O. Platelets Guide the Formation of Early Metastatic Niches. *Proc. Natl. Acad. Sci. U. S. A.* **2014**, *111* (30), E3053–E3061. https://doi.org/10.1073/PNAS.1411082111/SUPPL_FILE/PNAS.201411082SI.PDF.
333. Sebastiano, M.; Momi, S.; Falcinelli, E.; Bury, L.; Hoylaerts, M. F.; Gresele, P. A Novel Mechanism Regulating Human Platelet Activation by MMP-2–Mediated PAR1 Biased Signaling. *Blood* **2017**, *129* (7), 883–895. https://doi.org/10.1182/BLOOD-2016-06-724245.
334. Que, W.; Chen, J. Knockdown of C-Met Inhibits Cell Proliferation and Invasion and Increases Chemosensitivity to Doxorubicin in Human Multiple Myeloma U266 Cells in Vitro. *Mol. Med. Rep.* **2011**, *4* (2), 343–349. https://doi.org/10.3892/MMR.2011.426.
335. Foda, H. D.; Zucker, S. Matrix Metalloproteinases in Cancer Invasion, Metastasis and Angiogenesis. *Drug Discov. Today* **2001**, *6* (9), 478–482. https://doi.org/10.1016/S1359-6446(01)01752-4.
336. Sophie Barillé, B.; lia Akhoundi, C.; Collette, M.; Mellerin, M.-P.; Rapp, M.-J.; Harousseau, J.-L.; gis Bataille, R.; Amiot, M. Metalloproteinases in Multiple Myeloma: Production of Matrix Metalloproteinase-9 (MMP-9), Activation of ProMMP-2, and Induction of MMP-1 by Myeloma Cells.
337. Parmo-Cabañas, M.; Molina-Ortiz, I.; Matías-Román, S.; García-Bernal, D.; Carvajal-Vergara, X.; Valle, I.; Pandiella, A.; Arroyo, A. G.; Teixidó, J. Role of Metalloproteinases MMP-9 and MT1-MMP in CXCL12-Promoted Myeloma Cell Invasion across Basement Membranes. *J. Pathol.* **2006**, *208* (1), 108–118. https://doi.org/10.1002/PATH.1876.
338. Guo, Y.; Cui, W.; Pei, Y.; Xu, D. Platelets Promote Invasion and Induce Epithelial to Mesenchymal Transition in Ovarian Cancer Cells by TGF-β Signaling Pathway. *Gynecol. Oncol.* **2019**, *153* (3), 639–650. https://doi.org/10.1016/J.YGYNO.2019.02.026.
339. Pan, S.; Hu, Y.; Hu, M.; Jian, H.; Chen, M.; Gan, L.; Zheng, P.; He, Y.; Wang, J. Platelet-Derived PDGF Promotes the Invasion and Metastasis of Cholangiocarcinoma by Upregulating MMP2/MMP9 Expression and Inducing EMT via the P38/MAPK Signalling Pathway. *Am. J. Transl. Res.* **2020**, *12* (7), 3577.
340. Martini, C.; Thompson, E. J.; Hyslop, S. R.; Cockshell, M. P.; Dale, B. J.; Ebert, L. M.; Woods, A. E.; Josefsson, E. C.; Bonder, C. S. Platelets Disrupt Vasculogenic Mimicry by Cancer Cells. *Scientific Reports 2020 10:1* **2020**, *10* (1), 5869-. https://doi.org/10.1038/s41598-020-62648-x.
341. Gould, S. T.; Darling, N. J.; Anseth, K. S. Small Peptide Functionalized Thiol-Ene Hydrogels as Culture Substrates for Understanding Valvular Interstitial Cell Activation and de Novo Tissue Deposition. *Acta Biomater.* **2012**, *8* (9), 3201. https://doi.org/10.1016/J.ACTBIO.2012.05.009.
342. Johnson, K. E.; Ceglowski, J. R.; Roweth, H. G.; Forward, J. A.; Tippy, M. D.; El-Husayni, S.; Kulenthirarajan, R.; Malloy, M. W.; Machlus, K. R.; Chen, W. Y.; Italiano, J. E.;

Battinelli, E. M. Aspirin Inhibits Platelets from Reprogramming Breast Tumor Cells and Promoting Metastasis. *Blood Adv.* **2019**, *3* (2), 198–211. https://doi.org/10.1182/BLOODADVANCES.2018026161.

343. Bulla, S. C.; Badial, P. R.; Silva, R. C.; Lunsford, K.; Bulla, C. Platelets Inhibit Migration of Canine Osteosarcoma Cells. *J. Comp. Pathol.* **2017**, *156* (1), 3–13. https://doi.org/10.1016/J.JCPA.2016.10.001.
344. Tong, H.; Li, K.; Zhou, M.; Wu, R.; Yang, H.; Peng, Z.; Zhao, Q.; Luo, K. Q. Coculture of Cancer Cells with Platelets Increases Their Survival and Metastasis by Activating the TGFβ/Smad/PAI-1 and PI3K/AKT Pathways. *Int. J. Biol. Sci.* **2023**, *19* (13), 4259. https://doi.org/10.7150/IJBS.85986.
345. Yoon, J.; Parish, C. R.; Blackburn, A. C.; Coupland, L. A. Potential Contrasting Effects of Platelets on the Migration and Invasion of Sarcomas versus Carcinomas. *Platelets* **2021**, 1–9. https://doi.org/10.1080/09537104.2020.1792433.
346. Bulla, S. C.; Badial, P. R.; Bulla, C. Canine Cancer Cells Activate Platelets via the Platelet P2Y12 Receptor. *J. Comp. Pathol.* **2022**, *192*, 41–49. https://doi.org/10.1016/J.JCPA.2022.01.002.
347. Cooke, A.; Cooke, N. M.; Spillane, C. D.; Sheils, O.; Kenny, D. Lenus: Research Repository Aspirin and P2Y12 Inhibition Attenuate Platelet-Induced Ovarian Cancer Cell Invasion. Item Type Article Aspirin and P2Y 12 Inhibition Attenuate Platelet-Induced Ovarian Cancer Cell Invasion. **2011**. https://doi.org/10.1186/s12885-015-1634-x.
348. Zarà, M.; Canobbio, I.; Visconte, C.; Canino, J.; Torti, M.; Guidetti, G. F. Molecular Mechanisms of Platelet Activation and Aggregation Induced by Breast Cancer Cells. *Cell. Signal.* **2018**, *48*, 45–53. https://doi.org/10.1016/J.CELLSIG.2018.04.008.
349. Kunicki, T. J.; Nugent, D. J. The Genetics of Normal Platelet Reactivity. *Blood* **2010**, *116* (15), 2627. https://doi.org/10.1182/BLOOD-2010-04-262048.
350. Orellana, R.; Kato, S.; Erices, R.; Bravo, M. L.; Gonzalez, P.; Oliva, B.; Cubillos, S.; Valdivia, A.; Ibañez, C.; Brañes, J.; Barriga, M. I.; Bravo, E.; Alonso, C.; Bustamente, E.; Castellon, E.; Hidalgo, P.; Trigo, C.; Panes, O.; Pereira, J.; Mezzano, D.; Cuello, M. A.; Owen, G. I. Platelets Enhance Tissue Factor Protein and Metastasis Initiating Cell Markers, and Act as Chemoattractants Increasing the Migration of Ovarian Cancer Cells. *BMC Cancer* **2015**, *15* (1), 290. https://doi.org/10.1186/S12885-015-1304-Z.
351. Lin, K. T.; Yeh, Y. M.; Chuang, C. M.; Yang, S. Y.; Chang, J. W.; Sun, S. P.; Wang, Y. S.; Chao, K. C.; Wang, L. H. Glucocorticoids Mediate Induction of MicroRNA-708 to Suppress Ovarian Cancer Metastasis through Targeting Rap1B. *Nat. Commun.* **2015**, *6*. https://doi.org/10.1038/NCOMMS6917.
352. Looi, C. K.; Hii, L. W.; Ngai, S. C.; Leong, C. O.; Mai, C. W. The Role of Ras-Associated Protein 1 (Rap1) in Cancer: Bad Actor or Good Player? *Biomedicines* **2020**, *8* (9), 334. https://doi.org/10.3390/BIOMEDICINES8090334.
353. Mele, S.; Devereux, S.; Pepper, A. G.; Infante, E.; Ridley, A. J. Calcium-RasGRP2-Rap1 Signaling Mediates CD38-Induced Migration of Chronic Lymphocytic Leukemia Cells. *Blood Adv.* **2018**, *2* (13), 1551–1561. https://doi.org/10.1182/BLOODADVANCES.2017014506.
354. Chuang, Y. C.; Wu, H. Y.; Lin, Y. L.; Tzou, S. C.; Chuang, C. H.; Jian, T. Y.; Chen, P. R.; Chang, Y. C.; Lin, C. H.; Huang, T. H.; Wang, C. C.; Chan, Y. L.; Liao, K. W. Blockade of ITGA2 Induces Apoptosis and Inhibits Cell Migration in Gastric Cancer. *Biol. Proced. Online* **2018**, *20* (1), 10. https://doi.org/10.1186/S12575-018-0073-X.

355. Liu, Z.; Zhan, Y.; Tu, Y.; Chen, K.; Liu, Z.; Wu, C. PDZ and LIM Domain Protein 1(PDLIM1)/CLP36 Promotes Breast Cancer Cell Migration, Invasion and Metastasis through Interaction with α-Actinin. *Oncogene 2015 34:10* **2014**, *34* (10), 1300–1311. https://doi.org/10.1038/onc.2014.64.
356. Lei, Y.; He, L.; Li, Y.; Hou, J.; Zhang, H.; Li, G. PDLIM1 Interacts with HK2 to Promote Gastric Cancer Progression through Enhancing the Warburg Effect via Wnt/β-Catenin Signaling. *Cell Tissue Res.* **2024**, *395* (1), 105–116. https://doi.org/10.1007/S00441-023-03840-Z.
357. Adams, J. The Proteasome: A Suitable Antineoplastic Target. *Nature Reviews Cancer 2004 4:5* **2004**, *4* (5), 349–360. https://doi.org/10.1038/nrc1361.
358. Manasanch, E. E.; Orlowski, R. Z. Proteasome Inhibitors in Cancer Therapy. *Nat. Rev. Clin. Oncol.* **2017**, *14* (7), 417–433. https://doi.org/10.1038/NRCLINONC.2016.206.
359. Hideshima, T.; Nakamura, N.; Chauhan, D.; Anderson, K. C. Biologic Sequelae of Interleukin-6 Induced PI3-K/Akt Signaling in Multiple Myeloma. *Oncogene* **2001**, *20* (42), 5991–6000. https://doi.org/10.1038/SJ.ONC.1204833.
360. Mitsiades, C. S.; Mitsiades, N.; Poulaki, V.; Schlossman, R.; Akiyama, M.; Chauhan, D.; Hideshima, T.; Treon, S. P.; Munshi, N. C.; Richardson, P. G.; Anderson, K. C. Activation of NF-KappaB and Upregulation of Intracellular Anti-Apoptotic Proteins via the IGF-1/Akt Signaling in Human Multiple Myeloma Cells: Therapeutic Implications. *Oncogene* **2002**, *21* (37), 5673–5683. https://doi.org/10.1038/SJ.ONC.1205664.
361. Corre, J.; Labat, E.; Espagnolle, N.; Hébraud, B.; Avet-Loiseau, H.; Roussel, M.; Huynh, A.; Gadelorge, M.; Cordelier, P.; Klein, B.; Moreau, P.; Facon, T.; Fournié, J. J.; Attal, M.; Bourin, P. Bioactivity and Prognostic Significance of Growth Differentiation Factor GDF15 Secreted by Bone Marrow Mesenchymal Stem Cells in Multiple Myeloma. *Cancer Res.* **2012**, *72* (6), 1395–1406. https://doi.org/10.1158/0008-5472.CAN-11-0188.
362. Tarkun, P.; Birtas Atesoglu, E.; Mehtap, O.; Musul, M. M.; Hacihanefioglu, A. Serum Growth Differentiation Factor 15 Levels in Newly Diagnosed Multiple Myeloma Patients. *Acta Haematol.* **2014**, *131* (3), 173–178. https://doi.org/10.1159/000354835.
363. Yang, H.; He, Y.; Qu, F.; Zhu, J.; Deng, L.; Jiang, F.; Wu, X.; Chen, Y.; Kashif, A.; Wang, X. Maraviroc Enhances Bortezomib Sensitivity in Multiple Myeloma by Inhibiting M2 Macrophage Polarization via PI3K/AKT/RhoA Signaling Pathway in Macrophages. *Cell Division* **2025**, *20* (1), 5-. https://doi.org/10.1186/S13008-025-00145-1/FIGURES/6.
364. Zhang, H.; Du, Z.; Tu, C.; Zhou, X.; Menu, E.; Wang, J. Hypoxic Bone Marrow Stromal Cells Secrete MiR-140-5p and MiR-28-3p That Target SPRED1 to Confer Drug Resistance in Multiple Myeloma. *Cancer Res.* **2024**, *84* (1), 39–55. https://doi.org/10.1158/0008-5472.CAN-23-0189.
365. Balsas, P.; Galán-Malo, P.; Marzo, I.; Naval, J. Bortezomib Resistance in a Myeloma Cell Line Is Associated to PSMβ5 Overexpression and Polyploidy. *Leuk. Res.* **2012**, *36* (2), 212–218. https://doi.org/10.1016/J.LEUKRES.2011.09.011.
366. Yasui, H.; Hideshima, T.; Ikeda, H.; Jin, J.; Ocio, E. M.; Kiziltepe, T.; Okawa, Y.; Vallet, S.; Podar, K.; Ishitsuka, K.; Richardson, P. G.; Pargellis, C.; Moss, N.; Raje, N.; Anderson, K. C. BIRB 796 Enhances Cytotoxicity Triggered by Bortezomib, Heat Shock Protein (Hsp) 90 Inhibitor, and Dexamethasone via Inhibition of P38 Mitogen-Activated Protein Kinase/Hsp27 Pathway in Multiple Myeloma Cell Lines and Inhibits

Paracrine Tumour Growth. *Br. J. Haematol.* **2007**, *136* (3), 414–423. https://doi.org/10.1111/J.1365-2141.2006.06443.X.
367. Li, J.; Zhang, X.; Shen, H.; Guo, J.; Wang, X.; Liu, J. Bortezomib Promotes Apoptosis of Multiple Myeloma Cells by Regulating HSP27. *Mol. Med. Rep.* **2019**, *20* (3), 2410–2418. https://doi.org/10.3892/MMR.2019.10467.
368. Besse, L.; Besse, A.; Mendez-Lopez, M.; Vasickova, K.; Sedlackova, M.; Vanhara, P.; Kraus, M.; Bader, J.; Ferreira, R. B.; Castellano, R. K.; Law, B. K.; Driessen, C. A Metabolic Switch in Proteasome Inhibitor-Resistant Multiple Myeloma Ensures Higher Mitochondrial Metabolism, Protein Folding and Sphingomyelin Synthesis. *Haematologica* **2019**, *104* (9), E415–E419. https://doi.org/10.3324/HAEMATOL.2018.207704.
369. Soriano, G. P.; Besse, L.; Li, N.; Kraus, M.; Besse, A.; Meeuwenoord, N.; Bader, J.; Everts, B.; Den Dulk, H.; Overkleeft, H. S.; Florea, B. I.; Driessen, C. Proteasome Inhibitor-Adapted Myeloma Cells Are Largely Independent from Proteasome Activity and Show Complex Proteomic Changes, in Particular in Redox and Energy Metabolism. *Leukemia* **2016**, *30* (11), 2198–2207. https://doi.org/10.1038/LEU.2016.102.
370. Maiso, P.; Huynh, D.; Moschetta, M.; Sacco, A.; Aljawai, Y.; Mishima, Y.; Asara, J. M.; Roccaro, A. M.; Kimmelman, A. C.; Ghobrial, I. M. Metabolic Signature Identifies Novel Targets for Drug Resistance in Multiple Myeloma. *Cancer Res.* **2015**, *75* (10), 2071–2082. https://doi.org/10.1158/0008-5472.CAN-14-3400.
371. Radziwon-Balicka, A.; Medina, C.; O'Driscoll, L.; Treumann, A.; Bazou, D.; Inkielewicz-Stepniak, I.; Radomski, A.; Jow, H.; Radomski, M. W. Platelets Increase Survival of Adenocarcinoma Cells Challenged with Anticancer Drugs: Mechanisms and Implications for Chemoresistance. *Br. J. Pharmacol.* **2012**, *167* (4), 787–804. https://doi.org/10.1111/J.1476-5381.2012.01991.X.
372. Ishikawa, S.; Miyashita, T.; Inokuchi, M.; Hayashi, H.; Oyama, K.; Tajima, H.; Takamura, H.; Ninomiya, I.; Ahmed, A. K.; Harman, J. W.; Fushida, S.; Ohta, T. Platelets Surrounding Primary Tumor Cells Are Related to Chemoresistance. *Oncol. Rep.* **2016**, *36* (2), 787–794. https://doi.org/10.3892/OR.2016.4898/HTML.
373. Liang, X.; Wang, H.; Zhou, J.; Zhu, J.; Jiao, X.; Zhai, Z. Platelets Form Aggregates on the Surface of AML Cells Via CD62P/PSGL-1 and Release TGF-B1 to Promote Drug Resistance. *Blood* **2024**, *144* (Supplement 1), 5809–5809. https://doi.org/10.1182/BLOOD-2024-210121.
374. Dutta, D.; Liu, J.; Wen, K.; Kurata, K.; Fulciniti, M.; Gulla, A.; Hideshima, T.; Anderson, K. C. BCMA-Targeted Bortezomib Nanotherapy Improves Therapeutic Efficacy, Overcomes Resistance, and Modulates the Immune Microenvironment in Multiple Myeloma. *Blood Cancer Journal 2023 13:1* **2023**, *13* (1), 184-. https://doi.org/10.1038/s41408-023-00955-y.
375. Bianchi, G.; Oliva, L.; Cascio, P.; Pengo, N.; Fontana, F.; Cerruti, F.; Orsi, A.; Pasqualetto, E.; Mezghrani, A.; Calbi, V.; Palladini, G.; Giuliani, N.; Anderson, K. C.; Sitia, R.; Cenci, S. The Proteasome Load versus Capacity Balance Determines Apoptotic Sensitivity of Multiple Myeloma Cells to Proteasome Inhibition. *Blood* **2009**, *113* (13), 3040–3049. https://doi.org/10.1182/BLOOD-2008-08-172734.